Contents

List of Figures

Chapter 8: Discussion

List of Abbreviations

4E-BP	the eukaryotic initiation factor 4E binding protein
AMP	Antimicrobial peptide
APC/C	Anaphase promoting complex/cyclosome
attA	AttacinA
bp	base pair
BSA	Bovine Serum Albumin
Cdk	Cyclin dependent kinase
cDNA	complementary DNA
CLAP	Chymostatin, Leupeptin, Antipain, Pepstatin A
C-terminus	Carboxyl terminus
Cyc	Cyclin
DAPI	4', 6-diamidino-2-phenylindole
DEPC	Diethyl pyrocarbonate
Dfs	Dominant female sterile
Dilp	Drosophila insulin-like peptide
DMEM	Dulbecco's modified Eagle's medium
DMSO	Dimethyl sulphoxide
DNA	Deoxyribonucleotide
dNTP	2'-deoxyribonucleoside 5'-triphosphate
dpt	Diptericin
drs	Drosomycin
Dscam	Down syndrome cell adhesion molecule
DTT	Dithiothreitol
EBR	Ephrussi Beadle Ringer's Solution
ECL	Enhanced Chemiluminescence
EDTA	Ethylenediamine-N,N,N',N'-tetraacetic acid
EMS	Ethylmethane Sulfonate
FBS	Fetal Bovine Serum
FOXO	Forkhead box, subgroup O
GFP	Green Fluorescent Protein
GNBP	Gram-negative-binding protein
HCl	Hydrochloric acid
HEPES	N-(2-hydroxyethyl)piperazine-N'-(2-ethanesulfonic acid)
His	Histidine
hr	hour
HRP	Horseradish peroxidase
IGF	Insulin-like growth factor

Imd	Immune deficiency
InR	Insulin receptor
IPS	Insulin-producing cells
IRAKs	Interleukin-1 receptor associated kinases
IRS	Insulin receptor substrate
JNK	c-jun N-terminal kinase
kb	kilobase-pairs(s)
kDa	kiloDalton(s)
LB	Luria-Bertani medium
N-terminus	Amino terminus
ºC	Degree Celsius
OD	Optical Density
PAGE	Polyacrylamide Gel Electrophoresis
PBS	Phosphate Buffered Saline
PCR	Polymerase Chain Reaction
PGRPs	Peptidoglycan-recognition proteins
PH	Pleckstrin homology
PIP2	Phosphatidylinositol-4,5-phosphate
PIP3	Phosphatidylinositol-3,4,5-phosphate
PMSF	Phenylmethyl Sulfonyl Fluoride
pRb	Product of retinoblastoma
RNA	Ribonucleic acid
RNAi	RNA-mediated interference
RNase	Ribonuclease
rp49	Ribosomal protein 49
Rpm	Revolutions per minute
RT-PCR	Reverse Transcriptase - Polymerase Chain Reaction
SDS	Sodium Dodecyl Sulfate
SDS-PAGE	Sodium Dodecyl Sulphate Polyacrylamide Gel Electrophoresis
SNP	Single nucleotide polymorphism
TAE	Tris acetate buffer with EDTA
TAK	TGF-β-activated kinase
TE	Tris buffer with EDTA
TLRs	Toll-like receptors
TOR	Target of rapamycin
TORC1	Target of rapamycin complex 1
TORC2	Target of rapamycin complex 2
Tris	Tris[hydroxymethyl]aminomethane
Triton X-100	Octylphenol ethoxylate

TSC	Tuberous sclerosis complex
Tween-20	Polyoxyethylene-sorbitan monolaurate
UAS	Upstream Activating Sequence
wt	wild type

Abstract

Poly is a novel, essential protein in *Drosophila melanogaster*, loss of function of which results in late larval lethality. Importantly, Poly is evolutionarily conserved with a human homologue. *poly* mutation was isolated in a P-element mutagenesis screen that aimed to generate a larger collection of single P-element induced mutants. Mutant *poly* larvae are characterized by extreme larval longevity without pupation, formation of melanotic masses, smaller imaginal discs and brains, and abnormal nuclear morphology in neuroblasts. During the course of my project, I attempted to identify cellular processes and pathways that Poly might be involved in. Interestingly, my data suggest that Poly is a novel interactor and regulator of Insulin receptor/target of rapamycin (InR/TOR) signalling in *Drosophila*.

Linking environmental cues to cell growth and metabolism is an essential process that multicellular organisms need to accomplish successfully for normal development. InR/TOR signalling is a highly conserved pathway that mediates the link between the environment and cellular processes such as growth, metabolism and ageing. My analysis in *Drosophila* suggests that Poly interacts physically with the InR and mutation of Poly leads to an overall down-regulation of InR/TOR signalling in *Drosophila* as revealed by decreases in the phosphorylation levels of Akt, S6K and 4E-BP - all downstream effectors of this pathway. In addition, loss of *poly* results in constitutive activation of autophagy in *Drosophila* fat body and a decrease in stored triglyceride levels. Furthermore, I show that localisation and levels of Poly protein are dependent on insulin action in both *Drosophila* and human cells. Together, these data suggest that Poly is a novel mediator of InR signalling that promotes an increase in cell growth and metabolism.

Taking into consideration the observed *poly* mutant phenotype, I also investigated the potential involvement of Poly during cell cycle progression and the *Drosophila* innate immune response. While my analysis suggests that *poly* loss of function does not have a direct effect on cell cycle progression, alteration of Poly has consequences on various aspects of the *Drosophila* innate immune response. Therefore, I conclude that the *Drosophila* innate immune response is a cellular process in which Poly plays a crucial role.

Chapter 1: Introduction

My Ph.D. project in the Heck laboratory focused on the functional characterization of a novel gene named *poly* in *Drosophila melanogaster*. The initial phenotypic characterization of *poly* mutants had already been done by other members of the Heck laboratory by the time I started my Ph.D. My project focused on elucidation of cellular processes and pathways that Poly might be involved in. Since, at the time, we had very few indications about the molecular function of Poly, this project allowed me to explore and gain knowledge about various aspects of cell biology.

This thesis comprises five Results chapters, Material and Methods and a Discussion chapter. During the Introduction Chapter, I have firstly introduced the use of *Drosophila* as a model system in biological research as well as some of the important genetic tools available in *Drosophila* and those that I have made use of during the course of my project. I have then briefly summarised the cell cycle and its regulation, as part of my project focused on investigation of a potential role for Poly during cell cycle control. In the remaining part of the Introduction Chapter, I have reviewed pathways including Insulin Receptor/Target of Rapamycin signalling and pathways involved in the *Drosophila* innate immune response as my data suggest involvement of *Drosophila* in these processes. Finally, I concluded the Introduction Chapter by giving the background of *poly* mutation as well as the phylogenetic and structural analysis of the protein consisting of the work that has been done previously by other members of the Heck laboratory.

1.1 *Drosophila melanogaster* as a model organism

Drosophila melanogaster, or with the more commonly used name, the fruit fly, has been a widely used model organism in biology since early 20th century when Thomas Hunt Morgan and colleagues first set up the famous Fly Room at Columbia University. Even at this very early stage, research carried out in *Drosophila* played a major pioneering role in the discovery of essential basic biological processes such as the identification of chromosomes as the basis of heredity about a century ago (BRIDGES 1916; MORGAN 1910). Since these early days, the number of research groups using *Drosophila* as a model organism to study various cellular and biological processes has greatly increased. Many advantageous features that flies possess make them the model organism of choice for a great number of scientists.

Firstly, its small size makes *Drosophila* a model organism that is very easy and cheap to store in the laboratory environment. *Drosophila* regeneration time is only about 10 days at room temperature and females have high fecundity, which allows the study of subsequent generations within a short period of time. Also, fruit flies are dimorphic which makes female and male sexes very easily distinguishable from each other.

The genome of *Drosophila* only consists of 4 chromosomes and the males (which are the heterogametic sex) do not undergo meiotic recombination, making genetic studies easier. Furthermore, the existence of "balancer chromosomes", which are characterized by a number of chromosomal inversions that prevent recombination, makes it possible to maintain homozygous lethal alleles as heterozygous stocks.

Drosophila has a well defined life-cycle and a range of different tissue types which allow the study of gene expression as well as various other cellular processes at different developmental stages and in different tissue types. For example, *Drosophila* larvae have giant chromosomes called "polytenes" which result from continuous endoreplication events in the larval salivary glands. The study of the banding pattern in polytene chromosomes was one of the pioneer works that has brought insight into the developmental regulation of transcriptional activity and gene expression (ASHBURNER 1975). Interestingly, polytene chromosomes are still being successfully used to uncover mechanistics of transcriptional activity (RAFFA *et al.* 2005).

The *Drosophila* genome was first sequenced and published in 2000 (ADAMS *et al.* 2000). To date, it is known to contain 165 million base pair and an estimated number of 14000 genes. Mutations in a large number of *Drosophila* genes are available in worldwide stock centres and these are readily accessible which makes the study of a great number of genes possible. The information about various aspects of *Drosophila melanogaster* genome as well as the existence of mutant lines is available through FlyBase (http://flybase.org/).

Apart from all the practical advantages that *Drosophila* offers, evolutionarily conservation of genes between flies and higher eukaryotes makes research carried out in flies applicable to humans. Interestingly, about 77% of all known human genes involved in diseases have homologues in *Drosophila* genome (REITER *et al.* 2001). Therefore, flies have been efficiently used to model various human diseases ranging from neurodegenerative diseases to cancer and diabetes (BROUGHTON *et al.* 2005; FEANY and BENDER 2000; LEOPOLD and PERRIMON 2007; TENENBAUM 2003).

Interestingly, a number of important genes involved in human biology were first discovered in *Drosophila*. As an example, we could give the Toll receptor gene which was firstly identified in *Drosophila* as a gene involved in embryonic axis formation (ANDERSON *et al.* 1985).

In the remaining part of this section I will be describing the life cycle of *Drosophila* followed by the description of two powerful genetic tools available in *Drosophila* including the *UAS/GAL4* system for directed gene expression and the Flp/FRT technique for the generation of mitotic clones.

1.1.1 Life cycle of Drosophila

Drosophila melanogaster is a holometabolous insect that undergoes a complete metamorphosis by passing through four distinct developmental stages: embryo, larvae, pupae and adult (Figure 1.1). Like other ectothermic species, its developmental period is temperature dependent. Females lay eggs shortly after fertilisation takes place. At 25°C, the embryonic stage lasts about 24 hours before the embryo hatches into the first larval instar. The first two larval stages (first and second instar) last 24 hours each, whereas the third larval instar stage lasts 48 hours and terminates by formation of the puparium. About 4 days later, the adult fly ecloses from the pupae, having undergone a complete metamorphosis. Overall, at 25°C the eclosion of an adult takes about 9-10 days. The life cycle period becomes longer at lower temperature and faster at higher temperature. *Drosophila* can survive at temperatures from 16°C up to 30°C (ASHBURNER *et al.* 2005)

In more detail, the embryonic stage starts with 13 rapid and synchronized syncytial divisions that last about 2 hours each (FOE 1989). The syncitial divisions

are followed by the formation of cytoplasm around these nuclei therefore forming the blastoderm. Maternally loaded mRNA coming from the female's ovaries is used to drive the syncitial cell division events (BATE and ARIAS 1993).

During the first two larval instars and the first half of the third instar, *Drosophila* larvae expand greatly in mass mainly due to continuous feeding. At the late third instar larval stage, larvae leave the food and start wandering on the walls of the containement vial searching for a suitable place to pupate. Metamorphosis into the adult fly takes place inside the puparium and within 4-5 days the young adult fly ecloses with unexpanded wings and a non-pigmented body. Developmental timing at a given temperature as well as various larval physiological features, such as the morphology of mouth hooks and spiracles, makes it possible to distinguish between different larval instars (ASHBURNER *et al.* 2005; GREENSPAN 1997; ROBERTS 1998).

1.1.2 Genetic tools available in Drosophila

One of the main reasons for the success of *Drosophila* as a model system is the availability of various genetic tools that makes it possible to carry out forward genetic screens to uncover genetic interactions involved in a given biological process (ST JOHNSTON 2002).

In the early days, scientists who were using *Drosophila* as a model organism were mainly focusing on isolating naturally occurring mutations that gave a visible phenotype. However, techniques were soon developed to induce mutations of various *Drosophila* genes. Two most commonly used strategies to generate mutant alleles in *Drosophila* are mutagenesis via P-element transposition and chemical mutagenesis by ethyl methane sulphonate (EMS) administration.

P-elements are transposons that are found naturally in the *Drosophila* genome. When they are induced to transpose, their insertion into a gene can lead to a mutation. Mutated genes can be identified easily by using the P-element sequence as a "tag". The disadvantage of this technique is that some parts of the genome are hot spots and others are cold spots for P-element insertion. A large collection of P-element insertions has already been generated and is available in stock centres (SPRADLING *et al.* 1999).

Feeding flies with EMS leads to a very high frequency of mutation which makes EMS mutagenesis more efficient than P-element transposition. EMS mutagenesis mostly leads to single base pair changes that result in missense or nonsense mutations. The main disadvantage of EMS mutagenesis has been the difficulty to map the single base pair change to a specific gene. However, the development of single nucleotide polymorphism (SNP) maps seems to be solving this problem to a large extent (BERGER *et al.* 2001).

Genetic screens in *Drosophila,* which aim to uncover a great number of genes involved in a given biological process, have a history of success. The most famous example is the Nobel Prize winning Heidelberg screen that described mutations affecting body patterning in the embryo (NUSSLEIN-VOLHARD and WIESCHAUS 1980). This screen carried out by Christiane Nusslein-Volhard and Eric Wieschaus was the first time that anyone successfully attempted to isolate, in a multicellular organism, a large number of genes affecting one biological process, and therefore it is considered as a revolutionary genetic screen. But at this early stage, this screen had its own limitations such as the inability to identify maternal effect genes and genes affecting the internal structures in the embryo. Since then, more sophisticated

genetic tools have become available in *Drosophila* which made it possible to design more sophisticated screens. One such commonly used genetic tool is the *Gal4-UAS* system.

Directed gene expression in *Drosophila* is achieved by using the *Gal4-UAS* system (BRAND and PERRIMON 1993; DUFFY 2002). The yeast transcription factor *Gal4* binds to the Upstream Activator Sequence (*UAS*) and promotes transcription of the gene of interest situated downstream of the *UAS* (Figure 1.2). In *Drosophila*, there are a number of "enhancer trap" lines that have the *Gal4* gene inserted nearby a number of genomic enhancer therefore allowing the expression of *Gal4* in a tissue specific manner. Therefore, the over-expression of the gene of interest in a tissue specific manner is achieved by crossing the relevant *Gal4* enhancer trap line with the transgenic flies that carry the *UAS* sequence followed by the gene of interest.

Gal4-UAS system is commonly used in genetic screens where the overexpression of the gene of interest in a particular tissue gives a scorable phenotype (RORTH 1996; RORTH *et al.* 1998). Adult eye has been a widely used tissue for such screens. The fly eye is composed of around 800 ommatidia, the correct formation of which is tightly regulated by various cell signalling events (TIO *et al.* 1996). Disruption to these cell signalling events leads to rough eye phenotype which is an easily scorable phenotype and does not affect the viability of the fly. If the eye specific over-expression of the gene of interest by using the *Gal4-UAS* system leads to rough eye phenotype, this opens to possibility to carry out a screen whereby one would be looking for modifiers of the rough eye. Mutations in other genes might be acting as the "suppressor" or the "enhancer" of the rough eye phenotype resulting from the over-expression of the gene of interest. In this way,

identification of suppressors and enhancers allows the discovery of novel genetic interactions (MUKHERJEE *et al.* 2005).

Another useful genetic tool available in *Drosophila* is the generation of mutant mitotic clones in a heterozygous mutant background by using the Flp/FRT system (THEODOSIOU and XU 1998). Yeast flipase (Flp) recombinase mediates the recombination between FRT sites in the yeast 2μ plasmid. Site specific recombination in *Drosophila* is achieved by expression of *Flp* recombinase in transgenic flies that have FRT sites inserted on chromosome arms with the mutation of interest located distally to the FRT site (Figure 1.3). If the site specific recombination takes place between FRT sites situated on homologous chromosomes following the DNA replication in a larvae heterozygous for the mutation of interest, and the daughter chromatids segregate appropriately one of the daughter cells will inherit two copies of the mutations whereas the other daughter cell will be wild type regarding the mutation.

Generation of mutant clones were successfully carried out on larval imaginal discs and fat body (SCOTT *et al.* 2007; SIMON 1994). An important advantage of this technique is that it allows the direct comparison of homozygous mutant versus heterozygous cells side-by-side within the same tissue. Furthermore, it allows the functional study of essential genes in a tissue specific manner that would otherwise be lethal following the loss of function at the whole organism.

An early example of a screen that used the generation of mitotic clones in imaginal discs successfully identified genes involved in tumourous growth, such as the tumour suppressor gene *warts,* by looking at phenotypes that were scorable in adults (XU *et al.* 1995).

Another important application of the use of this technique has been the generation of germline mutant clones. Generation of mutant germline clones allows the study of the zygotic function of the genes which would have otherwise been impossible due to the maternal loading of the gene product from the heterozygous mother. This technique combines the use of dominant female-sterile (DFS) mutations and FRT sites allowing therefore the production of eggs only in germline cells resulting from mitotic recombination, and therefore lacking the DFS mutation but remaining homozygous for the mutation of interest (CHOU *et al.* 1993; CHOU and PERRIMON 1996). Similarly to somatic mitotic clones, germline clones have been widely used in genetic screens to reveal the zygotic effect of genes without the masking by the maternally loaded gene product (PERRIMON *et al.* 1996).

Put together, all these previously described features make *Drosophila melanogaster* a powerful model organism in which it is possible to carry out elegant genetic screens, to identify novel genes and cellular processes as well as to model various human diseases.

1.2. The Cell Cycle

The cell division cycle is the process whereby the cell replicates its DNA and divides to give rise to two identical daughter cells. Development of multicellular organisms requires sophisticated regulation and coordination of the cell cycle with external cell division promoting or inhibiting stimuli. In fact, disruption of the cell cycle is involved in the development of diseases, such as cancer, highlighting the requirement of non-aberrant progression of cell cycle for normal development (VERMEULEN *et al.* 2003).

The cell cycle is considered to consist of four major stages: Gap phases (G1 and G2) and the Synthetic (S) phase that can be called by the general term interphase, and mitosis (M) during which the nuclear division takes place (Figure 1.4). Mitosis is further divided into four sequential phases that include prophase, metaphase, anaphase and telophase. Important regulators of cell cycle progression called cyclin-dependent kinases (Cdks) and their binding partners, cyclins, are important regulators of the transition between different phases of the cell cycle (EVANS *et al.* 1983; MORGAN 1995; PINES 1991; PINES 1995). Cdks belong to a family of serine/threonine protein kinases and they become activated at stage specific points of the cell cycle. Although the protein levels of Cdks remain constant, levels of their activating cyclins fluctuate throughout the cell cycle in a stage specific manner therefore ensuring stage specific activation of Cdks. Furthermore, important regulatory checkpoints exist throughout the cell cycle (HARTWELL and WEINERT 1989). Recognition of damaged DNA might result in the arrest of cell cycle in Gap phases or suppression of the initiation and/or elongation phases of DNA replication during S phase. As a response to damaged DNA, expression of repair genes can be triggered or, entry into cellular senescence can be promoted if the damage is not repairable (LUKAS *et al.* 2004; MELO and TOCZYSKI 2002).

1.2.1 G1 phase

G1 phase is a gap phase in which the cell is preparing for DNA replication. During G1 phase cells make the decision whether to enter a quiescent, non-dividing state named G0 during which they might differentiate into specialised cells. A combination of Cyclin D with Cdk4 and Cdk6 is important for the entry into G1

phase (SHERR *et al.* 1994). An important substrate of Cdk4/6-Cyclin D complex is the product of retinoblostama tumour suppressor gene (pRb) which upon phosphorylation promotes the release and activation of the transcription factor E2F-1 (BUCHKOVICH *et al.* 1989; COQUERET 2002; KATO *et al.* 1993). When activated, E2F-1 directs transcription of genes such as Cyclin E. Later on during G1 phase, the association of Cyclin E with Cdk2 is necessary for progression into the following S phase (OHTSUBO *et al.* 1995).

DNA damage detected at the G1/S checkpoint results in prevention of the entry into S phase therefore avoiding replication of damaged DNA. G1/S checkpoint is sensitive to induction of p53 levels that is induced in response to DNA damage (KO and PRIVES 1996; LEVINE 1997).

1.2.2 S phase

Synthetic or S phase is the stage of the interphase during which replication of DNA takes place. The association of Cyclin A with Cdk2 is required for S phase progression (GIRARD *et al.* 1991; WALKER and MALLER 1991). In addition to DNA replication, the duplication of centrosomes also takes place during S phase (DOXSEY 2001). Furthermore, the formation of a physical link between sister chromatids by the cohesin complex happens during this phase of the cell cycle (BLOW and DUTTA 2005; BLOW and TANAKA 2005).

The recognition of damaged DNA at S phase checkpoint results in disturbance of DNA replication by interference of the initiation and elongation phases (PAINTER 1986; PAULOVICH and HARTWELL 1995).

1.2.3 G2 phase

G2 is the gap phase before the onset of mitosis. The association of Cyclin B with Cdk1 takes place during late G2 phase and it is involved in the entry to mitosis (ARELLANO and MORENO 1997; KING *et al.* 1994). Furthermore, Cdk1/Cyclin A complex forms during late G2 phase and it is needed for the entry into mitosis. Another important checkpoint, exists at G2/M transition. In case of DNA damage detection, entry into mitosis is mainly prevented via inhibition of Cdk1 (SANCHEZ *et al.* 1997; ZENG *et al.* 1998). Furthermore, separation of centrosomes which form the spindle poles takes place during G2 phase.

1.2.4 Mitosis

Prophase

Prophase is the first stage of mitosis and is characterized by important changes in the cell. Chromosome condensation and the formation of sister chromatids take place during prophase. Kinetochores, which are protein structures involved in the movement of chromosomes during mitosis, start forming at the centromeres (AULT and RIEDER 1994). Several histone phosphorylation events mediate important processes during prophase: phosphorylation of histone H3 by aurora B kinase (ADAMS et al. 2001) leads to unfolding of local chromatin which is likely to contribute to binding of condensin complex (HIRANO 2002). Furthermore, histone H1 gets phosphorylated by Cdk1-CyclinB (SWANK et al. 1997). In addition, microtubules are reorganized and form astral arrays around the centrosomes which facilitates the separation of sister chromatids at later stages of mitosis (POLLARD and EARNSHAW 2007).

Metaphase

At the transition from prophase to metaphase, the break down of nuclear envelope takes place. The important event of metaphase is the formation of the "metaphase plate" which involves attachment of microtubules to kinetochores and is followed by the alignment of all chromosomes in the middle of the spindle poles (POLLARD and EARNSHAW 2007). An important checkpoint called the "spindle checkpoint" ensures the correct alignment of chromosomes at this stage. In case of error detection during the spindle checkpoint, the metaphase-anaphase transition is prevented (AMON 1999).

Anaphase

The onset of anaphase is triggered by a decrease in Cdk1 function due to the degradation of proteins such as Cyclin B and securing, which is promoted by the anaphase-promoting complex/cyclosome (APC/C) function (IRNIGER 2002). During anaphase sister chromatids move towards opposite poles and the spindle poles start separating from each other.

Telophase and Cytokinesis

The separation of sister chromatids, the reformation of nuclear envelopes around segregated chromosomes and decondensation of chromosomes take place during telophase. Furthermore, the partitioning of the cytoplasm called cytokinesis begins during telophase. Cytokinesis in animal cells is triggered by the contraction of a fibrous ring mainly involving actin and myosin, whereas in plant cells the rigid cell wall requires a cell plate formation in the middle of the separated nuclei. The outcome of successful completion of this process is the formation of two identical daughter cells (POLLARD and EARNSHAW 2007).

1.3 Insulin receptor/Target of Rapamycin (InR/TOR) Signalling

Availability of nutrients and growth factors as well as cellular energy levels are major determinant factors that regulate cell growth and metabolism. The Insulin receptor/target of rapamycin (InR/TOR) pathway is the major signalling pathway that links cellular growth and energy homeostasis to such environmental factors. Importantly InR/TOR signalling is an evolutionarily well-conserved pathway that serves a similar function from flies to humans, in nutrient sensing and regulation of growth and metabolism, making it possible the use of model organisms to uncover the mechanism and regulation of this signalling pathway (GREWAL 2009; WULLSCHLEGER *et al.* 2006).

1.3.1 Overview of InR/TOR signalling

A number of phosphorylation events mediate signalling through InR/TOR pathways (Figure 1.5). The initial activation of the pathway starts by binding of insulin or insulin like growth factors (IGF) to insulin receptor (InR) which results in autophosphorylation of the InR (VAN OBBERGHEN *et al.* 2001). The activation of InR by the biding of its ligand leads to recruitment and phosphorylation of key tyrosine residues on insulin receptor substrate (IRS). PI3K binds to phosphorylated IRS which results in conversion of phosphatidylinositol-4,5-phosphate (PIP2) into phosphatidylinositol-3,4,5-phosphate (PIP3). The accumulation of PIP3 is antagonized by the action of the phospholipid dephosphatase and tumour suppressor PTEN, which dephosphorylates PIP3 (SULIS and PARSONS 2003). The important outcome of the accumulation of the lipid second messenger PIP3 is the recruitment of both PDK1 and the serine/threonine kinase Akt near the plasma membrane. Akt is

an important downstream effector of PI3K and it has a pleckstrin homology (PH) domain that allows the binding of PIP3. In fact, the binding of PIP3 to this PH domain and the subsequent recruitment of Akt to the plasma membrane is the rate-limiting step for its activation. PDK1 is the kinase that is responsible for the phosphorylation and the subsequent activation of Akt. The activation of Akt has two important consequences. Firstly, it results in phosphorylation and the subsequent retention of the forkhead transcription factor Foxo in the cytoplasm therefore preventing Foxo accomplishing its role as a transcription factor (DEMONTIS and PERRIMON 2009; KAESTNER *et al.* 2000; KOPS *et al.* 2002). Amongst target genes of Foxo, there are a number of genes involved in control of metabolism (BAKER and THUMMEL 2007). Secondly, Akt activity results in phosphorylation and the subsequent inactivation of TSC2 (tuberous sclerosis complex 2) in response to insulin (CAI *et al.* 2006; GAO and PAN 2001; POTTER *et al.* 2001). TSC2 exists as a heterodimer with TSC1 and TSC1/TSC2 complex acts as an inhibitor of TOR complex 1 (TORC1) in its active form. However the inactivation of TSC1/TSC2 complex promotes the binding of the small GTPase Rheb to TOR therefore resulting in the activation of TORC1 (LONG *et al.* 2005).

At this point it is worth underlining that TOR exists as part of two distinct complexes (BHASKAR and HAY 2007). The signalling cascade summarised above involves upstream regulation of TOR complex 1 (TORC1) which comprises the rapamycin sensitive adaptor protein Raptor making TORC1 subject to the inhibitory action of rapamycin. However, the adaptor protein Rictor that is part of the TOR complex 2 (TORC2) is insensitive to the action of rapamycin (LOEWITH *et al.* 2002). The upstream regulation as well as the downstream effects of TORC2 still remains to

be fully elucidated however there is evidence that shows that Akt is subject to phosphorylation by TORC2 (GUERTIN *et al.* 2006; JACINTO *et al.* 2006; SARBASSOV *et al.* 2005). Furthermore, it was shown that in yeast TORC2 is mainly involved in actin reorganization (JACINTO *et al.* 2004).

The activation of TORC1 has a number of downstream effects that contribute between them to an increase in cell growth and metabolism. TORC1 activity results in phosphorylation of the p70 ribosomal protein S6 kinase and eukaryotic translation initiation factor 4E binding protein (4E-BP) which contributes to an increase in protein synthesis. Ribosome biogenesis, which accounts for a large part of cellular energy consumption, is also increased as a consequence of TORC1 activity (WULLSCHLEGER *et al.* 2006). Furthermore, an important outcome of TORC1 activity is the inhibition of autophagy (SCOTT *et al.* 2004).

Autophagy is the process whereby part of the cytoplasmic content is delivered to lysosomes for degradation. It is a non-selective process of degradation and acts as a very important survival mechanisms during times when nutrients are scarce in the environment (CUERVO 2004; LEVINE and KLIONSKY 2004; MIZUSHIMA and KLIONSKY 2007). The most common trigger for autophagy is nutrient withdrawal and various studies have shown the importance of signalling via InR/TOR pathway during the regulation of autophagy (SCOTT *et al.* 2007; SCOTT *et al.* 2004). Interestingly, mechanisms of autophagic vesicle formation appear to be well conserved from yeast to higher eukaryotes. The important mediator of autophagy is an organelle named the autophagasome. Part of the cytoplasm is engulfed in a double membrane vesicle to form the autophagasome. The outer membrane of the autophagosome later fuses with the endosome and then the

lysosome. The intermediate step during which the autophagosome fuses with the endosome is thought to provide the double membrane vesicle with the necessary machinery to subsequently allow fusion with the lysosome. After fusion with the lysosome, this new organelle is called the autolysosome or the autophagolysosome. The inner membrane and the contents of this vesicle are degraded by the lysosomal hydrolases and the breakdown products are released into the cytosol where they can serve as a nutrient source during starvation (MIZUSHIMA 2007).

The importance of signalling via InR/TOR is reflected by the influence of this pathway in important processes such as control of ageing, metabolism and growth. The involvement of InR/TOR signalling in such a wide range of important cellular processes highlights the importance of elucidating the mechanism of action as well as novel components this pathway.

1.3.2 InR/TOR signalling and ageing

There is increasing evidence suggesting that down-regulation of signalling via InR/TOR pathway delays the aging process, therefore increasing lifespan in a number of organisms including yeast, worms, flies as well as mammals. In yeast, the *tor1*Δ mutant shows extended replicative and chronological life span (KAEBERLEIN *et al.* 2007). Similarly in worm, mutants in worm homologues of TOR and S6K show extended longevity (HANSEN *et al.* 2007). Furthermore in *Drosophila*, mutation of TOR as well as over-expression of TSC1 or TSC2, which act as negative regulators of TOR, lead to a significant life span increase (KAPAHI *et al.* 2004; LUONG *et al.* 2006). Also, the deletion of cells producing *Drosophila* insulin-like peptides (Dilps) results in extension of lifespan (BROUGHTON *et al.* 2005). Interestingly, recent

research carried out in *Drosophila* showed that rapamycin administration to adult flies results in lifespan extension (BJEDOV *et al.*). The analysis of the mechanism of this lifespan extension following rapamycin administration suggested that the increase in longevity acts through alteration in both autophagy and protein translation. Finally, mutation of S6K1 in mice leads to increased longevity suggesting that the effect of InR/TOR signalling on aging is an evolutionarily conserved process (SELMAN *et al.* 2009).

1.3.3 InR/TOR signalling and the control of metabolism

InR/TOR signalling is involved in various aspects of metabolism including lipid metabolism, glucose homeostasis and amino acid biosynthesis. In fact various metabolic disorders, including type 2 diabetes and obesity, were associated with insulin insensitivity highlighting the importance of this pathway for the adequate metabolic function. Research carried out both in mammals and model organisms such as *Drosophila* has been of major importance in uncovering involvement of InR/TOR signalling function in the control of metabolism. For example it was shown that mammalian TORC1 is involved during adipogenesis as rapamycin addition inhibits adipocyte differentiation (KIM and CHEN 2004). Also, S6K mutant mice were found to exhibit reduced levels of adipose tissue and fat accumulation due to increased β oxidation (UM *et al.* 2004). The differentiation of preadipocytes is blocked by constitutive expression of active Foxo1 whereas over-expression of the dominant-negative form of Foxo1 restores adipocyte differentiation of fibroblasts isolated from InR deficient mice (NAKAE *et al.* 2003). In addition, constitutive Foxo

activation in liver and pancreatic β cells was found to cause hyperglycemia (NAKAE *et al.* 2002).

In *Drosophila*, there are seven insulin-like peptides (Dilp1-7) that the complete functions of which still remain to be fully understood (BROGIOLO *et al.* 2001; IKEYA *et al.* 2002). A cluster of median neurosecretory cells located in the *Drosophila* brain named the insulin producing cells (IPCs) are responsible for the secretion of Dilps (BROGIOLO *et al.* 2001; BROUGHTON *et al.* 2005; IKEYA *et al.* 2002). It was shown that *dilp* expression depends on specific nutritional cues like insulin in humans. For example, the expression of *dilp3* and *dilp5* is reduced in response to low carbohydrate levels whereas lowering amino acid levels does not have an affect (COLOMBANI *et al.* 2003; IKEYA *et al.* 2002). Furthermore, ablation of IPCs results in increased levels of glucose as well as in a mild increase in lipid storage therefore suggesting a diabetic phenotype (BROUGHTON *et al.* 2005). These findings therefore highlight the possibility to use *Drosophila* as a powerful genetic model for the study of the mechanisms of diabetes.

Interestingly a novel component of InR/TOR pathway named melted, which has an impact on lipid metabolism, was discovered in a genetic screen carried out in *Drosophila* (TELEMAN *et al.* 2005b). Melted is a protein with a plecstrin homology (PH) domain that appears to be essential for its function. Melted is thought to act upstream of TOR as it was found to bind TSC1 leading therefore to recruitment of TSC1/TSC2 heterodimer near the plasma membrane. Furthermore, Melted is thought to promote phosphorylation of dFoxo and TSC2 by Akt in response to the activation of signalling via InR. Importantly, mutations in *melted* leads to reduced lipid levels without having an affect on sugar levels therefore suggesting its

involvement during lipid metabolism. Melted has homologues in worms, mice and humans suggesting the importance of the elucidation of its function for the studies of InR/TOR involvement during the control of metabolic function.

1.3.4 InR/TOR signalling and growth

As described earlier, signalling via InR/TOR pathway contributes to growth via its downstream effects on processes such as transcription and translation. Genetic analysis of various InR/TOR mutants in *Drosophila* revealed the importance of this pathway during the regulation of body and tissue size. For example, hypomorphic *InR* mutant in *Drosophila* or some heteroallelic combinations of *InR* mutations are characterized by significant reduction in body size that can go down to ~ 50% (BROGIOLO *et al.* 2001; CHEN *et al.* 1996). Similar phenotypes are observed in animals that are mutant for the *Drosophila* insulin receptor substrate chico (BOHNI *et al.* 1999). Mutations in the tumour repressor *Pten* result in an increase in cell size whereas as expected its over-expression leads to a reduction in cell growth (GOBERDHAN *et al.* 1999; SCANGA *et al.* 2000). Furthermore, although mutations in *Drosophila S6K* give rise to viable adults, these flies are significantly reduced in size highlighting that an intact signalling is needed for normal growth (MONTAGNE *et al.* 1999). These examples demonstrate the importance of the use of *Drosophila* as a model system to elucidate the effect of various components of InR/TOR signalling on regulation of cell size.

Importantly, activities of various components of InR/TOR signalling were found altered in a number of human cancers. One of the most striking examples of this is the development of hematomas in a great number of organs in individuals with

mutations in Tsc1/Tsc2 complex (KWIATKOWSKI 2003). Similarly, loss of Pten function as well as an increase of Akt function were identified to be a characteristics of a subset of human cancers (INOKI *et al.* 2005; SANSAL and SELLERS 2004). Therefore, elucidating the exact mechanism by which InR/TOR signalling regulates growth would be an important step towards the identification of the molecular basis of cancer developement.

1.4 *Drosophila* innate immunity

Multicellular organisms have evolved effective immune mechanisms to battle invading pathogens. All metzoans are equipped by an effective innate immune system that involves recognition of the pathogen followed by phagocytosis and synthesis of various antimicrobial peptides targeting elimination of the invader (JANEWAY and MEDZHITOV 2002; MEDZHITOV and JANEWAY 2000). Along with innate immunity the mammalian immune system includes an additional branch of immune response called adaptive immunity. Adaptive immunity involves generation of large repertoire of receptors in the lymphocytes via gene rearrangements. Another important difference between adaptive and innate immune responses is that adaptive immune response is capable of remembering previously encountered pathogen and therefore is characterized by memory. Interestingly it was shown that innate immune response promotes the trigger of an effective adaptive immune response suggesting that both innate and adaptive immune responses work together (FEARON and LOCKSLEY 1996; SCHNARE *et al.* 2001).

Drosophila immune system consists solely of innate immune response. Therefore the use of *Drosophila* as a model system has been very useful to elucidate

pathways and cellular processes involved in the innate immune response. There are two major branches of innate immunity in *Drosophila* involving humoral and cellular immune responses. The important outcome of the humoral immune response is the generation of antimicrobial peptides by the fat body in response to activation of two important pathways: Toll signalling and Immune deficiency (Imd) pathways (HOFFMANN 2003; HOFFMANN and REICHHART 2002). The cellular immune response involves phagocytosis and/or encapsulation of invaders by the action of blood cells (GOVIND 2008; HOFFMANN 2003; HOFFMANN and REICHHART 2002; WILLIAMS 2007). In the following part of this section I will be describing Imd and Toll signalling pathways as mediators of humoral immune response followed by description of *Drosophila* blood cells and their involvement during the cellular immune response.

1.4.1 Toll signalling pathway during humoral immune response in Drosophila

Signalling via Toll receptor is mainly involved in defense against Gram-positive bacterial and fungal infection. Toll receptor activation is triggered by binding of Spaetzle protein which is similar to mammalian neutrotrophins. The binding of Spaetzle to Toll receptor with high affinity is made possible by a proteolytic cascade that is activated as an early response to infection. The resulting mature form of Spaetzle bind to the Toll receptor as a dimer leading therefore to activation of subsequent components of the pathway (Figure 1.6) (DELOTTO and DELOTTO 1998; MIZUGUCHI *et al.* 1998; WEBER *et al.* 2003). The intracytoplasmic domain of Toll receptor interacts with three important proteins: MyD88, Pelle and Tube (HORNG and MEDZHITOV 2001; SUN *et al.* 2002; TAUSZIG-DELAMASURE *et al.*

2002). MyD88 and Tube act as adaptor proteins in this complex whereas Pelle serves a function similar to mammalian interleukin-1 receptor associated kinases (IRAKs). Two important NF-κB transcription factors that are activated in response to Toll activation are Dorsal and Dorsal-related immunity factor (DIF) (IP *et al.* 1993; MANFRUELLI *et al.* 1999; MENG *et al.* 1999; RUTSCHMANN *et al.* 2000a). DIF is activated solely in adults (IP *et al.* 1993) whereas Dorsal can be activated both in adults and larvae in response to Toll activation (MANFRUELLI *et al.* 1999). In the absence of immune stimulus, Dorsal and DIF are held in the cytoplasm by their association with another protein named Cactus. Their activation and subsequent nuclear translocation are achieved by the phosphorylation and proteasomic degradation of Cactus (FERNANDEZ *et al.* 2001; NICOLAS *et al.* 1998). The exact details and mechanistics of this activation process still remain to be fully understood. The movement of Dorsal and/or DIF into the nucleus leads to transcriptional activation of antimicrobial peptide (AMP) gene expression. Two important AMPs that are expressed in response to Toll activation are Drosomycin (LEMAITRE *et al.* 1995b) and Defensin (BRENNAN *et al.* 2007). Drosomycin is known to be involved in fight against fungal infection whereas Defensin acts against Gram-positive bacteria.

Toll has eight additional homologues in the *Drosophila* genome (Toll-2 to Toll-9) which all have various developmental roles (KAMBRIS *et al.* 2002; TAUSZIG *et al.* 2000). Interestingly, Toll is the only one that has been identified to have an additional role during the humoral immune response in *Drosophila*. Furthermore unlike mammalian Toll-like receptors (TLRs), the expression of Toll receptors in

Drosophila is not restricted to only immune responsive tissues (KAMBRIS *et al.* 2002; TAUSZIG *et al.* 2000).

As described earlier the interaction of a cleaved form of Spaetzle, rather than a pathogenic inducer with Toll, results in activation of signalling. However it is thought that the recognition of pathogenic inducers are achieved by a number of circulating recognition proteins called peptidoglycan-recognition proteins (PGRPs) and Gram-negative-binding proteins (GNBPs) (GOBERT *et al.* 2003; MICHEL *et al.* 2001). These proteins circulating in the blood are likely to recognize Gram-positive bacteria activating the proteolytic cascade that results in cleavage of Spaetzle. Interestingly, mutations in two members of these protein families (PGRP-A and GNBP-1) result in increased sensitivity to Gram-positive bacterial infection underlining their importance during immune response to Gram-positive bacterial infection (GOBERT *et al.* 2003; MICHEL *et al.* 2001). Furthermore, a circulating protease called Persephone was identified to be involved in cleavage of Spaetzle in response to fungal infection (LIGOXYGAKIS *et al.* 2002).

1.4.2 Imd signalling pathway during humoral immune response in Drosophila

Signalling via Imd pathway is involved mainly, although not solely, in the fight against Gram-negative bacterial infection. Imd is a 25 kDa protein that shows strong similarities to mammalian TNF-receptor-interactor protein (GEORGEL *et al.* 2001). Imd interacts with three important downstream components (Figure 1.7). The first one of these downstream players is *Drosophila* FADD which directly associates and forms a complex with Imd (LEULIER *et al.* 2002; NAITZA *et al.* 2002). TGF-β-activated kinase 1 (TAK1) is a MAP kinase that acts downstream of

Imd/FADD complex (VIDAL *et al.* 2001). The third downstream component is the complex that comprises *Drosophila* homologues of IKK-β and IKK-γ/NEMO (RUTSCHMANN *et al.* 2000b; SILVERMAN *et al.* 2000). The NF-κB transcription factor involved in Imd pathway is called Relish. The activation and subsequent nuclear translocation of Relish requires the endoproteolytic cleavage of its own inhibitory ankyrin-repeat sequences (STOVEN *et al.* 2000). Activation of the IKK-β/IKK-γ complex by TAK1 activity leads to phosphorylation of Relish and it is necessary for its cleavage (SILVERMAN *et al.* 2000). Furthermore *Drosophila* caspase-8 homologue DREDD, that can bind both to FADD and Relish, was identified to directly cleave Relish (LEULIER *et al.* 2000; SILVERMAN *et al.* 2000). Activation of Relish leads to its tranlocation into the nucleus where it can activate the expression of various AMPs including Diptericins, Drosocins and Attacins (GEORGEL *et al.* 1993; LEMAITRE *et al.* 1995a; LEVASHINA *et al.* 1998).

An interesting finding came from the sophisticated microarray analysis that suggested involvement of TAK1 activity in promoting signalling through c-jun N-terminal kinase (JNK) apart from activating Relish transcription factor (BOUTROS *et al.* 2002). According to these findings the branching downstream TAK1 leads to activation of JNK as well as Relish at the same time in response to stimulation of Imd pathway, allowing therefore the coordination of antibacterial defence and tissue repair.

Interestingly, another member of the PGRP family called PGRP-LC is an important protein involved in recognition of Gram-negative bacteria in *Drosophila* (CHOE *et al.* 2002; GOTTAR *et al.* 2002). Unlike blood borne PGRP-SA involved in Toll activation, PGRP-LC is a transmembrane protein. Mutations in PGRP-LC

result in mild phenotypes suggesting that it is likely to be acting together with other components of a complex for the recognition of Gram-negative bacterial infection.

1.4.3 **Drosophila** *blood cells and cellular immunity*

Blood cells or hemocytes are the mediators of cellular immune response in *Drosophila*. Cellular immune response mainly consists of phagocytosis and encapsulation during which hemocytes act as key players of immune surveillance. Hemocytes can be subdivided into three subclasses, including plasmatocytes, lamellocytes and crystal cells, based on their morphological differences as well as distinct cellular functions (EVANS *et al.* 2003).

Plasmatocytes are round cells that appear around 8-10 μm in size and they form the most abundant class of hemocytes (LANOT *et al.* 2001; LEBESTKY *et al.* 2000). The primary function of plasmatocytes is phagocytosis, during which they engulf apoptotic cells and cell debris as well as invading pathogens contributing therefore to cellular immune response (LANOT *et al.* 2001; RIZKI and RIZKI 1978; TEPASS *et al.* 1994). So far, a limited number of genes have been identified which are implicated in plasmatocyte mediated phagocytosis. Amongst these genes involved in pathogen recognition by plasmatocytes are scavenger receptor (dS-CI) (RAMET *et al.* 2001) and PGRP-LC (RAMET *et al.* 2002b) that as indicated earlier are also involved during humoral immune response. Another important protein that was shown to be involved in bacterial binding by plasmatocytes is the Ig superfamily receptor Down syndrome cell adhesion molecule (Dscam) (WATSON *et al.* 2005). A great number of isoforms that can potentially be generated through alternative splicing of Dscam (theoretically around 38,000) suggests the possibility that Dscam

alone could be able to provide a high number of receptors that are involved in pathogen recognition by plasmatocytes (WATSON *et al.* 2005).

It was shown previously that the absence of plasmatocyte mediated phagocytosis results in sensitivity to pathogens. Apart from their involvement in cellular immune response as professional phagocytes, plasmatocytes also produce AMPs contributing therefore to humoral immunity (DIMARCQ *et al.* 1997; SAMAKOVLIS *et al.* 1990).

The second class of hemocytes are crystal cells that are around 10-12 μm in size and are characterized by the crystalline inclusions they contain giving them therefore their name (LANOT *et al.* 2001). Crystal cells are involved in melanisation response and they are thought to provide phenoloxidase activity (DE GREGORIO *et al.* 2002a; RAMET *et al.* 2002a; RIZKI *et al.* 1985). Phenoloxidase activity converts phenol to quinone which polymerizes as melanin (CHOSA *et al.* 1997; DE GREGORIO *et al.* 2002a). Importantly melanin, as well as nitric oxide and hydrogen peroxide released by this reaction are toxic to pathogens.

The third class of hemocytes are lamellocytes which are flat, large cells of around 15-40 μm in size (NAPPI 1975; RIZKI and RIZKI 1992). Lamellocytes are easily morphologically distinguishable from other hemocyte subtypes by their large size. Lamellocytes are important players involved in the encapsulation of pathogens that are too large to be engulfed by phagocytosis. For example their differentiation in the hemolymph is triggered upon parasitisation by the wasp *Leptopolina boulardi* whereas bacterial invasion does not illicit this response (CARTON and NAPPI 2001; RIZKI and RIZKI 1992).

Encapsulation response in *Drosophila* involves all three subtypes of hemocytes. The entry of the wasp egg into the hemocoel leads to the release of plasmatocytes from the lymph gland (LANOT *et al.* 2001) as well as from sessile population of plasmatocytes located under the larval cuticle (ZETTERVALL *et al.* 2004) followed by the switch of plasmatocytes from non-adhesive to adhesive form. Plasmatocytes then start to adhere and spread at the surface of the wasp eggs (RUSSO *et al.* 1996; WILLIAMS *et al.* 2005) and this spreading step requires the action of the small GTPase Rac2 (WILLIAMS *et al.* 2005). In the mean time, lamellocyte differentiation takes place (CARTON and NAPPI 1997; MEISTER and LAGUEUX 2003). Lammellocytes start attaching to a plasmatocyte surrounded wasp egg allowing the wasp egg to be isolated from the hemocoel (RUSSO *et al.* 1996). The attachement of lamellocytes requires Rac2 (WILLIAMS *et al.* 2005) and β_2-integrin Myospehroid (IRVING *et al.* 2005) action. Therefore, it is likely that various cell adherence and cell shape change events are involved during the encapsulation process. Finally, melanisation reaction triggered by crystal cells takes place and causes the capsule to be covered by a brown layer (RUSSO *et al.* 1996).

Mediators of both humoral and cellular immunity described in this section contribute to innate immune response in *Drosophila* providing therefore an efficient protection against a wide range of pathogenic invaders.

1.5 Background of Poly

The *poly* mutation was isolated in a P-element mutagenesis screen that aimed to generate a large collection of single P-element induced mutations in *Drosophila* (KARPEN and SPRADLING 1992). Prof. Margarete Heck took part in this screen

carried out in 1989 during her post-doctoral training. Following isolation by Prof. Margarete Heck, members of the Heck lab carried out phenotypic characterization of the *poly* mutation over the next years. The gene sequence was identified in 1995.

poly^{05137} is a late larval lethal mutation and the P-element insertion that led to the *poly*^{05137} allele was mapped in the only intron of the CG9829 gene, localising to 87E7-8 (Figure 1.8.A). The *poly*^{05137} insertion leads to an absence of *poly* mRNA as assessed by Northern blotting and RT-PCR, and Poly protein revealed by immunoblotting. However, we were able to show that the expression of the overlapping CG8790 gene was not affected by the P-element insertion in the *poly*^{05137} allele as revealed by RT-PCR analysis (Figure 1.8.B-D). Therefore, we concluded that *poly*^{05137} allele was a loss of function mutation. Furthermore, successful rescue of *poly*^{05137} lethality was achieved during the rescue experiment carried out by Dr. Sharron Vass by using a Gal4 driver under the control of the heatshock promoter to direct expression of a *UAS-poly* transgene during larval development.

Expression analysis of the *poly* gene revealed high levels of mRNA and protein in the first 4 hours of embryogenesis, suggesting maternal loading of the *poly* mRNA, and possibly protein, into oocytes. In the following 16 hours, Poly protein levels decreased but were still higher than those observed throughout the reminder of development (Figure 1.9). Therefore, *poly* expression seems to be strongest in embryos but continues throughout the course of development.

poly mutant animals are characterized by a number of interesting phenotypic features. When homozygous mutant larvae were examined, the morphology of various tissues appeared abnormal: the brain, ring gland, salivary glands and

imaginal discs were reduced in size compared to heterozygous siblings and wild type animals, suggesting a potential cell growth and/or proliferation defect (Figure 1.10.A). At that time, research carried out in the Heck laboratory was focused on control of cell cycle progression in *Drosophila*. This is the reason why further characterization of Poly was considered to be important and relevant.

Mutant larval neuroblasts were characterized by abnormally shaped nuclei (Figure 1.10.B), though mitotic figures, evident until 9 days of development, appeared normal. These lobulated nuclei resemble the nuclei of mammalian polymorphonuclear leukocytes, thus suggesting the name *poly*.

A careful investigation of the developmental timing by Dr. Sharron Vass revealed that *poly* mutants show delayed development. Mutants animals reach early third instar larval stage later than their heterozygous siblings and wild type larvae. This developmental delay can go up to 24-48 hours at 25°C. More interestingly, mutant larvae exhibit extended third instar larval lives that can go up to 21 days. However, *poly* larvae die before reaching the pupation suggesting that *poly* gene product is essential for reaching adulthood.

During the lengthened third instar larval phase, melanotic masses appeared in the hemolymph of *poly* mutants, increasing in size and number with time (Figure 1.10.C). Numerous melanotic masses can be detected in the body cavity of *poly* mutant larvae during the extended third instar developmental stage.

Poly gene product is a 251 amino acid long protein with no obvious functional motifs. However, Poly appears to be evolutionarily conserved in higher eukaryotes. Importantly, Poly also has a human homologue (*Hs*Poly) (Figure 1.11).

As no obvious motifs were apparent in the Poly protein sequence, database searches and phylogenetic analysis were employed to investigate which other proteins appeared similar. Analysis carried out by a former post-doctoral fellow from the Heck laboratory, Dr. Neville Cobbe, identified the orthologue of Poly in *Saccharomyces cerevisiae* as the Elp6 protein (Figure 1.12.A), part of the Elongator complex that, in association with the RNA polymerase II holoenzyme, is responsible for transcriptional elongation (KROGAN and GREENBLATT 2001; WINKLER *et al.* 2001). Although, the Elongator holocomplex appears to be conserved in composition and function between yeast, humans and *Arabidopsis* (HAWKES *et al.* 2002; NELISSEN *et al.* 2005), there is no *in vivo* evidence yet for the involvement of Poly during transcriptional elongation a part from the phylogenetic analysis that suggested Elp6 as the distant homologue of Poly in yeast.

In order to predict the protein structure of Poly, Dr. Neville Cobbe carried out extensive database searches for more distant homologues of Poly and identified several proteins for which structural data were available, including KaiC from cyanobacteria (PATTANAYEK *et al.* 2004), an archaeal KaiC-like protein (KANG *et al.* 2009) and RadB proteins (AKIBA *et al.* 2005), each of which are members of the RecA/Rad51/DCM1 superfamily of ATP-dependent recombinases (LEIPE *et al.* 2000; LIN *et al.* 2006). All these proteins appeared to display a similar overall confirmation with a core of several beta sheets surrounded by alpha helices thereby allowing a model of the protein structure to be developed for Poly (Figure 1.12.B).

1.6. Aims of this Ph.D. project

Poly is a novel, essential and more importantly, evolutionarily conserved protein. Furthermore, as previously described, mutation in *poly* results in an intriguing phenotype characterized by pleiotropic effects in *Drosophila*. All these features make Poly an interesting as well as important protein for which cellular function deserved to be elucidated.

When I started my Ph.D. project in the Heck Laboratory, although much of the phenotypic characterization of the mutant had already been performed, the pathways and cellular processes that Poly might be involved in were still unknown. Therefore the aim of my project was to identify at least some of the cellular processes that Poly might be involved in.

Taking into consideration observed mutant phenotype, our first hypothesis for the function of Poly was its potential involvement during cell cycle progression. Therefore I investigated this by carrying out a mosaic clonal analysis in *Drosophila* eye imaginal discs described in Chapter 3.

In the meantime, we wanted to adopt an unbiased approach to identify protein interactors of Poly as this would give us indications about what cellular processes Poly might be involved in. Interestingly, the insulin receptor was identified as a protein interactor of Poly. I describe the identification of insulin receptor as a protein interactor of Poly and the characterization of the consequences of the interaction of Poly with insulin receptor in Chapters 4 and 5.

Again, taking into consideration the *poly* mutant phenotype, I investigated the involvement of Poly during the *Drosophila* innate immune response. I present these results in Chapter 6.

Finally, a minor part of my project summarized in Chapter 7, consisted of the generation of reagents such as antibodies and constructs for the study of the human homologue of Poly as ultimately much of the research on Poly will be carried out in higher eukaryotic systems.

Chapter 2: Material and Methods

2.1 Maintenance of *Drosophila* stocks

Flies were propagated in plastic bottles or vials containing 'Dundee' maize medium (recipe below). To fatten larvae before larval dissection, yeast paste diluted with water was placed in the vial. Flies were usually kept at room temperature or 25˚C with tipping into a new vial once every 10 days or at 18˚C with tipping into a new vial once every month. Genetic crosses were performed using virgin female flies collected as soon as possible after eclosion. Fly stocks used in this thesis are listed in Table 2.1.

Dundee maize medium: 14 litres water, 150 g agar, 1100 g glucose, 620g brewer's yeast, 1000 g maize meal, 80 g dried yeast, 38 g nipagin (p-hydroxy benzoic acid methyl ester), 380 ml absolute alcohol, 45 ml propionic acid

Table 2.1 Drosophila Stocks used in this study

Strain	Source
Canton S	Bloomington *Drosophila* Stock Center (USA)
poly^{05137}/TM6B	Heck laboratory
FRT82Bpoly^{05137}/TM6B	Heck laboratory
InR^{05545}/TM6B	Bloomington *Drosophila* Stock Center (USA)
Akt^{04226}/TM6B	Bloomington *Drosophila* Stock Center (USA)
S6K^{07084}/TM6B	Bloomington *Drosophila* Stock Center (USA)
UAS-GFP	Bloomington *Drosophila* Stock Center (USA)
Hml-Gal4	Dr. Michael Williams, University of Aberdeen
GMR-Gal4,UAS-poly	Heck laboratory
Cg-Gal4	Bloomington *Drosophila* Stock Center (USA)
UAS-InR^{A1325D}	Bloomington *Drosophila* Stock Center (USA)
FRT82B	Bloomington *Drosophila* Stock Center (USA)
FRT82BlacZ/TM6B	Bloomington *Drosophila* Stock Center (USA)
FRT82BGFP	Bloomington *Drosophila* Stock Center (USA)
UAS-poly	Heck laboratory

2.2 Fly crosses

Virgin females (about 5-10) from one stock were collected and crossed with 2-3 males from the desired stock. Flies were left to mate and lay eggs for 3 days. The parents were removed from the vials and the progeny were allowed to eclose in the same vial. Crosses were carried out at 18, 25 or 27˚C according to the requirements of the experiment.

2.3 Commonly used reagents and buffers

Aprotinin

Stock at 1.4 mg/ml in 0.9% NaCl and 0.9% benzyl alcohol, used at 1.4 µg/ml (Calbiochem).

BSA

Bovine Serum Albumin, 30% stock solution (Sigma, A3299).

CLAP

1 mg/ml chymostatin, 1 mg/ml leupeptin, 1 mg/ml antipain, 1 mg/ml pepstatin A (Sigma) in DMSO (dimethyl sulfoxide).

Coomassie Brilliant Blue Stain

0.5% Coomassie Blue (Sigma) in 100% methanol.

Coomassie Blue Stain Diluent

35% methanol, 14% acetic acid.

Coomassie Blue Fast Destain

35% methanol, 10% acetic acid.

Coomassie Blue Slow Destain

10% methanol, 7% acetic acid.

DAPI

4',6-diamidino-2-phenylindole (Sigma), stock solution at 1 mg/ml in dH_2O, stored at –20˚C. Used at 0.1 μg/ml (1:10,000 dilution) unless otherwise stated.

DTT

Stock solution at 1M dithiothreitol (Fisher) in dH_2O stored at –20˚C.

EDTA

Ethylenediamine-N,N,N',N'-tetraacetic acid, Stock solution 0.5 M solution in dH_2O, pH 8.0.

Ephrussi-Beadle Ringer's solution (EBR) (10X)

1.3 M NaCl, 47 mM KCl, 19 mM $CaCl_2$, 100 mM HEPES, pH 6.9.

Ethidium Bromide (EtBr)

Stock solution at 10 mg/ml in dH_2O, used at 300 ng/ml (Sigma).

Formaldehyde

16% Formaldehyde ampules (methanol free) (TAAB, F017).

Immunoblot stripping solution

100 mM β-mercaptoethanol, 2% SDS, 62.5 mM Tris, pH 6.7.

LB (Luria-Bertrani broth)

1% Bacto-tryptone, 0.5% Bacto-yeast extract, 1% NaCl, pH 7.4.

Molecular weight markers

SeeBlue Plus2 prestained standard for proteins (Invitrogen, LC5925).

100 kb DNA ladder (Promega, G210A).

1 kb DNA ladder (Promega, G571A).

MOPS SDS-PAGE electrophoresis buffer (20X)

1 M 3-(N-morpholino) propane sulphonic acid, 1 M Tris base, 2% SDS, 20.5 mM EDTA, pH 7.7.

Mowiol mounting solution

10% Mowiol 4-88 (Calbiochem), 20% Glycerol in PBS.

Phosphate Buffered Saline (PBS) (Dulbecco's) (10X)

1.37 M NaCl, 26.8 mM KCl, 14.7 mM KH_2PO_4, 64.6 mM Na_2HPO_4, pH 7.4.

PBS-T

Dulbecco's PBS with 0.1% TritonX-100 (diluted from 10% w/v stock solution of TritonX-100 in water).

PMSF (Phenylmethylsulfonyl fluoride)

0.1 M stock solution in ethanol, used at 1 mM concentration (Sigma).

RIPA (10X)

20 mM Tris-HCl (pH 7,5), 150 mM NaCl, 1 mM Na_2EDTA, 1 mM EGTA, 1%NP-40, 1% sodium deoxycholate, 2.5 sodium pyrophosphate, 1mM β-glyceriohosphate, 1mM Na_3VO_4, 1 μg/ml leupeptin.

TBS (Tris-buffered saline) (1X)

137 mM NaCl, 20 mM Tris base, pH 7.6 (with HCl).

TBS-T

TBS with 0.05% Tween-20.

TAE (1X)

40 mM Tris-acetate, 1 mM EDTA, pH 8.0.

TE (1X)

10 mM Tris-HCl, 1 mM EDTA, pH 8.

Towbin buffer (protein transfer solution)

25 mM Tris (Sigma 7-9, code-T1378), 20% methanol, 250 mM Glycine (Sigma) 0.1% SDS.

3X SDS-PAGE sample buffer

6% SDS, 150 mM upper buffer (0.5 M trizma-base, pH 6.8), 30% Glycerol, 0.03% Bromophenol blue, 6 mM EDTA.

5X loading dye for DNA agarose gels

17.5% Ficoll 400, 100 mM EDTA, pH 8.0, 2.5% SDS, 0.25% Bromophenol blue, 0.25% Xylene cyanol FF.

2.4 Plasmid DNA isolation

For small scale DNA isolation, one colony from a selective plate was inoculated in 3 ml of LB with appropriate antibiotic and bacterial cells were cultured overnight at 37°C with shaking. One ml of this culture was collected for plasmid DNA isolation. Small scale plasmid DNA extraction was performed using QIAprep Spin®MiniPrep Kit (Qiagen, 27106), according to manufacturer's instructions. The large scale isolation (up to 50 ml) was performed using Qiafilter® Plasmid Maxi Kit (Qiagen, 12243), according to the manufacturer's instructions.

To confirm positive constructs, restriction enzyme digestion of plasmids was performed in 1.5 ml eppendorf tubes as follows: a mixture including 5-8 µl of plasmid DNA (mini preps), 1 µl of 10X buffer (New England Biolabs), 1 µl of restriction enzyme (New England Biolabs) was prepared and the volume was brought to 10 µl with sterile deionized water. Restriction digestion was normally performed at 37°C for 2-4 hours. The size of the fragments was determined by electropheresing a small amount of the digest on agarose gel along with a DNA marker ladder.

2.5 Agarose gel electroporesis

Agarose gels were usually prepared at a concentration of 1% SeaKem LE Agarose (BioWhittaker Molecular Applications) containing 300 ng/ml of ethidium bromide in 1X TAE buffer. Gels were electrophoresed in electrophoresis tanks (Owl Scientific Plastics) in 1X TAE buffer. Different gel sizes were used according to the number of samples and/or the degree of separation required. Gel size: mini (50 ml, run at 70-80 V), midi (100 ml, run at 100 V) and maxi (300 ml, run at 150 V).

2.6 Purification of DNA from agarose gels

Electrophoresis was performed in low-melt agarose gels (MacroSieve LM agarose, Flowgen) containing 300 ng/ml ethidium bromide. 1X TAE buffer was used and the desired bands were excised under UV illumination using a glass cover slip and placed into 1.5 ml Eppendorf tubes. DNA was purified from the agarose gel by using Qiagen's QIAquick® Gel Extraction Kit as per manufacturer's instructions (Qiagen, 28704).

2.7 Purification of DNA from PCR reactions

DNA products from PCR reactions were usually purified using the QIAquick® PCR Purification Kit (Qiagen, 28704). The entire PCR reaction was used and 5 volumes of the SpinBind reagent were added. The DNA was finally purified using the Spin Filter columns by following the manufacturer's instructions and the DNA was eluted in 25 µl of elution buffer.

2.8 Amplification of plasmid DNA by PCR

PCR reactions were performed in a 50 µl volume containing 500 nM of each forward and reverse primer, 1.5 mM of $MgCl_2$, 200 µM of each dNTP, 100 ng of plasmid DNA and 1 µl Expand High Fidelity enzyme (3.5 U/µl, Roche, 11732650001). PCR reactions were performed in a Biometra Personal Cycler according to the following protocol: a) 95°C for 5 minutes, b) 95°C for 30 seconds, c) 55°C-58°C for 30 seconds, d) 72°C for 2-4 minutes (time is dependent on the size of the product designed), (step b-d were repeated for 30 cycles), 72°C for 7 minutes and eventually held at 4°C.

2.9 Ligations

All ligations were performed using T4 DNA ligase from Promega or New England Biolabs with appropriate reaction buffer at 16-18˚C overnight. An insert:vector molar ratio of 3:1 was routinely used.

2.10 Sequencing of DNA samples from plasmids

Sequencing reactions were performed using 250-500 ng of template DNA in conjunction with 3.2 pmol of the appropriate primer and 4 µl of Big Dye terminator cycle sequencing kit version 3.1 (Perkin Elmer, Applied Biosystems), in a total reaction volume of 20 µl. The reactions were performed in a Biometra Personal Cycler according to the following protocol: a) 95°C for 5 minutes, b) 95°C for 30 seconds, c) 55°C for 15 seconds, d) 60°C for 4 minutes (b-d were repeated for 25 cycles), and eventually held at 4°C.

The reactions were then transferred to 0.2 ml tubes and taken to the University of Edinburgh Sequencing facility at Ashworth building for loading onto an ABI prism sequencer. Primers used in sequencing reactions are listed in Table 2.2.

Table 2.2 Primers used for sequencing of the constructs in Chapter 7

Primer name	Primer sequence
GFP-C1F	5'-CCAACGAGAAGCGCGATCAC-3'
GFP-C1R	5'-GCAACTAAAACCTCTACAAATGTGG-3'
GFP-N1 PN1	5'-ATGGGCGGTAGGCGTGTA-3'
GFN1 PN13	5'-TACGTCGCCGTCAGCTC-3'

2.11 RNA extraction

2.11.1 RNA extraction from larvae

RNA from larvae was extracted using RNeasy ® Mini Kit (Qiagen, 74104) according to manufacturer's instructions. The equivalent of 5 wild type larvae were collected in RNA*later* (Qiagen, 76104) to stabilize larval tissue. The larvae were then transferred to 350 μl of RLT buffer containing 3.5 μl of β-mercaptoethanol and homogenised using a hand pestle and then the mixture was transferred into a QIAshredder spin column, followed by centrifugation for 2 minutes. 350 μl of 70% ethanol was added to homogenised lysate. After mixing well by pipetting, 700 μl of the mixture was transferred to an RNeasy spin column and centrifuged for 15 seconds. The column was then washed twice with 500 μl of RPE buffer, followed by

centrifuging for 1 minute after each addition. Finally, 50 µl of the RNase-free water was added to the column to elute RNA.

2.11.2 RNA extraction from adult flies

Around 8-10 adult flies were homogenized in 600 µl Trizol (Invitrogen, 15596018) by using a mortar and pestle chilled on dry ice and homogenates were transferred to room temperature for 5 minutes. 120 µl of chloroform was added to 600 µl of homogenate. Tubes were vortexed for 15 seconds and left at room temperature for 3 minutes. Samples were centrifuged at 12,000 rpm for 15 minutes at 4°C. The aqueous phase was transferred to fresh tubes and 8 µl of RNA MATRIX® (Anachem, 1007204) was added. Samples were vortexed and agitated for 5 minutes followed by centrifugation at 12,000 rpm for 1 minute to obtain a pellet. The supernatant was removed and 300 µl of wash buffer was added. The pellet was resuspended in RNA MATRIX® wash buffer (Anachem, 1007203) and samples then centrifuged at 12,000 rpm for 1 minute and the washing step was repeated twice. After the final wash step the supernatant was discarded and the pellet was resuspended in 20 µl RNAse free water. Samples were incubated at 60°C for 12 minutes followed by a centrifugation at 12,000 rpm for 1 minute. The supernatant containing the isolated RNA was transferred to a separate fresh tube for use in subsequent experiments.

2.12 RT-PCR reaction

RT-PCR reactions were performed using Superscript™III reverse transcriptase (Invitrogen, 18080044) in 20 μl reactions. The reactions contained 1 μg of RNA, 1 μl of 150 ng/μl random hexamers, 1 μl of each dNTP (10 mM stocks) and 1 μl of DEPC water. This mixture was incubated at 65°C for 5 minutes and placed on ice for 1 minute. Then 4 μl of 5X first strand buffer, 1 μl of 0.1M DTT, 1 μl of RNase out (40 U/μl) and 1 μl of Superscript™III reverse transcriptase (200 U/μl) was added to the mixture and the reactions were performed in the Biometra Personal Cycler according to the following protocol: 50°C for 60 minutes and then 70°C for 15 minutes. The cDNA was then ready to serve as template for PCR or quantitative PCR (qPCR) reactions.

2.13 PCR reaction on cDNA and genomic DNA

PCR reactions to amplify fragments of cDNA and genomic DNA were performed by the Taq DNA polymerase (Roche, 11146173001). Each 25 μl reaction contained 800 nM of forward and reverse primer, 1.5 mM of $MgCl_2$, 400 μM of each dNTP, 2 μl of DNA template and 0.2 μl of Taq DNA polymerase (5 U/μl). PCR reactions were performed in the Biometra Personal Cycler according to the following protocol: a) 95°C for 5 minutes, b) 95°C for 30 seconds, c) 55°C for 30 seconds, d) 72°C for 45 seconds (b-d were repeated for 28 or 30 cycles), 72°C for 7 minutes and subsequently held on 4°C. Table 2.3 of primers used in this thesis.

Table 2.3 Primers used for PCR reactions on genomic DNA and cDNA described in Chapter 3 and 4 respectively

Primer	Primer sequence	Product size
Dm rp49F	5'-AGGGGTATCGACAACAGAGTG-3'	122 bp
Dm rp49R	5'-CACCAGGAACTTCTTGAATC-3'	
Poly F	5'-AAGTGAATCCCTTGCCACCA-3'	301 bp
Poly R	5'-CCCCTGGAAAATGTTCGTATT-3'	
FRT F	5'-GCTTTGAAGTTCCTATTCCGAA-3'	408 bp
FRT R	5'-CAGGAAACAGCTATGACCATG-3'	
P(z)	5'-CGACGGGACCACCTTATGTTAT-3'	210bp
Poly-intron	5'-AGTGTTTTGGCACTGGGACT-3'	

2.14 Quantification of mRNA using real-time PCR

qPCR was performed using the LightCycler® 480 System and the LightCycler® 480 probes Master kit (Roche, 04707494001). Primers and probes used were designed by Universal Probe Library Assay Design Center (https://www.roche-applied-science.com/sis/rtpcr/upl/index.jsp?id=uplct_000000) by entering the CG number of the corresponding gene. The PCR mix was added to 2.2 μl of water, 0.2 μl of 100 μM forward and reverse primer mix, 0.1 μl of appropriate Hydrolysis Probe and 5 μl of the probe master mix. 7.5 μl reaction mix was loaded into LightCycler® 480 Multiwell plate (Roche, 04729749001) and 2.5 μl of the cDNA (diluted at 1:10) added to each well. qPCR reactions were performed with following steps: Pre-incubation at 95°C for 10 seconds, 55°C for 15 seconds, 72°C for 1 second, the last three steps were repeated 60 cycles and subsequently reactions

were cooled at 4°C for 10 seconds. Table 2.3 is the list of the primers and probes used in this thesis.

Table 2.4 Primers and probes used for qPCR reactions described in Chapter 4 and 6

Gene ID	Primers	Primer sequence	Probe #
4E-BP	4E-BPF	5'-CCAGATGCCCGAGGTGTA-3'	22
	4E-BPR	5'-AGCCCGCTGGTAGATAAGTTT-3'	
AttacinA	attAF	5'-CACAATGTGGTGGGTCAGG-3'	149
	attAR	5'-GGCACCATGACCAGCATT-3'	
Relish	relF	5'-CCCACAAACAGCTAAGGACC-3'	94
	relR	5'-TAAAGGCCTCAAAGCAGAGC-3'	
Diptericin	dptF	5'-GGGGATTACCAAAGCTTCA-3'	151
	dptR	5'-TCAACTCAATTTGGCCATTCT-3'	
Actin5C	Actin5CF	5'-AGACACCAAACCGAAAGACTTAAT-3'	132
	Actin5CR	5'-ACATGCCAGAGCCGTTGT-3'	

2.15 Extraction of genomic DNA

6-7 flies were homogenized in 120 μl lysis buffer (100 mM Tris pH 9, 100 mM EDTA, 1% SDS) using a hand held pestle in 1.5 ml eppendorf tubes. Lysates were incubated at 70°C for 30 minutes. 75 μl of 8M potassium acetate was added and then samples incubated for 30 minutes on ice. 500 μl of phenol/chlorofom (1:1) was added and the sample was vortexed for 30 seconds. The lysate was centrifuged for 5 minutes at 13,000 rpm and the supernatant transferred into a fresh tube with 1 ml of ethanol. The samples were left at room temperature for 4 hours followed by centrifugation at 13,000 rpm to pellet the DNA. Pellets were washed with 70%

ethanol and centrifuged. The liquid was removed from the tube and the samples air-dried. 50 μl of nuclease free water was added to the tube for re-suspension of DNA.

2.16 Cloning of HsPoly vectors for transfection into human cells

DNA fragments encoding full length HsPoly coding sequence were generated by PCR from cDNA clones and inserted in-frame into pEGFP-N1 or pEGFP-C1 (Clontech) vectors. The following primers were used to generate HsPoly sequence for expression in human cells.

Table 2.5 Primers used for cloning HsPoly into GFP constructs described in Chapter 6

Primer name	Primer sequence
HsPolyGFPC1F	5'-GAAGATCTTCTATGTTCGTGGAACTTAATAAC-3'
HsPolyGFPC1R	5'-GGAATTCCTCACAGAACAGCAGGAGACAT-3'
HsPolyGFPN1 F	5'-GAAGATCTATGTTCGTGGAACTTAATAAC-3'
HsPolyGFPN1 R	5'-CGGAATTCCGTCACAGAACAGCAGGAGACAT-3'

2.17 Transfection of A375 cells with HsPoly constructs

Transfections were performed with lipofectamine™2000 (Invitrogen, 11668-019) according to manufacturer's protocol. The day before transfection, 3-4 x 10^5 A375 cells were seeded in DMEM containng 10% FBS in 6 well plates and cultured to 90% confluence. Samples for transfection were prepared as follows: 4 μg of plasmid DNA in 10 μl of lipofectamine 2000 was added to 250 μl of OPTI-MEM® (Gibco, 11058) in distinct 1.5 ml eppendorf tubes and the mixtures were incubated at

room temperature for 5 minutes. After incubation, DNA and lipofectamine 2000 solution were mixed together and incubated for 15 minutes at room temperature. The 500 µl mixture was added to a well containing pre-seeded cells and 1.5 ml of OPTI-MEM®. The cells were incubated at 37°C in a CO_2 incubator for 4 hours and then the OPTI-MEM® was exchanged for DMEM containing 10% FBS.

2.18 Preparation of protein extracts for immunoblotting

2.18.1 Preparation of larval extracts for immunoblotting

15-20 wandering 3rd instar larvae of the appropriate genotype were removed from culture vials, transferred to 1.5 ml tubes, and rinsed 3 times in (1X EBR. 300 µl of cold lysis buffer 1X EBR, 10 mM EDTA, 10 mM DTT, 1 µg/ml of each chymostatin, leupeptin, antipain, and pepstatin (CLAP, Sigma), 1 mM phenylmethanesulfonyl fluoride (PMSF, Sigma), and 1 unit of Aprotinin (Calbiochem)) was added to the tubes. PhoSTOP tablet (Roche, 04906877001) was added into the lysis buffer according to manufacturer's instructions. The larvae were then homogenised using a motorised hand pestle starting at lowest speed and gently increasing the speed to the maximum for 2 minutes. 150 µl of preheated (70˚C) 3X SDS-PAGE Sample Buffer (+10 mM DTT) was added to the homogenate and the tube placed at 100˚C for 10 min. Particulate matter was centrifuged at 13,000 rpm for 2 min, and supernatant transferred to a fresh tube. Samples were stored at -20˚C until required.

2.18.2 Preparation of protein extracts from cultured cell lines

Medium was removed from each well of a 6 well plate and cells rinsed with PBS. 200 μl of RIPA lysis buffer (NEB, 9806) with protease inhibitors (Roche Protease Inhibitor Cocktail Tablets, 14150700) was then added into each well. Cells were scraped with cell scraper and the lysate transferred to a 1.5 ml eppendorf. The lysate was mixed with 100 μl of 3X SDS-PAGE sample buffer and the mixture was sonicated 5 times (2 second sonications, with a 5 second interval between sonications), and subsequently boiled for 10 minutes. To remove the debris, the tube was centrifuged at 13,000 rpm for 2 minutes at 4°C, and the supernatant collected and stored at -20°C until required.

2.19 Electrophoresis of protein samples

Protein samples were resolved at 170 V by SDS-PAGE on precast 4-12% Bis-Tris pre-cast gels (Novex) in 1X MOPS buffer for 1 hour.

2.20 Coomassie blue staining of protein gels

To observe protein bands, polyacrylamide gels were stained with Coomassie Blue (0.5% Coomassie Blue in methanol) diluted 1:5 in Stain Diluent Solution (35% methanol, 14% acetic acid in dH_2O) for 1 hour (or overnight) at RT. The gel was then destained with Fast Destain solution (35% methanol, 10% acetic acid in dH_2O) for 1 hour at room temperature and destained further with Slow Destain solution (10% methanol, 7% acetic acid in dH_2O) for 1 hour (or overnight) at room temperature. The gel was subsequently dried with a gel dry system (Novex,

N12387) and then placed between two layers of DryEAse mini cellophane (Invitrogen, NC2380) with a supplement of the Gel-Dry™ drying solution (Invitrogen, LC 4025), and dried overnight at room temperature.

2.21 Transfer of SDS-PAGE gels to nitrocellulose membranes and immunoblotting

The SDS-PAGE gel was assembled in the transfer cassette with the order of (negative cathode) - sponge/ Whatman blotting paper / gel / nitrocellulose membrane (Sigma, Z613657) / Whatman blotting paper/ sponge – (positive anode). The cassette was placed in a transfer tank with transfer buffer (25 mM Tris, 192 mM glycine, 0.1 % SDS and 20% methanol) and the transfer was performed at 450 mA for 3.5 hours at 4°C.

After transfer, the nitrocellulose membrane was rinsed with water and stained with Ponceau-S (0.2% Ponceau-S in 3% trichloroacetic acid) to check the efficiency of transfer and then washed by TBS-T (20 mM Tris pH 7.4, 150 mM NaCl, 0.1% Tween-20) buffer. The membrane was blocked in 5% skimmed milk powder (Sainsburys) solution prepared in TBS-T for 1 hour at room temperature. The membrane was incubated with primary antibodies at appropriate dilutions (5% milk or 5% BSA in TBS-T) for 1 hour at room temperature or overnight at 4°C. To remove excess antibody, the membrane was washed with TBS-T 3 times with 5 minutes each. The membrane was incubated with horseradish peroxidase-linked (HRP) secondary antibody (1:10,000 in 5% skimmed milk in TBS-T) at room temperature for 1 hour. The membrane was washed with TBS-T 6 times with 5 minutes each. Antibody signal was detected by 1 minute incubation with ECL

reagent (GE Healthcare, RPN2106) followed by development with Lumi-Film Chemiluminescent detection film (Roche, REF 11666657001). The antibodies used in this study are listed in Table 2.6 below.

Table 2.6 The list of primary and secondary antibodies used in immunoblotting

Antibody	Host animal	Source, Catalogue number	Dilution
Anti-DmPoly	Rabbit	Generated by Diagnostics Scotland for the Heck laboratory against the His-tagged recombinant protein and validated by Sharron Vass, Bryce Nelson and Ekin Bolukbasi	1:1000
Anti-HsPoly A7718	Rabbit	Generated by Genosphere for the Heck laboratory against the antigen LGMGAVAVLDFIHYC	1:1000, 1:500
Anti-HsPoly A7719	Rabbit	Generated by Genosphere for the Heck laboratory against the antigen LGMGAVAVLDFIHYC	1:1000, 1:500
Anti-actin	Rabbit	Sigma (A20066)	1:1000
Anti-Akt	Rabbit	Cell signalling (9272)	1:500
Anti-pAkt	Rabbit	Cell signalling (4054)	1:500
Anti-GFP	Mouse	Sigma (G6539)	1:1000
Anti-lsd2	Rabbit	Ronal Kuhnlein (Max Planck Gesellscharft)	1:2000
Anti-pS6K	Rabbit	Cell Siganling (9209)	1:500
Anti-tubulin	Mouse	Sigma (T5168)	1:5000
Anti-4E-BP	Rabbit	Cell signalling	1:500
Anti-mouse HRP	Sheep	Amersham (NA931V)	1:10,000
Anti-rabbit HRP	Donkey	Amersham (NA9340V)	1:10,000

2.22 Stripping of probed nitrocellulose membrane

Nitrocellulose membranes that were already used for immunoblotting were stripped of the primary antibody in order to be used for further immunoblotting with different primary antibodies. The membrane was washed twice in TBS-T for 15 minutes each time and incubated in Stripping Solution for 30 minutes at 65˚C. The membrane was then rinsed several times with TBS-T and washed twice for 10 minutes each time in TBS-T and then for 1-2 hours at room temperature (or overnight at 4˚C) with TBS-T. The membrane was ready to be used for another antibody probing.

2.23 Immunoprecipitation

50 µl of 0-5 hr wild type embryos (raised at 18°C) were homogenized in 1 ml of cold lysis buffer (100 mM NaCl, 10 mM EDTA, 50 mM Tris-Cl pH 7.6, 0.1% Triton-X100, 10 µg/ml of CLAP, 50 µg/ml PMSF and 1 unit of aprotonin) and briefly sonicated. The antibody or pre-immune serum was coupled to 40 µl of Dynal magnetic beads (Invitrogen) at 1:5 ratio and added to pre-cleared embryo lysates overnight. 10% of each sample was subjected to immunoblot analysis to ensure successful immunoprecipitation of Poly while the remaining 90% of sample was resolved on precast 4-12% Bis-Tris polyacrylamide gels (Novex) and stained with Colloidal Coomassie Blue (Invitrogen). Comparable molecular weight regions of interest were excised from each lane (preimmune- and immune-precipitations) and mass spec analysis performed (Gerard Cagney, Conway Institute, University College Dublin).

2.24 Mass spectrometry

SDS–PAGE gels were cut into slices and the proteins digested in-gel with trypsin according to the method of Shevchenko and co-workers (SHEVCHENKO *et al.* 1996). The resulting peptide mixtures were resuspended in 1% formic acid and analysed by nano-electrospray liquid chromatography mass spectrometry (Nano-LC MS/MS). An HPLC instrument (Dionex, UK) was interfaced with an LTQ ion trap mass spectrometer (ThermoFinnigan, CA). Chromatography buffer solutions (Buffer A: 5% acetonitrile and 0.1% formic acid; Buffer B: 80% acetonitrile and 0.1% formic acid) were used to deliver a 60 min gradient (35 min to 45% Buffer B, 10 min to 90%, hold 10 min, 3 min to 5%, hold for 15 min). A flow rate of 2 µl min^{-1} was used at the electrospray source. One full scan was followed by ten MS/MS events, and the duty cycle programmed to enforce dynamic exclusion for 2 min. In-house proteomics pipeline software (Proline) was used to process data. Spectra were searched using the Sequest algorithm (YATES *et al.* 1995) against SwissProt.2007.04.19 database restricted to *D. melanogaster* entries. Proteins with a) Peptide Prophet probability score greater than 0.99 (KELLER *et al.* 2002), and b) identified by a minimum of two different peptide spectra, were automatically accepted, while spectra for the minority of proteins identified by single spectra were manually analyzed for quality.

2.25 Larval manipulations

Prior to dissections or protein extractions, 10-15 2nd instar larvae were transferred to a fresh vial supplemented with fresh yeast paste. Manipulations were carried out when larvae reached early third instar stage (as determined by their

physiological features including their mouth-hooks and spiracles). For starvation experiments, early third instar larvae were starved in 20% sucrose solution for 3-4 hr prior to dissection.

2.26 Triglyceride assay on larval extracts

Triglyceride assay on larvae was carried out as described by (GRONKE *et al.* 2003). Briefly, 6 whole larvae corresponding to each genotype were collected and placed in 500 µl of 0.05% Tween 20 and homogenised using a Polytron apparatus, followed by heat incubation at 70°C for 5 minutes. The samples were centrifuged for 1 minute at 3500 rpm and 350 µl of the supernatant was transferred to a new vial and centrifuged for 3 minutes at 2500 rpm. 600 µl of Thermo Infinity Trig solution (Thermo Electron, 981786) was added to 75 µl of isolated supernatant and the absorbance at 540 nm was measured following incubation for 30 minutes. Similarly, protein content was determined by adding 10 µl of isolated supernatant to Bradford reagent (Sigma, B6916) and reading the absorbance at 595 nm. The triglyceride levels were normalized to corresponding protein levels.

2.27 Lysotracker staining

Lysotracker staining was performed as described (HENNIG *et al.* 2006). Fat body from fed or starved larvae was dissected in PBS, and incubated for 2 minutes in 100 nM LysoTracker Red DND-99 (Molecular Probes, L7528), with 1 µM Hoechst 33342 (Molecular Probes, H3570) in PBS. Fat bodies were mounted with PBS on a glass slide and tissues were visualized by using an Olympus AX-70 Provis epifluorescence microscope, and images captured with a Hamamatsu Orca II CCD

camera. Images were captured using SmartCapture 3 and processed using Adobe Photoshop software.

2.28 Cell culture

A375 and HeLa cells were maintained in Dulbecco's modified Eagle's medium (DMEM) (Gibco, 41966) supplemented with 10% fetal bovine serum (FBS) (Gibco, 10106). Cells were grown to 80-90% confluence before overnight serum withdrawal.

For insulin stimulation, serum starved cells were treated with 100 nM insulin (Sigma, I0516). Cells were treated with 20 nM rapamycin (Cell Signaling Technology, 9904) during the overnight serum starvation.

2.29 Immunofluorescence

Immunofluorescence experiments were carried out on human cultured cells, larval hemocytes and larval eye imaginal discs. Antibodies used in all immunofluorescence experiments are listed in Table 2.7 at the end of this section.

2.29.1 Immunofluorescence on human cultured cells

Cells were grown on coverslips in 6-well plates overnight. Cells were rinsed in PBS for 3 min followed by a 3 min fixation in PBS containing 4% paraformaldehyde (diluted from 16% ampoules). Fixative was removed by a 2 min wash in PBS. Cells were permeabilised by a 5 min incubation in PBS + 0.5% Triton

X-100 followed by a 1 hr block in PBS containing 3% BSA. Subsequently, four 5 minute PBS-T washes were performed. Primary antibody was diluted in PBS+0.3% BSA+0.1% Triton X-100 and incubated on the cover slips for 1 hr at room temperature. Cells were washed twice for 5 min followed by a 1 hr secondary antibody incubation diluted in PBS+0.3% BSA+0.1% Triton X-100. Subsequently, four 5 minute PBS-T washes were performed. DAPI was included in the penultimate wash at 0.1 μg/ml concentration.

2.29.2 Phalloidin staining of hemocytes

Third instar larvae were bled on multispot microscope slides (Hendley-Essex) using a pair of forceps and a 25 gauge needle in 20 μl of PBS. Cells were left to settle on the slide for 1 hour at room temperature in a humidified chamber to allow adherence to the slide. Cells were fixed with 20 μl of 3.7% paraformaldehyde (prepared by carrying out 1:10 dilution of the 37% stock solution) in PBS for 5 minutes. Cells were washed with PBS for 5 minutes followed by a 5 minute permeabilisation in PBS with 0.1% Triton X-100. Following an additional wash in PBS, cells were incubated at room temperature with Alexafluor-phalloidin diluted at 1:40 in PBS containing 1% BSA. Following the antibody incubation cells were washed in PBS twice with 5 minute washes. Cells were incubated with DAPI diluted in PBS (1:5,000 dilution) for 5 minutes followed by a 5 minute PBS wash. Cells were mounted with a drop of mowiol by gently lowering a coverslip on the top of the slide. Antibodies used in this study are listed in Table 2.7.

2.29.3 Antibody staining of hemocytes

Third instar larvae were bled on multispot microscope slides (Hendley-Essex) using a pair of forceps and a 25 gauge needle in 20 μl of PBS. Cells were left to settle on the slide for 1 hour at room temperature in a humidified chamber to allow adherence to the slide. Cells were fixed with 20 μl of 3.7% paraformaldehyde in PBS for 5 minutes. Cells were washed with PBS for 5 minutes, followed by a 5 minute permeabilization in PBS with 0.1% Triton X-100. Following an additional 5 minute wash in PBS the blocking step was performed by incubating cells in PBS containing 3% BSA for one hour. Cells were then incubated with primary antibody diluted in block solution overnight at 4°C. The following day cells were washed in PBS three times and incubated at room temperature with secondary antibody diluted in PBS containing 3% BSA. Following the secondary antibody incubation cells were washed twice in PBS for 5 minutes. Cells were incubated with DAPI diluted in PBS (1:5000 dilution) for 5 minutes followed by a 5 minute wash in PBS. Cells were mounted with a drop of mowiol by gently lowering a coverslip on the top of the slide. Antibodies used in this study are listed in Table 2.7.

2.29.4 Immunofluorescence on eye imaginal discs

Third instar larval discs were dissected in PBS and fixed for 30 minutes in 7.4 % formaldehyde solution in PBS (diluted from 37% formaldehyde solution). Eye discs were washed four times for 10 minutes in the wash solution (PBS with 0.3 % Triton-X 100). Discs were blocked for 30 minutes in PBS containing 10% normal goat serum and 0.3 % Triton-X 100. Discs were incubated at 4°C overnight with primary antibody diluted in the blocking solution to the appropriate concentration.

The following day, discs were washed four times for 10 minutes in wash solution and blocked for an additional 30 minutes in blocking solution. Discs were then incubated with the secondary antibody that (diluted in the blocking solution) for two hours at room temperature. At the end of the secondary antibody incubation, eye discs were washed four times in the wash solution, and with the addition of DAPI (at 1:10,000 dilution) in the third wash. Finally eye discs were mounted on glass slides with mowiol.

Table 2.7 List of antibodies used immunofluorescence experiments described in Chapters 2, 3 and 5

Fluorescently labelled probes		**Source**	**Dilution**
Alexa Fluor 488 phalloidin		Invitrogen (A12379)	1:500 1:40, (hemocyte staining)
Alexa Fluor 594 phalloidin		Invitrogen (A12381)	1:500, 1:40 (hemocyte staining)
DAPI (1mg/ml in water)		Sigma (D9564)	1:10,000
Primary antibody	**Animal**	**Source**	**Dilution**
Anti-HsPoly Rb1162	Rabbit	Generated by Diagnostics Scotland for the Heck laboratory against the GST-tagged recombinant protein and validated by Sharron Vass and Ekin Bolukbasi	1: 1000
Anti-HsPoly A7718	Rabbit	Generated by Genosphere for the Heck laboratory against the antigen LGMGAVAVLDFIHYC	1:1000
Anti-HsPoly A7719	Rabbit	Generated by Genosphere for the Heck laboratory against the antigen LGMGAVAVLDFIHYC	1:1000
Anti-Cyclin E	Mouse	Hybridoma Bank, University of Iowa	1:50
Anti-βGal	Mouse	Hybridoma Bank, University of Iowa	1:50
Anti-L1	Mouse	Istvan Ando, University of Szeged	1:1
Anti-PH3	Mouse	Cell Signalling (9701)	1:100
Anti-Dm-Poly	Rabbit	Heck laboratory	1:1000
Anti-Hs-Poly	Rabbit	Heck laboratory	1:1000
Anti-Hs-Poly-A7718	Rabbit	Heck laboratory	1:1000, 1:500
Anti-Hs-Poly-A7719	Rabbit	Heck laboratory	1:1000, 1:500
Secondary antibody	**Animal**	**Source**	**Dilution**
Anti-mouse Alexa 488	Donkey	Molecular Probes (A21202)	1:500
Anti-mouse Alexa 594	Donkey	Molecular Probes (A21203)	1:500
Anti-rabbit Alexa 488	Donkey	Molecular Probes (A21206)	1:500
Anti-rabbit Alexa 594	Donkey	Molecular Probes (A21207)	1:500

2.30 Microscopy

All slides (apart from eye imaginal disc preperations) were examined with an Olympus Provis microsope, equipped with epifluorescence optics. Images were captured with an Orca II CCD camera (Hamamatsu) and Smart-capture 3 software (Digital Scientific). Microscopy on larval eye imaginal discs was performed using a DeltaVision (Applied Precision Inc.) set up on an Olympus micsorsope and deconvolved using Delta Vision software. All images were processed using Adobe Photoshop software.

2.31 Bacterial infection and survival experiments

Salmonella typhimurium, Pseudomonas aeruginosa were used as Gram-negative bacterial strains. *Enterococcus faecalis* was used as a Gram-positive strain. All strains were grown on standard Luria-Bertrani media (LB) overnight. For septic infections, 25-30 male and 25-30 female flies, between 5-7 days old (giving therefore a total number of 50-60 adult flies for each injection experiment) were picked in the upper part of the thorax with a glass needle previously dipped into the bacterial solution. Oral infection with *Pseudomonas aeruginosa* was carried out as follows: 40 μl of an overnight culture was added to 3 ml of LB and incubated for around 3 hours at 37°C with agitation until an OD_{600} of 0.7 was obtained. The cultures were diluted at 1:1 ratio with sterile 5% sucrose solution bringing the final OD_{600} to around 0.35. The mixture was dotted on sheets of Whatman paper. Around 10 slides of paper (cut out as circles of 3 cm in diameter) were used for addition of 1 ml of the solution. Flies survival was followed at several time points at 25°C. The infection

was renewed each 24 hours by changing by addition of fresh sheets dotted with fresh bacterial solution.

2.32 Wasp infection and encapsulation assay

The encapsulation assay was done according to published methods (SORRENTINO *et al.* 2002). Briefly, 2 days before parasitisation, fly strains were crossed and kept at room temperature. Four or five females of *L. boulardi* G486 were allowed to infest at room temperature for 2 hours, after which vials containing *Drosophila* larvae were left at room temperature for 40-42 hours. After this time, larvae were collected, washed in PBS, and then viewed under a stereomicroscope for the presence of a dark capsule. Larvae in which no dark capsule was observed were dissected in 20 μl PBS to determine whether they had been parasitized. Larvae containing eggs from parasitoid that had not darkened by this time were scored as non-encapsulated. Non-parasitised larvae were excluded from the count.

2.33 Microarray analysis

Microarray analysis was carried out by FlyChip (Cambridge). Three biological samples each consisting of 5-7 early third instar larvae corresponding to each genotype were homogenized in Trizol and samples sent to FlyChip. Subsequent RNA extraction and microarray analysis were carried out by FlyChip service according to protocols described on their website (http://www.flychip.org.uk/).

2.34 Statistical analysis

Unpaired two-tailed Student's t-test was used to determine statistical significance in real-time PCR experiments and TAG assay described in Chapters 4 and 6. Data were analysed using Microsoft Excel.

Chapter 3: Mosaic clonal analysis in larval eye imaginal discs to investigate the state of cell cycle progression upon *poly* mutation

3.1 Introduction

The *Drosophila* compound eye consists of 800 ommatidia with a precise organisation which is essential to its function. Each ommatidium is generated by nineteen precursor cells whose well defined plan is tightly controlled by specific cell proliferation events. Therefore the *Drosophila* eye has become an efficient model system to study cell proliferation (BAKER and YU 2001; READY *et al.* 1976).

The development of the retina begins in the monolayer epithelium of the third instar larval imaginal disc. Differentiation of the cells within the eye imaginal disc is a spatially and temporally controlled developmental mechanism. Differentiation starts at the posterior of the eye disc and sweeps anteriorly (BAKER 2001) via the "morphogenetic furrow" (MF). A cell cycle arrest in G1 phase takes place within the MF (READY *et al.* 1976; THOMAS *et al.* 1994). Anterior to the MF, cell proliferation takes place randomly and as cells enter the MF they arrest at G1 phase. Cells exit from the posterior of the MF either as one of the five precursor cells that have already been specified and ready to start ommatidial recruitment or undifferentiated surrounding cells that have not joined a precluster. This latter class of cells undergoes a final round of mitosis called second mitotic wave (SMW) that is necessary to produce enough cells to complete eye development (BAKER 2001; THOMAS *et al.* 1994). Because distinct phases of the cell cycle are tightly regulated

during the SMW, eye imaginal disc development provides a good model to investigate cell cycle defects upon various mutations (BAKER and YU 2001). Cyclin-depedent kinases (Cdks) and their binding partner cyclins are the main regulators of the cell cycle progression in eukaryotes. Distinct phases of cell cycle are triggered by specific combinations of Cdks/cyclins facilitating tight regulation of cell proliferation. Cyclins are subject to degradation by ubiquitin-dependent proteolysis following phosphorylation/dephosphorylation events and interaction with cyclin dependent kinase inhibitors. The Cyclin protein family is evolutionarily well conserved. All five family members - Cyclin A, B, C, D and E - are found both in humans and *Drosophila* suggesting that they are likely to have distinct but conserved functions (KOFF *et al.* 1991; LAHUE *et al.* 1991; LEHNER and O'FARRELL 1990; LEOPOLD and O'FARRELL 1991; LEW *et al.* 1991; MOTOKURA *et al.* 1991; PINES and HUNTER 1990; WHITFIELD *et al.* 1989; XIONG *et al.* 1991).

The small larval brain and imaginal discs phenotype observed in *poly* mutants has been commonly associated with mutants that are characterized by dysregulation of the cell cycle (GATTI and BAKER 1989). Therefore we hypothesized that the phenotype observed in *poly* larvae might be indicative of the disturbance of normal cell cycle progression upon *poly* mutation. I decided to test this hypothesis by looking at the state of the cell cycle in *poly* mutant clones generated in mosaic eye imaginal discs. As described in the Introduction chapter, mosaic clonal analysis is a powerful genetic tool available in *Drosophila* that aims to generate patches of homozygous mutant tissue on a heterozygous background. Cell cycle progression in *poly* mutant clones was investigated by assessing the levels by immunofluorescence

of a number of cell cycle cyclins in the mutant patches and comparing them to the surrounding non-mutant tissue.

3.2 Results

3.2.1 Generation of FRT82B poly^{05137}/TM6B flies

The first step towards the mosaic clonal analysis of *poly* in the eye imaginal discs was the placement of the P-element insertion leading to the *poly*^{05137} mutation on the same arm as the FRT site on the right arm of the third chromosome. The crossing scheme for placing the mutation of interest on the same arm as the FRT site has previously been described in detail (XU and RUBIN 1993). Therefore following previously published work describing the generation of mosaics, a crossing scheme was planned for recombining the P-element insertion leading to *poly*^{05137} on the same arm as the FRT site situated at the base of the right arm of the third chromosome. This crossing scheme is schematised in detail in Figure 3.1.

As described in Figure 3.1 the neomycin resistance cassette associated with the FRT site allows selection of flies bearing the FRT site on neomycin-containing media. Out of 18 lines that showed neomycin resistance resulting from the second round of crossing (Figure 3.1.B), only one line that was named "line 7" had gone through meiotic recombination appropriately placing the *poly*^{05137} mutation on the same arm as the FRT site, therefore giving flies with the following genotype: P(neoFRT)82B*poly*^{05137}/TM6B. The presence of both the neomycin resistance cassette/FRT site and P-element insertion leading to *poly*^{05137} mutation was further confirmed by genomic PCR on line 7 (Figure 3.2).

3.2.2 Generation of poly *mutant clones in third instar eye imaginal disc*

After molecularly confirming that "line 7" had the correct genotype bearing both the FRT site and the *poly*^{05137} mutation on the same chromosome arm, the technique for generating clones in the eye imaginal disc was optimized. This optimization was necessary as in some cases the over-proliferation of wild type cells leads to failure of the detection of mutant clones. This can be overcome by carrying out the clonal analysis on a *minute* background (BLAIR 2003). Therefore, it was essential to check if it was possible to detect *poly* mutant patches before planning any further investigation.

Both *hs-flp* and *eyeless-flp* lines that express the recombination enzyme flipase following heat-shock and in the same expression pattern as the *eyeless* gene respectively, were previously used to successfully generate mutant clones in the eye imaginal disc (BAONZA and FREEMAN 2005; BRUMBY and RICHARDSON 2003). However, in our analysis I used *eyeless-flp* line in order to avoid the heat-shock step that might in some cases lead to variability.

In the first step control crosses established in which flies bearing only the FRT site without the *poly*^{05137} insertion was used in order to determine if the technique was working efficiently. Control crosses revealed patches of tissue lacking GFP expression in the eye imaginal disc isolated from the larvae with the following genotype: *eyFLP; FRT82B-GFP/FRT82B* (Figure 3.3.A). Therefore, in the next step crosses were carried out using line 7 and patches of tissue lacking GFP expression indicating *poly* mutation were detected in eye imaginal discs isolated from larvae of genotype *eyFLP;FRT82B-GFP/FRT82B-poly*^{05137} (Figure 3.3.B).

These observations confirmed that it was possible to generate *poly* mutant clones in the eye imaginal disc using "line 7" and expressing flipase in the *eyeless* pattern.

3.2.3 Investigation of Cyclin E and Cyclin A levels suggests no disruption of progression into S phase in **poly** *mutant clones generated in the eye imaginal disc*

Earlier work carried out in *Drosophila* embryos revealed that the pattern of Cyclin E expression correlated with the pattern of endoreplication during *Drosophila* embryogenesis (KNOBLICH *et al.* 1994). Furthermore, embryos that lacked Cyclin E showed reduced BrdU incorporation and many cells appeared to arrest before the entry into S phase. In addition, over-expression of Cyclin E was enough to induce G1-arrested cells to enter S phase. Taken together, these observations suggested that Cyclin E was the primary trigger of S phase (KNOBLICH *et al.* 1994).

I started my investigation of cell cycle progression in the absence of *poly* by assessing Cyclin E levels in *poly* mutant clones generated in the eye imaginal disc. It should be noted that in this experiment as an alternative approach to the method described in the previous section, transgenic flies bearing lacZ marker instead of GFP was used, allowing therefore the detection of *poly* mutant clones by the lack of β-galactosidase staining. Staining for Cyclin E was not disrupted in β-galactosidase negative clones suggesting that Cyclin E levels are not affected by *poly* mutation (Figure 3.4). However Cyclin E staining appeared rather uniform across the eye disc whereas previous work has shown an intense band of staining suggesting accumulation of Cyclin E behind the MF indicative of a population of cells that were

entering S phase (MOBERG *et al.* 2001). Therefore further investigation of S phase was carried out using an antibody recognizing Cyclin A.

It is known that the association of Cyclin A with Cdk1 during late G2 phase is a necessary step for the entry into mitosis. In mammalian cells it has also been shown that the CycA/Cdk2 complex can induce entry into S phase from G1 (RESNITZKY *et al.* 1995; ROSENBERG *et al.* 1995). However elucidating the role of Cyclin A during the onset of S phase has been more challenging in *Drosophila* as cells can go through S phase without any disruption in the absence of Cyclin A (KNOBLICH and LEHNER 1993; LEHNER and O'FARRELL 1989). But it was shown that over-expression of Cyclin A compensates for the lack Cyclin E allowing cells to enter S phase (SPRENGER *et al.* 1997). Furthermore, ectopic expression of Cyclin A induces cells to get into S phase as indicated by an increase in BrdU incorporation (BAONZA and FREEMAN 2005). Also, in *Drosophila* embryos over-expression of a Cyclin A inhibitor leads to a block in S phase entry (AVEDISOV *et al.* 2000). Therefore, although its role is more complex and less well defined, there is substantial evidence for the involvement of Cyclin A in the onset of S phase in *Drosophila*.

In order to obtain a more accurate conclusion regarding the onset of S phase upon *poly* mutation, Cyclin A levels were assessed in mosaic eye imaginal discs. Cyclin A levels appeared to be the same in *poly* mutant clones (indicated by the lack of GFP) and the surrounding wild type tissue (Figure 3.5).

Taken together, my observations suggest that the levels of two important cyclins involved in the onset of S phase are not affected upon *poly* mutation.

Therefore mutation of *poly* does not appear to lead in a disturbance of progression into S phase.

3.2.4 Investigation of Cyclin B levels suggests no disruption of the G2/M transition in poly *mutant clones generated in the eye imaginal disc*

Cyclin B is a marker of cells that have passed the checkpoint but not divided so therefore it accumulates at G2/M transition (ARELLANO and MORENO 1997). In the larval eye imaginal discs, Cyclin B is absent in G1 arrested cells of the MF, but starts being detectable in columns of cells posterior to the MF. In fact, surprisingly it was shown that in the eye imaginal disc the accumulation of Cyclin B starts at very low levels at S phase resulting therefore in a slight overlap with BrdU labelling and reaches its maximum at the G2/M transition. At mitosis, Cyclin B is degraded leading to its absence in late mitotic cells (BAKER and YU 2001; KNOBLICH and LEHNER 1993).

In order to assess whether *poly* mutation resulted in disruption of the progression of G2 to M phase, mosaic eye imaginal discs were stained with an antibody that recognizes Cyclin B. An intense staining for Cyclin B behind the MF was detected possibly indicating its accumulation in cells that have gone through the G1/S checkpoint but that had not divided yet. The accumulation of Cyclin B along this band was not disrupted in *poly* mutant clones (Figure 3.6).

My results indicate that cells lacking Poly accumulate Cyclin B at the same levels as wild type cells. This suggests that *poly* cells reach the G2/M transition phase without any disruption. Therefore Poly function appears not to be required for progression of cell cycle through the G2/M transition.

3.2.5 Investigation of PH~3 levels suggests no disruption of mitosis in **poly** *mutant clones generated in the eye imaginal disc*

I started the analysis of the cell cycle progression in *poly* mutant clones by looking at the progression from G1 into S phase by assessing Cyclin E and A levels. Subsequently the progression to the G2/M transition was analyzed by investigating Cyclin B levels. To our surprise, none of these stage-specific cell cycle markers showed any difference in *poly* mutant clones compared to the neighbouring tissue. Therefore in the next step, cells undergoing mitosis were visualized by looking at phosphorylation levels of histone 3 (P~H3) at serine 10 (HENDZEL *et al.* 1997). It was previously shown that mitosis occur in a more random fashion than a very synchronous S phase posterior to the MF (BAONZA and FREEMAN 2005). Staining of mosaic eye imaginal discs with P~H3 was in agreement with this previously published data in that it showed a more random distribution of the mitosis. However, removal of Poly in the eye imaginal disc did not cause a block to mitosis as P~H3 staining was not disrupted in *poly* mutant patches revealed by the lack of GFP (Figure 3.7).

This observation suggests that mitosis is not blocked in the absence of functional Poly in the eye imaginal disc.

3.3 Discussion

I carried out the mosaic clonal analysis on larval eye imaginal discs starting from the initial hypothesis that small brains and the absence of imaginal discs observed in *poly* mutants might be due to a major cell cycle defect in mutant animals. If Poly was primarily involved in the regulation of the cell cycle we might expect to

see disruption of major stage-specific cell cycle markers upon *poly* mutation. Investigation of S phase by the assessment of Cyclin E and A levels and the G2/M transition by the assessment of Cyclin B levels revealed no difference in the levels of these cell cycle stage-specific cyclins in *poly* homozygous clones and the surrounding tissue. This result suggested that corresponding cell cycle stages were not dysregulated in mutant clones. In addition, PH~3 staining was not altered suggesting that cells lacking *poly* can go through mitosis without any discernible aberrations.

In *Drosophila,* Cyclin D and its partner Cdk4 form a complex and it was shown to be primarily an important regulator of cell growth (DATAR *et al.* 2000; MEYER *et al.* 2000; PROBER and EDGAR 2000). While I had wanted to assess Cyclin D levels in *poly* mutant clones to determine whether *poly* results primarily in the dysregulation of Cyclin D (indirectly affecting cell growth), I was not able to obtain anti-cyclin D antibodies as the reagent was not commercially available and my efforts of contacting groups who had already published the use of Cyclin D antibodies (DUMAN-SCHEEL *et al.* 2002) did unfortunately not lead to a successful outcome.

In summary mosaic clonal analysis in *poly* mutant clones did not reveal an obvious disruption of cell cycle progression suggesting that Poly does not appear to have a direct role to play in cell cycle progression.

Chapter 4: Identification of the insulin receptor as a protein interactor of Poly and investigation of the role of Poly in insulin receptor signalling

4.1 Introduction

A protein's function in the cell may be defined by its other interactions with other proteins. Therefore, identification of protein-protein interactions is a powerful way of scrutinizing the unknown function of proteins as well as identifying missing players involved in a cellular pathway. Sophisticated protein analysis approaches, such as mass spectrometry, that have become readily available over the recent years have made possible the discovery of previously unknown protein interactions (FIGEYS *et al.* 2001; SHIIO *et al.* 2002)

The success rate of isolation of a protein of interest by immunoprecipitation followed by the recovery of protein complexes depends on various parameters such as the abundance of the protein, the rates of association and dissociation as well as the stability of the protein and its interactions. However when the optimal technical parameters are met, this approach is very powerful mainly due to high accuracy and unambiguous identification of interacting proteins.

As Poly was a functionally uncharacterized protein at the start of my PhD project, we decided that identification of binding partners of Poly by mass spectrometry analysis would be a useful and unbiased approach to dissect the function of Poly in the cell. The use of this approach was possible due to the availability of good antibodies generated by our lab recognizing the endogenous Poly

protein. The native protein was immunoprecipitated from wild type *Drosophila* embryonic extracts and binding partners of Poly were identified by mass spectrometry. *Drosophila* Insulin receptor (InR) was identified as a significant Poly interacting protein which led us to further investigate the nature and consequences of an interaction of Poly with InR signalling.

Signalling through the Insulin Receptor/Target of Rapamycin (InR/TOR) pathway is one of the key regulators of cellular energy homeostasis and growth (WULLSCHLEGER *et al.* 2006). Importantly, the InR/TOR pathway is evolutionarily conserved amongst metazoa (GREWAL 2009; WULLSCHLEGER *et al.* 2006). Thus, studies carried out using *Drosophila* as a model system have played a major role in expanding our understanding of the mechanism as well as downstream consequences of signalling via this pathway (BRITTON *et al.* 2002; HENNIG *et al.* 2006; PUIG *et al.* 2003). In humans, aberrations of InR/TOR signalling lead to various metabolic syndromes, such as diabetes and obesity, as well as to development of tumours (MANNING 2004).

As described more in depth in the Introduction chapter, cascade of phosphorylation events mediates signalling through the InR/TOR pathway (Figure 1.5). The binding of insulin to the InR leads to phosphorylation of IRS (Insulin Receptor Substrate) by InR. IRS acts as a recruitment site for PI3K (phosphatidylinositol 3-kinase), which in turn catalyses the conversion of PIP_2 (phosphatidylinositol [4,5]-bisphosphate) into PIP_3 (phosphatidylinositol [3,4,5]-trisphosphate) at the cell membrane. PIP_3 recruits PDK1 and Akt to the membrane where Akt gets phosphorylated and activated by PDK1. Phosphorylated Akt signals to and inhibits the TSC (Tuberous Sclerosis Complex, Tsc1/Tsc2) (CAI *et al.* 2006;

GAO and PAN 2001; POTTER *et al.* 2001). In its active form, TSC acts as an inhibitor of the small GTPase Rheb (LONG *et al.* 2005). TOR is activated by Rheb and is thereby integrated into this signalling process.

TOR exists as part of two different complexes: TORC1 and TORC2. Activation of TORC1 has various downstream effects contributing to an increase in cell growth and proliferation. For example, TORC1 directly phosphorylates S6K and 4E-BP, resulting in an increase in ribosome biogenesis and m7G cap-dependent translation (WULLSCHLEGER *et al.* 2006). In addition, autophagy is inhibited by TORC1 activation (SCOTT *et al.* 2004). Akt is phosphorylated by the TORC2 complex (SARBASSOV *et al.* 2005). A negative feedback loop signals back to IRS through S6K ensuring shut off of the TOR signalling pathway above a certain level (RADIMERSKI *et al.* 2002). Signalling downstream of Akt phosphorylates the forkhead-like transcription factor Foxo which leads to its exclusion from the nucleus, thereby preventing the transcription of Foxo target genes (MARR *et al.* 2007; PUIG and TJIAN 2005; TELEMAN *et al.* 2005a).

I analyzed the genetic interactions between Poly and other components of the InR/TOR pathway and I investigated the consequences of the loss of function of *poly* by looking at the activity of various downstream effectors of InR/TOR signalling. Taken together, my results suggest that *poly* loss of function results in decrease of signalling via InR/TOR pathway. In light of my results, I suggest that Poly is a positive regulator of InR/TOR signalling.

4.2 Results

4.2.1 Identification of the insulin receptor as a physical interactor of Poly by mass spectrometry

The sequence of the *poly* gene (encoding a protein of 251 amino acids) was unique showing no motifs indicative of function. We therefore decided to adopt an unbiased approach to determine the pathways and processes in which Poly might be involved. In order to identify proteins physically interacting with Poly, immunoprecipitation using an antibody generated to recombinant his-tagged Poly was performed using 0 to 5 hour *Drosophila* embryo extracts (Figure 4.1 A, B). Initial immunoprecipitation experiments were done with the guidance of the former post-doctoral fellow from the Heck Lab, Dr. Bryce Nelson. Samples were analyzed using tandem mass spectrometry. Immunoprecipitates with pre-immune serum were used as control samples. Amongst the five Poly binding proteins identified with significant scores, the insulin receptor scored the highest and was represented by numerous peptides in two distinct bands (Figure 4.1 C). This result suggests that Poly and InR are components of the same protein complex, and that Poly may play a role in the InR signalling pathway.

4.2.2 Examination of InR *mutant larvae reveals decreased Poly levels and the appearance of melanotic masses*

Considering the physical binding of Poly to the InR, I assessed the level of Poly in various InR signalling mutants. Strikingly, the level of Poly was dramatically decreased in InR^{05545} mutant larvae, whereas levels in *Akt1* mutant

larvae (Akt1 is situated downstream of InR) were unaffected (Figure 4.2 A). Interestingly, semi-quantitative assessment of *poly* mRNA levels revealed that *poly* transcript levels were unchanged in the *InR* mutants (Figure 4.2 B) suggesting that the difference in protein levels might be due to decreased translation or increased degradation of Poly in the absence of InR.

Further evidence of a connection between Poly and the InR came from the observation of homozygous InR^{05545} mutants that were reported previously to be embryonic lethal (FERNANDEZ *et al.* 1995). I noticed that a number of homozygous InR^{05545} animals reached the third instar larval stage. In fact, Poly protein levels in Figure 4.2 A were assessed by immunoblotting third instar InR^{05545} larval extracts. Interestingly, some of these mutant *InR* larvae exhibited a greatly extended third larval instar and developed melanotic masses that were superficially similar to those observed in *poly* mutants (Figure 4.2 C). These observations suggest that loss of InR leads to a decrease in Poly and that InR^{05545} mutants exhibit phenotypic features similar to those of *poly* mutant larvae.

4.2.3 Mutations in Akt *and* S6K *lead to suppression of a rough eye phenotype induced by over-expression of* poly

I hypothesized that there should be genetic interactions between *poly* and components of the InR signalling pathway. Consequences of such interactions may be evident by their effects on the activity of downstream effectors of the InR pathway.

Therefore *poly* was over-expressed in adult fly eyes, using a *UAS-poly* transgene under control of a *GMR-Gal4* driver (FREEMAN 1996) which led to a rough

eye phenotype containing disorganized ommatidia at 27°C. Disruption of InR/TOR signalling through mutation of either *dAkt1* or *dS6K* led to a striking suppression of the *poly*-induced rough eye phenotype (Figure 4.3 A, B) suggesting an intact InR/TOR signalling cascade was required for Poly to exert its effects.

4.2.4 Activity of Akt, S6K and 4E-BP is down-regulated upon poly *loss of function*

I hypothesized that if *dAkt* and *dS6K* mutants can act as suppressors of the *poly* over-expression phenotype, the activity of these kinases might be altered in *poly* mutant animals. Therefore early third instar larval extracts were probed with antibodies that recognize specifically the phosphorylated (active) forms of dAkt and dS6K. Indeed, the phosphorylation levels of both dAkt and dS6K were decreased upon mutation of *poly* (Figure 4.4 A, B). These data suggested that the activity of both dAkt and dS6K, and likely their cell growth promoting effects, were decreased in *poly* mutant animals.

4E-BP, the translation initiation factor eIF-4E binding protein is another important downstream effector of TOR. Phosphorylation of 4E-BP by TOR leads to its dissociation from the m7G-cap binding protein eIF-4E, thereby allowing activation of cap-dependent translation with consequent positive effects on cell growth (HAY and SONENBERG 2004). Disruption of InR/TOR signalling has two effects on 4E-BP: increased transcription due to increased Foxo activity and a simultaneous decrease in phosphorylation of 4E-BP resulting in its binding to eIF-4E and inhibition of cap-dependent translation (MARR *et al.* 2007).

In order to test whether mutation of *poly* also had an effect on d4E-BP, the level of d4E-BP transcript was assessed by real-time PCR. Consistent with a

decrease in InR/TOR signalling, the level of d4E-BP transcript was almost 3-fold greater in *poly* mutant larvae compared to control animals (Figure 4.4 C). Furthermore, immunoblotting revealed that d4E-BP was hypophosphorylated in *poly* mutant extracts compared to wild type extracts (Figure 4.4 D). Taken together, these results suggest a decrease in cap-dependent protein translation upon loss of Poly.

4.2.5 Autophagy is constitutively active in the fat body of **poly** *larvae*

One important downstream consequence of the activation of InR/TOR signalling is the inhibition of autophagy. Autophagy is a cellular response to starvation whereby the cytoplasm is engulfed in small double-membrane enclosed vesicles, the contents of which are degraded by the autophagic machinery. Breakdown products then serve as a nutrient source for the cell until more nutrients become available in the environment. Alterations of the autophagic pathway have been found to be involved in cancer and neurodegenerative diseases (LEVINE and KROEMER 2008; MIZUSHIMA *et al.* 2008). Starvation-induced autophagy, in response to nutrient deprivation, takes place in the larval fat body (SCOTT *et al.* 2004). *Drosophila* also undergoes programmed autophagy at developmentally defined time points to facilitate tissue remodelling during metamorphosis (BUTTERWORTH *et al.* 1988; BUTTERWORTH and FORREST 1984; JUHASZ *et al.* 2003; RUSTEN *et al.* 2004). In *Drosophila*, the larval fat body serves a similar function to the mammalian liver by acting as a nutrient storage organ, and has commonly been used to examine the autophagic pathway during both starvation-induced and developmentally regulated autophagy (JUHASZ *et al.* 2007; SCOTT *et al.* 2007; SCOTT *et al.* 2004). While the fat

body from fed larvae does not exhibit autophagy, autophagy becomes activated within a short period of amino acid starvation.

TOR activity directly inhibits starvation-induced autophagy, while various components of InR signalling (such as InR and Akt, acting upstream of TOR), also behave as negative regulators of autophagy. I hypothesized that if *poly* acts in InR signalling, the state of autophagy should be altered in *poly* mutant fat body. This hypothesis was tested by carrying out Lysotracker staining on wild type and *poly* mutant fat body. Lysotracker recognizes acidic organelles such as active lysosomes and therefore is used commonly to monitor the state of autophagy (SCOTT *et al.* 2004). At the absence of any autophagic activity lystotracker staining positive bright spots are absent. However, lysotracker positive puncta become quickly apparent upon activation of autophagy due to the activity of lysosomic enzymes. In agreement with published findings (SCOTT *et al.* 2004), no Lysotracker puncta were observed in fed wild type early third instar fat body (Figure 4.5 A, left). However, Lysotracker puncta became apparent following a 4 hour amino acid starvation, due to activation of autophagy (Figure 4.5 A, right). Strikingly, Lysotracker puncta were abundantly clear in fed *poly* early third instar fat bodies suggesting that autophagy was constitutively active in the fat body of *poly* mutants (Figure 4.5 B, left).

4.2.6 **poly** *loss of function leads to an increase in autophagic cell death as indicated by increased cleaved Caspase-3 staining*

Autophagy and programmed cell death are two processes that have been shown to be closely related but the exact nature of their relationship has been difficult to elucidate. Autophagic cell death is characterized by degradation of the

dying cell by its own lysosomal enzymes and therefore differs from apoptotic cell death in which the dying cell is eliminated by phagocytosis. It was previously shown that increased levels of autophagy could lead to cell death (BERRY and BAEHRECKE 2007; SCOTT *et al.* 2007). For example increased levels of autophagy due to the clonal over-expression of *Atg1* in the wing disc result in increased cell death as indicated by cleaved caspase-3 staining in the *Atg-1* over-expression clones (SCOTT *et al.* 2007).

I had already shown *poly* loss of function leads to constitutive activation of autophagy in the fat body. Therefore I wanted to investigate whether loss of function of *poly* has a similar effect resulting in an increased cell death. As the generation of mosaic imaginal discs allows the comparison of the mutant versus non-mutant tissue side by side, I generated *poly* loss of function clones in eye imaginal discs. Staining of mosaic eye imaginal discs with an antibody specifically recognizing the programmed cell death marker cleaved caspase-3 revealed an increase in cleaved caspase-3 levels in *poly* mutant clones indicated by the lack of ß-galactosidase staining (Figure 4.6 A,B). Staining for cleaved caspase-3 was not detectable in the neighbouring non-mutant tissue.

This observation suggests that loss of *poly* leads to an increase in cell death. Taking into consideration evidence suggesting that increased levels of autophagy leading to increased levels of cell death, I propose that this increase in cell death is likely to be resulting from up-regulated levels of autophagy.

4.2.7 Triglyceride levels are decreased in **poly** *mutant larvae*

Drosophila has been successfully used to study metabolic regulation as fruit flies share many of the metabolic functions as mammalian organisms (BAKER and THUMMEL 2007). As discussed earlier the larval fat body, a tissue similar to mammalian liver and white adipose tissue, is the place of energy homeostasis regulation where storage of excess energy takes place in the form of glycogen and lipid. The main form of lipid storage in larval fat body is triglycerides. Not surprisingly, the break down of larval fat body and consequent release of energy allows *Drosophila* to go through metamorphosis. Activation of signalling through InR pathway promotes anabolic metabolism as well as storage of nutrient sources such as triglycerides (SALTIEL and KAHN 2001).

My previous observations suggested down-regulation of InR/TOR signalling in *poly* mutant larvae as indicated by the decrease in phosphorylation levels of Akt, S6K, 4E-BP as well as the constitutive activation of autophagy in the larval fat body. Therefore, in the next step I investigated if the down-regulation of InR/TOR activity was also reflected at the metabolic level in the storage of triglycerides. In order to assess this, a triglyceride (TAG) assay was carried out on wild type and *poly* mutant larvae. TAG levels were normalized to total protein levels to have an accurate quantification of lipids per unit of mass. In agreement with a decrease in InR/TOR signalling, triglyceride to protein ratios were found to be around half of the levels seen in the wild type larvae (Figure 4.7 A).

Lipid storage droplet 2 (LSD2) protein has been previously identified as the perilipin homologue of *Drosophila*. Lsd2 is localized on the outer membrane of lipid droplets that are the storage organelles for triglycerides (GRONKE *et al.* 2007;

TEIXEIRA *et al.* 2003). Taking into consideration the reduced TAG levels in *poly* mutants, Lsd2 levels were assessed in extracts of wild type and *poly* mutant larvae. In agreement with observation of reduced TAG levels, *poly* mutant larvae showed decreased levels of Lsd2 protein (Figure 4.7 B). Interestingly, immunoblotting on wild type extracts with Lsd2 antibody revealed multiple bands that are likely to correspond to phosphorylated states of the Lsd2 protein (WELTE *et al.* 2005). Intriguingly, the lower bands were particularly absent in *poly* mutants suggesting a possible absence of Lsd2 phosphorylation in *poly* mutants.

These results demonstrate a reduction in triglyceride storage as well as in levels of lipid droplet associated protein Lsd2 in *poly* mutant animals. Taken together these observations suggest down-regulation of anabolic metabolism in mutant animals. This is in consistence with a decrease in InR/TOR signalling whose activity promotes anabolic metabolism.

4.3 Discussion

Our data reveal an essential involvement of Poly in InR signalling, an important pathway linking the nutritional status of cells to metabolism and cell growth (BRITTON *et al.* 2002). The two kinases, Akt and S6K, are key effectors of InR/TOR signalling integrated into the pathway at two distinct levels. The Akt kinase is located upstream in this pathway and has a critical role in promoting cell growth. Dysregulation of Akt was found to be involved in various diseases such as type-2 diabetes and cancer (BELLACOSA *et al.* 2005; ENGELMAN *et al.* 2006). Phosphorylation of Akt substrates contributes to a range of cellular processes including cell growth, proliferation and survival (MANNING and CANTLEY 2007).

S6K kinase is one of the most downstream effectors of InR/TOR signalling and is subject to phosphorylation and activation by TOR. Activation of S6K leads to an increase in translation through its phosphorylation and activation of ribosomal protein S6 (WULLSCHLEGER *et al.* 2006). Furthermore, as explained in the results section, 4E-BP is another important downstream effector of InR/TOR signalling which when phosphorylated leads to an increase in cap-dependent translation (HAY and SONENBERG 2004).

Several observations suggest that Poly acts upstream in the InR signalling pathway. The phosphorylation and presumed activity of both dAkt and dS6K kinases and 4E-BP were downregulated in *poly* larvae. This would result in a decrease in InR/TOR signalling in the absence of Poly. The hypothesis that Poly acts in the activation of both dAkt and dS6K is also supported by genetic data that revealed suppression of the *poly*-induced rough eye phenotype by mutations in *dAkt* and *dS6K*. These two kinases would act as suppressors only if they are situated downstream of *poly* in the signalling pathway.

Our biochemical data revealed that Poly and InR are members of the same protein complex. Intriguingly, the level of Poly protein was decreased in *InR* larval extracts in a manner independent of transcript levels suggesting that a fraction of Poly protein may be unstable and subject to degradation in the absence of InR. Indeed, there are numerous examples of such instability if one partner of a protein complex is absent (CIAPPONI *et al.* 2004; SAVVIDOU *et al.* 2005; VASS *et al.* 2003). It should however be noted that the assessment of *poly* transcript levels shown in Figure 4.2 B was not done in a fully quantitative manner. Assessment of *poly* mRNA

by techniques such real-time PCR in the future will give a better understanding of relative in *poly* transcript levels in wild type and *InR* mutant larvae.

Autophagy is constitutively active in the fat bodies of *poly* mutant larvae. Autophagy is a multi-step, catabolic process used for nutrient recycling during development and times of starvation requiring autophagy-related *ATG* genes first identified in yeast (KLIONSKY *et al.* 2003; THUMM *et al.* 1994; TSUKADA and OHSUMI 1993), but highly conserved amongst eukaryotes. Recent studies demonstrated that over-expression of only one of these genes, *Atg1*, was sufficient to induce autophagy and inhibit cell growth in the *Drosophila* fat body (SCOTT *et al.* 2007). TOR activity is responsible for the inhibition of autophagy under cell growth promoting conditions. However, downregulation of InR/TOR signalling due to unfavourable nutritional conditions suppresses the inhibitory effect of TOR on autophagy. The observation of constitutively active autophagy in *poly* fat body is in agreement with the observation of downregulation of InR/TOR signalling as indicated by decreased phosphorylation levels of Akt, S6K and 4E-BP proteins.

I compared the *poly* mutant phenotype to that of other mutations defective in InR/TOR signalling. An extreme larval longevity phenotype has been observed in other cell growth mutants such as *Tor* (ZHANG *et al.* 2000) and the *InR* mutant (this study). The observation that a small fraction of *InR* mutant larvae that reach the third instar larval stage also develop melanotic masses highlights the phenotypic similarities of loss of function mutations in both *poly* and *InR*. This suggests that *poly* and *InR* gene products may be functionally related in the InR/TOR signalling pathway.

As mentioned earlier, two important consequences of InR signalling activity are the promotion of cell growth and metabolism. Here, I show evidence that anabolic metabolism is down-regulated in *poly* loss of function mutants as suggested by decreased triglyceride levels as well as decreased levels of lipid droplet associated protein Lsd2. Importantly the absence of lower molecular weight bands in mutant extracts suggested that the phosphorylation of Lsd2 might specifically be reduced in *poly* mutants. As part of future work, it will be important to determine whether this observation indeed reflects a reduction of specifically phosphorylated versions of Lsd2. This could be achieved by phosphatase addition to protein extracts followed by immunoblotting with Lsd2 antibody in order to determine whether levels of Lsd2 appear similar in wild type and mutant extracts upon the loss of phosphorylation.

Furthermore, reduced tissue sizes, such as the small larval brain and imaginal discs, are likely to result from a defect in cell growth as cell proliferation did not appear to be directly affected in the mosaic clonal analysis in the eye imaginal disc as described in Chapter 3. Although a qualitative assessment by microsocopy of the cell size in tissues such as the fat body allows me to conclude that cell size in *poly* mutants appear to be reduced, a more quantitative approach for the assessment of cell size is needed in order to definitively conclude the effect of *poly* loss of function on cell size. I have tried to obtain a quantitative assessment of cell size by carrying out a flow cytometry approach on larval brains as other groups have previously used this technique on larval brains as well as imaginal discs (HENNIG *et al.* 2006; PAGE *et al.* 2005). Unfortunately this technique has proven to be unsuccessful in my hands due to the difficulties in dissociating the brain tissue into single cells by trypsinization.

Overall my results suggest that Poly is a novel interactor of InR in *Drosophila* and that *poly* loss of function results in down-regulation of InR/TOR signalling as revealed by the decrease in activity of various downstream effectors of this pathway. I propose that Poly is situated upstream in the InR/TOR signalling pathway and that it forms a protein complex with InR upon activation of the signalling. The important consequence of this interaction is the positive regulation of the signalling via InR/TOR pathway therefore Poly acts as a positive regulator of InR/TOR signalling. However, it should be noted that the mass spectrometry analysis that revealed the formation of a complex between InR and Poly was carried out on immunoprecipitates prepared from embryonic extracts. Embryonic extracts naturally contain both activated and non-activated forms of InR. Therefore in order to confirm this hypothesis, it will be essential in the future to determine at which activation state of the InR/TOR signalling the complex formation between InR and Poly takes place. This important point could be addressed by carrying out insulin stimulation experiments on *Drosophila* S2 cell culture followed by mass spectrometry analysis. The analysis of protein complex formation of Poly on pre- and post-insulin stimulated S2 cells would allow us to determine whether the protein complex containing InR and Poly is indeed forming upon the activation of the signalling.

Chapter 5: Investigation of Poly levels and distribution in *Drosophila* and human cells following activation of the InR/TOR pathway

5.1 Introduction

Linking cell growth and metabolism to environmental cues is an essential process that multicellular organisms need to accomplish successfully for normal development. Nutrient levels in the cellular environment show fluctuations leading therefore to continuous cycles of growth stimulatory and starvation conditions for the organism. For example following feeding, the increase in glucose levels leads to a rise in insulin levels which in its turn leads to a number of metabolic triggers that result in glucose storage. However during the converse fasting state, the reduction in insulin levels leads to glucose production in the liver. Therefore signalling through the InR/TOR pathway has evolved so that it can respond promptly to rapid changes in nutrient levels taking place in the environment (PUIG *et al.* 2003).

It has been previously shown that there are dynamic changes at the levels as well as subcellular localisation of various components of the InR/TOR pathway depending on the activity of the signalling via this pathway (PUIG *et al.* 2003; PUIG and TJIAN 2005; VALOVKA *et al.* 2003). It is likely that these changes take place in order to allow cells to respond to fluctuations of nutrients. An interesting example of this is the regulation of the subcellular localisation of the transcription factor Foxo in response to the activation of InR. Upon activation of InR signalling by insulin binding, Foxo is phosphorylated by Akt leading to its retention in the cytoplasm.

This leads to transcriptional down-regulation of Foxo target genes. However, decrease of the InR signalling activity leads its translocation into the nucleus where it can activate the transcription of its target genes (PUIG *et al.* 2003).

Interestingly, *4E-BP* and *InR* are amongst various target genes of Foxo. Expression levels of *4E-BP* and *InR* are regulated by Foxo action. As explained in Chapter 4 transcriptional up-regulation of *4E-BP* reflects down-regulation of cell growth and metabolism (PUIG *et al.* 2003). The case of the regulation of *InR* transcription by Foxo activity is also intriguing. The increase of *InR* expression levels by Foxo transcriptional activity under starvation conditions leads to an increase in InR at the cell membrane. The cell becomes more "sensitized" allowing a rapid response to changes in insulin-like peptide levels in the environment (PUIG and TJIAN 2005).

Taking such examples into consideration, that suggest that cellular distribution and levels of various InR/TOR signalling components might be affected by the activity levels of this pathway, and the biochemical and genetic data that suggested involvement of Poly in InR/TOR signalling, I decided to investigate if the cellular Poly levels and/or subcellular localization were changed following the activation of InR/TOR signalling. I started this investigation by analysing cellular levels and distribution of the human homologue of Poly in HeLa cells by immunofluorescence followed by similar analysis on *Drosophila* hemocytes.

5.2 Results

5.2.1. HsPoly staining in HeLa cells appears to redistribute and/or increase following insulin stimulation

Our mass spectrometry data suggested physical interaction of Poly with InR. The involvement of Poly in InR/TOR signalling was further confirmed by genetic interaction of Poly with downstream components of InR signalling and the dysregulation of their activity following *poly* loss of function in *Drosophila*. I next wanted to assess whether Poly levels in the cell were dependent on activity of InR. As mentioned earlier, Poly also has a human homologue (denoted HsPoly) (Figure 1.11) and InR/TOR signalling is well conserved from flies to higher eukaryotes. Human cell lines offer clearer morphology (as they are larger) than *Drosophila* cells to visualize various subcellular compartments by immunofluorescence. Therefore I decided to carry out analysis of the effect of the insulin stimulation on protein levels and subcellular localization of Poly in HeLa cells by using an antibody raised to HsPoly.

I carried out a time course experiment during which overnight serum-starved HeLa cells were stimulated with insulin for 60 and 90 minutes. Interestingly, staining for HsPoly appeared to be significantly brighter following insulin stimulation. This increase of HsPoly staining was already apparent following 60 minutes of stimulation and appeared maximal following insulin treatment for 90 minutes (Figure 5.1 A). As HeLa cells offered a suitable morphology to distinguish different cellular compartments, it appeared that this increase in HsPoly levels was more concentrated near the nuclear area of cells.

To determine whether this increase in HsPoly staining following insulin stimulation was dependent on TOR inhibition, I incubated HeLa cells with rapamycin during the overnight starvation prior to treatment with insulin. Indeed, rapamycin treatment prevented the increase in HsPoly staining following insulin stimulation (Figure 5.1 B). HsPoly remained evenly distributed throughout the cytoplasm and nucleus even following 90 minutes of insulin treatment in cells that had been previously incubated with rapamycin.

Taken together, these observations suggest that the increase in HsPoly concentrated in the nuclear area is responsive to the stimulatory action of insulin in a TOR dependent manner. Importantly, these results further suggest a possible role for Poly in InR/TOR signalling, not only in *Drosophila*, but also in human cells.

I had planned to carry out further analysis of the levels and distribution of HsPoly following insulin stimulation under various InR/TOR signalling inhibitory conditions by immunofluorescence and by immunoblotting on HeLa cells, as they offer an easily tractable system to carry out such cell biology experiments. However unfortunately, the antibodies generated against HsPoly were detoriated due to their unsuitable storage at this early stage of my experiments. Therefore, I had to carry out the remaining part of my analysis on *Drosophila* cells.

5.2.2 Poly staining in Drosophila larval hemocytes appear to increase following insulin stimulation

Insulin stimulation experiments carried out on HeLa cells showed a dramatic change in HsPoly staining following insulin stimulation in a rapamycin sensitive manner. I next wanted to assess whether *Drosophila* Poly levels in the cell were

dependent on activity of InR in *Drosophila* cells too. To this end, a timecourse experiment was set up whereby wild type larval hemocytes were isolated by bleeding early third instar larvae. Hemocytes were then stimulated with 200 nM insulin for 75 minutes. Interestingly, the staining for Poly was significantly increased following insulin stimulation for 75 minutes as revealed by the immunofluorescence data (Figure 5.2).

The experiment was repeated, but this time by starving the larvae for 3 hours in 20% sucrose solution prior to bleeding. The purpose of the larval starvation was to mimic the overnight serum starvation carried out on HeLa cells and to achieve the inactivation of the pathway prior to insulin stimulation in order to determine if this had a greater effect on Poly distribution. Hemocytes were then stimulated with 200 nM insulin for 15 and 75 minutes. Interestingly, staining for Poly was increased at both 15 minute and 75 minute time points (Figure 5.3).

This observation suggested that activation of signalling via InR by insulin action leads to an increase in Poly staining in *Drosophila* hemocytes. This increase in Poly staining appears to be a quick response that is detectable following only 15 minutes of insulin stimulation.

5.2.3 Poly staining in Drosophila larval hemocytes appears to increase following constitutive activation of InR

Results described above revealed that Poly staining in the cell increases following insulin stimulation. In a complementary experiment, Poly levels were assessed in hemocytes expressing a constitutively active form of InR. A single amino acid change (A1325D) in *Drosophila* InR leads to its constitutive activation

(DIANGELO *et al.* 2009). Therefore, the over-activation of InR signalling in the larval hemocytes was achieved by expressing the *UAS-InR*^{A1325D} transgene under the control of the Hml-Gal4 driver. Interestingly, hemocytes over-expressing the constitutively activated form of InR showed increased staining for Poly particularly localized near the nuclear area that was similar to observations obtained in HeLa cells following the stimulation with insulin (Figure 5.4, immunofluorescence on these cells was carried out by the MSc student Mei Xuan Lye). Interestingly, hemocytes over-expressing a constitutively active form of InR were strikingly increased in size (Figure 5.4B) compared to control hemocytes (Figure 5.4A). This observation is in agreement with the growth promoting downstream effects of the activation of InR/TOR signalling.

This result suggests that similarly to what is observed upon insulin stimulation, over-expression of the constitutively active form of InR leads to an increase in Poly staining. Importantly this increase of staining is concentrated near the nuclear are similar the observations obtained from the analysis of the HsPoly localisation upon stimulation of HeLa cells.

5.2.4 Immunoblotting on fat body and whole larval extracts suggest that Poly levels are increased upon constitutive activation of InR in the fat body

I have tried to carry out immunoblotting on hemocytes isolated from larvae in order to link the immunofluorescence data to total protein levels. However unfortunately immunoblotting attempts on hemocytes have not been very successful in my hands due to limited number of hemocytes that I was able be isolated from larvae, therefore not giving enough protein levels to be detected on immunoblots.

Therefore in a complementary approach, I have decided to carry out immunoblots on larvae over-expressing constitutively activated form of InR in their fat bodies. The over-activation of InR signalling in the larval fat body was achieved by expressing the *UAS-InR*^{A1325D} transgene under the control of the Cg-Gal4 driver. Poly protein levels were assessed by immunoblotting whole larval protein extracts as well as extracts prepared from dissected larval fat bodies. Strikingly, Poly protein levels were higher in whole larval and fat body extracts isolated from animals over-expressing the constitutively active form of InR compared to control animals (Figure 5.5).

This observation suggests that the levels of Poly are dependent on activation of signalling via InR. More importantly, there is a positive correlation between Poly protein levels and the activity of InR. This might reflect a positive feedback loop whereby Poly levels are up-regulated following the activation of signalling via InR. Furthermore, this result is particularly intriguing taking into account my previous observation that revealed a significant decrease in Poly levels in larvae mutant for *InR* (Chapter 4, Figure 4.2.A).

5.3 Discussion

I have detected an increase in Poly staining by immunofluorescence following activation of InR/TOR signalling in two different systems including *Drosophila* and human cells. A possible explanation for this observation would be an active translocation of Poly following insulin stimulation and therefore the activation of the InR/TOR pathway, leading to its localization in or closer to the nuclear area, thus explaining the intense HsPoly staining observed in insulin

stimulated HeLa cells as well as in hemocytes over-expressing constitutively active form of InR. In this case, we could speculate an active role for Poly in the nucleus, such gene expression regulation, following activation of the InR pathway. This would be the opposite situation to the one observed for Foxo transcription factor which is excluded from the nucleus following the activation of InR/TOR signalling. Another possible explanation for the observed immunofluorescence results could be an overall increase in total Poly protein levels. Also, a combination of both of these possible mechanisms –a movement into the nucleus as well as an increase in total protein levels- could be contributing to observed in increased staining. Immunoblotting on stimulated HeLa cells and hemocytes is an important experiment that needs to be achieved successfully in order to determine the contribution of a potential increase in total protein levels to observed increase in staining.

However, I carried out immunoblotting on larvae over-expressing the constitutively active form of InR in the fat body. Immunoblotting results revealed an increase in Poly in larvae expressing constitutively active form of InR. This suggests that in the fat body, over-activation of InR/TOR signalling leads to an increase in total Poly protein levels. Therefore, in a similar way an increase in overall Poly protein levels might be contributing, at least partly, to observed increase in Poly staining by immunofluorescence.

Overall these observations suggest that staining and distribution of Poly in both *Drosophila* and human cells are dependent on activity of InR signalling. Interestingly, the increase in Poly staining appears to be mostly localised near the nuclear area in insulin stimulated HeLa cells and hemocytes over-expressing the constitutively active form of InR. Also the over-expression of the constitutively

active form of InR in the larval fat body results in increased total Poly protein levels by immunoblotting which suggests that Poly protein levels can be dependent on the activity levels of InR/TOR signalling. Importantly, similar results obtained in both *Drosophila* and human cells led me to speculate that HsPoly might have a similar role in promoting InR signalling in human cells. This is a significant finding deserving further investigation.

Taking into consideration the biochemical, genetic and cell biology data discussed in Chapter 4 and the results discussed in this Chapter, I propose that the change in cellular distribution and levels of Poly upon insulin stimulation might be necessary for Poly to accomplish its role as a positive regulator of InR/TOR pathway. Importantly, the striking increase in HsPoly staining following insulin stimulation of HeLa cells and the increase in nuclear Poly localisation in hemocytes over-expressing the constituvely active form of InR, might be reflecting an active role for Poly in the nucleus. I speculate that the mechanism of action for Poly as a positive regulator of InR/TOR signalling may involve a function for Poly in the nucleus, such as transcription, and that Poly may be exerting its cell metabolism and growth promoting effects via its role in the nucleus.

Chapter 6: Investigation of the potential involvement of Poly during the cellular and innate immune response in *Drosophila*

6.1 Introduction

As described in detail in my Introductory Chapter, *Drosophila* is equipped with a sophisticated innate immune system that makes it a suitable model organism to study various signalling pathways and cellular processes involved in the immune response. The innate immune response in *Drosophila* can be divided into two main branches: cellular immune response and humoral immune response. *Drosophila* blood cells -or hemocytes- are the main mediators of the cellular immune response against invading pathogens (WILLIAMS 2007) whereas Imd and Toll pathways are the two important signalling pathways involved during the humoral immune response (HOFFMANN 2003; HOFFMANN and REICHHART 2002). Additionanl evidence suggests that infection by Gram-negative bacteria results mainly in activation of the Imd pathway, whereas Gram-positive bacteria or fungal infection strongly stimulates Toll signalling. Activation of the Imd and/or Toll pathways leads to transcription of a set of genes encoding antimicrobial peptides (AMPs) such as *attacin, diptericin* and *drosomycin* (HOFFMANN 2003; HOFFMANN and REICHHART 2002).

poly mutants are characterized by the development of melanotic masses in their body cavity at third instar larval stage. Development of melanotic masses has been previously linked to dysregulation of signalling pathways involved in the *Drosophila* immune response and/or processes involved in hemocyte formation (LEMAITRE *et al.* 1995b; MINAKHINA and STEWARD 2006; NAPPI *et al.* 2005).

Furthermore, microarray analysis suggested up-regulation of a number of genes involved in immunity upon *poly* loss of function (Heck lab, unpublished data). Therefore I decided to investigate whether Poly function might be involved during the innate immune response in *Drosophila*. Investigation of Poly function during both cellular and humoral immune responses was carried out during this study. Analysis of the cellular immune response was carried out on *poly* mutant larvae whereas the main part of the investigation of the humoral immune response was carried out on a *poly* over-expression background in adult flies. Results that I will be describing in this Chapter show that both cellular and humoral immune responses are affected upon *poly* loss of function and over-expression respectively, thus suggesting an involvement of Poly in *Drosophila* immunity.

6.2 Results

6.2.1 Actin staining of hemocytes isolated from poly *mutant larvae reveals cells morphologically similar to lamellocytes*

poly mutant larvae are characterized by the appearance of melanotic masses in the third instar larval body cavity. The appearance of melanotic masses was previously linked to aberrations in pathways involved in *Drosophila* immune response and various studies have reported the involvement of *Drosophila* blood cell mediated immune response in the formation of melanotic masses (LAVINE and STRAND 2002). In fact, it was shown that the melanotic mass phenotype observed in *Toll* gain of function and *cactus* loss of function mutants can be attributed to the

over-proliferation of larval hemocytes (LAVINE and STRAND 2002; LEMAITRE *et al.* 1995b; QIU *et al.* 1998).

Taking into consideration the prevalence of melanotic masses in *poly* mutants and the involvement of hemocytes during formation of melanotic masses in *Drosophila* larvae, I decided to investigate whether *poly* loss of function resulted in abnormalities in larval hemocyte formation and/or differentiation. To examine the morphology of hemocytes, third instar larvae were bled onto microscope slides and hemocytes were stained with phalloidin to visualize the actin cytoskeleton. Phalloidin staining of wild type hemocytes revealed cells that were round in appearance (Figure 6.1A). As expected, these round cells correspond to the previously published morphology of plasmatocytes, which are the largest population of hemocyte subtype observed in healthy larvae. Interestingly, actin staining on *poly* hemocytes revealed the appearance of a great number of cells that were much larger in size (Figure 6.1B). The appearance of these large cells was consistently observed in numerous bleeds isolated from *poly* mutant larvae. The morphology of the large cells observed in *poly* mutant hemocytes was very similar to the morphology of previously published lamellocytes (TOKUSUMI *et al.* 2009; WILLIAMS 2009), suggesting that *poly* loss of function might be leading to an abnormal lamellocyte differentiation in non-parasitized larvae. Although extensive cell counts to determine the exact number of cells belonging to two different classes of hemocyte morphology in *poly* mutants was not performed, I was able to see that lamellocyte-like shaped cells occurred consistently at high frequency (around ~50% of the total hemocyte population) in the hemolymph isolated from all *poly* mutants. However,

cells with lamellocyte like morphology were never observed in the hemolyph isolated from wild type larvae.

6.2.2 **poly** *mutation leads to increased number of hemocytes*

Interestingly, a semi-quantitative observation of hemocytes isolated from both wild type and *poly* mutant larvae suggested that total hemocyte numbers isolated from *poly* larvae were higher than hemocyte numbers isolated from wild type larvae (Figure 6.2A). In order to quantitate hemocyte numbers for each genotype, control and *poly* mutant larvae were bled and hemocytes isolated from each genotype were counted by after DAPI staining. Cell counts were carried out on a large number of larvae for each genotype, in order to have a statistically significant estimation of cell numbers for both wild type and *poly* larvae. Interestingly, hemocyte numbers isolated from *poly* larvae appeared to be significantly increased compared to hemocyte numbers isolated from wild type larvae (Figure 6.2B, Cell counts presented in this Figure were carried out by a MSc by Research mini-project student, Swati Naidu). However, it should be noted that the observed difference in cell counts might be resulting from different adhesive properties of hemocytes isolated from larvae of two different genotypes. As described in the Material and Methods chapter, hemocytes are allowed to adhere to coated slides by incubating them in PBS for one hour. In the future in order to rule out the possibility of hemocyte from two different genotypes having different adhesive properties, it will be important to observe by phase microscopy the PBS solution containing the larval hemolymph post-incubation. This would allow us to determine the relative abundance of hemocytes in the post-incubation hemolymph and to determine the

relative adhesive properties of hemocytes isolated from each genotype. A more accurate conclusion can then drawn concerning the relative hemocyte abundance isolated from each genotype.

6.2.3 **poly** *mutation results in the appearance of lamellocytes in the absence of pathogen invasion*

Actin staining revealed the appearance of large hemocytes in *poly* larvae that were morphologically similar to lamellocytes. In order to confirm that these cells were indeed lamellocytes, immunostaining using an antibody that specifically recognizes lamellocytes was carried out on hemocytes isolated from control and *poly* larvae. The L1 antibody recognizes Attila-L1 that was previously shown to be a lamellocyte specific marker (HONTI *et al.* 2009; KURUCZ *et al.* 2007). In agreement with previously published data hemocytes isolated from wild type larvae showed little, if any, staining for L1 antibody suggesting the absence of lamellocytes in healthy larvae (Figure 6.3A). Interestingly, in agreement with our previous actin staining of *poly* hemocytes, a great number of hemocytes isolated from *poly* larvae were positive for the L1 antigen suggesting the presence of lamellocytes in *poly* mutants (Figure 6.3B). This result suggests that *poly* loss of function leads to the aberrant appearance of lamellocytes in *poly* mutant larvae even in the absence of any invading pathogen.

6.2.4 **poly** *mutants fail to encapsulate wasp eggs following parasitisation*

Drosophila hemocytes are responsible for the removal of foreign organisms by phagocytosis or encapsulation. As outlined in my Introductory Chapter, upon insertion of eggs of the parasitic wasp *Leptopilina boulardi* into the hemocoel of second instar larvae, an encapsulation reaction that engages all three subtypes of hemocytes is triggered. Encapsulation leads to a coating generated by hemocytes around the wasp egg, isolating it from the rest of the larval body cavity. Earlier steps of the encapsulation process involves the release of plasmatocytes from the lymph gland and possibly from a sessile compartment located beneath the larval cuticle (CARTON and NAPPI 1997; WILLIAMS 2007).

Investigation of hemocyte numbers, morphology and subtypes isolated from *poly* third instar larvae revealed an increased number of total hemocytes as well as the unexpected presence of lamellocytes in non-parasitsed mutant larvae. Thus as a next step, I wanted to investigate whether the cellular immune response mediated by hemocytes was affected in *poly* mutant larvae. A direct way of testing the functionality of *poly* mutant hemocytes is to carry out a wasp parasitisation experiment, followed by an encapsulation assay. Therefore, wild type and *poly* homozygous mutant as well as *poly* heterozygous second instar larvae were parasitized by the avirulent *Leptopilina boulardi* wasp strain G486. Following 30-40 hours of parasitisation, third instar larvae were dissected and the presence of the wasp egg as well as the melanisation state of the wasp egg were scored. Melanisation of the wasp egg is considered as a successful encapsulation reaction. Melanised capsules surrounding wasp eggs were easily detected in the hemocoel of wild type control larvae as well as heterozygous $poly^{05137}$/TM6B larvae. Strikingly,

melanisation did not take place around the wasp eggs laid in the hemocoel of *poly* homozygous larvae (Figure 6.4, the encapsulation assay presented in this figure was done in collaboration with Dr. Michael J. Williams, University of Aberdeen).

The lack of melanization around the wasp eggs found in the hemocoel of *poly* mutants suggests that *poly* loss of function leads to a strong defect in encapsulation of *Leptopilina boulardi* wasp eggs in parasitized larvae. This is particularly surprising taking into consideration 1) the increased number of hemocytes, and 2) especially the presence of lamellocytes in non-parasitized *poly* larvae.

6.2.5 Microarray analysis and quantitative PCR in **poly** *mutant larvae suggest up-regulation of genes involved in the humoral immune response in* **Drosophila**

Microarray analysis is a powerful approach for identifying differential gene expression and it was previously successfully employed in *Drosophila* (TELEMAN *et al.* 2008; ZINKE *et al.* 2002). As at the start of my PhD project, we did not have any information about the pathways and processes that Poly might be involved in, we have decided to adopt an unbiased approach to identify differential gene expression between the wild type and *poly* mutant third instar larvae to obtain directions about the cellular processes and pathway that it might be involved in. Therefore microarray analysis was carried out in order to identify genes that were differentially expressed in early third instar *poly* mutant larvae compared to wild type larvae. Interestingly, analysis of the differentially expressed genes revealed that a number of genes involved in the humoral immune response in *Drosophila* were up-regulated in *poly* mutants (Figure 6.5). Taking into consideration the appearance of melanotic masses in *poly* homozygous mutant larvae and the observed defect during the cellular

immune response, I decided to further investigate the potential involvement of Poly during humoral immunity in *Drosophila*.

I have my investigation by confirming via real-time PCR the microarray data that suggested differential expression of various genes involved in innate immune response in *poly* mutants.

Relish (rel) is the NF-κB transcription factor that is activated upon stimulation of the Imd pathway (LEMAITRE *et al.* 1995a). In agreement with microarray data, real-time PCR revealed a close to two-fold increase in *rel* transcript levels in *poly* mutant larvae compared to wild type larvae (Figure 6.6).

Diptericin (dpt) and *Attacin A (attA)* are two antimicrobial peptide-encoding genes that are transcribed in response to transcriptional activation of the Imd pathway (GEORGEL *et al.* 1993; LEMAITRE *et al.* 1995a). Therefore, the activation of the Imd pathway leads to transcription of *dpt* and *attA* via Rel activity. Assessment of *attA* and *dpt* mRNA levels by real-time PCR revealed up-regulation of both genes in *poly* mutant larvae, thus confirming the microarray data (Figure 6.7).

Drosomycin (drs) is another antimicrobial peptide involved in *Drosophila* immunity (LEMAITRE *et al.* 1995b). Transcription of *drs* is activated upon the stimulation of Toll signalling. Given that *drs* levels were found to be up-regulated in *poly* larvae during the microarray analysis, attempts were made to quantify transcription levels of *drs* in wild type and *poly* larvae. Unfortunately, I was not able to obtain a definitive answer from these experiments as various primer and probe combinations that were used in these real-time PCR experiments did not give a reliable standard curve, making it therefore impossible to draw a reliable conclusion out of these experiments.

These observations suggest that both microarray and quantification of gene expression by real-time PCR show up-regulation of *rel, dpt,* and *attA* which are all mediators of signalling via the Imd pathway.

6.2.6 poly *over-expression in hemocytes results in susceptibility to* Salmonella typhimurium *infection*

Taking into consideration the microarray and real-time PCR results that revealed an increased expression of immunity related genes in *poly* mutants, I decided to investigate whether alteration of Poly function would affect *Drosophila* immunity *in vivo* by monitoring the survival of flies following pathogen infection. The microarray analysis and real-time PCR were carried out on *poly* mutant larvae. Unfortunately it was not possible to carry out similar survival investigations on the mutant background as the $poly^{05137}$ allele is larval lethal. Therefore survival analysis was carried out on *poly* over-expression background to achieve alteration of normal Poly levels. To this end, a *UAS-poly* transgene was over-expressed in *Drosophila* hemocytes under the control of the hemocyte specific *Hml-Gal4* driver. Survival of flies following infection by three different bacterial pathogens was monitored.

Flies over-expressing Poly in hemocytes (*Hml-Gal4>UAS-poly*) and control flies (*Hml-Gal4> UAS-GFP* and *Hml-Gal4> +*) were injected with Gram-negative pathogen *Salmonella typhimurium* overnight cultures. Survival of flies corresponding to each genotype was monitored over the following days. During the course of the same experiment, flies from each genotype were injected with LB broth alone as a control. A dramatic decrease in the survival of flies over expressing *UAS-poly* in hemocytes was observed following 24 hours post-injection (Figure 6.8). At

the 24 hour time point, control flies of genotypes *Hml-Gal4> UAS-GFP* and *Hml-Gal4> +*, showed around 65% and 75% of survival respectively, whereas the survival of flies over-expressing *UAS-poly* under the control of hemocyte specific driver was around 30%. Similarly, at 48 hours post-injection, the survival of flies over-expressing *poly* in the hemocytes fell to 25% whereas the survival of control flies remained significantly higher. Flies injected with LB broth alone did not show any significant change in their survival rate over the course of the experiment remained around (their survival rate remained high, ~90-100%). Taken together, these observations suggest that *poly* over-expression in hemocytes results in sensitivity to *Salmonella typhimurium* infection.

6.2.7 **poly *over-expression in hemocytes does not affect survival following* Entereococcus faecalis *infection***

In my next approach, the effect of *poly* over-expression on survival following infection by the Gram-positive pathogen *Enterococcus faecalis* was investigated. In order to investigate whether *poly* over-expression had an affect on survival following *Entereococcus faecalis* infection, control flies (of genotypes *Hml-Gal4> UAS-GFP* and *Hml-Gal4> +*) and flies over-expressing *poly* in hemocytes (*Hml-Gal4> UAS-poly*) were injected with *Enterococcus faecalis* cultures grown in LB broth (with OD= 0.35). Interestingly, the survival of flies in all three genotypes appeared to be similar during the course of the experiment. Though, strikingly both flies over-expressing *poly* in the hemocytes and control flies showed a decline in their survival as soon as 5 hours post-infection (Figure 6.9). The survival of flies was monitored over a total of 9 hours which did not reveal a difference between the survival of flies

over-expressing *poly* in the hemocytes versus control flies. These results suggest that *poly* overexpression in the hemocytes does not affect survival of flies following *Enterococcus faecalis* infection.

6.2.8 poly *over-expression in hemocytes results in susceptibility to* Pseudomonas aeruginosa *infection*

poly over-expression in hemocytes resulted in sensitivity to the Gram-negative pathogen *Salmonella typhimurium*, however it did not have appear to have an effect on the survival following infection by the Gram-positive bacteria *Enterococcus faecalis*. In order to determine whether the sensitivity of flies over-expressing *poly* in the hemocytes is specific to Gram-negative bacteria, infection experiments were carried out using another Gram-negative pathogen, *Pseudomonas aeruginosa*. As the success of *Pseudomonas* "oral infection" was previously published by other groups (AVET-ROCHEX *et al.* 2005; AVET-ROCHEX *et al.* 2007; BERGERET *et al.* 2008), flies were fed with bacterial broth (OD=0.70) mixed with sterile sucrose solution at 1:1 dilution. Sterile sucrose solution diluted in LB broth alone was used in control experiments. *Pseudomonas aeruginosa* oral infection resulted in significant sensitivity of flies over-expressing *poly* in hemocytes compared with control flies of genotype *Hml-Gal4> UAS-GFP* and *Hml-Gal4> +* (Figure 6.10). At around 20 hours post-infection, the survival rate of *poly* over-expressing flies dropped to around 60%, whereas the survival of control flies remained at 100%. The survival of flies over-expressing *poly* in hemocytes appeared to decrease significantly compared with control flies over a total of 58 hours post-

infection. These observations suggest that Poly over-expression in hemocytes leads to sensitivity to *Pseudomonas aeruginosa* introduced by feeding.

Taken together, these observations suggest that *poly* over-expression results in sensitivity to Gram-negative bacteria as suggested by decreased survival rates following *Salmonella typhimurium* and *Pseudomonas aeruginosa* infections. However *poly* over-expression does not have any consequences on sensitivity and/or resistance to Gram-positive bacteria as the survival rates remain the same following infection by *Enterococcus faecalis*.

6.2.9 Investigation of attA *levels following* Pseudomonas aeruginosa *feeding*

Over-expression of *poly* in hemocytes leads to sensitivity to Gram-negative bacteria. Gram-negative bacterial infection leads to strong stimulation of the Imd pathway. The larval fat body and plasmatocytes are involved in synthesis of antimicrobial peptides (AMPs) in response to pathogen infection. As mentioned earlier, *attA* and *dpt* are two AMPs transcribed in response to the Imd pathway activation (GEORGEL *et al.* 1993; LEMAITRE *et al.* 1995a). Therefore, I hypothesized that over-expression of *poly* in hemocytes might be interfering with AMP synthesis resulting in the observed sensitivity to Gram-negative infection.

In order to investigate whether AMP levels were affected by poly over-expression, *attA* levels were quantified by real-time PCR before and 18 hours after the oral infection with *Pseudomonas aeruginosa* in control flies and flies over-expressing *poly* in their hemocytes. As expected *attA*, levels were significantly increased in control flies 18 hours following infection. Surprisingly, *attA* expression levels also significantly increased at 18 hours post-infection in flies over-expressing

poly suggesting that AMP induction following bacterial infection was not affected in these flies (Figure 6.11). However, the induction of *attA* levels seemed to be greater in controls compared to flies over-expressing *poly*. The *attA* levels appeared to be induced by 5 to 6 fold in control flies, whereas the induction of *attA* was only around 2 fold in flies over-expressing *poly*. Therefore, in order to investigate the relative induction of *attA* in control flies and flies over-expressing *poly* in their hemocytes, *attA* levels obtained post-infection were normalized to basal *attA* levels corresponding to each genotype. Interestingly, the analysis of *attA* expression showed that *attA* increased to a less extent in flies over-expressing *poly* compared to control flies (Figure 6.12). Indeed, the induction of *attA* appeared to be significantly different between the two genotypes.

Therefore, although the expression of *attA* is induced in both control flies and flies over-expressing *poly* in their hemocytes, the extent of this induction is greater in control flies. The limited induction of *attA* could be contributing to the sensitivity of flies over-expressing *poly* in hemocytes to Gram-negative bacteria infection.

6.3 Discussion

Results described in this Chapter suggest that normal levels of Poly are required for functional immunity in *Drosophila*. I investigated function of Poly during both cellular and humoral immune responses *in vivo* by examining both *poly* mutant and over-expression background, respectively.

The cellular immune response is impaired in *poly* mutant larvae as suggested by the failure of encapsulation of parasitic wasp eggs. This failure is observed despite the increased number of hemocytes and the constitutive appearance of

lamellocytes that are important mediators of the encapsulation process. A possible explanation for the lack of encapsulation could be a functional defect of lamellocytes produced in *poly* non-parasitised larvae. This would suggest that although lammellocyte differentiation is readily taking place even in the absence of an invading pathogen, these lamellocytes abnormally present in *poly* mutant larvae are actually not able to fulfil their functional requirements upon pathogen invasion. Alternatively, since the lamellocytes are already present in the hemolymph, the failure to encapsulate following parasitisation could be attributed to a functional defect of plasmatocytes. The adhesion of plasmatocytes is an essential step during the encapsulation of wasp eggs and mutants that fail to successfully complete plasmatocyte adhesion were shown to also exhibit encapsulation defects following parasitisation (IRVING *et al.* 2005). Therefore, failure of *poly* mutant plasmatocytes to adhere to the surface of wasp eggs could be another possible explanation for the observed encapsulation defect. As part of future work, a direct way of testing this hypothesis will be to carry out staining using plasmatocyte specific antibodies on wasp eggs isolated from the hemocoel of *poly* mutants to determine whether plasmatocytes can be detected on the surface of wasp eggs.

The lethality of *poly* mutants at the larval stage led me to investigate the function of Poly during the humoral immune response in adults over-expressing *poly* rather than the *poly* mutant background. Survival analysis of flies following three different bacterial pathogens suggested that over-expression of Poly in hemocytes resulted in increased sensitivity to Gram-negative bacterial infection. Imd signalling is strongly induced upon Gram-negative bacterial invasion. Therefore, I hypothesized that the failure to fight Gram-negative bacterial infection in *poly* over-

expressing flies might be due to a failure to suitably activate the Imd pathway. However, quantitative assesement of *attA* expression levels as a read-out of the activity of the Imd pathway revealed that *attA* expression was increased both in control flies and flies over-expressing *poly*. The extent of this increase appeared to be less in *poly* over-expressing flies, thus possibly acting as a contributing factor to their increased sensitivity to Gram-negative bacteria.

Hemocytes in adult *Drosophila* are also responsible for the phagocytosis and internalisation of pathogens (BERGERET *et al.* 2008). Therefore, another possible contributing factor for the reduced survival rate of flies over-expressing *poly* in their hemocytes following Gram-negative bacterial infection could be the failure to internalize and phagocytose the invading pathogen. This hypothesis could be tested by performing a quantitative phagocytosis assay on *Hml-Gal4 >UAS-poly* hemocytes using fluorescently labelled pathogens. In fact, this work is ongoing in order to optimize a quantitative phagocytosis assay to determine whether altering Poly levels in hemocytes leads to a defect in phagocytosis.

Taken together, my observations suggest the involvement of Poly in cellular and humoral immunity in *Drosophila*. Interestingly, the defect in cellular in immune response was detected upon *poly* loss of function, whereas the defect in humoral immune response was observed following *poly* over-expression in adult hemocytes. Therefore I speculate that the fine-tuning of Poly levels in *Drosophila* hemocytes might be needed in order to accomplish a successful immune response. In order to determine whether normal Poly levels are needed for a successful immune response, as part of future work it would be necessary to investigate whether the over-expression of *poly* in hemocytes results also in an alteration of the cellular immune

response in larvae. Furthermore, investigation of the sensitivity/resistance to bacterial infection in adult flies that lack *poly* specifically in hemocytes is an avenue of future investigation. However, the survival analysis of flies specifically lacking *poly* in their hemocytes will require the generation of transgenic flies that bear an RNAi construct for *poly*. Unfortunately Poly RNAi flies are currently not available from existing stock centres, though they may become available in the future.

Chapter 7: Generation of reagents for the study of HsPoly

7.1 Introduction

Availability of powerful reagents, such as antibodies and plasmid constructs, is essential for successful conduction of various cell biology experiments. In fact, the availability of high affinity antibodies raised against recombinant his-tagged *Drosophila* Poly was key to identification of the physical interaction of Poly with InR as revealed by the immunoprecipitation and mass spectrometry analysis described in Chapter 4. Antibodies that had previously been generated in the Heck laboratory against HsPoly and that were used in insulin stimulation experiments on HeLa cells (described in Chapter 5) had unfortunately deteriorated over storage. Therefore, in order to be able to carry out functional characterization of the human homologue of Poly, I decided to generate tagged HsPoly constructs and additional antibodies recognizing HsPoly. The availability of such reagents for HsPoly would allow us to analyse cellular localisation of the protein therefore giving insights into the function of HsPoly in the cell, as well as to investigate potential interacting protein binding partners. Importantly, these experiments would make it possible to further characterize the interaction of Poly with InR signalling in a mammalian system which would be complementary to the work carried out in *Drosophila*. In this chapter I will describe the generation and primary characterization of peptide antibodies and tagged plasmid constructs of HsPoly.

7.2 Results

7.2.1 Generation of peptide antibodies for the study of HsPoly

The results I described in Chapter 5 revealed intriguing observations which suggested that cellular levels and distribution of HsPoly are affected by insulin stimulation of cells. This was the first evidence suggesting a potential involvement for HsPoly in InR signalling. Therefore, we wanted to further analyze the role for HsPoly in InR signalling in mammalian cells. The deterioration of previously generated antibodies (Chapter 5) recognizing the bacterially expressed GST-tagged HsPoly fusion protein resulted in the need to generate additional antibodies. Since producing peptide antibodies is a less time consuming process than making antibodies recognising fusion protein antibodies, we have decided to adopt a peptide antibody approach as used previously in the lab (COBBE *et al.* 2009; SAVVIDOU *et al.* 2005).

HsPoly is a 266 amino acid long protein. Taking into consideration the predicted tertiary structure of HsPoly, a unique peptide sequence of 15 amino acids was chosen for injection into animals (Figure 7.1A). This selected polypeptide sequence is predicted to be exposed on the surface of the modelled protein structure. Position of the peptide sequence is indicated on the predicted protein structure model shown in Figure 7.1B. The selected peptide sequence -LGMGAVAVLDFIHYC- was synthesized by Genosphere Biotechnologies (Paris) and injected into two rabbits resulting in two antisera, named A7718 and A7719.

Antibodies were tested at 1:500 dilution for reactivity by immunoblotting on A375 melanoma cell lysates. A7718 and A7719 antibodies showed a similar banding pattern by immunoblotting with three predominant bands at 44, 54 and 60

kDa (Figure 7.2). Importantly, these bands were absent in the preimmune serum. Furthermore, immunblotting with both A7718 and A1119 revealed the same banding pattern. In an attempt to reduce the non-specific background banding pattern, immunoblotting with A7718 and A7719 was repeated on cell lysates by using them at 1:1000 dilution. The use of the antibodies at a lower concentration showed predominant appearance of a band at 44 kDa (Figure 7.3). The expected size of HsPoly is 30 kDa. Therefore, the size of the observed predominant band by immunoblotting is ~14 kDa larger than the predicted size of total HsPoly. This discrepancy in size might be due to a post-translational processing of the gene product or the electrophoresis conditions of the gel. One possible way of concluding whether A7718 and A7719 are in fact recognizing HsPoly would be to carry out an immunoprecipitation followed by mass spectrometry analysis. Alternatively, RNAi depletion of HsPoly on human cells followed by immunoblotting with A7718 and A7719 antibodies would help us to determine whether these reagents are indeed recognizing the correct protein.

To further characterize the peptide antibodies, also a series of immunofluorescence experiments was carried out on A375 cells using A7718 and A7719 antibodies. Preimmune serum for each of these antibodies were used in the experiment as control to dissect the specific staining pattern for the immune sera. All sera were used at 1:1000 dilution. The staining pattern and intensity of preimmune and immune sera of A7718 appeared to be similar. However in some cells stained with the immune sera, stronger staining localized in the nuclear area was detectable (Figure 7.4). The observed stronger nuclear staining with A7718 that is absent in the immune serum might be reflecting specific staining.

Immunofluorescence by using A7719 immune serum revealed stronger staining than its corresponding preimmune serum. This result suggesting that A7719 is likely to be a suitable reagent to visualise HsPoly by immunofluorescence. The staining pattern observed by using A7719 antibody was characterized by signal throughout the cytoplasm as well as the nucleus. However the signal was stronger in the nucleus (Figure 7.5).

Insulin stimulation experiment described in Chapter 5 was carried out on A375 cells by using the A7719 antibody. Staining with A7719 antibody revealed cytoplasmic and nuclear pattern with a stronger intensity in the nucleus prior to insulin stimulation. However, staining with A7719 antibody was not affected by insulin action and remained similar following 60 and 90 minutes of stimulation with insulin (Figure 7.6) failing therefore to repeat results that was obtained with previously used HsPoly antibodies.

7.2.2 GFP-tagged construct of HsPoly

Over-expression of tagged versions of a protein is a successful approach to dissect subcellular localisation as well as cellular dynamics of the protein of interest (MARTINEZ *et al.* 2006; UHLES *et al.* 2003). Furthermore, it is possible to perform immunoprecipitation experiments on tagged proteins for the identification of potential protein-protein interactions (PANKIV *et al.* 2007). Therefore as a complementary approach to the use of antibodies, I wanted to generate tagged versions of HsPoly. To this end, I cloned GFP fusions of HsPoly constructs (N and C-terminal) into CMV (cytomegalovirus) promoter-driven expression vectors (Figure 7.7). A375 cells were transiently transfected with C- and N-terminally GFP

tagged full-length HsPoly plasmids and cells were then fixed and stained for DNA, while GFP signal was observed directly by fluorescence microscopy. During transfection experiments, a construct expressing GFP alone was used as a control. Immunofluorescence on transfected cells revealed cells exhibiting two different kinds of localisation that were distinguishable from each other. In some cells, visualisation of N- and C-terminally GFP-tagged HsPoly staining revealed signal throughout the cytoplasm and nucleus, sometimes showing a stronger staining around the nucleus (Figure 7.8). Interestingly, in some other cells aside from this pattern of staining, I was able to detect appearance of small aggregated dots exhibiting intense GFP staining (Figure 7.9). Furthermore, this pattern was observed consistently in multiple transfection experiments with both N- and C-terminally tagged constructs.

Moreover, some of the cells over-expressing both GFP alone and GFP-tagged HsPoly were found to exhibit abnormally shaped nuclei (Figure 7.8B-C and Figure 7.9A-B). Quantitative analysis of cells revealed that 70% and 76% of the total cells over-expressing GFP alone and GFP-tagged HsPoly respectively were characterized by abnormally shaped nuclei. Since the percentages of cells characterized by abnormally shaped nuclei are very close for cells over-expressing the control construct and GFP-tagged HsPoly constructs, it is likely that this phenotype is not due to the over-expression of HsPoly. The observed nuclear phenotype could be caused by reagents used during the transfection protocol.

To further confirm HsPoly expression, A375 cells were transfected with C-terminally GFP-tagged HsPoly construct. Cell lysates were prepared 24 hours after transfection and blotted with a monoclonal antibody recognizing GFP. As expected,

immunoblotting of cell lysates isolated from control cells transfected with GFP construct revealed a band at 26kDa which corresponds to the predicted protein size of GFP. Extracts isolated from cells transfected with C-terminally tagged HsPoly revealed a band at ~ 52 kDa (Figure 7.10) that was absent in cells transfected with GFP alone. The size of total HsPoly protein is 30 kDa. Although it is 4kDa less than the expected size, the band observed at 52 kDa is likely to correspond to the size of the GFP tag fused to HsPoly. This observation suggests that A375 cells express GFP-tagged HsPoly at high enough levels to detect it by immunoblotting by using a GFP antibody.

In order to determine whether it was possible to detect an increase in GFP-tagged HsPoly or other changes in cellular distribution following activation of InR signalling, an insulin stimulation experiment was carried out. Briefly following 24 hours of transfection, cells were serum starved overnight prior to insulin stimulation. Unfortunately the majority of cells died after the overnight serum starvation making it impossible to carry out further analysis. The experiment was repeated by changing the duration of transfection to 16 hours and 32 hours. Unfortunately all these attempts were unsuccessful as the overnight starvation following transfection led to the death of cells at both of these time points.

7.3 Discussion

The initial characterization of the peptide antibodies raised against HsPoly revealed a predominant band at 44 kDa by immunoblotting which is 14 kDa higher than the anticipated size. Importantly, immunblotting by using both A7718 and A7719 revealed similar banding patterns. More optimizations of the immunoblotting

methods, such as the use of different types of detergents, would be a good approach to determine whether different conditions give rise to appearance of a predominant band at a size closer to the predicted size of HsPoly. An alternative way of determining whether A7718 and A7719 antibodies recognize HsPoly would be to carry out immunoblotting on cells that had been RNAi depleted for HsPoly. Also in a complementary approach, it would be relevant to carry out immunoblotting by using A7718 and A7718 antibodies on cells that had been transfected with the GFP-tagged construct of HsPoly to determine whether these reagents are able to recognize the tagged protein.

However immunoblotting on cells transfected with GFP-HsPoly constructs by using an anti-GFP antibody gave a single band at around 52 kDa that was absent in control cells transfected with the GFP construct alone. This observed size for the GFP tagged HsPoly is very close to the expected size of the tagged protein (the expected size of HsPoly is 30 kDa and the GFP tag is 26 kDa giving 56 kDa for the expected size of the GFP tagged HsPoly). Therefore, this observation leads me to conclude that the size of endogenous HsPoly should be indeed at around 30 kDa and that A7718 and A7719 peptide antibodies unfortunately fail to detect HsPoly by immunoblotting.

The characterization of the peptide antibodies by immunofluorescence suggested that immune serum of A7719 antibody reveals a stronger signal than the corresponding preimmune serum. However, a less predominant difference was detected between the immune serums of A7718 that showed a more nuclear staining in some cells compared to its corresponding preimmune serum. Therefore, I suggest that A7719 is likely to be a more suitable antibody for the use in

immunofluorescence experiments. But unfortunately, insulin stimulation followed by immunofluorescence carried out with A7719 immune serum on A375 cells that had been stimulated did not show an alteration in levels and/or distribution of HsPoly.

Transient expression of GFP-tagged versions of the protein of interest is a complementary approach to investigate the protein's cellular localisation and dynamics. In fact, GFP-tagged versions of components of InR signalling, such as InR and Foxo, have been successfully used for this purpose by other groups (MARTINEZ *et al.* 2006; UHLES *et al.* 2003). Transient expression of GFP-tagged constructs of HsPoly revealed two distinct patterns: cytoplasmic and nuclear staining with and without appearance of aggregated dots. Appearance of aggregated dots was not observed in previously carried out immunofluorescence experiments described in Chapter 5. Similarly, immunofluorescence using peptide antibodies described in this chapter did not reveal formation of aggregates.

The aggregates observed following GFP-tagged HsPoly transfection superficially resembled aggresome-like induced structures (ALIS) that serve as compartments of polyubiquitinated misfolded proteins prior to their degradation (BJORKOY *et al.* 2005; LELOUARD *et al.* 2004; PANKIV *et al.* 2007; SZETO *et al.* 2006).

It has been previously shown that induction of stress conditions such as heat shock or increase of oxidative stress promotes the formation of ALIS. Interestingly, it was also shown that even the addition of transfection reagents alone to cultured cells is sufficient to favour stress conditions leading to formation of ALIS (SZETO *et al.* 2006). Therefore, I propose that the observation of aggregates in cells transfected

with GFP-tagged HsPoly might be due to formation of ALIS following transfection alone. In order to determine whether this is the case, it is necessary to determine whether GFP-tagged HsPoly aggregates are ubiquitinated protein particles. This can be achieved by carrying out immunofluorescence with an anti-ubiquitin antibody on GFP-tagged HsPoly transfected cells. Furthermore, if the observed aggregates are structures similar to ALIS one might expect to observe an increase in number following stress inducing condition such as heat shock or increased oxidative stress. Therefore, further investigation needs to be carried out in order to determine whether aggregates observed during the transfection experiments are storage of misfolded proteins or they in fact represent functional GFP-tagged HsPoly.

I have tried to repeat the insulin stimulation experiment on cell that had been transfected with GFP-tagged HsPoly. However, I was not able to get any results out of this experiment due to a very high death rate of cells after the transfection followed by overnight serum starvation. Observed increased death of transfected cells might be due to over-expression of HsPoly. However, further optimization of the transfection protocol along with the insulin stimulation protocol would be required in order to clarify this point and to determine whether under different conditions (such as shorter serum starvation) it is possible to get enough number of cells to carry out the insulin stimulation on.

GFP-HsPoly was detectable by immunoblotting suggesting that tagged protein could accumulate within cells. Transient expression of GFP-tagged proteins was previously used in immunoprecipitation experiments to identify protein-protein interactions (PANKIV *et al.* 2007). Therefore, in future work immunoprecipitation of

GFP-HsPoly from A375 cells followed by mass spectrometry analysis could be performed to identify proteins interacting with the human homologue of Poly.

Chapter 8: Discussion

8.1. Cell cycle distribution is not affected following *poly* loss of function: is the defect in cell proliferation or cell growth?

Two distinct types of tissue with different types of cell cycle comprise the majority of *Drosophila* larva. The major part of the larva is composed of endoreplicative tissue, such as the larval fat body and salivary glands, that have exited mitosis, but showing high levels of polyploidy and continuous increase in cell size. The second type of tissue, including brains and imaginal discs, are comprised of actively proliferating cells which differentiate into various adult structures during metamorphosis.

As *poly* mutants showed rudimentary imaginal discs, we hypothesized whether this defect could be due to a major proliferative dysregulation. However, investigation of cell cycle progression in *poly* mutant clones did not reveal an alteration in the distribution of cell cycle stages in mutant clones (Chapter 3). Furthermore, data described in Chapters 4 and 5 suggested that Poly is a positive regulator of InR/TOR signalling. The effect of InR/TOR signalling on control of cell cycle progression has been more complicated to elucidate than its effect on other cell growth promoting mechanisms such as protein synthesis (WANG and PROUD 2009). There is evidence that shows that mammalian TORC1 (mTORC1) activity affects the G1/S phase transition via its effects on cyclins, such as Cyclin D (HLEB *et al.* 2004; TAKUWA *et al.* 1999), and Cdk-inhibitor proteins such as p21 and p27 (LEUNG-PINEDA *et al.* 2004). Also, the inhibitory effect of rapamycin was shown to prevent

entry from G1 into S phase (AVEROUS *et al.* 2008; HLEB *et al.* 2004; LUO *et al.* 1996). Furthermore, mTORC1 activity was also found to promote entry into mitosis via its positive regulatory effect on cdc2/Cyclin B function (SMITH and PROUD 2008).

However, in *Drosophila,* the effect of mutations in various components of InR/TOR signalling on cell proliferation and cell cycle distribution has been difficult to determine and at times even contradictory to the data obtained in mammalian organisms (WU *et al.* 2007). Mutation in *InR* was found to result in a reduction in cell number (BROGIOLO *et al.* 2001). Similarly, loss of function of *dTOR* leads to an increased number of cells in G1 phase and fewer cells in S and G2 phases resulting therefore in decreased mitotic activity and number of total cells (ZHANG *et al.* 2000). On the other hand, mutations in *dAkt* (SCANGA *et al.* 2000; VERDU *et al.* 1999) and *dS6K* (MONTAGNE *et al.* 1999) do not show an effect on cell number or the distribution of cell cycle phases. Perhaps not surprisingly, it has been proposed that there might be points in the InR/TOR pathway where signals affecting cell proliferation and cell growth diverge (GAROFALO 2002).

In light of the interaction of Poly with the InR/TOR pathway, I have tried to interpret the data obtained from mosaic clonal analysis on eye imaginal discs that suggested normal distribution of various stage-specific cell cycle markers in *poly* mutant clones. I propose that similar to mutations in *dAkt* and *dS6K*, mutation in *poly* does not affect progression of cell cycle. Therefore, I conclude that Poly is likely to perform its function via the cell growth promoting branch of InR/TOR signalling without affecting the cell proliferation.

8.2. Poly is a novel positive regulator of InR/TOR signalling

The data I have presented in this thesis show that Poly is a novel interactor of InR/TOR signalling in *Drosophila melanogaster*. Investigation of the consequences of *poly* loss of function in mutant larvae reveals down-regulation of signalling via the InR/TOR pathway therefore I suggest that Poly plays a role as a positive regulator of this signalling pathway. In light of my data, I propose a model in which a complex between Poly and InR is formed upon activation of insulin signalling (Figure 8.1). The activation of signalling leads to an alteration in subcellular localisation of Poly and its translocation into the nucleus. I speculate that Poly might be performing a role in the nucleus that is essential for its growth promoting function. This role may potentially involve the regulation of transcription and gene expression in the nucleus. The expression of Poly's target genes may be contributing to promotion of cell growth via the increase in the activity of positive effectors of InR/TOR signalling pathway such as Akt and S6K, as well as the inhibition of negative regulators of cell growth such as autophagy, and an increase in anabolic metabolism. The inhibition of InR/TOR signalling by rapamycin may lead to the exclusion of Poly from the nucleus, blocking expression of its target genes.

Down-regulation of InR/TOR signalling upon *poly* loss of function is indicated by a decrease in d4E-BP and dS6K phosphorylation levels suggesting therefore a decrease in overall protein synthesis. Furthermore, loss of *poly* leads to constitutive activation of autophagy, mimicking a starvation-like state such what is observed in *Tsc1/Tsc2* over-expressing and *dTOR* mutant animals. I propose that both the decrease in protein synthesis and the activation of autophagy observed in *poly* mutants should result in a decrease in size. In agreement with this hypothesis,

initial analysis of the *poly*^{2} allele (KLUSZA and DENG) (a very recently published hypomorphic allele of *poly* that shows few surviving homozygous adults), revealed that *poly*^{2} flies were much smaller in size than wild type animals. Interestingly, previous research showed that the small number of *dS6K* mutant that reach the adulthood are dwarfs, highlighting the importance of an intact InR/TOR signalling pathway for normal growth (MONTAGNE *et al.* 1999). Further characterization and analysis will be done on the surviving *poly*^{2} adult flies in the future in order to determine the effect of a milder mutation in *poly* on body and organ size.

As described previously in the Introduction and Chapter 5, an important downstream effect of the InR/TOR pathway is the control of metabolism in various organisms including flies. For example, *4E-BP* mutants show increased sensitivity to starvation (TELEMAN *et al.* 2005a). Interestingly, it was previously shown that the loss of *PTEN* function in *Drosophila* nurse cells results in accumulation of activated Akt in the cytoplasm. The activation of Akt is responsible for the formation of enlarged lipid droplets along with an increase in the expression of the *Drosophila* homologue of the lipid-droplet associated protein perillipin (Lsd2) in the cytoplasm (VERESHCHAGINA and WILSON 2006). Also *lsd2* mutants are characterized by decreased TAG levels (TEIXEIRA *et al.* 2003). These findings highlight the effect of the activation of InR/TOR signalling on lipid storage in *Drosophila*. Consistent with a down-regulation of InR/TOR signalling in the absence of *poly*, both Lsd2 and TAG levels are reduced in *poly* mutant animals. Therefore I propose that Poly function also affects metabolism via its interaction with InR/TOR pathways and acts as a positive regulator of anabolic metabolism.

Signalling via the TOR/InR pathway has an important effect on life span and ageing as suggested by an increase in lifespan of *tor* mutants in *Drosophila* (ZHANG *et al.* 2000). Therefore I suggest that increased third instar larval life observed in *poly* mutant animals (up to 21 days) may be attributed to the down-regulation of InR/TOR signalling. It would be interesting and relevant in the future to assess whether adult flies heterozygous for the *poly* mutation also exhibit an alteration in their lifespan compared to control flies to gain insight into the effect of Poly function on the control of lifespan and ageing. Furthermore, an analysis of the effect of rapamycin feeding on the lifespan of *poly* heterozygous mutant and control flies will be important to determine whether the effect of rapamycin on the lifespan differs between these two genotypes.

Due to the lack of any known functional motifs, we were unable to firmly predict the function of the Poly protein. But interestingly the phylogenetic analysis carried out by Dr. Neville Cobbe (Heck lab) suggested a potential involvement of Poly in transcription due to its distant homology to the yeast Elp6 protein. This phylogenetic data is in agreement with the proposed model in which dynamic changes in the cellular localisation of Poly in an InR/TOR signalling depending manner mediates the mechanism of action of Poly. Based on the immunofluorescence carried out on *Drosophila* hemocytes and HeLa cells that suggested an increase in staining for HsPoly following insulin stimulation of cells and the phylogenetic analysis I propose that Poly might have a role during transcription. The cell growth and metabolism-stimulatory output of Poly function can be exerted via its effects on transcriptional control. However, in order to obtain evidence for such involvement during gene expression regulation, further *in vivo*

analysis needs to be carried out to assess whether there is indeed a role for Poly in transcription. Also, in the future it will be important to carry out the biochemical fractionation of cells followed by immunoblotting in order assess relative Poly levels in the nucleus versus the cytoplasm upon insulin stimulation of cells.

8.3 Poly: a cross point between the innate immune response and InR/TOR signalling?

A successful immune response and regulation of growth and metabolism are amongst the basic important requirements for normal development of an organism. Interestingly, there is increasing evidence suggesting that these two processes are likely to be co-regulated and interlinked (HOTAMISLIGIL 2006). For example, it is now clear that type 2 diabetes is also characterized by chronic inflammation (WELLEN and HOTAMISLIGIL 2005). Therefore, increasing effort is being put into elucidating the mechanism by which metabolic dysfunction might be connected to alteration of the immune response.

Importantly, the *Drosophila* fat body is an essential organ involved in both metabolic function and the immune response. Apart from being the main lipid storage tissue, the *Drosophila* fat body has the essential role of synthesizing antimicrobial peptides during the humoral innate immune response. There are increasing arenas of study suggesting that there should be cross-talk between InR/TOR signalling and the immune response to regulate the cellular energy balance in response to infection. In fact, it was previously shown that *foxo* mutants exhibit resistance to *Mycobacterium marinum* and that *Akt* activity is reduced following *Mycobacterium marinum* infection (DIONNE *et al.* 2006). Furthermore, mutation in

4E-BP results in sensitivity to *Staphylococcus epidermis* (BERNAL and KIMBRELL 2000). A recent study has also shown that the activation of Toll signalling results in a decrease of InR/TOR activity as suggested by reduced TAG and phospho-Akt levels (DIANGELO *et al.* 2009). Taken together, these data suggest that metabolic and growth control should be coordinated in *Drosophila* as well, however the nature of this interaction remains unclear.

In addition to an involvement of Poly in InR/TOR signalling, my results suggest that normal levels of Poly are needed for the innate immune response in *Drosophila*. Poly over-expression in hemocytes resulted in increased sensitivity to Gram-negative bacterial infection and antimicrobial peptide levels appear to be significantly up-regulated in *poly* mutant larvae. These observations could be due to either a direct or an indirect effect of Poly on humoral immunity.

Poly over-expression could be affecting the immune reponse indirectly via its overall effect on cell growth and metabolism. Recent evidence demonstrated that the activity of InR/TOR signalling was reduced following activation of the immune response (DIANGELO *et al.* 2009). In a model whereby Poly indirectly affects the immune response, the over-expression of Poly could be resulting in up-regulation of InR/TOR signalling via its positive regulatory effect. This up-regulation of InR/TOR pathway may prevent energy "relocation" from cell growth and anabolic processes towards the battle against bacteria during infection. In this scenario, the observed decreased survival of Poly over-expressing flies upon infection would be an indirect consequence of the overall up-regulation of InR/TOR signalling.

However, I suggest that Poly function may have a more direct consequence on the activity of the innate immune response. One of the reasons for this suggestion

is that in flies showing increased bacterial sensitivity, the over-expression was carried out only in hemocytes. Therefore, I propose that the effect of a limited over-expression of Poly on the survival of flies is too major to be solely considered as an indirect effect. Intriguingly, the sensitivity of *poly* over-expressing flies appears to be specific to Gram-negative bacteria. I propose that this specificity might be due to an effect of Poly function on Imd signalling pathway, as this pathway is the main activity involved in fighting Gram-negative bacterial infection. So a model in which Poly function affects immunity in a more direct fashion would involve a location for Poly at an important intersection between the InR/TOR pathway and the immune response. Poly may function as a co-regulatory factor of the immune response with cell growth and metabolism.

In this model (Figure 8.2), I propose that Poly could have an inhibitory effect on the innate immune response (possibly via the Imd pathway), alongside a positive regulatory effect on the InR/TOR pathway. Therefore the function of Poly in the cell might be characterized by a dichotomy of action via which Poly regulates the cell growth and metabolism as well as the immune response. Under normal conditions, Poly could be suppressing the activity of the innate immune response and promoting growth at the same time. Infection could result in suppression of Poly function leading therefore to suppression of its inhibitory effect on innate response as well as to a decrease in InR/TOR signalling. This might facilitate a shift of energy away from cell growth and anabolic processes towards the innate immune response. This model would also explain the observed up-regulation of antimicrobial peptide expression upon *poly* loss of function. The loss of *poly* function would lead to suppression of the inhibitory action of Poly on Imd pathway. This would result in

the activation of the signalling via this pathway and the subsequent transcription of corresponding antimicrobial genes, such as *attA* and *diptericin,* as revealed by the microarray analysis and the quantitative PCR.

According to my proposed model, sensitivity of *poly* over-expressing flies upon Gram-negative bacterial infection could be explained by an increased inhibitory effect of Poly function on the immune response. Interestingly, it was previously shown that a number of proteases are expressed in response to immune challenge (DE GREGORIO *et al.* 2002b). Therefore it is tempting to speculate that Poly might be subject to degradation by one or more of these proteases upon infection. In order to investigate this hypothesis, future work will address Poly levels following infection by various pathogens.

My results have additionally revealed an involvement of Poly in the cellular branch of innate immunity as suggested by the failure of *poly* mutants to encapsulate wasp eggs. Although mutants in various components of InR/TOR were found to exhibit altered survival to bacterial infection, encapsulation defects of InR/TOR signalling mutants have not been reported yet. Interestingly, a recent study showed that *InR* have increased numbers of hemocytes (STOFANKO *et al.* 2008) similar to *poly* mutants (Chapter 6). It will therefore be interesting to investigate whether mutants in other components of InR/TOR signalling show encapsulation defects similar to *poly* mutants. Such encapsulation defect would allow us to conclude whether this defect is a general feature of InR/TOR mutants or rather a more specific consequence of mutation in *poly*.

In conclusion, this study presents the first biochemical and genetic evidence for the involvement of Poly in the regulation of InR/TOR signalling in *Drosophila*.

While the details of Poly's mechanism of action remain to be elucidated, it is clear that the lack of Poly results in down-regulation of the downstream effects of this signalling pathway. Furthermore it will be extremely important to determine, given the evolutionary conservation of Poly, whether homologues of Poly serve a similar function in higher eukaryotes too. I presented evidence for the involvement of Poly during the innate immune response in *Drosophila*. In the future, it will be essential to determine if Poly's involvement during the immune response can be linked to its regulatory role in cell growth and metabolism. Ultimately, we should be able to decipher whether Poly acts as an important co-regulatory protein of the two crucial functions cell growth and metabolism and immune response.

Bibliography

ADAMS, M. D., S. E. CELNIKER, R. A. HOLT, C. A. EVANS, J. D. GOCAYNE *et al.*, 2000 The genome sequence of Drosophila melanogaster. Science **287:** 2185-2195.

ADAMS, R. R., M. CARMENA and W. C. EARNSHAW, 2001 Chromosomal passengers and the (aurora) ABCs of mitosis. Trends Cell Biol **11:** 49-54.

AKIBA, T., N. ISHII, N. RASHID, M. MORIKAWA, T. IMANAKA *et al.*, 2005 Structure of RadB recombinase from a hyperthermophilic archaeon, Thermococcus kodakaraensis KOD1: an implication for the formation of a near-7-fold helical assembly. Nucleic Acids Res **33:** 3412-3423.

AMON, A., 1999 The spindle checkpoint. Curr Opin Genet Dev **9:** 69-75.

ANDERSON, K. V., G. JURGENS and C. NUSSLEIN-VOLHARD, 1985 Establishment of dorsal-ventral polarity in the Drosophila embryo: genetic studies on the role of the Toll gene product. Cell **42:** 779-789.

ARELLANO, M., and S. MORENO, 1997 Regulation of CDK/cyclin complexes during the cell cycle. Int J Biochem Cell Biol **29:** 559-573.

ASHBURNER, M., 1975 The genetic and hormonal control of puffing in the salivary gland chromosomes of Drosophila. Sov J Dev Biol **5:** 97-107.

ASHBURNER, M., K. G. GOLIC and R. S. HAWLEY, 2005 *Drosophila* A Laboratory handbook. Cold Spring Harbor Laboratory Press, Cold Spring Harbor, New York, United States of America.

AULT, J. G., and C. L. RIEDER, 1994 Centrosome and kinetochore movement during mitosis. Curr Opin Cell Biol **6:** 41-49.

AVEDISOV, S. N., I. KRASNOSELSKAYA, M. MORTIN and B. J. THOMAS, 2000 Roughex mediates G(1) arrest through a physical association with cyclin A. Mol Cell Biol **20:** 8220-8229.

AVEROUS, J., B. D. FONSECA and C. G. PROUD, 2008 Regulation of cyclin D1 expression by mTORC1 signaling requires eukaryotic initiation factor 4E-binding protein 1. Oncogene **27:** 1106-1113.

AVET-ROCHEX, A., E. BERGERET, I. ATTREE, M. MEISTER and M. O. FAUVARQUE, 2005 Suppression of Drosophila cellular immunity by directed expression of the ExoS toxin GAP domain of Pseudomonas aeruginosa. Cell Microbiol **7:** 799-810.

AVET-ROCHEX, A., J. PERRIN, E. BERGERET and M. O. FAUVARQUE, 2007 Rac2 is a major actor of Drosophila resistance to Pseudomonas aeruginosa acting in phagocytic cells. Genes Cells **12:** 1193-1204.

BAKER, K. D., and C. S. THUMMEL, 2007 Diabetic larvae and obese flies-emerging studies of metabolism in Drosophila. Cell Metab **6:** 257-266.

BAKER, N. E., 2001 Cell proliferation, survival, and death in the Drosophila eye. Semin Cell Dev Biol **12:** 499-507.

BAKER, N. E., and S. Y. YU, 2001 The EGF receptor defines domains of cell cycle progression and survival to regulate cell number in the developing Drosophila eye. Cell **104:** 699-708.

BAONZA, A., and M. FREEMAN, 2005 Control of cell proliferation in the Drosophila eye by Notch signaling. Dev Cell **8:** 529-539.

BATE, M., and A. M. ARIAS, 1993 The developement of Drosophila melanogaster. Cold Spring Habor Laboratory Press, New York.

BELLACOSA, A., C. C. KUMAR, A. DI CRISTOFANO and J. R. TESTA, 2005 Activation of AKT kinases in cancer: implications for therapeutic targeting. Adv Cancer Res **94:** 29-86.

BERGER, J., T. SUZUKI, K. A. SENTI, J. STUBBS, G. SCHAFFNER *et al.*, 2001 Genetic mapping with SNP markers in Drosophila. Nat Genet **29:** 475-481.

BERGERET, E., J. PERRIN, M. WILLIAMS, D. GRUNWALD, E. ENGEL *et al.*, 2008 TM9SF4 is required for Drosophila cellular immunity via cell adhesion and phagocytosis. J Cell Sci **121:** 3325-3334.

BERNAL, A., and D. A. KIMBRELL, 2000 Drosophila Thor participates in host immune defense and connects a translational regulator with innate immunity. Proc Natl Acad Sci U S A **97:** 6019-6024.

BERRY, D. L., and E. H. BAEHRECKE, 2007 Growth arrest and autophagy are required for salivary gland cell degradation in Drosophila. Cell **131:** 1137-1148.

BHASKAR, P. T., and N. HAY, 2007 The two TORCs and Akt. Dev Cell **12:** 487-502.

BJEDOV, I., J. M. TOIVONEN, F. KERR, C. SLACK, J. JACOBSON *et al.*, Mechanisms of life span extension by rapamycin in the fruit fly Drosophila melanogaster. Cell Metab **11:** 35-46.

BJORKOY, G., T. LAMARK, A. BRECH, H. OUTZEN, M. PERANDER *et al.*, 2005 p62/SQSTM1 forms protein aggregates degraded by autophagy and has a protective effect on huntingtin-induced cell death. J Cell Biol **171:** 603-614.

BLAIR, S. S., 2003 Genetic mosaic techniques for studying Drosophila development. Development **130:** 5065-5072.

BLOW, J. J., and A. DUTTA, 2005 Preventing re-replication of chromosomal DNA. Nat Rev Mol Cell Biol **6:** 476-486.

BLOW, J. J., and T. U. TANAKA, 2005 The chromosome cycle: coordinating replication and segregation. Second in the cycles review series. EMBO Rep **6:** 1028-1034.

BOHNI, R., J. RIESGO-ESCOVAR, S. OLDHAM, W. BROGIOLO, H. STOCKER *et al.*, 1999 Autonomous control of cell and organ size by CHICO, a Drosophila homolog of vertebrate IRS1-4. Cell **97:** 865-875.

BOUTROS, M., H. AGAISSE and N. PERRIMON, 2002 Sequential activation of signaling pathways during innate immune responses in Drosophila. Dev Cell **3:** 711-722.

BRAND, A. H., and N. PERRIMON, 1993 Targeted gene expression as a means of altering cell fates and generating dominant phenotypes. Development **118:** 401-415.

BRENNAN, C. A., J. R. DELANEY, D. S. SCHNEIDER and K. V. ANDERSON, 2007 Psidin is required in Drosophila blood cells for both phagocytic degradation and immune activation of the fat body. Curr Biol **17:** 67-72.

BRIDGES, C. B., 1916 Non-Disjunction as Proof of the Chromosome Theory of Heredity (Concluded). Genetics **1:** 107-163.

BRITTON, J. S., W. K. LOCKWOOD, L. LI, S. M. COHEN and B. A. EDGAR, 2002 Drosophila's insulin/PI3-kinase pathway coordinates cellular metabolism with nutritional conditions. Dev Cell **2:** 239-249.

BROGIOLO, W., H. STOCKER, T. IKEYA, F. RINTELEN, R. FERNANDEZ *et al.*, 2001 An evolutionarily conserved function of the Drosophila insulin receptor and insulin-like peptides in growth control. Curr Biol **11:** 213-221.

BROUGHTON, S. J., M. D. PIPER, T. IKEYA, T. M. BASS, J. JACOBSON *et al.*, 2005 Longer lifespan, altered metabolism, and stress resistance in Drosophila from ablation of cells making insulin-like ligands. Proc Natl Acad Sci U S A **102:** 3105-3110.

BRUMBY, A. M., and H. E. RICHARDSON, 2003 scribble mutants cooperate with oncogenic Ras or Notch to cause neoplastic overgrowth in Drosophila. Embo J **22:** 5769-5779.

BUCHKOVICH, K., L. A. DUFFY and E. HARLOW, 1989 The retinoblastoma protein is phosphorylated during specific phases of the cell cycle. Cell **58:** 1097-1105.

BUTTERWORTH, F. M., L. EMERSON and E. M. RASCH, 1988 Maturation and degeneration of the fat body in the Drosophila larva and pupa as revealed by morphometric analysis. Tissue Cell **20:** 255-268.

BUTTERWORTH, F. M., and E. C. FORREST, 1984 Ultrastructure of the preparative phase of cell death in the larval fat body of Drosophila melanogaster. Tissue Cell **16:** 237-250.

CAI, S. L., A. R. TEE, J. D. SHORT, J. M. BERGERON, J. KIM *et al.*, 2006 Activity of TSC2 is inhibited by AKT-mediated phosphorylation and membrane partitioning. J Cell Biol **173:** 279-289.

CARTON, Y., and A. J. NAPPI, 1997 Drosophila cellular immunity against parasitoids. Parasitol Today **13:** 218-227.

CARTON, Y., and A. J. NAPPI, 2001 Immunogenetic aspects of the cellular immune response of Drosophilia against parasitoids. Immunogenetics **52:** 157-164.

CHEN, C., J. JACK and R. S. GAROFALO, 1996 The Drosophila insulin receptor is required for normal growth. Endocrinology **137:** 846-856.

CHOE, K. M., T. WERNER, S. STOVEN, D. HULTMARK and K. V. ANDERSON, 2002 Requirement for a peptidoglycan recognition protein (PGRP) in Relish activation and antibacterial immune responses in Drosophila. Science **296:** 359-362.

CHOSA, N., T. FUKUMITSU, K. FUJIMOTO and E. OHNISHI, 1997 Activation of prophenoloxidase A1 by an activating enzyme in Drosophila melanogaster. Insect Biochem Mol Biol **27:** 61-68.

CHOU, T. B., E. NOLL and N. PERRIMON, 1993 Autosomal P[ovoD1] dominant female-sterile insertions in Drosophila and their use in generating germ-line chimeras. Development **119:** 1359-1369.

CHOU, T. B., and N. PERRIMON, 1996 The autosomal FLP-DFS technique for generating germline mosaics in Drosophila melanogaster. Genetics **144:** 1673-1679.

CIAPPONI, L., G. CENCI, J. DUCAU, C. FLORES, D. JOHNSON-SCHLITZ *et al.*, 2004 The Drosophila Mre11/Rad50 complex is required to prevent both telomeric fusion and chromosome breakage. Curr Biol **14:** 1360-1366.

COBBE, N., K. M. MARSHALL, S. GURURAJA RAO, C. W. CHANG, F. DI CARA *et al.*, 2009 The conserved metalloprotease invadolysin localizes to the surface of lipid droplets. J Cell Sci **122:** 3414-3423.

COLOMBANI, J., S. RAISIN, S. PANTALACCI, T. RADIMERSKI, J. MONTAGNE *et al.*, 2003 A nutrient sensor mechanism controls Drosophila growth. Cell **114:** 739-749.

COQUERET, O., 2002 Linking cyclins to transcriptional control. Gene **299:** 35-55.

CUERVO, A. M., 2004 Autophagy: many paths to the same end. Mol Cell Biochem **263:** 55-72.

DATAR, S. A., H. W. JACOBS, A. F. DE LA CRUZ, C. F. LEHNER and B. A. EDGAR, 2000 The Drosophila cyclin D-Cdk4 complex promotes cellular growth. Embo J **19:** 4543-4554.

DE GREGORIO, E., S. J. HAN, W. J. LEE, M. J. BAEK, T. OSAKI *et al.*, 2002a An immune-responsive Serpin regulates the melanization cascade in Drosophila. Dev Cell **3:** 581-592.

DE GREGORIO, E., P. T. SPELLMAN, P. TZOU, G. M. RUBIN and B. LEMAITRE, 2002b The Toll and Imd pathways are the major regulators of the immune response in Drosophila. Embo J **21:** 2568-2579.

DELOTTO, Y., and R. DELOTTO, 1998 Proteolytic processing of the Drosophila Spatzle protein by easter generates a dimeric NGF-like molecule with ventralising activity. Mech Dev **72:** 141-148.

DEMONTIS, F., and N. PERRIMON, 2009 Integration of Insulin receptor/Foxo signaling and dMyc activity during muscle growth regulates body size in Drosophila. Development **136:** 983-993.

DIANGELO, J. R., M. L. BLAND, S. BAMBINA, S. CHERRY and M. J. BIRNBAUM, 2009 The immune response attenuates growth and nutrient storage in Drosophila by reducing insulin signaling. Proc Natl Acad Sci U S A.

DIMARCQ, J. L., J. L. IMLER, R. LANOT, R. A. EZEKOWITZ, J. A. HOFFMANN *et al.*, 1997 Treatment of l(2)mbn Drosophila tumorous blood cells with the steroid hormone ecdysone amplifies the inducibility of antimicrobial peptide gene expression. Insect Biochem Mol Biol **27:** 877-886.

DIONNE, M. S., L. N. PHAM, M. SHIRASU-HIZA and D. S. SCHNEIDER, 2006 Akt and FOXO dysregulation contribute to infection-induced wasting in Drosophila. Curr Biol **16:** 1977-1985.

DOXSEY, S. J., 2001 Centrosomes as command centres for cellular control. Nat Cell Biol **3:** E105-108.

DUFFY, J. B., 2002 GAL4 system in Drosophila: a fly geneticist's Swiss army knife. Genesis **34:** 1-15.

DUMAN-SCHEEL, M., L. WENG, S. XIN and W. DU, 2002 Hedgehog regulates cell growth and proliferation by inducing Cyclin D and Cyclin E. Nature **417:** 299-304.

ENGELMAN, J. A., J. LUO and L. C. CANTLEY, 2006 The evolution of phosphatidylinositol 3-kinases as regulators of growth and metabolism. Nat Rev Genet **7:** 606-619.

EVANS, C. J., V. HARTENSTEIN and U. BANERJEE, 2003 Thicker than blood: conserved mechanisms in Drosophila and vertebrate hematopoiesis. Dev Cell **5:** 673-690.

EVANS, T., E. T. ROSENTHAL, J. YOUNGBLOM, D. DISTEL and T. HUNT, 1983 Cyclin: a protein specified by maternal mRNA in sea urchin eggs that is destroyed at each cleavage division. Cell **33:** 389-396.

FEANY, M. B., and W. W. BENDER, 2000 A Drosophila model of Parkinson's disease. Nature **404:** 394-398.

FEARON, D. T., and R. M. LOCKSLEY, 1996 The instructive role of innate immunity in the acquired immune response. Science **272:** 50-53.

FERNANDEZ, N. Q., J. GROSSHANS, J. S. GOLTZ and D. STEIN, 2001 Separable and redundant regulatory determinants in Cactus mediate its dorsal group dependent degradation. Development **128:** 2963-2974.
FERNANDEZ, R., D. TABARINI, N. AZPIAZU, M. FRASCH and J. SCHLESSINGER, 1995 The Drosophila insulin receptor homolog: a gene essential for embryonic development encodes two receptor isoforms with different signaling potential. Embo J **14:** 3373-3384.
FIGEYS, D., L. D. MCBROOM and M. F. MORAN, 2001 Mass spectrometry for the study of protein-protein interactions. Methods **24:** 230-239.
FOE, V. E., 1989 Mitotic domains reveal early commitment of cells in Drosophila embryos. Development **107:** 1-22.
FREEMAN, M., 1996 Reiterative use of the EGF receptor triggers differentiation of all cell types in the Drosophila eye. Cell **87:** 651-660.
GAO, X., and D. PAN, 2001 TSC1 and TSC2 tumor suppressors antagonize insulin signaling in cell growth. Genes Dev **15:** 1383-1392.
GAROFALO, R. S., 2002 Genetic analysis of insulin signaling in Drosophila. Trends Endocrinol Metab **13:** 156-162.
GATTI, M., and B. S. BAKER, 1989 Genes controlling essential cell-cycle functions in Drosophila melanogaster. Genes Dev **3:** 438-453.
GEORGEL, P., M. MEISTER, C. KAPPLER, B. LEMAITRE, J. M. REICHHART *et al.*, 1993 Insect immunity: the diptericin promoter contains multiple functional regulatory sequences homologous to mammalian acute-phase response elements. Biochem Biophys Res Commun **197:** 508-517.
GEORGEL, P., S. NAITZA, C. KAPPLER, D. FERRANDON, D. ZACHARY *et al.*, 2001 Drosophila immune deficiency (IMD) is a death domain protein that activates antibacterial defense and can promote apoptosis. Dev Cell **1:** 503-514.
GIRARD, F., U. STRAUSFELD, A. FERNANDEZ and N. J. LAMB, 1991 Cyclin A is required for the onset of DNA replication in mammalian fibroblasts. Cell **67:** 1169-1179.
GOBERDHAN, D. C., N. PARICIO, E. C. GOODMAN, M. MLODZIK and C. WILSON, 1999 Drosophila tumor suppressor PTEN controls cell size and number by antagonizing the Chico/PI3-kinase signaling pathway. Genes Dev **13:** 3244-3258.
GOBERT, V., M. GOTTAR, A. A. MATSKEVICH, S. RUTSCHMANN, J. ROYET *et al.*, 2003 Dual activation of the Drosophila toll pathway by two pattern recognition receptors. Science **302:** 2126-2130.
GOTTAR, M., V. GOBERT, T. MICHEL, M. BELVIN, G. DUYK *et al.*, 2002 The Drosophila immune response against Gram-negative bacteria is mediated by a peptidoglycan recognition protein. Nature **416:** 640-644.
GOVIND, S., 2008 Innate immunity in Drosophila: Pathogens and pathways. Insect Sci **15:** 29-43.
GREENSPAN, R. J., 1997 Fly Pushing: The Theory and Practice of *Drosophila* Genetics. Cold Spring Harbor Laoratory Press, Cold Spring Harbor, New York, United States of America.
GREWAL, S. S., 2009 Insulin/TOR signaling in growth and homeostasis: a view from the fly world. Int J Biochem Cell Biol **41:** 1006-1010.

GRONKE, S., M. BELLER, S. FELLERT, H. RAMAKRISHNAN, H. JACKLE *et al.*, 2003 Control of fat storage by a Drosophila PAT domain protein. Curr Biol **13:** 603-606.

GRONKE, S., G. MULLER, J. HIRSCH, S. FELLERT, A. ANDREOU *et al.*, 2007 Dual lipolytic control of body fat storage and mobilization in Drosophila. PLoS Biol **5:** e137.

GUERTIN, D. A., D. M. STEVENS, C. C. THOREEN, A. A. BURDS, N. Y. KALAANY *et al.*, 2006 Ablation in mice of the mTORC components raptor, rictor, or mLST8 reveals that mTORC2 is required for signaling to Akt-FOXO and PKCalpha, but not S6K1. Dev Cell **11:** 859-871.

HANSEN, M., S. TAUBERT, D. CRAWFORD, N. LIBINA, S. J. LEE *et al.*, 2007 Lifespan extension by conditions that inhibit translation in Caenorhabditis elegans. Aging Cell **6:** 95-110.

HARTWELL, L. H., and T. A. WEINERT, 1989 Checkpoints: controls that ensure the order of cell cycle events. Science **246:** 629-634.

HAWKES, N. A., G. OTERO, G. S. WINKLER, N. MARSHALL, M. E. DAHMUS *et al.*, 2002 Purification and characterization of the human elongator complex. J Biol Chem **277:** 3047-3052.

HAY, N., and N. SONENBERG, 2004 Upstream and downstream of mTOR. Genes Dev **18:** 1926-1945.

HENDZEL, M. J., Y. WEI, M. A. MANCINI, A. VAN HOOSER, T. RANALLI *et al.*, 1997 Mitosis-specific phosphorylation of histone H3 initiates primarily within pericentromeric heterochromatin during G2 and spreads in an ordered fashion coincident with mitotic chromosome condensation. Chromosoma **106:** 348-360.

HENNIG, K. M., J. COLOMBANI and T. P. NEUFELD, 2006 TOR coordinates bulk and targeted endocytosis in the Drosophila melanogaster fat body to regulate cell growth. J Cell Biol **173:** 963-974.

HIRANO, T., 2002 The ABCs of SMC proteins: two-armed ATPases for chromosome condensation, cohesion, and repair. Genes Dev **16:** 399-414.

HLEB, M., S. MURPHY, E. F. WAGNER, N. N. HANNA, N. SHARMA *et al.*, 2004 Evidence for cyclin D3 as a novel target of rapamycin in human T lymphocytes. J Biol Chem **279:** 31948-31955.

HOFFMANN, J. A., 2003 The immune response of Drosophila. Nature **426:** 33-38.

HOFFMANN, J. A., and J. M. REICHHART, 2002 Drosophila innate immunity: an evolutionary perspective. Nat Immunol **3:** 121-126.

HONTI, V., E. KURUCZ, G. CSORDAS, B. LAURINYECZ, R. MARKUS *et al.*, 2009 In vivo detection of lamellocytes in Drosophila melanogaster. Immunol Lett **126:** 83-84.

HORNG, T., and R. MEDZHITOV, 2001 Drosophila MyD88 is an adapter in the Toll signaling pathway. Proc Natl Acad Sci U S A **98:** 12654-12658.

HOTAMISLIGIL, G. S., 2006 Inflammation and metabolic disorders. Nature **444:** 860-867.

IKEYA, T., M. GALIC, P. BELAWAT, K. NAIRZ and E. HAFEN, 2002 Nutrient-dependent expression of insulin-like peptides from neuroendocrine cells in the CNS contributes to growth regulation in Drosophila. Curr Biol **12:** 1293-1300.

INOKI, K., M. N. CORRADETTI and K. L. GUAN, 2005 Dysregulation of the TSC-mTOR pathway in human disease. Nat Genet **37:** 19-24.

IP, Y. T., M. REACH, Y. ENGSTROM, L. KADALAYIL, H. CAI *et al.*, 1993 Dif, a dorsal-related gene that mediates an immune response in Drosophila. Cell **75:** 753-763.

IRNIGER, S., 2002 Cyclin destruction in mitosis: a crucial task of Cdc20. FEBS Lett **532:** 7-11.

IRVING, P., J. M. UBEDA, D. DOUCET, L. TROXLER, M. LAGUEUX *et al.*, 2005 New insights into Drosophila larval haemocyte functions through genome-wide analysis. Cell Microbiol **7:** 335-350.

JACINTO, E., V. FACCHINETTI, D. LIU, N. SOTO, S. WEI *et al.*, 2006 SIN1/MIP1 maintains rictor-mTOR complex integrity and regulates Akt phosphorylation and substrate specificity. Cell **127:** 125-137.

JACINTO, E., R. LOEWITH, A. SCHMIDT, S. LIN, M. A. RUEGG *et al.*, 2004 Mammalian TOR complex 2 controls the actin cytoskeleton and is rapamycin insensitive. Nat Cell Biol **6:** 1122-1128.

JANEWAY, C. A., JR., and R. MEDZHITOV, 2002 Innate immune recognition. Annu Rev Immunol **20:** 197-216.

JUHASZ, G., G. CSIKOS, R. SINKA, M. ERDELYI and M. SASS, 2003 The Drosophila homolog of Aut1 is essential for autophagy and development. FEBS Lett **543:** 154-158.

JUHASZ, G., L. G. PUSKAS, O. KOMONYI, B. ERDI, P. MAROY *et al.*, 2007 Gene expression profiling identifies FKBP39 as an inhibitor of autophagy in larval Drosophila fat body. Cell Death Differ **14:** 1181-1190.

KAEBERLEIN, M., C. R. BURTNER and B. K. KENNEDY, 2007 Recent developments in yeast aging. PLoS Genet **3:** e84.

KAESTNER, K. H., W. KNOCHEL and D. E. MARTINEZ, 2000 Unified nomenclature for the winged helix/forkhead transcription factors. Genes Dev **14:** 142-146.

KAMBRIS, Z., J. A. HOFFMANN, J. L. IMLER and M. CAPOVILLA, 2002 Tissue and stage-specific expression of the Tolls in Drosophila embryos. Gene Expr Patterns **2:** 311-317.

KANG, H. J., K. KUBOTA, H. MING, K. MIYAZONO and M. TANOKURA, 2009 Crystal structure of KaiC-like protein PH0186 from hyperthermophilic archaea Pyrococcus horikoshii OT3. Proteins **75:** 1035-1039.

KAPAHI, P., B. M. ZID, T. HARPER, D. KOSLOVER, V. SAPIN *et al.*, 2004 Regulation of lifespan in Drosophila by modulation of genes in the TOR signaling pathway. Curr Biol **14:** 885-890.

KARPEN, G. H., and A. C. SPRADLING, 1992 Analysis of subtelomeric heterochromatin in the Drosophila minichromosome Dp1187 by single P element insertional mutagenesis. Genetics **132:** 737-753.

KATO, J., H. MATSUSHIME, S. W. HIEBERT, M. E. EWEN and C. J. SHERR, 1993 Direct binding of cyclin D to the retinoblastoma gene product (pRb) and pRb phosphorylation by the cyclin D-dependent kinase CDK4. Genes Dev **7:** 331-342.

KELLER, A., A. I. NESVIZHSKII, E. KOLKER and R. AEBERSOLD, 2002 Empirical statistical model to estimate the accuracy of peptide identifications made by MS/MS and database search. Anal Chem **74:** 5383-5392.

KIM, J. E., and J. CHEN, 2004 regulation of peroxisome proliferator-activated receptor-gamma activity by mammalian target of rapamycin and amino acids in adipogenesis. Diabetes **53:** 2748-2756.
KING, R. W., P. K. JACKSON and M. W. KIRSCHNER, 1994 Mitosis in transition. Cell **79:** 563-571.
KLIONSKY, D. J., J. M. CREGG, W. A. DUNN, JR., S. D. EMR, Y. SAKAI *et al.*, 2003 A unified nomenclature for yeast autophagy-related genes. Dev Cell **5:** 539-545.
KLUSZA, S., and W. M. DENG, poly is required for nurse-cell chromosome dispersal and oocyte polarity in Drosophila. Fly (Austin) **4:** 128-136.
KNOBLICH, J. A., and C. F. LEHNER, 1993 Synergistic action of Drosophila cyclins A and B during the G2-M transition. Embo J **12:** 65-74.
KNOBLICH, J. A., K. SAUER, L. JONES, H. RICHARDSON, R. SAINT *et al.*, 1994 Cyclin E controls S phase progression and its down-regulation during Drosophila embryogenesis is required for the arrest of cell proliferation. Cell **77:** 107-120.
KO, L. J., and C. PRIVES, 1996 p53: puzzle and paradigm. Genes Dev **10:** 1054-1072.
KOFF, A., F. CROSS, A. FISHER, J. SCHUMACHER, K. LEGUELLEC *et al.*, 1991 Human cyclin E, a new cyclin that interacts with two members of the CDC2 gene family. Cell **66:** 1217-1228.
KOPS, G. J., R. H. MEDEMA, J. GLASSFORD, M. A. ESSERS, P. F. DIJKERS *et al.*, 2002 Control of cell cycle exit and entry by protein kinase B-regulated forkhead transcription factors. Mol Cell Biol **22:** 2025-2036.
KROGAN, N. J., and J. F. GREENBLATT, 2001 Characterization of a six-subunit holo-elongator complex required for the regulated expression of a group of genes in Saccharomyces cerevisiae. Mol Cell Biol **21:** 8203-8212.
KURUCZ, E., B. VACZI, R. MARKUS, B. LAURINYECZ, P. VILMOS *et al.*, 2007 Definition of Drosophila hemocyte subsets by cell-type specific antigens. Acta Biol Hung **58 Suppl:** 95-111.
KWIATKOWSKI, D. J., 2003 Tuberous sclerosis: from tubers to mTOR. Ann Hum Genet **67:** 87-96.
LAHUE, E. E., A. V. SMITH and T. L. ORR-WEAVER, 1991 A novel cyclin gene from Drosophila complements CLN function in yeast. Genes Dev **5:** 2166-2175.
LANOT, R., D. ZACHARY, F. HOLDER and M. MEISTER, 2001 Postembryonic hematopoiesis in Drosophila. Dev Biol **230:** 243-257.
LAVINE, M. D., and M. R. STRAND, 2002 Insect hemocytes and their role in immunity. Insect Biochem Mol Biol **32:** 1295-1309.
LEBESTKY, T., T. CHANG, V. HARTENSTEIN and U. BANERJEE, 2000 Specification of Drosophila hematopoietic lineage by conserved transcription factors. Science **288:** 146-149.
LEHNER, C. F., and P. H. O'FARRELL, 1989 Expression and function of Drosophila cyclin A during embryonic cell cycle progression. Cell **56:** 957-968.
LEHNER, C. F., and P. H. O'FARRELL, 1990 The roles of Drosophila cyclins A and B in mitotic control. Cell **61:** 535-547.
LEIPE, D. D., L. ARAVIND, N. V. GRISHIN and E. V. KOONIN, 2000 The bacterial replicative helicase DnaB evolved from a RecA duplication. Genome Res **10:** 5-16.

LELOUARD, H., V. FERRAND, D. MARGUET, J. BANIA, V. CAMOSSETO *et al.*, 2004 Dendritic cell aggresome-like induced structures are dedicated areas for ubiquitination and storage of newly synthesized defective proteins. J Cell Biol **164:** 667-675.

LEMAITRE, B., E. KROMER-METZGER, L. MICHAUT, E. NICOLAS, M. MEISTER *et al.*, 1995a A recessive mutation, immune deficiency (imd), defines two distinct control pathways in the Drosophila host defense. Proc Natl Acad Sci U S A **92:** 9465-9469.

LEMAITRE, B., M. MEISTER, S. GOVIND, P. GEORGEL, R. STEWARD *et al.*, 1995b Functional analysis and regulation of nuclear import of dorsal during the immune response in Drosophila. Embo J **14:** 536-545.

LEOPOLD, P., and P. H. O'FARRELL, 1991 An evolutionarily conserved cyclin homolog from Drosophila rescues yeast deficient in G1 cyclins. Cell **66:** 1207-1216.

LEOPOLD, P., and N. PERRIMON, 2007 Drosophila and the genetics of the internal milieu. Nature **450:** 186-188.

LEULIER, F., A. RODRIGUEZ, R. S. KHUSH, J. M. ABRAMS and B. LEMAITRE, 2000 The Drosophila caspase Dredd is required to resist gram-negative bacterial infection. EMBO Rep **1:** 353-358.

LEULIER, F., S. VIDAL, K. SAIGO, R. UEDA and B. LEMAITRE, 2002 Inducible expression of double-stranded RNA reveals a role for dFADD in the regulation of the antibacterial response in Drosophila adults. Curr Biol **12:** 996-1000.

LEUNG-PINEDA, V., Y. PAN, H. CHEN and M. S. KILBERG, 2004 Induction of p21 and p27 expression by amino acid deprivation of HepG2 human hepatoma cells involves mRNA stabilization. Biochem J **379:** 79-88.

LEVASHINA, E. A., S. OHRESSER, B. LEMAITRE and J. L. IMLER, 1998 Two distinct pathways can control expression of the gene encoding the Drosophila antimicrobial peptide metchnikowin. J Mol Biol **278:** 515-527.

LEVINE, A. J., 1997 p53, the cellular gatekeeper for growth and division. Cell **88:** 323-331.

LEVINE, B., and D. J. KLIONSKY, 2004 Development by self-digestion: molecular mechanisms and biological functions of autophagy. Dev Cell **6:** 463-477.

LEVINE, B., and G. KROEMER, 2008 Autophagy in the pathogenesis of disease. Cell **132:** 27-42.

LEW, D. J., V. DULIC and S. I. REED, 1991 Isolation of three novel human cyclins by rescue of G1 cyclin (Cln) function in yeast. Cell **66:** 1197-1206.

LIGOXYGAKIS, P., N. PELTE, J. A. HOFFMANN and J. M. REICHHART, 2002 Activation of Drosophila Toll during fungal infection by a blood serine protease. Science **297:** 114-116.

LIN, Z., H. KONG, M. NEI and H. MA, 2006 Origins and evolution of the recA/RAD51 gene family: evidence for ancient gene duplication and endosymbiotic gene transfer. Proc Natl Acad Sci U S A **103:** 10328-10333.

LOEWITH, R., E. JACINTO, S. WULLSCHLEGER, A. LORBERG, J. L. CRESPO *et al.*, 2002 Two TOR complexes, only one of which is rapamycin sensitive, have distinct roles in cell growth control. Mol Cell **10:** 457-468.

LONG, X., Y. LIN, S. ORTIZ-VEGA, K. YONEZAWA and J. AVRUCH, 2005 Rheb binds and regulates the mTOR kinase. Curr Biol **15:** 702-713.

LUKAS, J., C. LUKAS and J. BARTEK, 2004 Mammalian cell cycle checkpoints: signalling pathways and their organization in space and time. DNA Repair (Amst) **3:** 997-1007.

LUO, Y., S. O. MARX, H. KIYOKAWA, A. KOFF, J. MASSAGUE *et al.*, 1996 Rapamycin resistance tied to defective regulation of p27Kip1. Mol Cell Biol **16:** 6744-6751.

LUONG, N., C. R. DAVIES, R. J. WESSELLS, S. M. GRAHAM, M. T. KING *et al.*, 2006 Activated FOXO-mediated insulin resistance is blocked by reduction of TOR activity. Cell Metab **4:** 133-142.

MANFRUELLI, P., J. M. REICHHART, R. STEWARD, J. A. HOFFMANN and B. LEMAITRE, 1999 A mosaic analysis in Drosophila fat body cells of the control of antimicrobial peptide genes by the Rel proteins Dorsal and DIF. Embo J **18:** 3380-3391.

MANNING, B. D., 2004 Balancing Akt with S6K: implications for both metabolic diseases and tumorigenesis. J Cell Biol **167:** 399-403.

MANNING, B. D., and L. C. CANTLEY, 2007 AKT/PKB signaling: navigating downstream. Cell **129:** 1261-1274.

MARR, M. T., 2ND, J. A. D'ALESSIO, O. PUIG and R. TJIAN, 2007 IRES-mediated functional coupling of transcription and translation amplifies insulin receptor feedback. Genes Dev **21:** 175-183.

MARTINEZ, S. C., C. CRAS-MENEUR, E. BERNAL-MIZRACHI and M. A. PERMUTT, 2006 Glucose regulates Foxo1 through insulin receptor signaling in the pancreatic islet beta-cell. Diabetes **55:** 1581-1591.

MEDZHITOV, R., and C. JANEWAY, JR., 2000 Innate immune recognition: mechanisms and pathways. Immunol Rev **173:** 89-97.

MEISTER, M., and M. LAGUEUX, 2003 Drosophila blood cells. Cell Microbiol **5:** 573-580.

MELO, J., and D. TOCZYSKI, 2002 A unified view of the DNA-damage checkpoint. Curr Opin Cell Biol **14:** 237-245.

MENG, X., B. S. KHANUJA and Y. T. IP, 1999 Toll receptor-mediated Drosophila immune response requires Dif, an NF-kappaB factor. Genes Dev **13:** 792-797.

MEYER, C. A., H. W. JACOBS, S. A. DATAR, W. DU, B. A. EDGAR *et al.*, 2000 Drosophila Cdk4 is required for normal growth and is dispensable for cell cycle progression. Embo J **19:** 4533-4542.

MICHEL, T., J. M. REICHHART, J. A. HOFFMANN and J. ROYET, 2001 Drosophila Toll is activated by Gram-positive bacteria through a circulating peptidoglycan recognition protein. Nature **414:** 756-759.

MINAKHINA, S., and R. STEWARD, 2006 Melanotic mutants in Drosophila: pathways and phenotypes. Genetics **174:** 253-263.

MIZUGUCHI, K., J. S. PARKER, T. L. BLUNDELL and N. J. GAY, 1998 Getting knotted: a model for the structure and activation of Spatzle. Trends Biochem Sci **23:** 239-242.

MIZUSHIMA, N., 2007 Autophagy: process and function. Genes Dev **21:** 2861-2873.

MIZUSHIMA, N., and D. J. KLIONSKY, 2007 Protein turnover via autophagy: implications for metabolism. Annu Rev Nutr **27:** 19-40.

MIZUSHIMA, N., B. LEVINE, A. M. CUERVO and D. J. KLIONSKY, 2008 Autophagy fights disease through cellular self-digestion. Nature **451:** 1069-1075.

MOBERG, K. H., D. W. BELL, D. C. WAHRER, D. A. HABER and I. K. HARIHARAN, 2001 Archipelago regulates Cyclin E levels in Drosophila and is mutated in human cancer cell lines. Nature **413:** 311-316.

MONTAGNE, J., M. J. STEWART, H. STOCKER, E. HAFEN, S. C. KOZMA *et al.*, 1999 Drosophila S6 kinase: a regulator of cell size. Science **285:** 2126-2129.

MORGAN, D. O., 1995 Principles of CDK regulation. Nature **374:** 131-134.

MORGAN, T. H., 1910 Sex Limited Inheritance in Drosophila. Science **32:** 120-122.

MOTOKURA, T., T. BLOOM, H. G. KIM, H. JUPPNER, J. V. RUDERMAN *et al.*, 1991 A novel cyclin encoded by a bcl1-linked candidate oncogene. Nature **350:** 512-515.

MUKHERJEE, T., J. C. HOMBRIA and M. P. ZEIDLER, 2005 Opposing roles for Drosophila JAK/STAT signalling during cellular proliferation. Oncogene **24:** 2503-2511.

NAITZA, S., C. ROSSE, C. KAPPLER, P. GEORGEL, M. BELVIN *et al.*, 2002 The Drosophila immune defense against gram-negative infection requires the death protein dFADD. Immunity **17:** 575-581.

NAKAE, J., W. H. BIGGS, 3RD, T. KITAMURA, W. K. CAVENEE, C. V. WRIGHT *et al.*, 2002 Regulation of insulin action and pancreatic beta-cell function by mutated alleles of the gene encoding forkhead transcription factor Foxo1. Nat Genet **32:** 245-253.

NAKAE, J., T. KITAMURA, Y. KITAMURA, W. H. BIGGS, 3RD, K. C. ARDEN *et al.*, 2003 The forkhead transcription factor Foxo1 regulates adipocyte differentiation. Dev Cell **4:** 119-129.

NAPPI, A. J., 1975 Inhibition by parasites of melanotic tumour formation in Drosophila melanogaster. Nature **255:** 402-404.

NAPPI, A. J., F. FREY and Y. CARTON, 2005 Drosophila serpin 27A is a likely target for immune suppression of the blood cell-mediated melanotic encapsulation response. J Insect Physiol **51:** 197-205.

NELISSEN, H., D. FLEURY, L. BRUNO, P. ROBLES, L. DE VEYLDER *et al.*, 2005 The elongata mutants identify a functional Elongator complex in plants with a role in cell proliferation during organ growth. Proc Natl Acad Sci U S A **102:** 7754-7759.

NICOLAS, E., J. M. REICHHART, J. A. HOFFMANN and B. LEMAITRE, 1998 In vivo regulation of the IkappaB homologue cactus during the immune response of Drosophila. J Biol Chem **273:** 10463-10469.

NUSSLEIN-VOLHARD, C., and E. WIESCHAUS, 1980 Mutations affecting segment number and polarity in Drosophila. Nature **287:** 795-801.

OHTSUBO, M., A. M. THEODORAS, J. SCHUMACHER, J. M. ROBERTS and M. PAGANO, 1995 Human cyclin E, a nuclear protein essential for the G1-to-S phase transition. Mol Cell Biol **15:** 2612-2624.

PAGE, A. R., A. KOVACS, P. DEAK, T. TOROK, I. KISS *et al.*, 2005 Spotted-dick, a zinc-finger protein of Drosophila required for expression of Orc4 and S phase. Embo J **24:** 4304-4315.

PAINTER, R. B., 1986 Inhibition of mammalian cell DNA synthesis by ionizing radiation. Int J Radiat Biol Relat Stud Phys Chem Med **49:** 771-781.

PANKIV, S., T. H. CLAUSEN, T. LAMARK, A. BRECH, J. A. BRUUN *et al.*, 2007 p62/SQSTM1 binds directly to Atg8/LC3 to facilitate degradation of

ubiquitinated protein aggregates by autophagy. J Biol Chem **282:** 24131-24145.

PATTANAYEK, R., J. WANG, T. MORI, Y. XU, C. H. JOHNSON *et al.*, 2004 Visualizing a circadian clock protein: crystal structure of KaiC and functional insights. Mol Cell **15:** 375-388.

PAULOVICH, A. G., and L. H. HARTWELL, 1995 A checkpoint regulates the rate of progression through S phase in S. cerevisiae in response to DNA damage. Cell **82:** 841-847.

PERRIMON, N., A. LANJUIN, C. ARNOLD and E. NOLL, 1996 Zygotic lethal mutations with maternal effect phenotypes in Drosophila melanogaster. II. Loci on the second and third chromosomes identified by P-element-induced mutations. Genetics **144:** 1681-1692.

PINES, J., 1991 Cyclins: wheels within wheels. Cell Growth Differ **2:** 305-310.

PINES, J., 1995 Cyclins and cyclin-dependent kinases: a biochemical view. Biochem J **308 (Pt 3):** 697-711.

PINES, J., and T. HUNTER, 1990 Human cyclin A is adenovirus E1A-associated protein p60 and behaves differently from cyclin B. Nature **346:** 760-763.

POLLARD, T. D., and W. C. EARNSHAW, 2007 Cell Biology. SAUNDERS, An imprint of Elsevier Science, Philedelphia, United States of America.

POTTER, C. J., H. HUANG and T. XU, 2001 Drosophila Tsc1 functions with Tsc2 to antagonize insulin signaling in regulating cell growth, cell proliferation, and organ size. Cell **105:** 357-368.

PROBER, D. A., and B. A. EDGAR, 2000 Ras1 promotes cellular growth in the Drosophila wing. Cell **100:** 435-446.

PUIG, O., M. T. MARR, M. L. RUHF and R. TJIAN, 2003 Control of cell number by Drosophila FOXO: downstream and feedback regulation of the insulin receptor pathway. Genes Dev **17:** 2006-2020.

PUIG, O., and R. TJIAN, 2005 Transcriptional feedback control of insulin receptor by dFOXO/FOXO1. Genes Dev **19:** 2435-2446.

QIU, P., P. C. PAN and S. GOVIND, 1998 A role for the Drosophila Toll/Cactus pathway in larval hematopoiesis. Development **125:** 1909-1920.

RADIMERSKI, T., J. MONTAGNE, F. RINTELEN, H. STOCKER, J. VAN DER KAAY *et al.*, 2002 dS6K-regulated cell growth is dPKB/dPI(3)K-independent, but requires dPDK1. Nat Cell Biol **4:** 251-255.

RAFFA, G. D., G. CENCI, G. SIRIACO, M. L. GOLDBERG and M. GATTI, 2005 The putative Drosophila transcription factor woc is required to prevent telomeric fusions. Mol Cell **20:** 821-831.

RAMET, M., R. LANOT, D. ZACHARY and P. MANFRUELLI, 2002a JNK signaling pathway is required for efficient wound healing in Drosophila. Dev Biol **241:** 145-156.

RAMET, M., P. MANFRUELLI, A. PEARSON, B. MATHEY-PREVOT and R. A. EZEKOWITZ, 2002b Functional genomic analysis of phagocytosis and identification of a Drosophila receptor for E. coli. Nature **416:** 644-648.

RAMET, M., A. PEARSON, P. MANFRUELLI, X. LI, H. KOZIEL *et al.*, 2001 Drosophila scavenger receptor CI is a pattern recognition receptor for bacteria. Immunity **15:** 1027-1038.

READY, D. F., T. E. HANSON and S. BENZER, 1976 Development of the Drosophila retina, a neurocrystalline lattice. Dev Biol **53:** 217-240.

REITER, L. T., L. POTOCKI, S. CHIEN, M. GRIBSKOV and E. BIER, 2001 A systematic analysis of human disease-associated gene sequences in Drosophila melanogaster. Genome Res **11:** 1114-1125.

RESNITZKY, D., L. HENGST and S. I. REED, 1995 Cyclin A-associated kinase activity is rate limiting for entrance into S phase and is negatively regulated in G1 by p27Kip1. Mol Cell Biol **15:** 4347-4352.

RIZKI, T. M., and R. M. RIZKI, 1978 Larval adipose tissue of homoeotic bithorax mutants of Drosophila. Dev Biol **65:** 476-482.

RIZKI, T. M., and R. M. RIZKI, 1992 Lamellocyte differentiation in Drosophila larvae parasitized by Leptopilina. Dev Comp Immunol **16:** 103-110.

RIZKI, T. M., R. M. RIZKI and R. A. BELLOTTI, 1985 Genetics of a Drosophila phenoloxidase. Mol Gen Genet **201:** 7-13.

ROBERTS, D. B., 1998 *Drosophila* A Practical Approach. Oxford University Press Inc., New York, United States of America

RORTH, P., 1996 A modular misexpression screen in Drosophila detecting tissue-specific phenotypes. Proc Natl Acad Sci U S A **93:** 12418-12422.

RORTH, P., K. SZABO, A. BAILEY, T. LAVERTY, J. REHM *et al.*, 1998 Systematic gain-of-function genetics in Drosophila. Development **125:** 1049-1057.

ROSENBERG, A. R., F. ZINDY, F. LE DEIST, H. MOULY, P. METEZEAU *et al.*, 1995 Overexpression of human cyclin A advances entry into S phase. Oncogene **10:** 1501-1509.

RUSSO, J., S. DUPAS, F. FREY, Y. CARTON and M. BREHELIN, 1996 Insect immunity: early events in the encapsulation process of parasitoid (Leptopilina boulardi) eggs in resistant and susceptible strains of Drosophila. Parasitology **112 (Pt 1):** 135-142.

RUSTEN, T. E., K. LINDMO, G. JUHASZ, M. SASS, P. O. SEGLEN *et al.*, 2004 Programmed autophagy in the Drosophila fat body is induced by ecdysone through regulation of the PI3K pathway. Dev Cell **7:** 179-192.

RUTSCHMANN, S., A. C. JUNG, C. HETRU, J. M. REICHHART, J. A. HOFFMANN *et al.*, 2000a The Rel protein DIF mediates the antifungal but not the antibacterial host defense in Drosophila. Immunity **12:** 569-580.

RUTSCHMANN, S., A. C. JUNG, R. ZHOU, N. SILVERMAN, J. A. HOFFMANN *et al.*, 2000b Role of Drosophila IKK gamma in a toll-independent antibacterial immune response. Nat Immunol **1:** 342-347.

SALTIEL, A. R., and C. R. KAHN, 2001 Insulin signalling and the regulation of glucose and lipid metabolism. Nature **414:** 799-806.

SAMAKOVLIS, C., D. A. KIMBRELL, P. KYLSTEN, A. ENGSTROM and D. HULTMARK, 1990 The immune response in Drosophila: pattern of cecropin expression and biological activity. Embo J **9:** 2969-2976.

SANCHEZ, Y., C. WONG, R. S. THOMA, R. RICHMAN, Z. WU *et al.*, 1997 Conservation of the Chk1 checkpoint pathway in mammals: linkage of DNA damage to Cdk regulation through Cdc25. Science **277:** 1497-1501.

SANSAL, I., and W. R. SELLERS, 2004 The biology and clinical relevance of the PTEN tumor suppressor pathway. J Clin Oncol **22:** 2954-2963.

SARBASSOV, D. D., D. A. GUERTIN, S. M. ALI and D. M. SABATINI, 2005 Phosphorylation and regulation of Akt/PKB by the rictor-mTOR complex. Science **307:** 1098-1101.

SAVVIDOU, E., N. COBBE, S. STEFFENSEN, S. COTTERILL and M. M. HECK, 2005 Drosophila CAP-D2 is required for condensin complex stability and resolution of sister chromatids. J Cell Sci **118:** 2529-2543.

SCANGA, S. E., L. RUEL, R. C. BINARI, B. SNOW, V. STAMBOLIC *et al.*, 2000 The conserved PI3'K/PTEN/Akt signaling pathway regulates both cell size and survival in Drosophila. Oncogene **19:** 3971-3977.

SCHNARE, M., G. M. BARTON, A. C. HOLT, K. TAKEDA, S. AKIRA *et al.*, 2001 Toll-like receptors control activation of adaptive immune responses. Nat Immunol **2:** 947-950.

SCOTT, R. C., G. JUHASZ and T. P. NEUFELD, 2007 Direct induction of autophagy by Atg1 inhibits cell growth and induces apoptotic cell death. Curr Biol **17:** 1-11.

SCOTT, R. C., O. SCHULDINER and T. P. NEUFELD, 2004 Role and regulation of starvation-induced autophagy in the Drosophila fat body. Dev Cell **7:** 167-178.

SELMAN, C., J. M. TULLET, D. WIESER, E. IRVINE, S. J. LINGARD *et al.*, 2009 Ribosomal protein S6 kinase 1 signaling regulates mammalian life span. Science **326:** 140-144.

SHERR, C. J., J. KATO, D. E. QUELLE, M. MATSUOKA and M. F. ROUSSEL, 1994 D-type cyclins and their cyclin-dependent kinases: G1 phase integrators of the mitogenic response. Cold Spring Harb Symp Quant Biol **59:** 11-19.

SHEVCHENKO, A., M. WILM, O. VORM and M. MANN, 1996 Mass spectrometric sequencing of proteins silver-stained polyacrylamide gels. Anal Chem **68:** 850-858.

SHIIO, Y., S. DONOHOE, E. C. YI, D. R. GOODLETT, R. AEBERSOLD *et al.*, 2002 Quantitative proteomic analysis of Myc oncoprotein function. Embo J **21:** 5088-5096.

SILVERMAN, N., R. ZHOU, S. STOVEN, N. PANDEY, D. HULTMARK *et al.*, 2000 A Drosophila IkappaB kinase complex required for Relish cleavage and antibacterial immunity. Genes Dev **14:** 2461-2471.

SIMON, M. A., 1994 Signal transduction during the development of the Drosophila R7 photoreceptor. Dev Biol **166:** 431-442.

SMITH, E. M., and C. G. PROUD, 2008 cdc2-cyclin B regulates eEF2 kinase activity in a cell cycle- and amino acid-dependent manner. Embo J **27:** 1005-1016.

SORRENTINO, R. P., Y. CARTON and S. GOVIND, 2002 Cellular immune response to parasite infection in the Drosophila lymph gland is developmentally regulated. Dev Biol **243:** 65-80.

SPRADLING, A. C., D. STERN, A. BEATON, E. J. RHEM, T. LAVERTY *et al.*, 1999 The Berkeley Drosophila Genome Project gene disruption project: Single P-element insertions mutating 25% of vital Drosophila genes. Genetics **153:** 135-177.

SPRENGER, F., N. YAKUBOVICH and P. H. O'FARRELL, 1997 S-phase function of Drosophila cyclin A and its downregulation in G1 phase. Curr Biol **7:** 488-499.

ST JOHNSTON, D., 2002 The art and design of genetic screens: Drosophila melanogaster. Nat Rev Genet **3:** 176-188.

STOFANKO, M., S. Y. KWON and P. BADENHORST, 2008 A misexpression screen to identify regulators of Drosophila larval hemocyte development. Genetics **180:** 253-267.

STOVEN, S., I. ANDO, L. KADALAYIL, Y. ENGSTROM and D. HULTMARK, 2000 Activation of the Drosophila NF-kappaB factor Relish by rapid endoproteolytic cleavage. EMBO Rep **1:** 347-352.

SULIS, M. L., and R. PARSONS, 2003 PTEN: from pathology to biology. Trends Cell Biol **13:** 478-483.

SUN, H., B. N. BRISTOW, G. QU and S. A. WASSERMAN, 2002 A heterotrimeric death domain complex in Toll signaling. Proc Natl Acad Sci U S A **99:** 12871-12876.

SWANK, R. A., J. P. TH'NG, X. W. GUO, J. VALDEZ, E. M. BRADBURY *et al.*, 1997 Four distinct cyclin-dependent kinases phosphorylate histone H1 at all of its growth-related phosphorylation sites. Biochemistry **36:** 13761-13768.

SZETO, J., N. A. KANIUK, V. CANADIEN, R. NISMAN, N. MIZUSHIMA *et al.*, 2006 ALIS are stress-induced protein storage compartments for substrates of the proteasome and autophagy. Autophagy **2:** 189-199.

TAKUWA, N., Y. FUKUI and Y. TAKUWA, 1999 Cyclin D1 expression mediated by phosphatidylinositol 3-kinase through mTOR-p70(S6K)-independent signaling in growth factor-stimulated NIH 3T3 fibroblasts. Mol Cell Biol **19:** 1346-1358.

TAUSZIG, S., E. JOUANGUY, J. A. HOFFMANN and J. L. IMLER, 2000 Toll-related receptors and the control of antimicrobial peptide expression in Drosophila. Proc Natl Acad Sci U S A **97:** 10520-10525.

TAUSZIG-DELAMASURE, S., H. BILAK, M. CAPOVILLA, J. A. HOFFMANN and J. L. IMLER, 2002 Drosophila MyD88 is required for the response to fungal and Gram-positive bacterial infections. Nat Immunol **3:** 91-97.

TEIXEIRA, L., C. RABOUILLE, P. RORTH, A. EPHRUSSI and N. F. VANZO, 2003 Drosophila Perilipin/ADRP homologue Lsd2 regulates lipid metabolism. Mech Dev **120:** 1071-1081.

TELEMAN, A. A., Y. W. CHEN and S. M. COHEN, 2005a 4E-BP functions as a metabolic brake used under stress conditions but not during normal growth. Genes Dev **19:** 1844-1848.

TELEMAN, A. A., Y. W. CHEN and S. M. COHEN, 2005b Drosophila Melted modulates FOXO and TOR activity. Dev Cell **9:** 271-281.

TELEMAN, A. A., V. HIETAKANGAS, A. C. SAYADIAN and S. M. COHEN, 2008 Nutritional control of protein biosynthetic capacity by insulin via Myc in Drosophila. Cell Metab **7:** 21-32.

TENENBAUM, D., 2003 What's All the Buzz? Fruit Flies Provide Unique Model for Cancer Research. J Natl Cancer Inst **95:** 1742-1744.

TEPASS, U., L. I. FESSLER, A. AZIZ and V. HARTENSTEIN, 1994 Embryonic origin of hemocytes and their relationship to cell death in Drosophila. Development **120:** 1829-1837.

THEODOSIOU, N. A., and T. XU, 1998 Use of FLP/FRT system to study Drosophila development. Methods **14:** 355-365.

THOMAS, B. J., D. A. GUNNING, J. CHO and L. ZIPURSKY, 1994 Cell cycle progression in the developing Drosophila eye: roughex encodes a novel protein required for the establishment of G1. Cell **77:** 1003-1014.

THUMM, M., R. EGNER, B. KOCH, M. SCHLUMPBERGER, M. STRAUB *et al.*, 1994 Isolation of autophagocytosis mutants of Saccharomyces cerevisiae. FEBS Lett **349:** 275-280.

TIO, M., C. MA and K. MOSES, 1996 Extracellular regulators and pattern formation in the developing Drosophila retina. Biochem Soc Symp **62:** 61-75.

TOKUSUMI, T., R. P. SORRENTINO, M. RUSSELL, R. FERRARESE, S. GOVIND *et al.*, 2009 Characterization of a lamellocyte transcriptional enhancer located within the misshapen gene of Drosophila melanogaster. PLoS One **4:** e6429.

TSUKADA, M., and Y. OHSUMI, 1993 Isolation and characterization of autophagy-defective mutants of Saccharomyces cerevisiae. FEBS Lett **333:** 169-174.

UHLES, S., T. MOEDE, B. LEIBIGER, P. O. BERGGREN and I. B. LEIBIGER, 2003 Isoform-specific insulin receptor signaling involves different plasma membrane domains. J Cell Biol **163:** 1327-1337.

UM, S. H., F. FRIGERIO, M. WATANABE, F. PICARD, M. JOAQUIN *et al.*, 2004 Absence of S6K1 protects against age- and diet-induced obesity while enhancing insulin sensitivity. Nature **431:** 200-205.

VALOVKA, T., F. VERDIER, R. CRAMER, A. ZHYVOLOUP, T. FENTON *et al.*, 2003 Protein kinase C phosphorylates ribosomal protein S6 kinase betaII and regulates its subcellular localization. Mol Cell Biol **23:** 852-863.

VAN OBBERGHEN, E., V. BARON, L. DELAHAYE, B. EMANUELLI, N. FILIPPA *et al.*, 2001 Surfing the insulin signaling web. Eur J Clin Invest **31:** 966-977.

VASS, S., S. COTTERILL, A. M. VALDEOLMILLOS, J. L. BARBERO, E. LIN *et al.*, 2003 Depletion of Drad21/Scc1 in Drosophila cells leads to instability of the cohesin complex and disruption of mitotic progression. Curr Biol **13:** 208-218.

VERDU, J., M. A. BURATOVICH, E. L. WILDER and M. J. BIRNBAUM, 1999 Cell-autonomous regulation of cell and organ growth in Drosophila by Akt/PKB. Nat Cell Biol **1:** 500-506.

VERESHCHAGINA, N., and C. WILSON, 2006 Cytoplasmic activated protein kinase Akt regulates lipid-droplet accumulation in Drosophila nurse cells. Development **133:** 4731-4735.

VERMEULEN, K., D. R. VAN BOCKSTAELE and Z. N. BERNEMAN, 2003 The cell cycle: a review of regulation, deregulation and therapeutic targets in cancer. Cell Prolif **36:** 131-149.

VIDAL, S., R. S. KHUSH, F. LEULIER, P. TZOU, M. NAKAMURA *et al.*, 2001 Mutations in the Drosophila dTAK1 gene reveal a conserved function for MAPKKKs in the control of rel/NF-kappaB-dependent innate immune responses. Genes Dev **15:** 1900-1912.

WALKER, D. H., and J. L. MALLER, 1991 Role for cyclin A in the dependence of mitosis on completion of DNA replication. Nature **354:** 314-317.

WANG, X., and C. G. PROUD, 2009 Nutrient control of TORC1, a cell-cycle regulator. Trends Cell Biol **19:** 260-267.

WATSON, F. L., R. PUTTMANN-HOLGADO, F. THOMAS, D. L. LAMAR, M. HUGHES *et al.*, 2005 Extensive diversity of Ig-superfamily proteins in the immune system of insects. Science **309:** 1874-1878.

WEBER, A. N., S. TAUSZIG-DELAMASURE, J. A. HOFFMANN, E. LELIEVRE, H. GASCAN *et al.*, 2003 Binding of the Drosophila cytokine Spatzle to Toll is direct and establishes signaling. Nat Immunol **4:** 794-800.

WELLEN, K. E., and G. S. HOTAMISLIGIL, 2005 Inflammation, stress, and diabetes. J Clin Invest **115:** 1111-1119.
WELTE, M. A., S. CERMELLI, J. GRINER, A. VIERA, Y. GUO *et al.*, 2005 Regulation of lipid-droplet transport by the perilipin homolog LSD2. Curr Biol **15:** 1266-1275.
WHITFIELD, W. G., C. GONZALEZ, E. SANCHEZ-HERRERO and D. M. GLOVER, 1989 Transcripts of one of two Drosophila cyclin genes become localized in pole cells during embryogenesis. Nature **338:** 337-340.
WILLIAMS, M. J., 2007 Drosophila hemopoiesis and cellular immunity. J Immunol **178:** 4711-4716.
WILLIAMS, M. J., 2009 The c-src homologue Src64B is sufficient to activate the Drosophila cellular immune response. J Innate Immun **1:** 335-339.
WILLIAMS, M. J., I. ANDO and D. HULTMARK, 2005 Drosophila melanogaster Rac2 is necessary for a proper cellular immune response. Genes Cells **10:** 813-823.
WINKLER, G. S., T. G. PETRAKIS, S. ETHELBERG, M. TOKUNAGA, H. ERDJUMENT-BROMAGE *et al.*, 2001 RNA polymerase II elongator holoenzyme is composed of two discrete subcomplexes. J Biol Chem **276:** 32743-32749.
WU, M. Y., M. CULLY, D. ANDERSEN and S. J. LEEVERS, 2007 Insulin delays the progression of Drosophila cells through G2/M by activating the dTOR/dRaptor complex. Embo J **26:** 371-379.
WULLSCHLEGER, S., R. LOEWITH and M. N. HALL, 2006 TOR signaling in growth and metabolism. Cell **124:** 471-484.
XIONG, Y., T. CONNOLLY, B. FUTCHER and D. BEACH, 1991 Human D-type cyclin. Cell **65:** 691-699.
XU, T., and G. M. RUBIN, 1993 Analysis of genetic mosaics in developing and adult Drosophila tissues. Development **117:** 1223-1237.
XU, T., W. WANG, S. ZHANG, R. A. STEWART and W. YU, 1995 Identifying tumor suppressors in genetic mosaics: the Drosophila lats gene encodes a putative protein kinase. Development **121:** 1053-1063.
YATES, J. R., 3RD, J. K. ENG, A. L. MCCORMACK and D. SCHIELTZ, 1995 Method to correlate tandem mass spectra of modified peptides to amino acid sequences in the protein database. Anal Chem **67:** 1426-1436.
ZENG, Y., K. C. FORBES, Z. WU, S. MORENO, H. PIWNICA-WORMS *et al.*, 1998 Replication checkpoint requires phosphorylation of the phosphatase Cdc25 by Cds1 or Chk1. Nature **395:** 507-510.
ZETTERVALL, C. J., I. ANDERL, M. J. WILLIAMS, R. PALMER, E. KURUCZ *et al.*, 2004 A directed screen for genes involved in Drosophila blood cell activation. Proc Natl Acad Sci U S A **101:** 14192-14197.
ZHANG, H., J. P. STALLOCK, J. C. NG, C. REINHARD and T. P. NEUFELD, 2000 Regulation of cellular growth by the Drosophila target of rapamycin dTOR. Genes Dev **14:** 2712-2724.
ZINKE, I., C. S. SCHUTZ, J. D. KATZENBERGER, M. BAUER and M. J. PANKRATZ, 2002 Nutrient control of gene expression in Drosophila: microarray analysis of starvation and sugar-dependent response. Embo J **21:** 6162-6173.

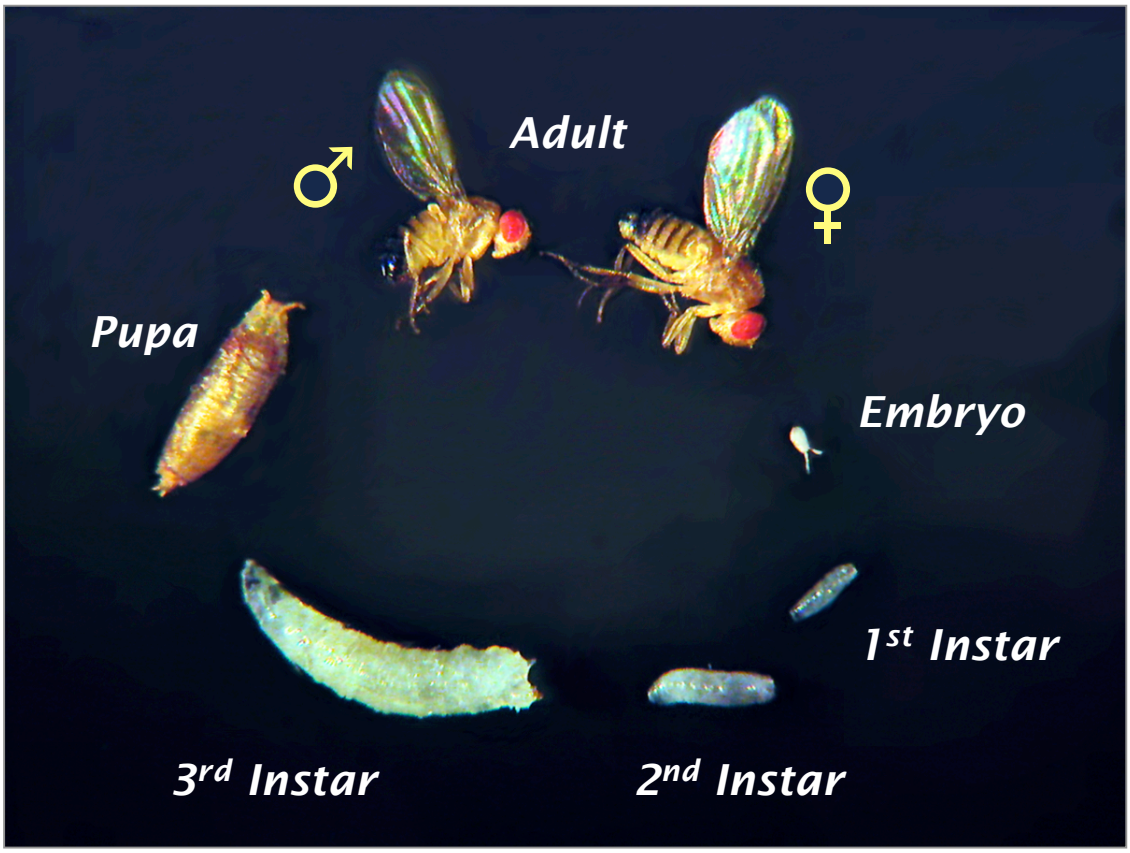

Figure 1.1. Life cycle of *Drosophila melanogaster*.

Drosophila goes through a complete metamorphosis passing through four different developmental stages including embryo, larva, pupa and finally the adult fly. The egg hatches into the first instar larva. Two additional larval instars follow the first instar larva while the animal keeps feeding and increasing in size and mass. Finally larvae undergo metamorphosis, during which pupa forms which later ecloses to give the adult fly (Image from Dr. Neville Cobbe).

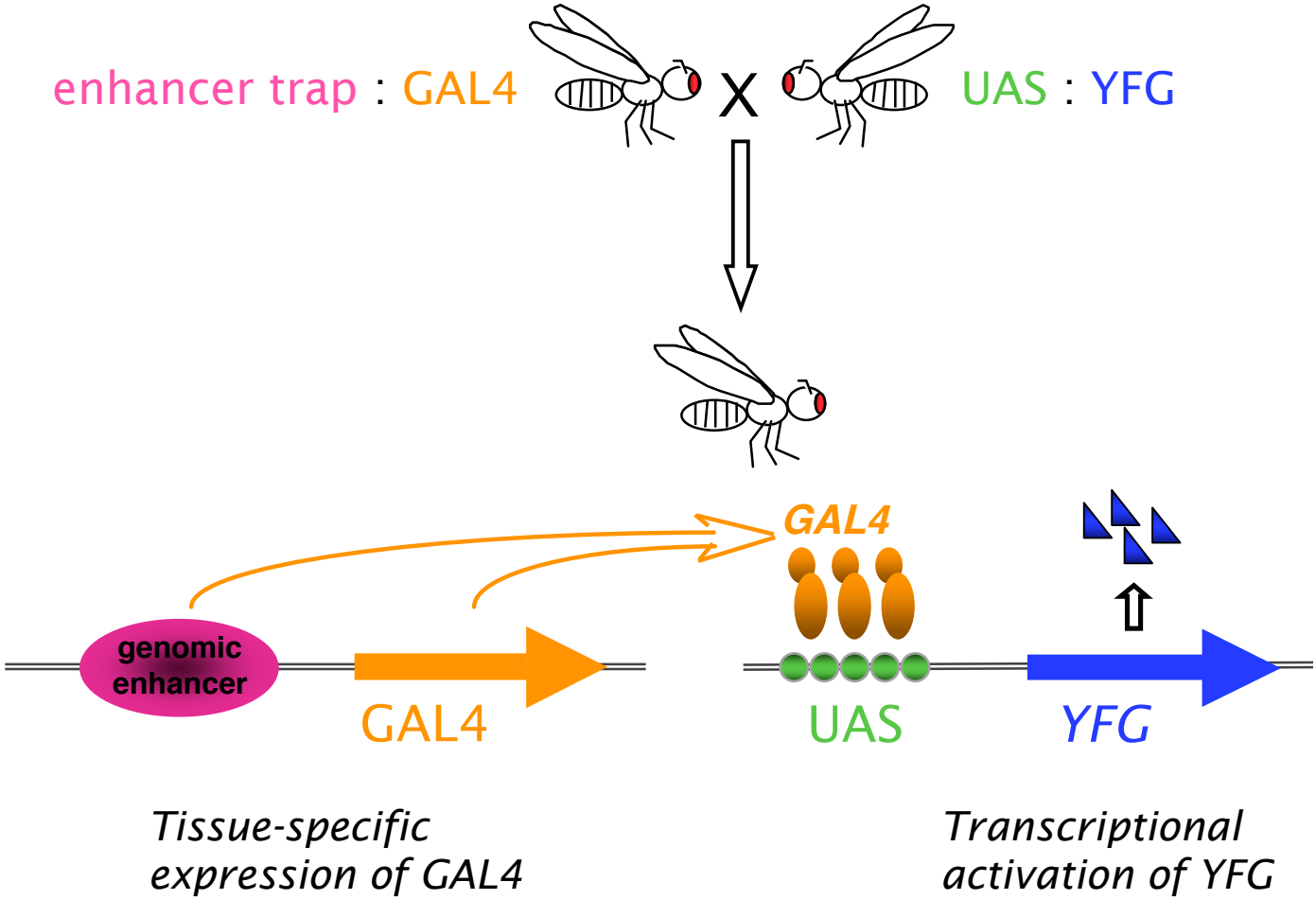

Figure 1.2. Directed gene expression by *UAS*-GAL4 system.

Directed gene expression in *Drosophila* is achieved by crossing an enhancer trap line expressing GAL4 transcription factor (shown in orange) under the control of a tissue specific promoter (shown in pink) with transgenic flies that have the *UAS* sequence (shown in green) inserted upstream of the gene of interest (your favourite gene, YFG shown in blue). In the resulting progeny GAL4 binds to *UAS* and therefore YFG is expressed in a tissue specific manner.

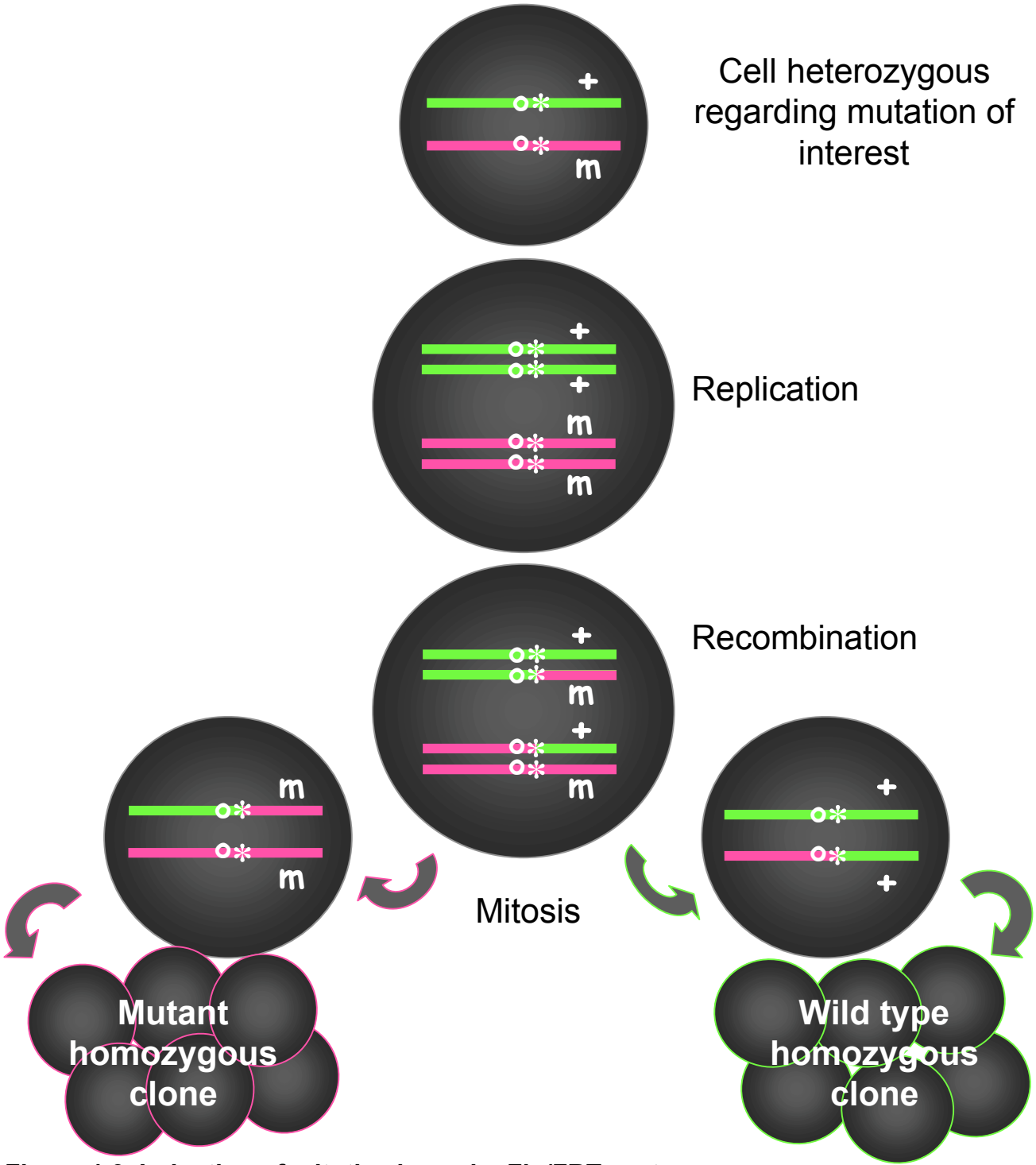

Figure 1.3. Induction of mitotic clones by Flp/FRT system.

In a cell heterozygous regarding the mutation of interest (mutation "m"), expression of FLP leads to mitotic recombination between FRT sites (indicated by asterisks) situated near the centrosome of chromosome arms. Following mitotic division, one daughter cell will inherit two copies of the mutation whereas the other cell will be wild type regarding the mutation. Subsequent proliferation of daughter cells results in wild type and mutant clones.

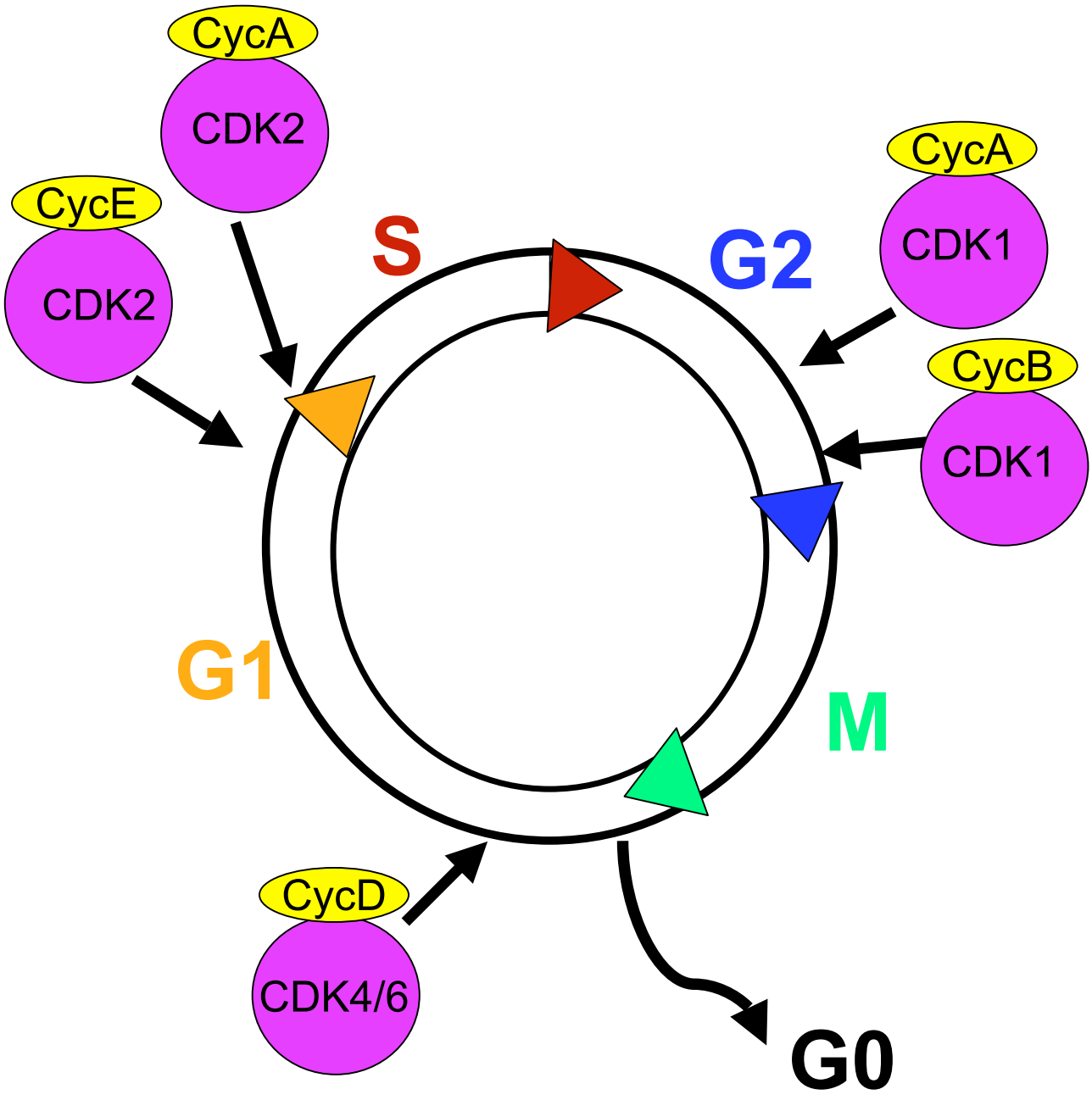

Figure 1.4. The stages of cell cycle.

Four stages of cell cycle includes G1, S, G2 and Mitosis (shown in orange, red, blue and green respectively). Cyclin-dependent kinases (Cdk, shown in purple) and their binding Cyclins (Cyc, shown in yellow) are important regulators of the cell cycle.

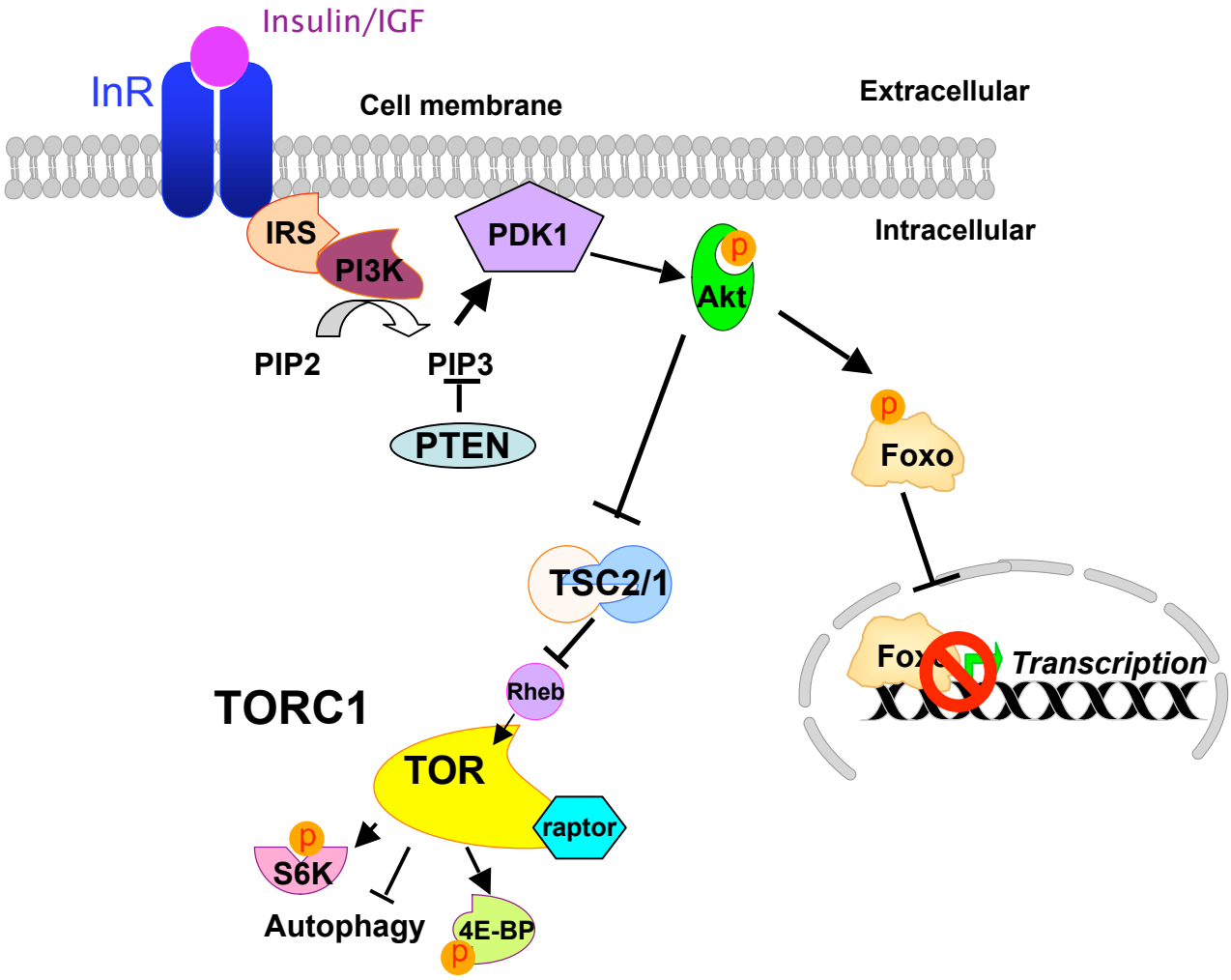

Figure 1.5. An overview of InR/TOR signalling pathway.

A number of phosphorylation events mediate signalling through the InR/TOR pathway. The binding of insulin or IGF activates the InR and leads in its turn to the activation PI3K via the IRS. Akt is recruited to the plasma membrane by PIP3 accumulation where it gets phosphorylated by PDK1 which has two important outcomes. One outcome is the phosphorylation and retention of Foxo transcription factor in the cytoplasm preventing it therefore from carrying out its function as a transcription factor. The other outcome is the inhibition of TSC2/1 complex which in its turn leads to the activation of TOR. TOR activation results in phosphorylation of S6K and 4E-BP which both contribute to an increase in translation and to inhibition of autophagy. The major outcome of the activation of this pathway is an increase in cellular growth and metabolism.

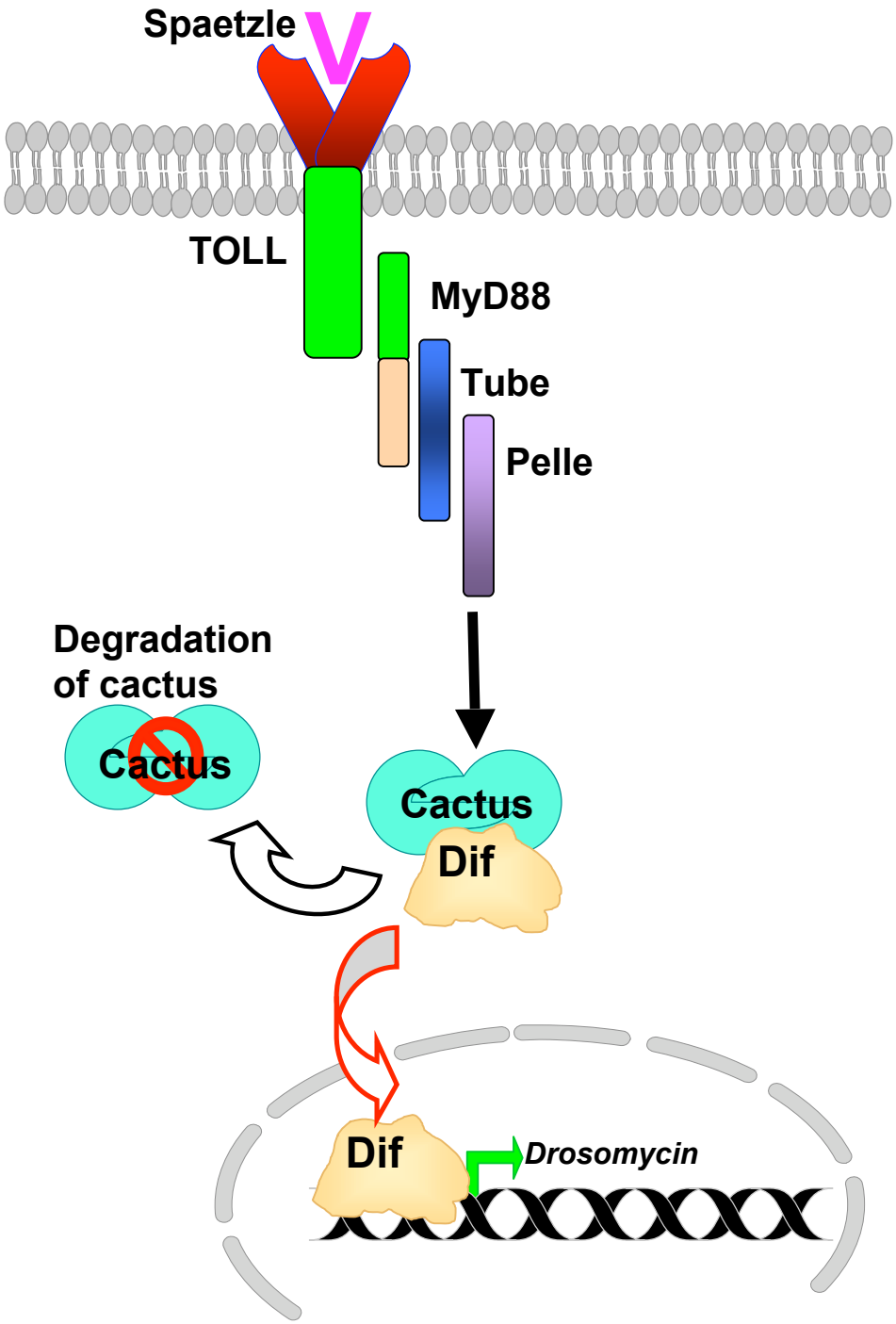

Figure 1.6. An overview of the Toll signalling pathway.

Toll signalling is activated following Gram-positive bacterial or fungal infection. The activation of the pathway results in expression of antimicrobial peptides such as Drosomycin that are involved in response against infection.

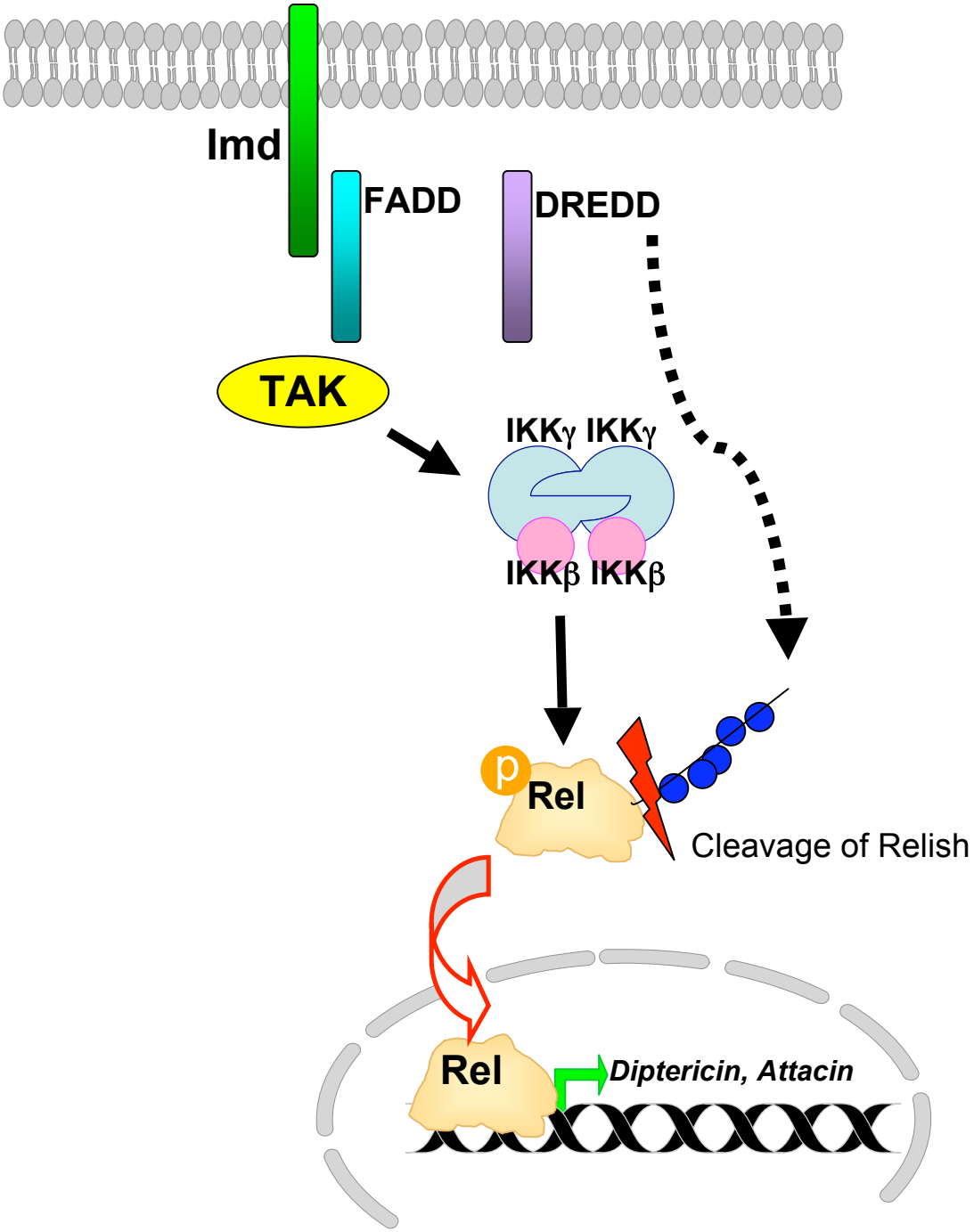

Figure 1.7. An overview of the Imd signalling pathway.

Imd pathway is mainly activated following Gram-negtive bacterial infection. The activation of the pathway results in cleavage of Relish transcription factor part of which can then move into the nucleus and direct the expression of antimicrobial peptide genes such as Diptericin and Attacin that are involved in the response against infection.

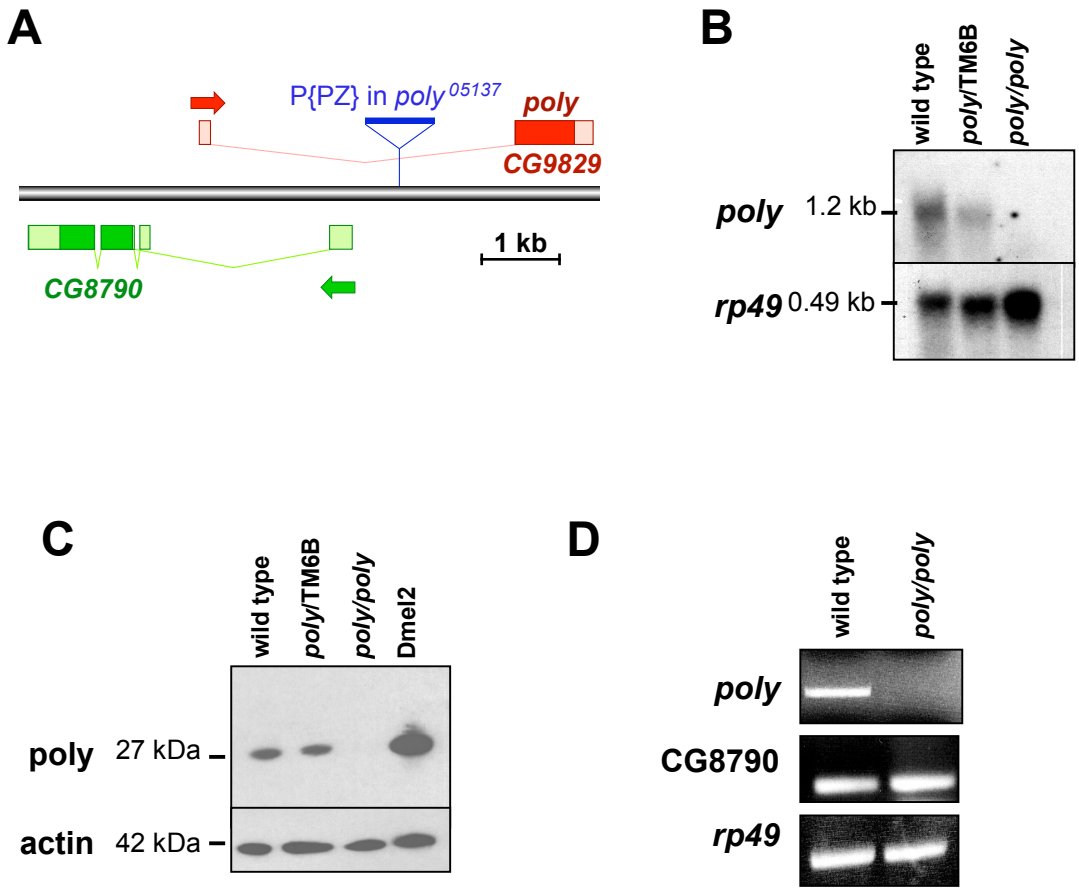

Figure 1.8. Gene map and *poly* expression analysis of *poly*^{5137} allele.

A) Gene map showing the P-element insertion into the first intron of *poly*. B, C) Northern and immunoblotting on extracts isolated from wild type, heterozygous and homozygous *poly* mutant third instar larvae showing the absence of Poly in homozygous mutant animals. Poly is present in Dmel2 cultured *Drosophila* cells. D) RT-PCR on extracts isolated from wild type and homozygous *poly* mutant third instar larvae showing that CG8790 expression levels are not affected in *poly*^{5137} allele. Data in panels B and C were generated by Prof. Margarete Heck and Dr. Sharron Vass respectively.

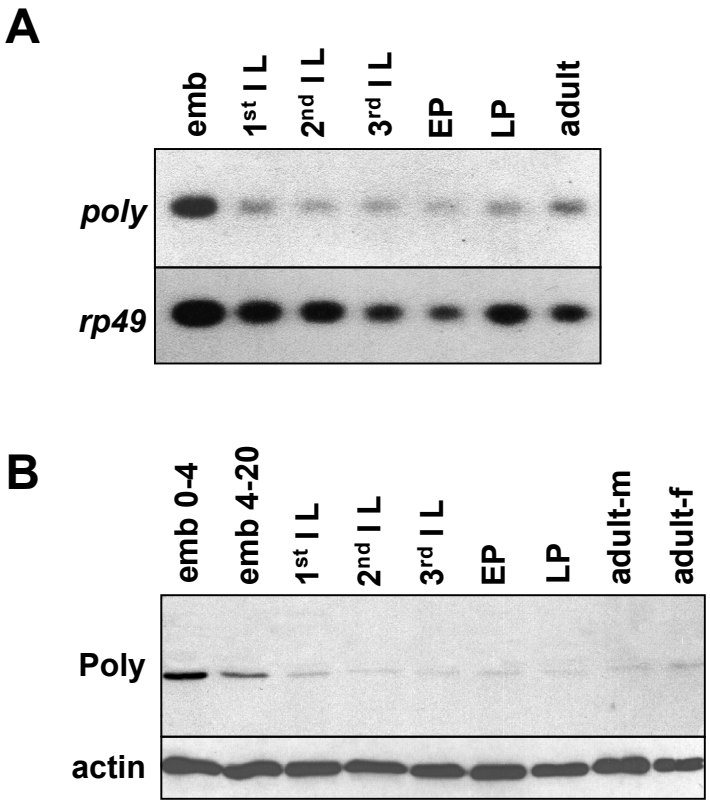

Figure 1.9. Expression analysis of *poly* mRNA and protein throughout development.

A) Northern blotting and B) Immunoblotting on extracts isolated at specific developmental stages of wild type animals showing Poly mRNA and protein expression levels. Data in this figure was generated by a former MSc by research student Victor Simossis.

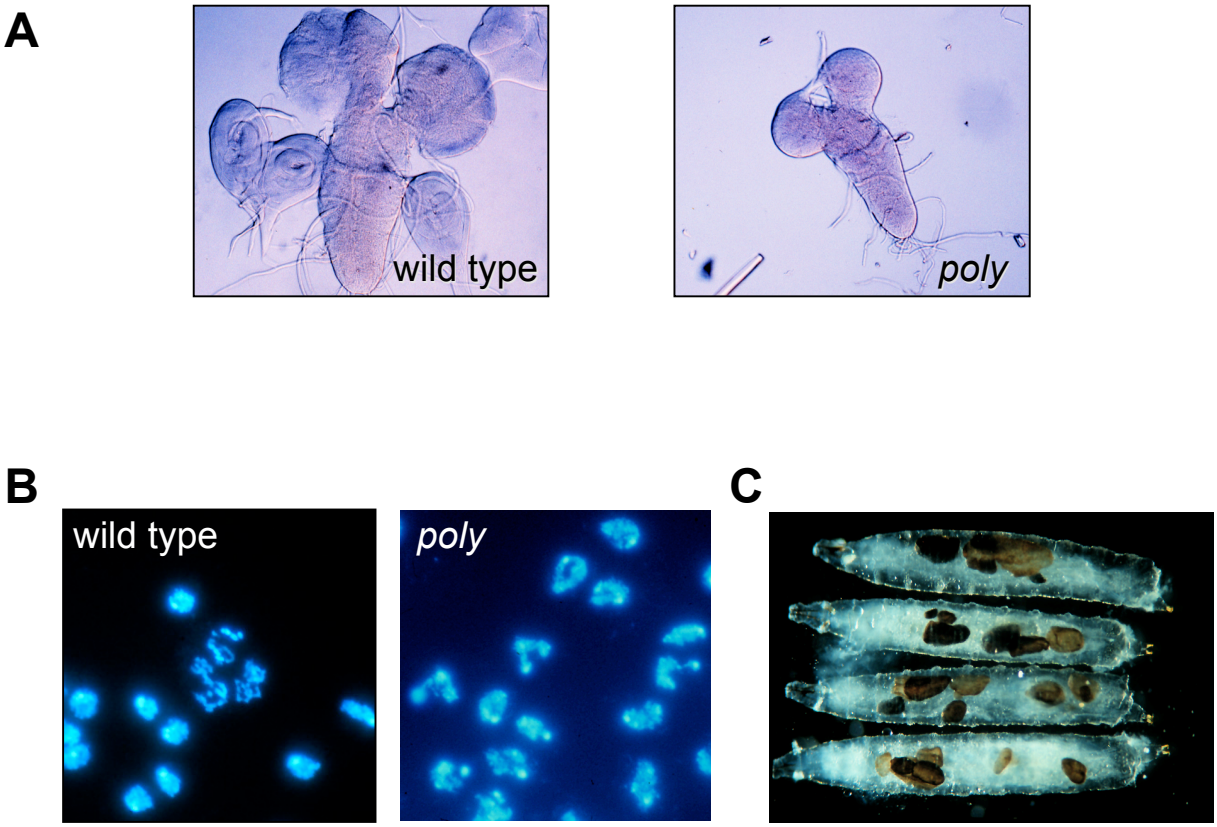

Figure 1.10. Morphology of various tissues in *poly* mutant larvae.

A) Third instar larval brain and imaginal discs dissected from wild type and *poly* animals. Note the reduced brain size and absence of imaginal discs in the homozygous *poly* mutant. B) DAPI staining of wild type and *poly* larval neuroblasts. Note the abnormally shaped nuclei in the homozygous *poly* mutant. C) Homozygous *poly* larvae start developing melanotic masses which increase in number with time. Data in this figure were generated by Prof. Margarete Heck and Dr. Sharron Vass.

Figure 1.11. Alignment of Poly homologues in other species.

Alignment showing Poly homologues conserved in *Homo sapiens* (Hs), *Danio rerio* (Dr), *Drosophila melanogaster* (Dm) and *Caenorhabditis elegans* (Ce).

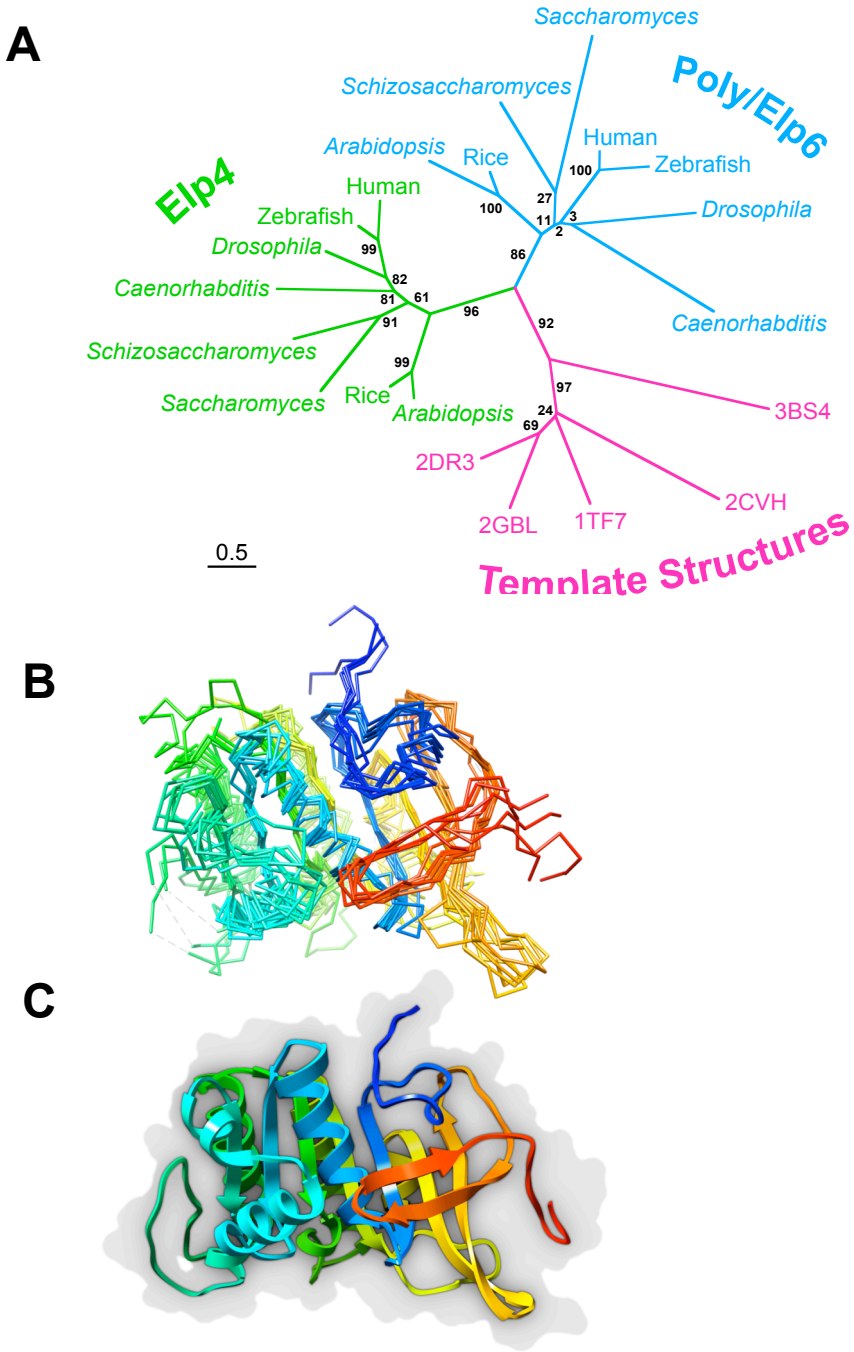

Figure 1.12. Phylogenetic and structural analysis of Poly.

A) Phylogenetic analysis suggested that Elp6 is the orthologue of Poly in yeast. Phylogenetic trees were calculated using TREE-PUZZLE, MrBayes and the Proml program of the PHYLIP Package after clustering of related sequences into smaller groups using SplitsTree4. Branch lengths were calculated by application of the WAG substitution matrix using TREE-PUZZLE. The proteins for which crystal structures were used as templates to model the structure of *Drosophila* Poly are indicated by their corresponding PDB codes. B) Superposition of seven structures used as templates for modelling the structure of Poly. C) Prediction of Poly protein structure using distant template structures suggests a core of beta sheets surrounded by alpha helices. Data in this figure was generated by Dr. Neville Cobbe.

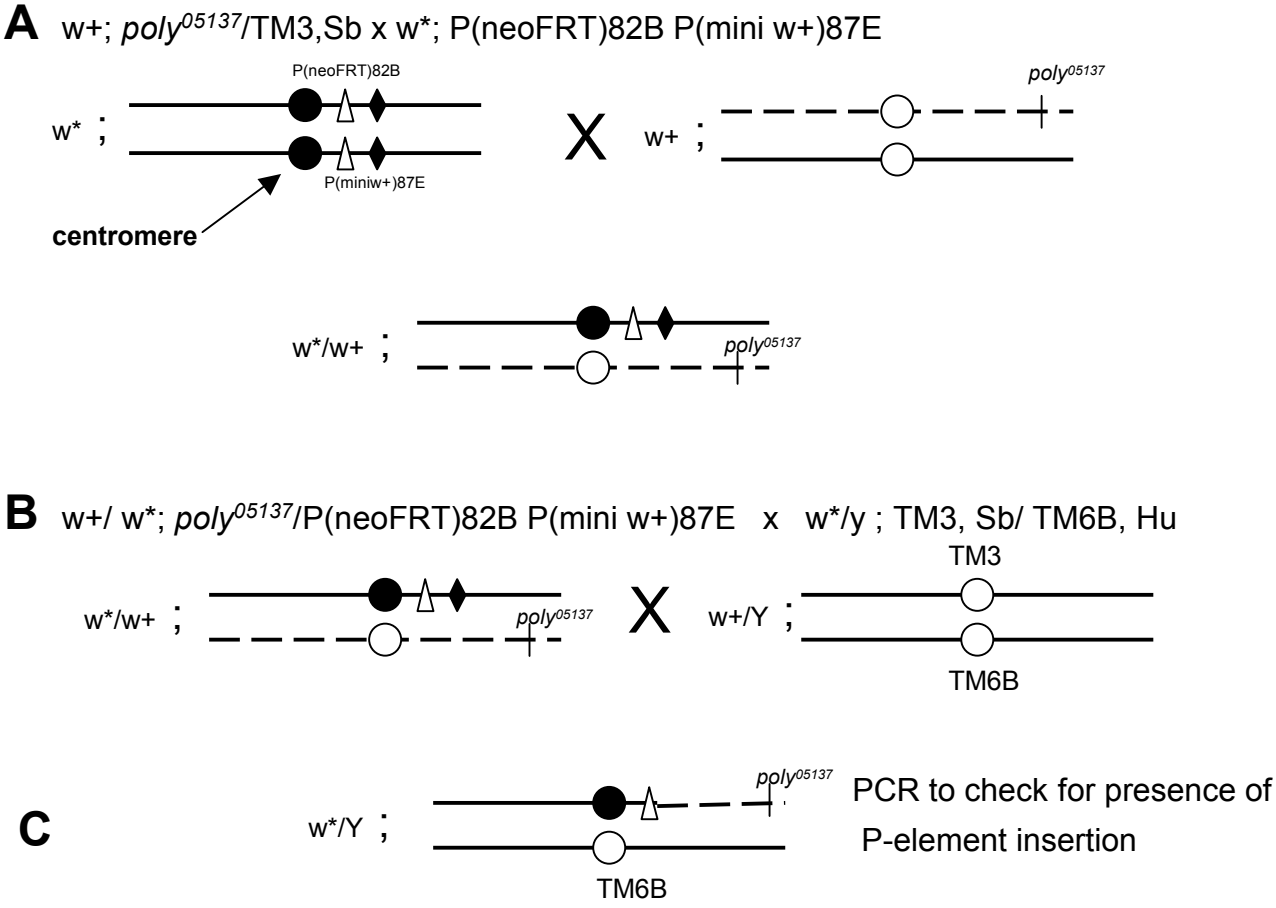

Figure 3.1. Crossing scheme for the generation of FRT82B*poly*^{05137}/TM6B flies.

A) *1st round of crossing:* Amongst the progeny resulting from this cross, non balancer females with the following genotype were selected: w+/ w*; *poly*^{05137}/P(neoFRT)82B P(mini w+)87E. The genomic location of *poly*^{05137} is distal to mini w+ marker. B) *Second round of crossing:* Non balancer female progeny resulting from the first cross were crossed to balancer males on neomycin containing media. Amongst the resulting progeny, flies that might have undergone female meiotic recombination between the FRT site and the *poly*^{05137} insertion were selected. Such meiotic recombination would lead the mini w+ marker on the distal end of the 3rd chromosome bearing the FRT site to be recombined away. Thus from the progeny of the second cross, male flies with white eye and neomycin resistance were selected. An individual line was established with each of these flies. At this point, selected flies could have one of the following genotypes: w*/y; P(neoFRT)82B/TM6B or P(neoFRT)82B*poly*^{05137}/TM6B. C) The existence of the P-element insertion leading to *poly*^{05137} mutation was verified by genomic PCR.

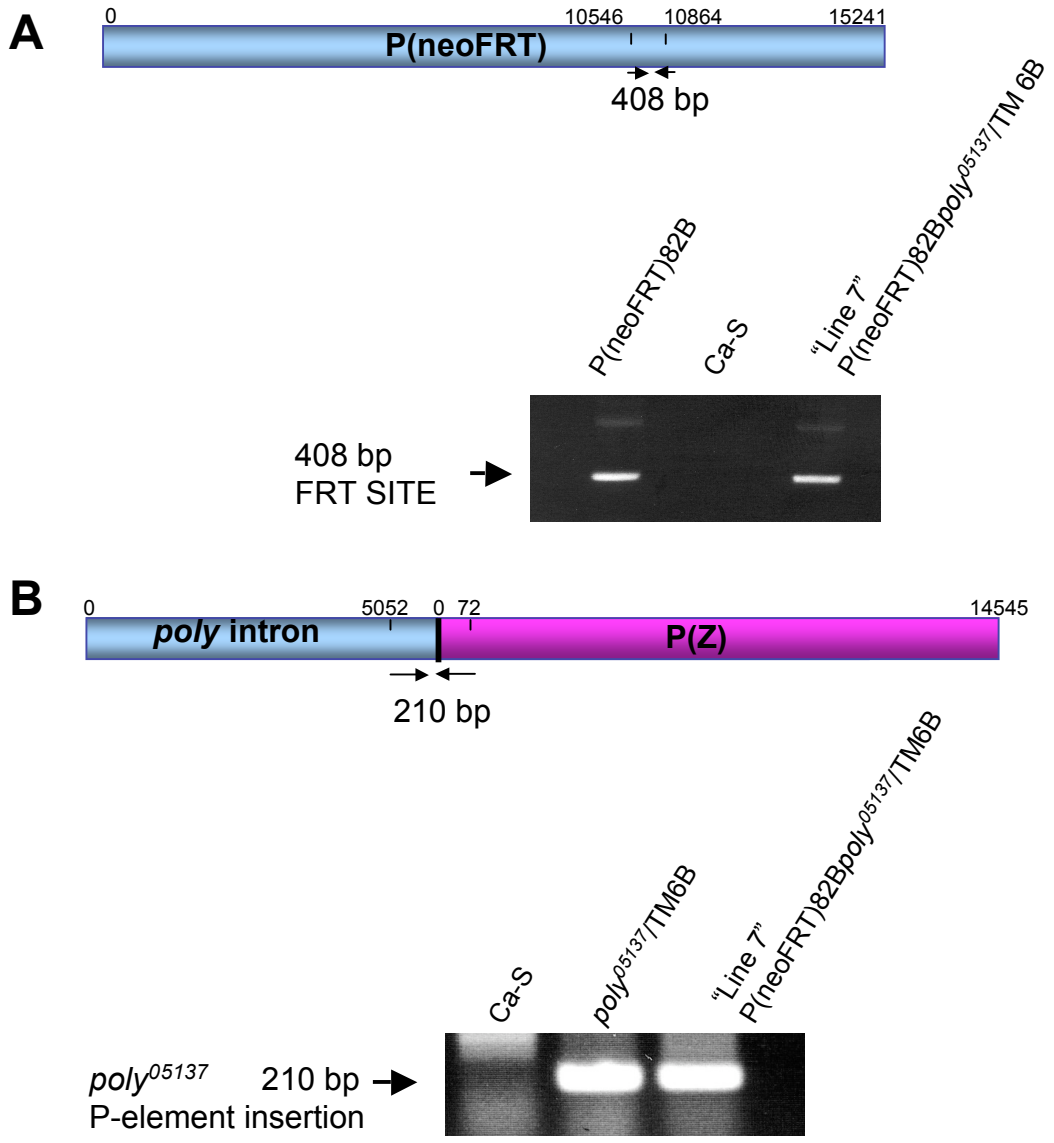

Figure 3.2. Genomic PCR was carried out on "Line 7" to confirm the presence of the FRT site and *poly*^{05137} P-element insertion.

A) Primers were designed on P(neoFRT) P-element sequence bearing both the FRT site and the neomycin resistance cassette to give a final PCR product of 408 base pairs. PCR on the genomic DNA revealed the presence of P(neoFRT) insertion in the positive control and in Line 7 whereas the band was absent in the wild-type negative control. B) Primers spaning the poly intron and the P(z) element were designed to detect the presence of *poly*^{05137} P-element insertion. PCR on the genomic DNA revealed the amplification of the *poly*^{05137} P-element in the positive control and Line 7 whereas the band was absent in wild-type negative controls.

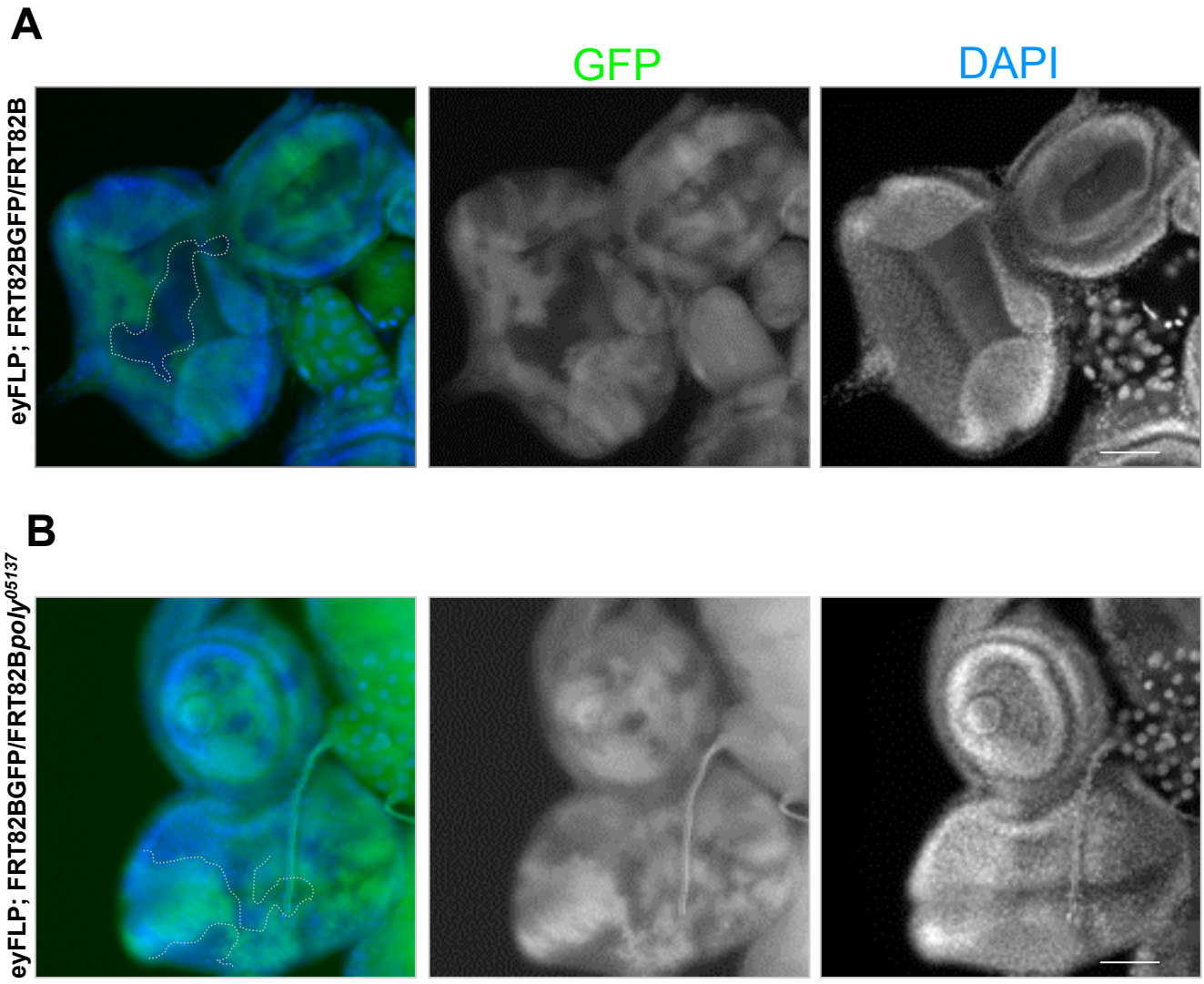

Figure 3.3. Generation of *poly* loss of function clones in third instar eye imaginal discs.

A) Immunofluorescence on eye imaginal discs dissected from control larvae of genotype *eyFLP; FRT82BGFP/FRT82B*. Clones resulting from mitotic recombination are indicated by the lack of GFP (green), DNA is stained by DAPI staining (blue). B) Immunofluorescence on eye imaginal disc dissected from flies of genotype *eyFLP; FRT82BGFP/FRT82Bpoly*^{05137}. *poly* loss of function clones resulting from mitotic recombination are indicated by the lack of GFP (green), DNA is stained by DAPI staining (blue) . Here, and in all subsequent disc figures, dotted lines outline the *poly* homozygous mutant clones. Scale bars represent 50 μm throughout.

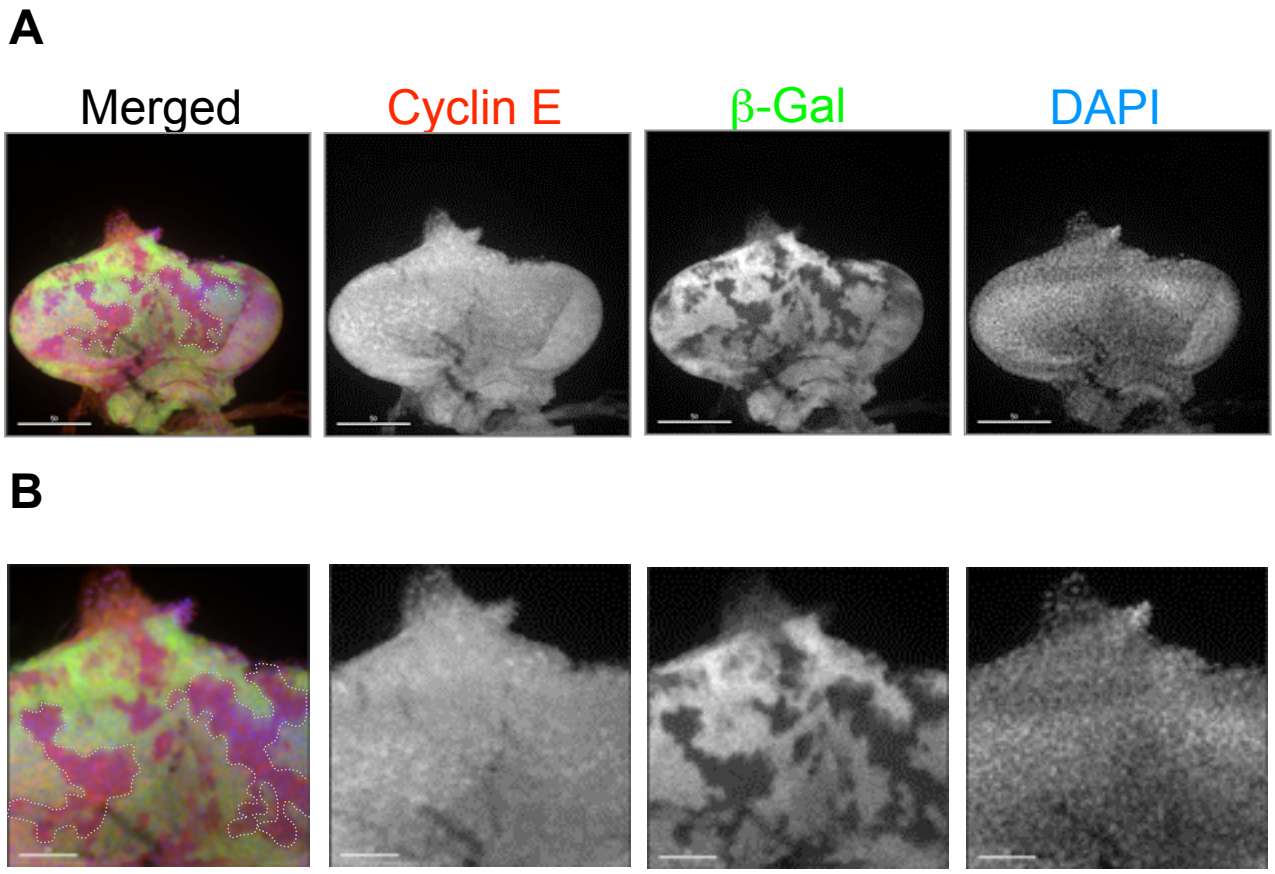

Figure 3.4. Cyclin E levels appear the same in *poly* loss of function clones and surrounding tissue.

(A, B) Images showing eye imaginal discs dissected from third instar larvae of the genotype *eyFLP; FRT82BB-lacz/FRT82Bpoly*^{05137} . Immunostaining was carried out for Cyclin E (red), β-galactosidase (green) and DNA (DAPI, blue). *poly* mutant clones are indicated by the lack of β-gal staining. Scale bars represent A) 50 and B) 20 μm.

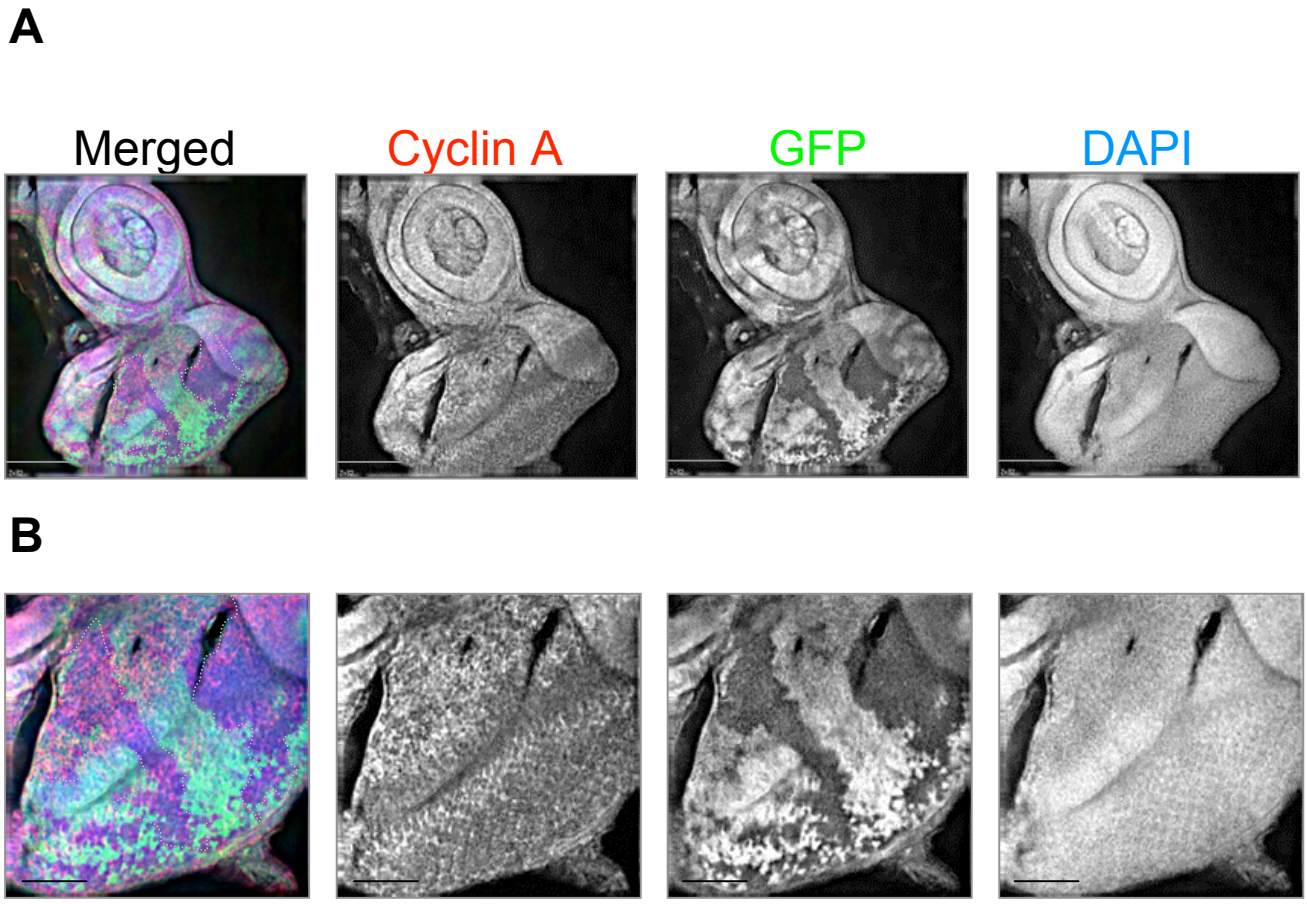

Figure 3.5. Cyclin A levels appear the same in *poly* loss of function clones and surrounding tissue.

(A, B) Images showing eye imaginal discs dissected from third instar larvae of the genotype *eyFLP; FRT82BGFP/FRT82Bpoly*^{05137}. Immunostaining was carried out for Cyclin A (red), GFP (green) and DNA (DAPI, blue). *poly* mutant clones are indicated by the lack of GFP. Scale bars represent A) 50 and B) 20 μm.

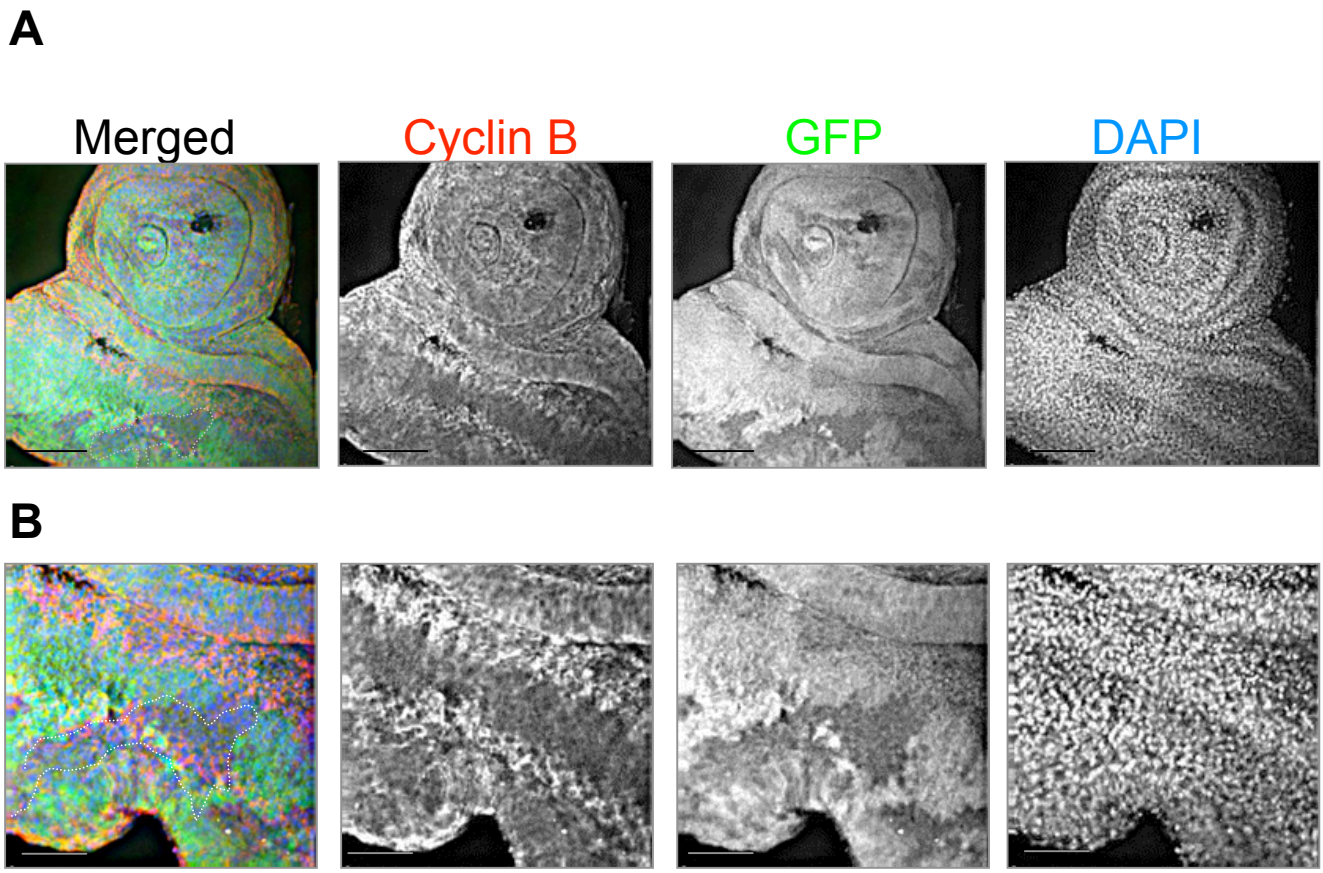

Figure 3.6. Cyclin B levels appear the same in *poly* loss of function clones and surrounding tissue.

(A, B) Images showing eye imaginal discs dissected from third instar larvae of the genotype *eyFLP; FRT82BGFP/FRT82Bpoly*$^{05137.}$ Immunostaining was carried out for Cyclin B (red), GFP (green) and DNA (DAPI, blue). *poly* mutant clones are indicated by the lack of GFP. Encircled region in both panels represent *poly* mutant clones. Panel B is a higher magnification of the image seen in panel A, mainly focusing on the the region bearing the encircled mutant clone. Scale bars represent A) 50 and B) 20 μm.

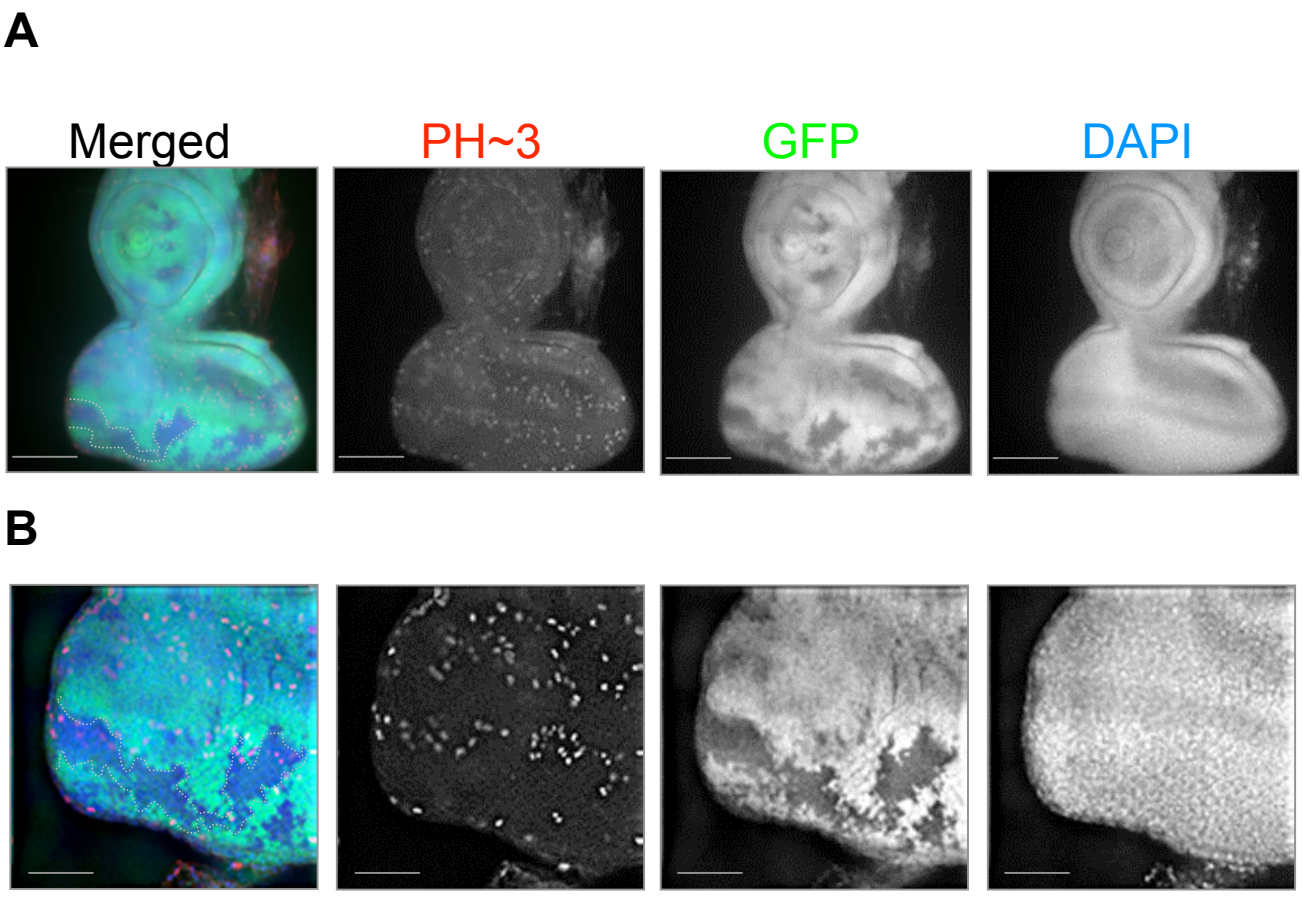

Figure 3.7. PH~3 levels appear the same in *poly* loss of function clones and surrounding tissue.

(A, B) Images showing eye imaginal discs dissected from third instar larvae of the genotype *eyFLP; FRT82BGFP/FRT82Bpoly05137.* Immunostaining was carried out for PH~3 (red), GFP (green) and DNA (DAPI, blue). *poly* mutant clones are indicated by the lack of GFP. Scale bars represent A) 50 and B) 20 μm.

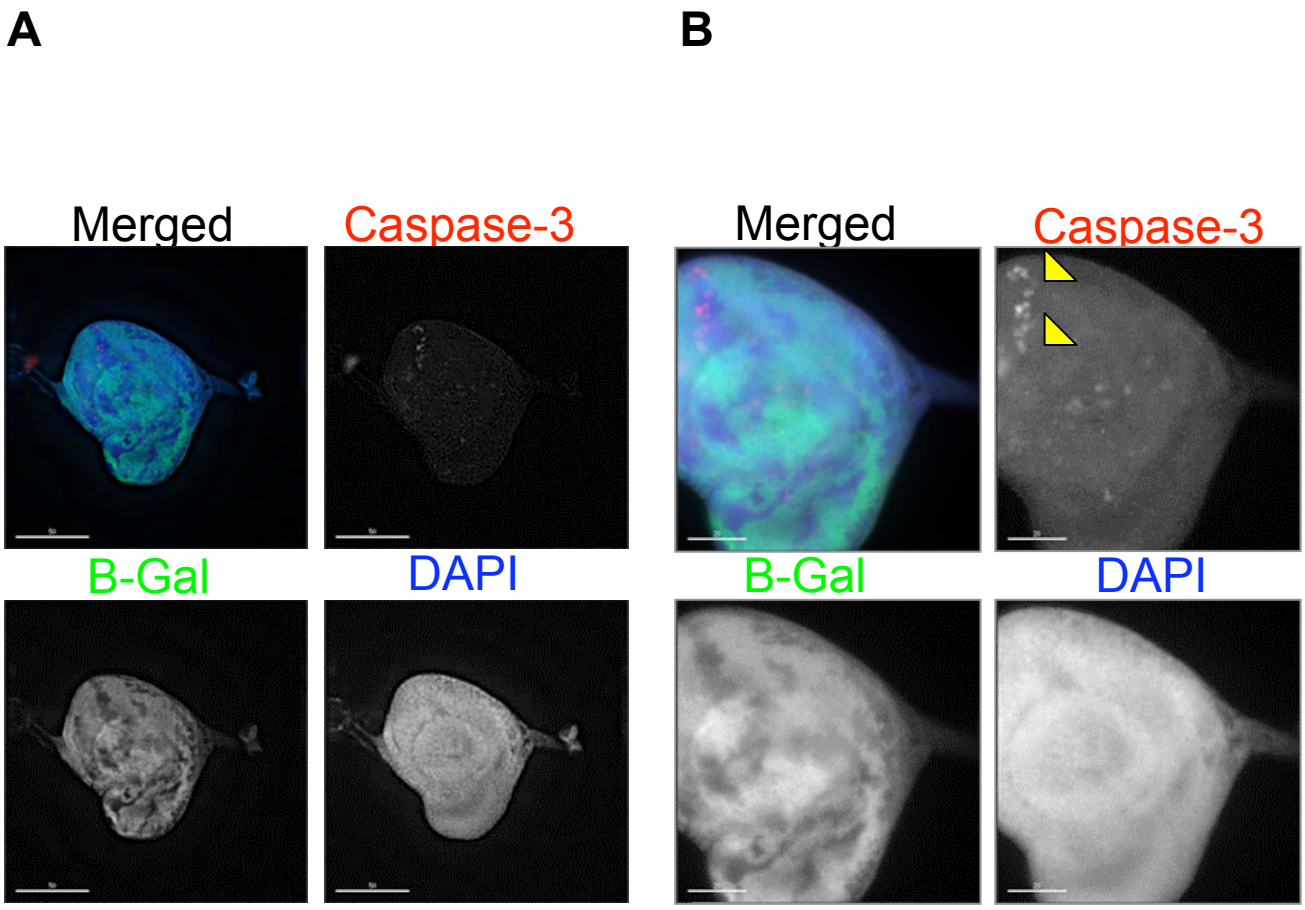

Figure x: (A, B) Images showing eye imaginal discs dissected from third instar larvae of the genotype eyeFLP; FRT82BB-Gal/FRT82B*poly*^{5137} . Immunostaining was carried out for claeved casp-3 (red), B-Galactosidase (green) and DNA (DAPI, blue). Poly mutant clones are indicated by the lack of B-Gal staining. Scale bars present 50 and 30 microns (?).

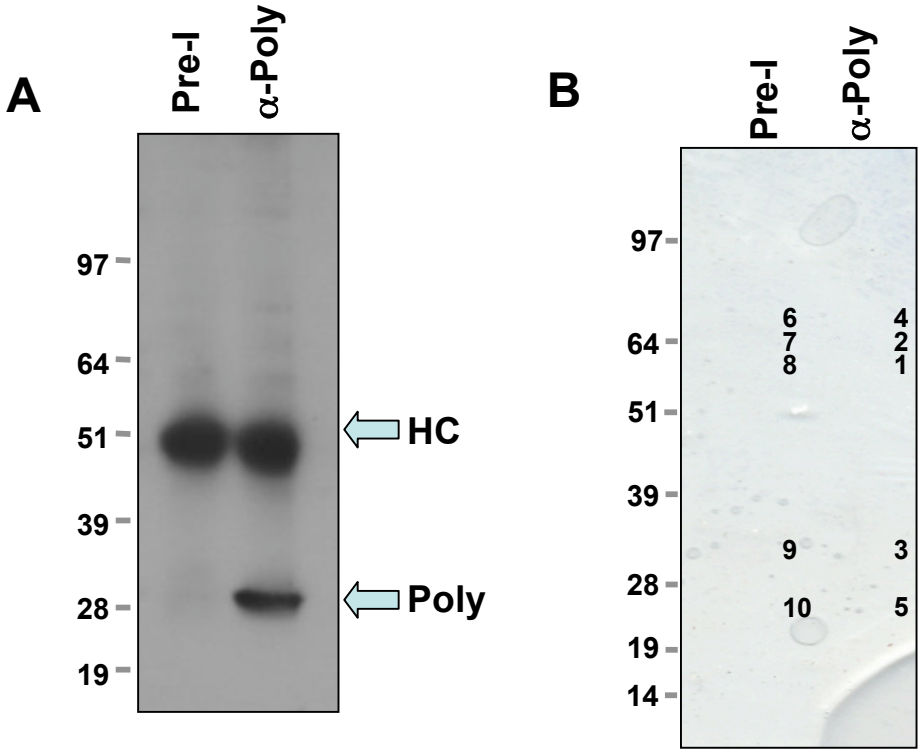

C

Band	Exp score	Unique/Total peptides	Protein
1	-13	4/7	Insulin-like receptor
2	-13	4/7	Insulin-like receptor
3	-5.3	3/3	E-Cadherin
4	-3	1/1	ATP-dependent RNA helicase (Rm62)
5	-2.5	2/2	Transient receptor potential cation channel subfamily A (TrpA1)

Figure 4.1. Poly interacts physically with the insulin receptor.

A) The antibody named anti-Poly 504 generated to recombinant his-tagged Poly can immunoprecipitate Poly from wild type *Drosophila* third instar larval extracts. The same antibody was used in for western blotting following immuniprecipitation. HC represents the heavy chain recognised by the secondary antibody reagent. Poly migrates at its predicted size of 28 kDa. B) Poly was immunoprecipitated from 0-5 hr wild type embryos using anti-Poly antibodies and compared to identical samples immunoprecipitated with pre-immune serum. Bands numbered 1-5 in the immunoprecipitate lane and their corresponding bands in the preimmune lane (numbered 6-10) were excised from the Coomassie blue stained gel and analyzed by mass spectrometry. C) Analysis of preimmune and immune-precipitation lanes by tandem mass spectrometry identified interacting proteins specifically found in the immune-precipitate sample. Insulin receptor was identified in bands 1 and 2. "Exp score" quantifies on a log scale (base 10) the expectation that the hit was achieved by chance, calculated using the program X!Tandem.

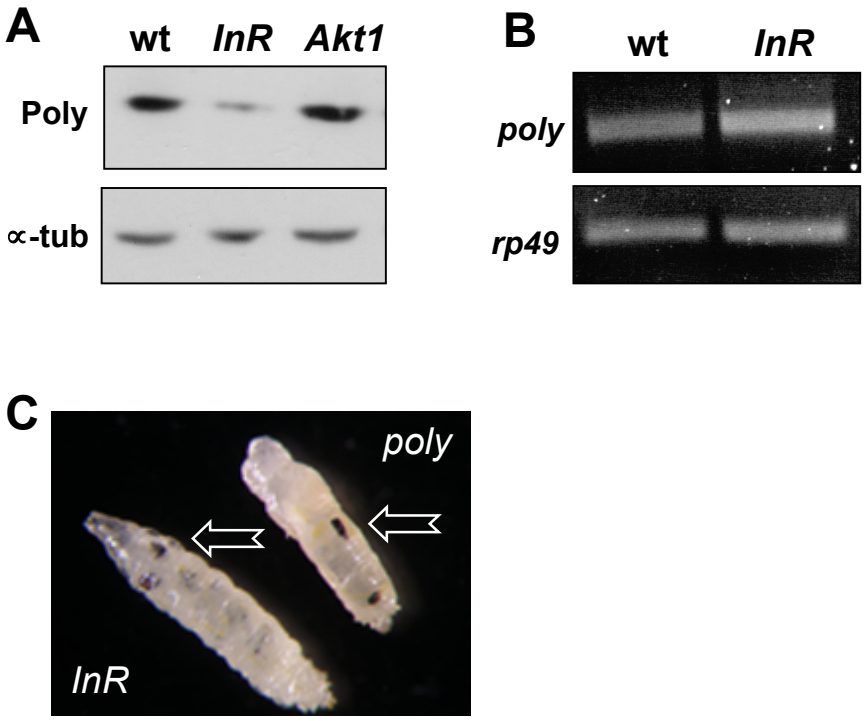

Figure 4.2. *InR* larvae show decreased Poly levels and appearance of melanotic masses.

A) Immunoblotting using anti-Poly antibody was carried out on wild type, InR^{05545}, and $Akt1^{04226}$ larval extracts. B) RT-PCR was performed using primers specific for *poly* and *rp49* on RNA extracted from wild type and InR^{05545} larvae. C) Arrows point melanotic masses observed in InR^{05545} and *poly* mutant larvae. Melanotic masses observed in both InR^{05545} and *poly* mutant larvae appeared to be superficially similar to each other.

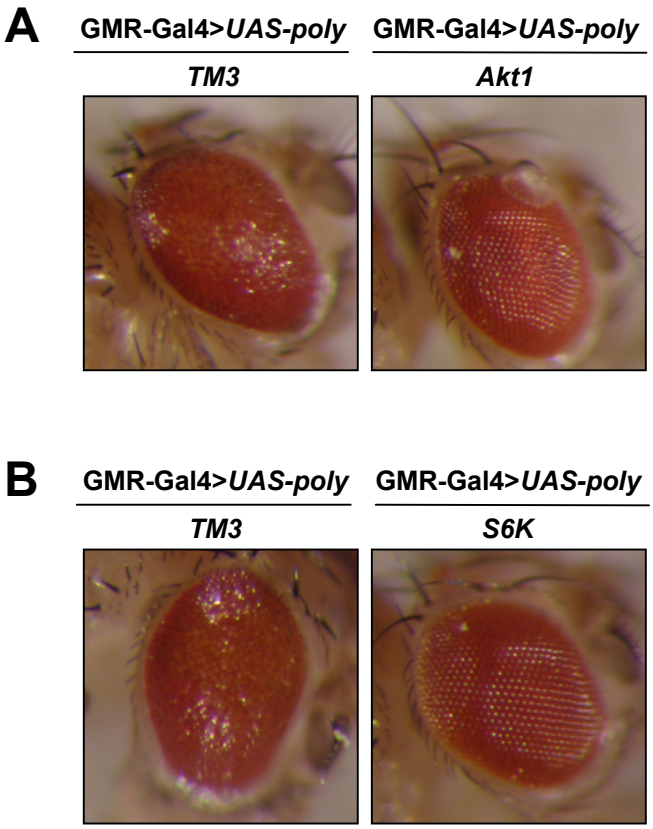

Figure 4.3. Mutations in *dAkt* and *dS6K* lead to suppression of the rough eye phenotype induced by *poly* over-expression.

A, B) Images showing *Drosophila* compound eyes. *UAS-poly* transgene was over-expressed under the control of the eye specific *GMR-Gal4* driver. Homozygous flies of genotype GMR-Gal4>*UAS-poly* were crossed with flies that were mutant in *Akt* and *S6K*. A,B) Left panels are images showing *Drosophila* compound eyes over-expressing one copy of *UAS-poly* under the control of GMR-Gal4 driver. A,B) Right panels are images of *Drosophila* compound eyes over-expressing one copy of *UAS-poly* under the control of GMR-Gal4 driver and bearing a mutation in A) *Akt* or B) *S6K*. TM3 represents the balancer chromosome carried by control sibling progeny.

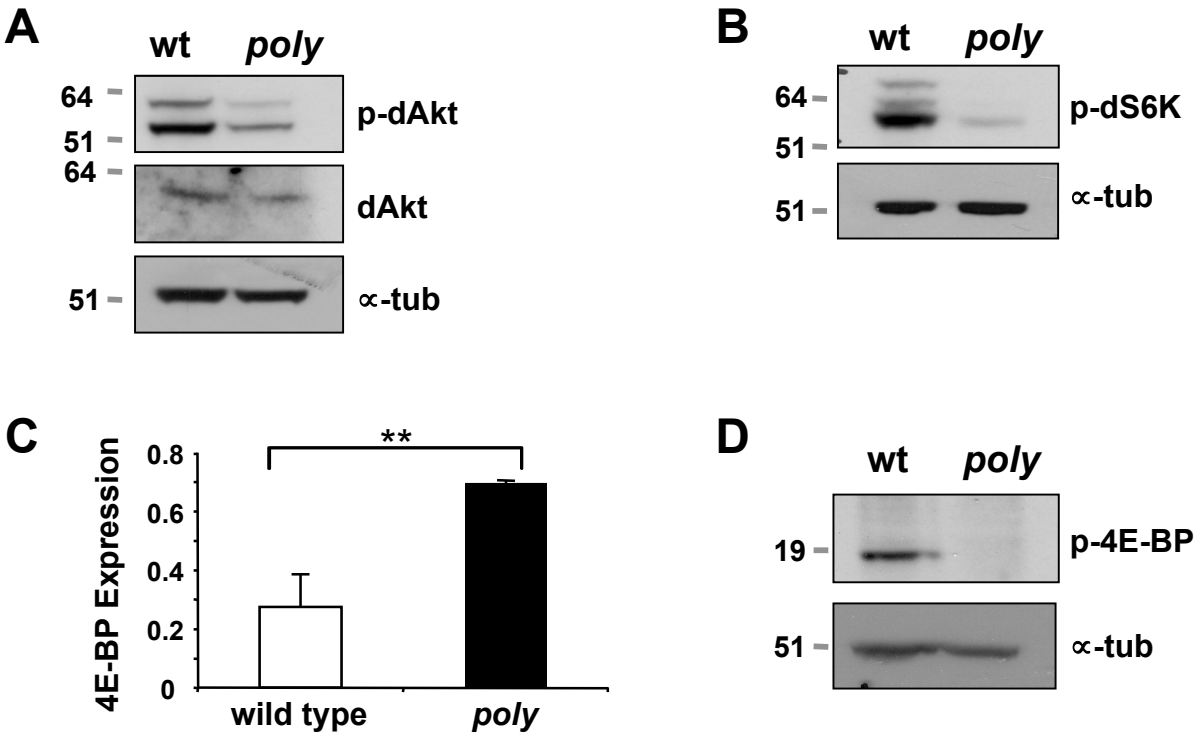

Figure 4.4. Activity of Akt, S6K and 4E-BP is down-regulated upon *poly* loss of function.

A, B) Immunoblotting of third instar larval extracts with phospho-specific antibodies to dAkt and dS6K reveals decreased phosphorylation of both kinases in *poly* larval extracts. C) d4E-BP transcript levels were assessed by real-time qPCR on RNA isolated from wild type and *poly* mutant larvae. d4E-BP levels were normalized to Actin5C levels. The error bars derive from reactions carried on biological triplicate samples. Double asterisk represents significant difference ($p<0.01$) in 4E-BP expression levels between wild type and *poly* larvae. D) Immunoblotting of third instar larval extracts showing decreased phosphorylation of d4E-BP in *poly* compared to wild type larvae.

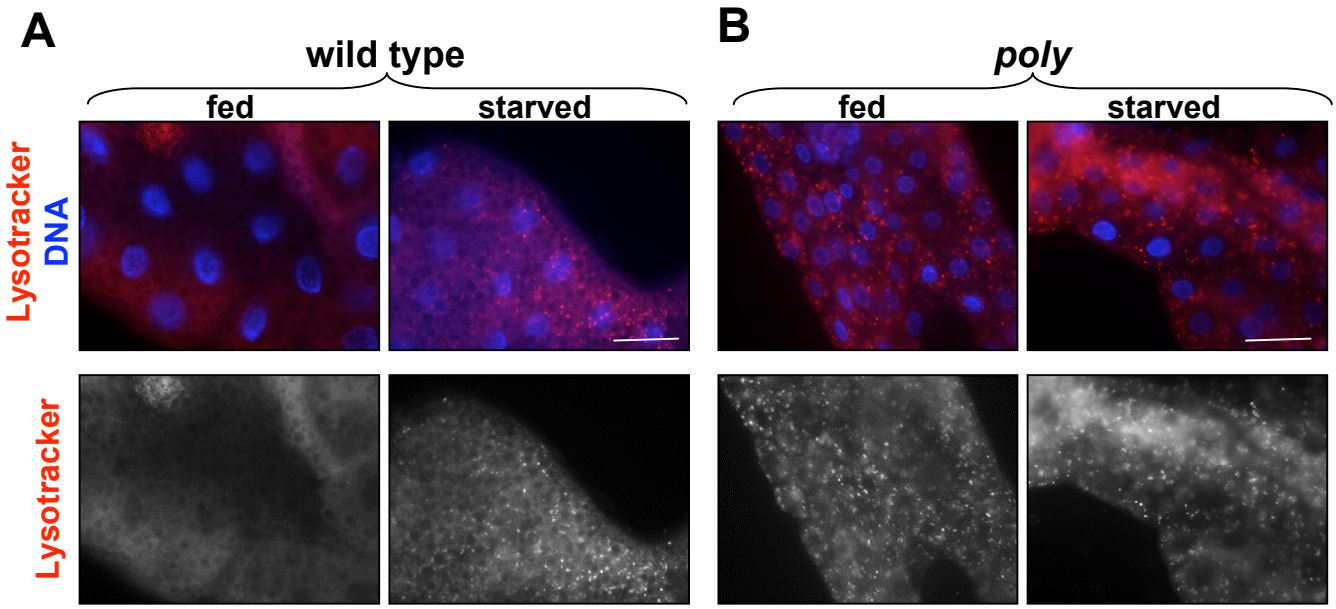

Figure 4.5. Poly is a regulator of the autophagic pathway.

A, B) Lysotracker (an acidic component-specific fluorescent dye) was used to monitor the state of autophagy in early third instar larval fat body. Autophagy was indicated by punctate Lysotracker staining. Live fat body tissues were stained with Lysotracker (red) and Hoechst 33342 to label DNA (blue). A, left panel) In early third instar larval fat body, no autophagy is evident. A, right panel) As indicated by Lysotracker positive bright spots, autophagy is active upon 4 hour amino acid starvation in 20% sucrose solution. B, left panel) Lysotracker positive spots can be detected in fed early third instar *poly* larval fat body, as well as in starved *poly* fat body. Scale bars represent 50 μm throughout.

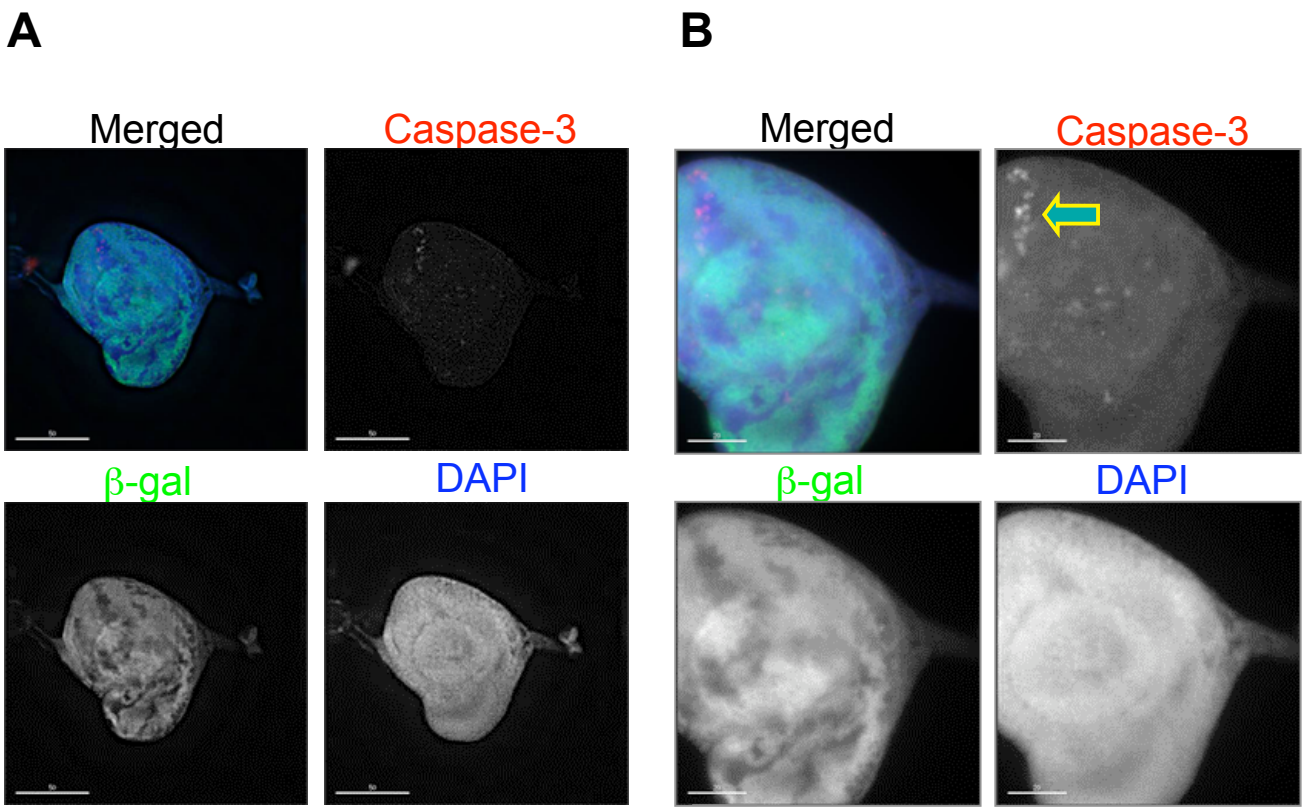

Figure 4.6. *poly* loss of function leads to increased Caspase-3 staining.

A, B) Images showing eye imaginal discs dissected from third instar larvae of the genotype *eyFLP; FRT82Bβ-Gal/FRT82Bpoly*^{05137}. Immunostaining was carried out for cleaved casp-3 (red), β-galactosidase (green) and DNA (DAPI, blue). *poly* mutant clones are indicated by the lack of β-Gal staining. Scale bars represent 50 and 30 μm for panel A and B respectively.

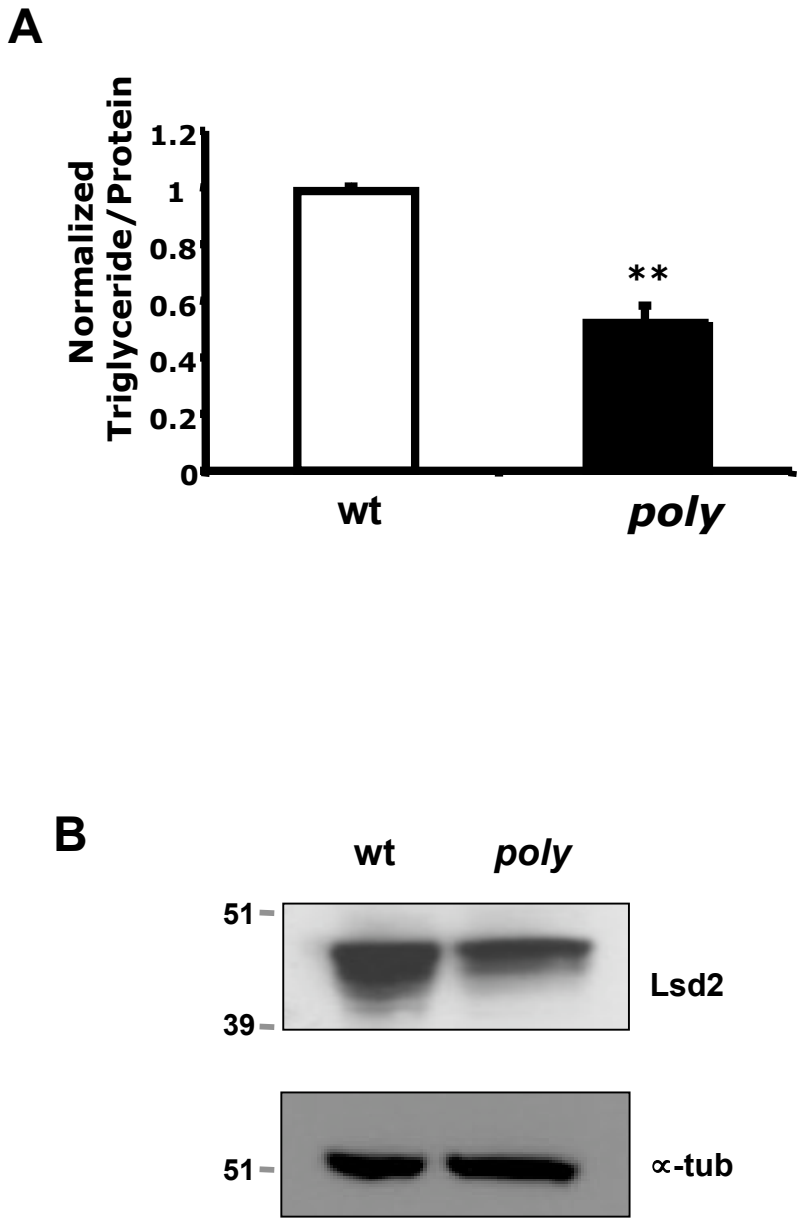

Figure 4.7. *poly* mutant larvae are characterized by reduced levels of triglycerides and Lsd2.

A) Triglyceride levels were assessed in wild type and *poly* mutant third instar larvae. Total triglyceride levels were normalized to total protein levels in order to get an accurate quantification. Error bars derive from biological triplicate of experiments. Error bars are derived from the standard deviation of three independent experiments. The unpaired two tailed t-test was used to compare the data from wild type and *poly* larvae. Double asterisk represents significant difference ($p<0.01$) in triglyceride levels between control larvae and *poly* mutants. B) Immunoblotting was carried out on larval extracts isolated from wild type and *poly* mutant larvae by using an antibody that specifically recognizes Lsd2 protein.

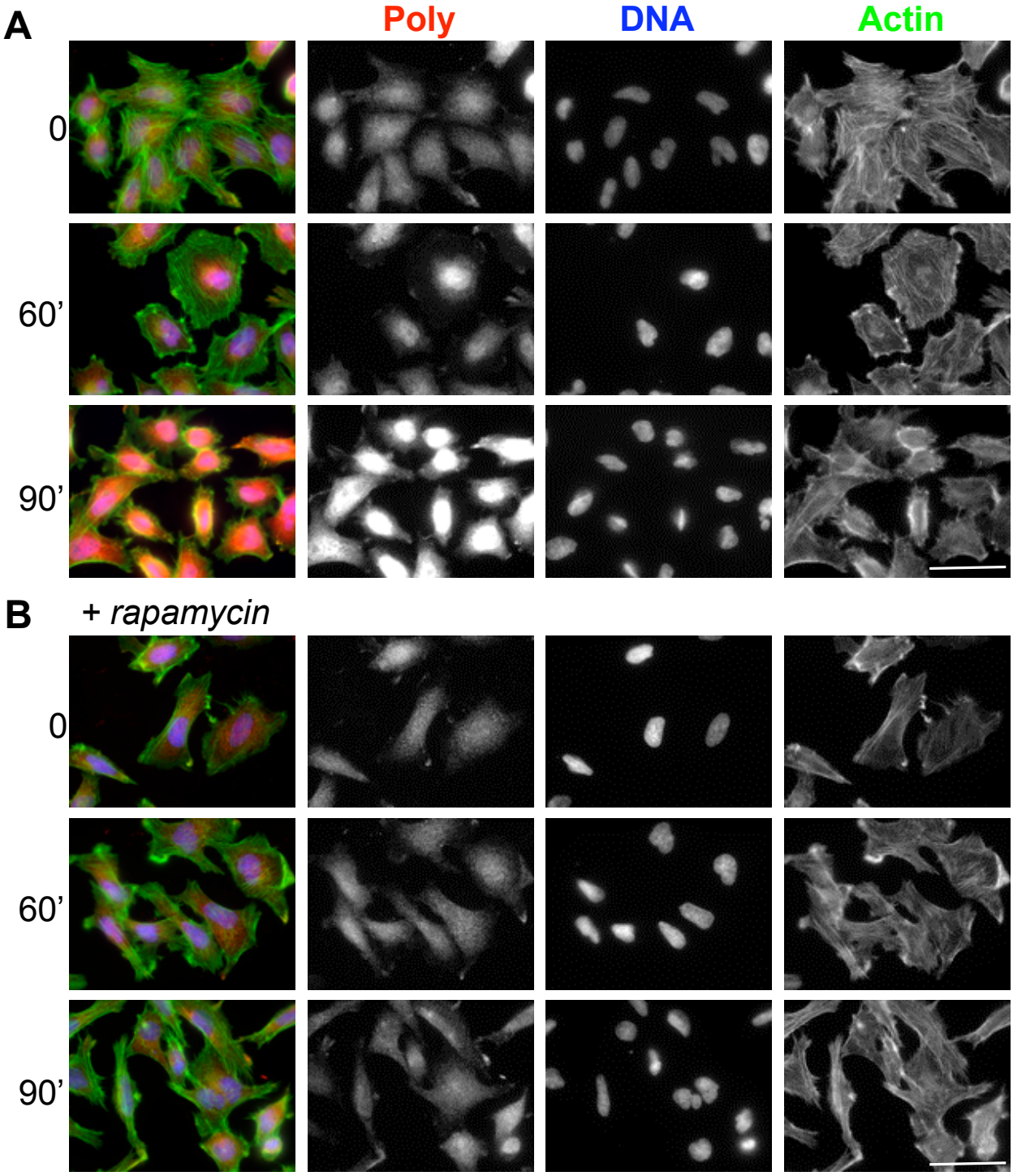

Figure 5.1. Insulin stimulation of HeLa cells leads to increase in HsPoly staining particularly localized in the nuclear area.

A) HeLa cells were serum starved overnight and then stimulated with 100 nM insulin for 60 and 90 minutes prior to immunostaining for actin (Alexafluor-488 phalloidin, green), DNA (DAPI, blue), and HsPoly (red). Staining for HsPoly (red) indicated accumulation near the nucleus is evident by 60 minutes, reaching a maximum following 90 minutes of insulin stimulation. B) The nuclear accumulation of HsPoly was inhibited by overnight incubation of cells with 20 nM of rapamycin prior to insulin treatment as in A. Scale bar presents 50 μm throughout.

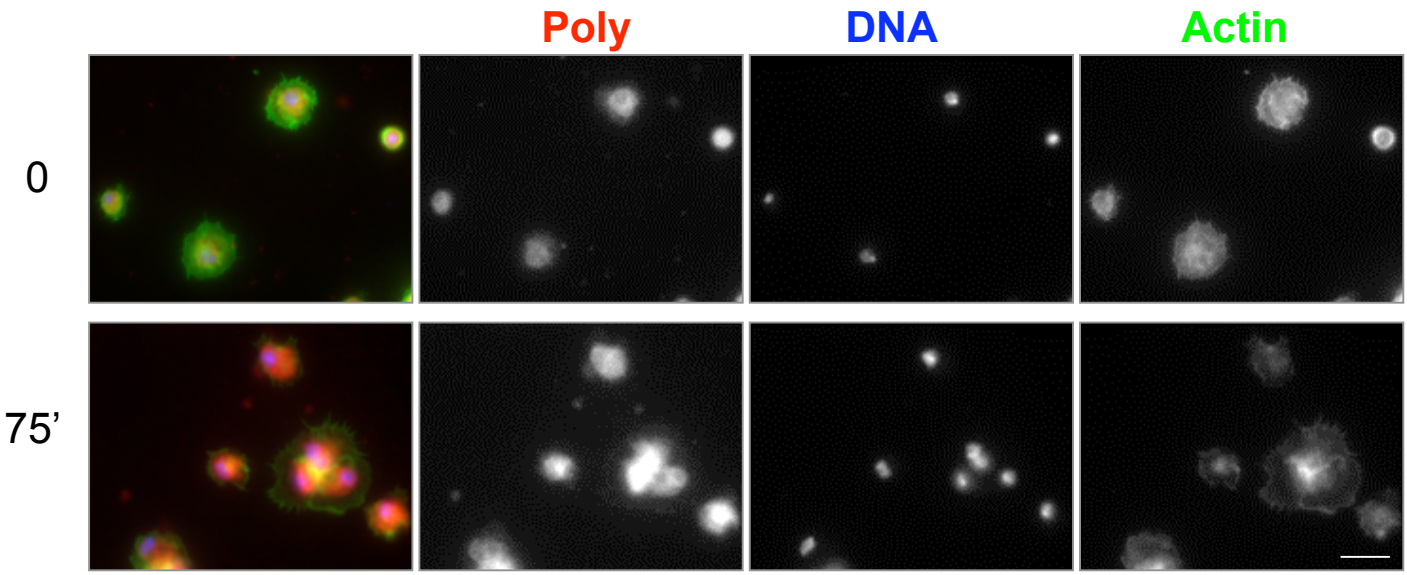

Figure 5.2. Poly immunostaining increases following stimulation of larval hemocytes with insulin.

Hemocytes were isolated by bleeding third instar larvae. Hemcoytes were then stimulated with 200 nM insulin for 75 minutes prior to immunostaining for actin (Alexafluor-488 phalloidin, green), DNA (DAPI, blue), and Poly (red). Staining for Poly (red) was stronger following 75 minutes of insulin stimulation. Scale bar presents 20 μm.

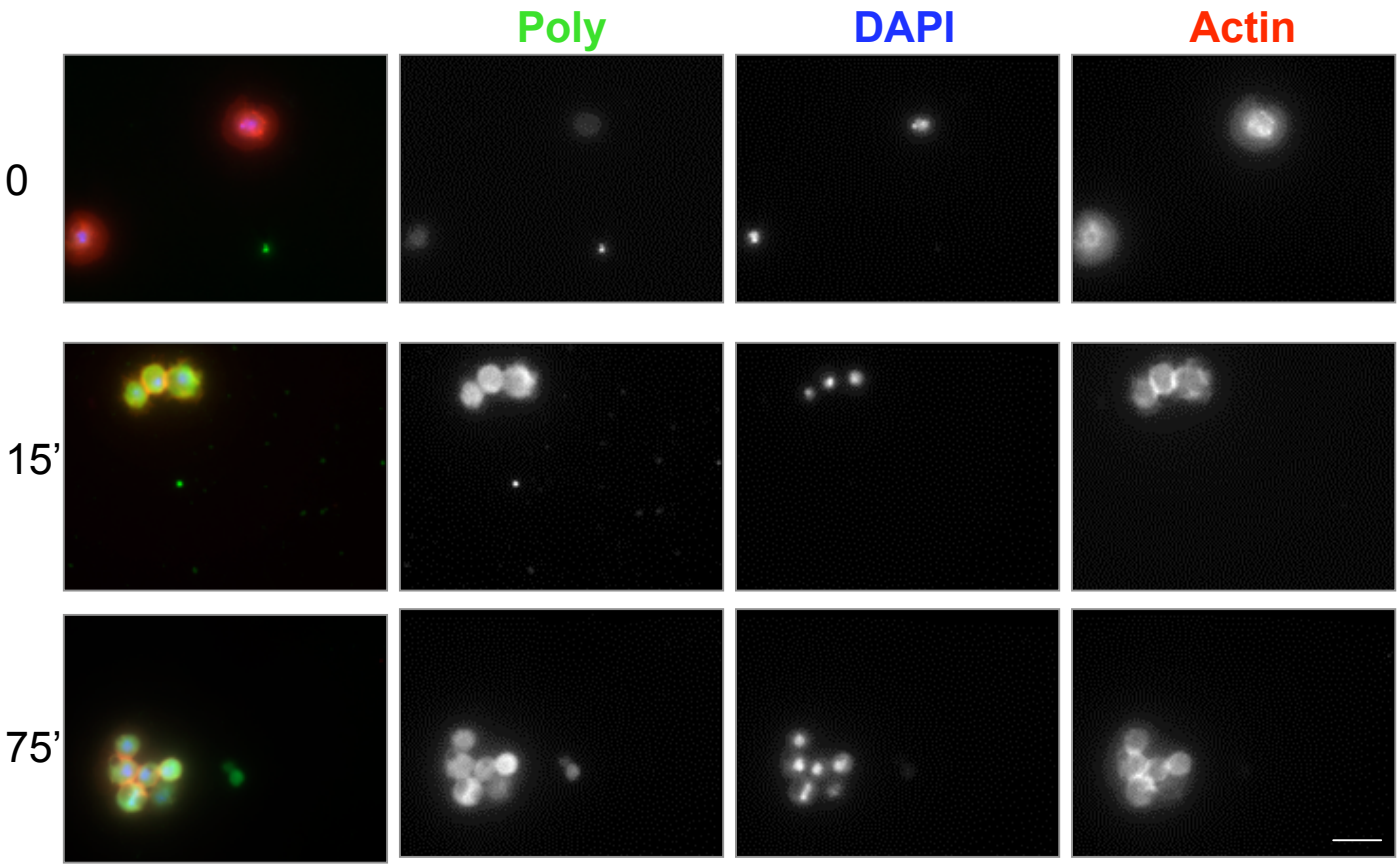

Figure 5.3. Poly immunostaining increases following insulin stimulation of hemocytes isolated from larvae that had previously been starved.

Hemocytes were isolated by bleeding third instar larvae. Larvae were starved for 3 hours in 20% sucrose solution prior to bleeding. Hemcoytes were then stimulated with 200 nM insulin for 15 an 75 minutes prior to immunostaining for actin (Alexafluor-594 phalloidin,red), DNA (DAPI, blue), and Poly (green). Staining for Poly (red) was stronger following both 15 and 75 minutes of insulin stimulation. Scale bar presents 20 μm.

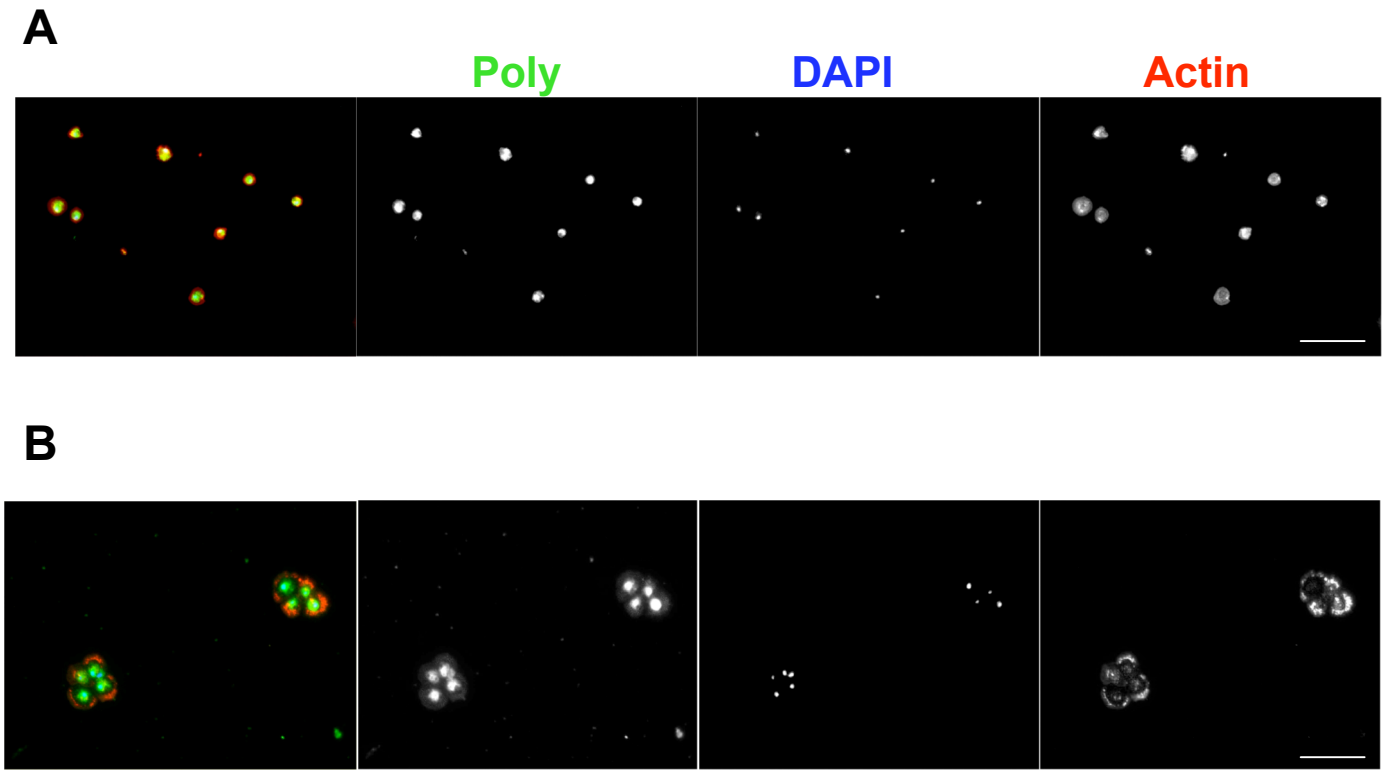

Figure 5.4. Poly immunostaining is increased in the nuclear area in hemocytes over-expressing constitutively active form of the InR.

Hemocytes were isolated by bleeding third instar A) control larvae and larvae B) over-expressing the constitutively active form of *UAS-InR*^{A1325D} under the control of Hml-Gal4. Hemcoytes were immunostained for actin (Alexafluor-594 phalloidin,red), DNA (DAPI, blue), and Poly (green). Hemocytes isolated from larvae over-expressing the constitutively active form of InR showed an increased strong nuclear staining which was absent in hemocytes isolated from control larvae. Scale bar presents 40 μm. Data in this figure was generated by the MSc by research student Mei Xuan Lye.

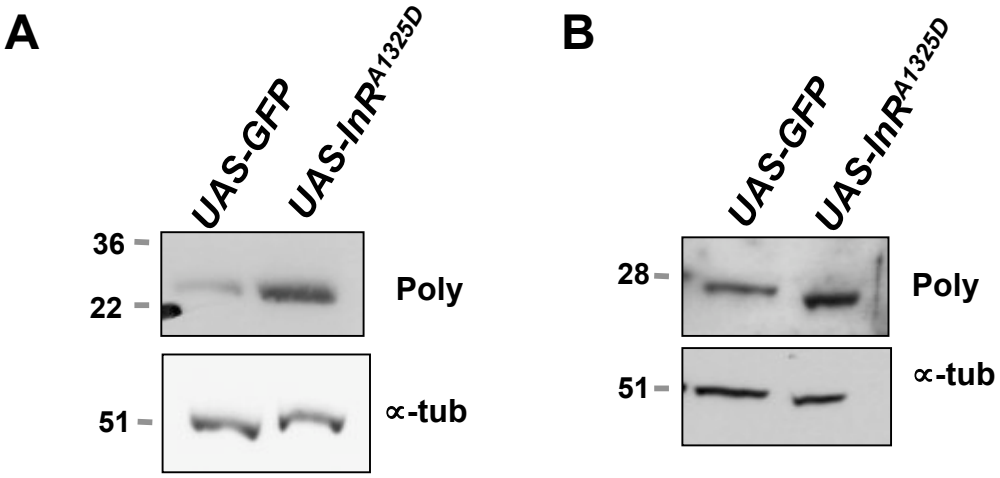

Figure 5.5. Poly levels are increased in larvae expressing a constitutively active form of the InR.

Immunoblotting of third instar larval extracts using an antibody specific to Poly reveals increased Poly levels in larvae over-expressing *UAS-InR^{A1325D}* under the control of Cg-Gal4 driver compared to *UAS-GFP;Cg-Gal4* control animals. Extracts were prepared from A) isolated fat body and B) whole larvae.

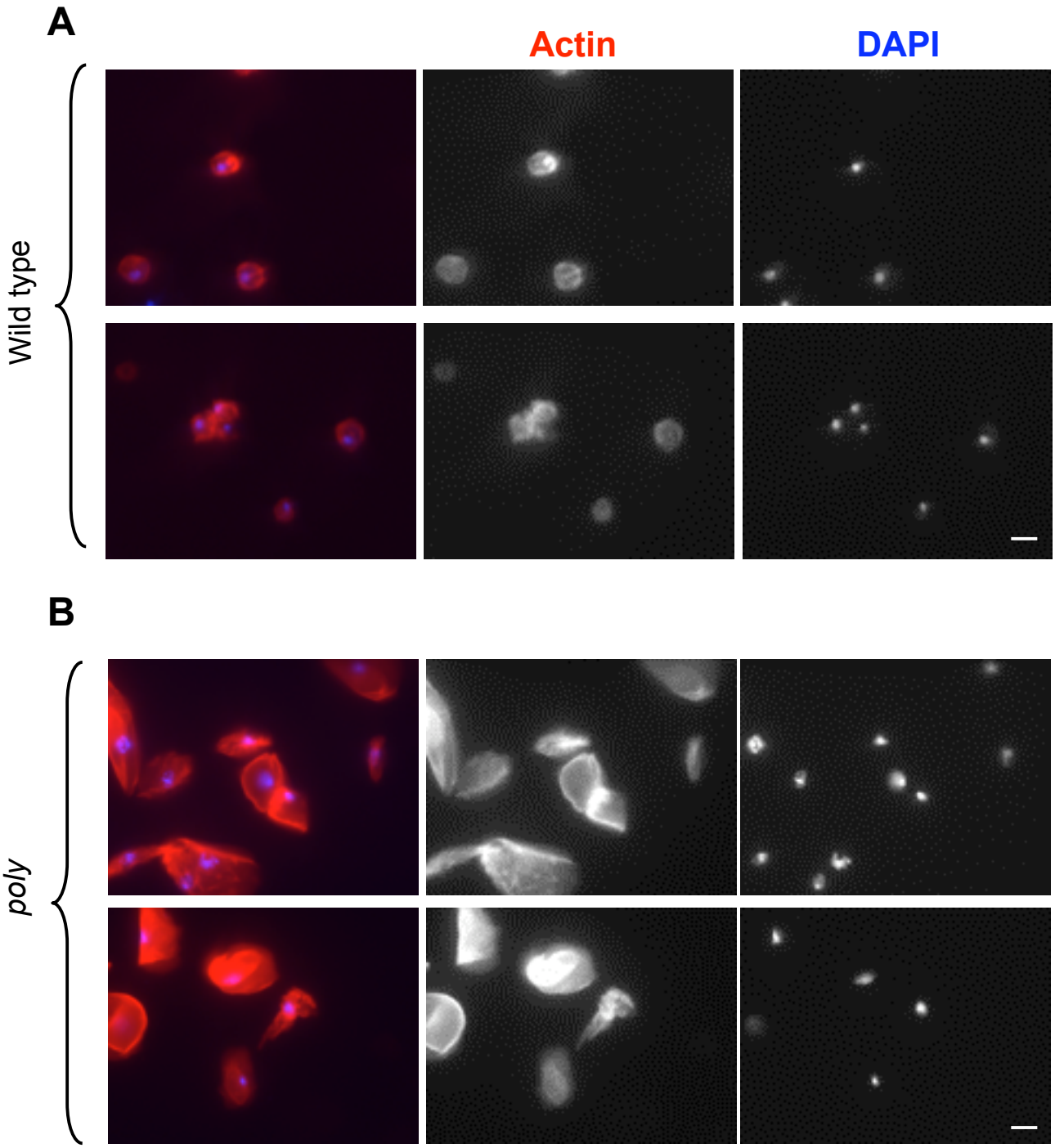

Figure 6.1. Actin staining of hemocytes isolated from wild type and *poly* mutant third instar larvae.

Hemocytes were isolated by bleeding third instar A) wild type and B) *poly* larvae. Hemocytes were then stained for actin (Phalloidin-Alexafluor-594, red) and DNA (DAPI, blue). Staining for actin cytoskeleton (red) of *poly* mutants revealed the appearance of cells that were much larger in size which were absent from wild type larvae. Scale bar presents 20 μm.

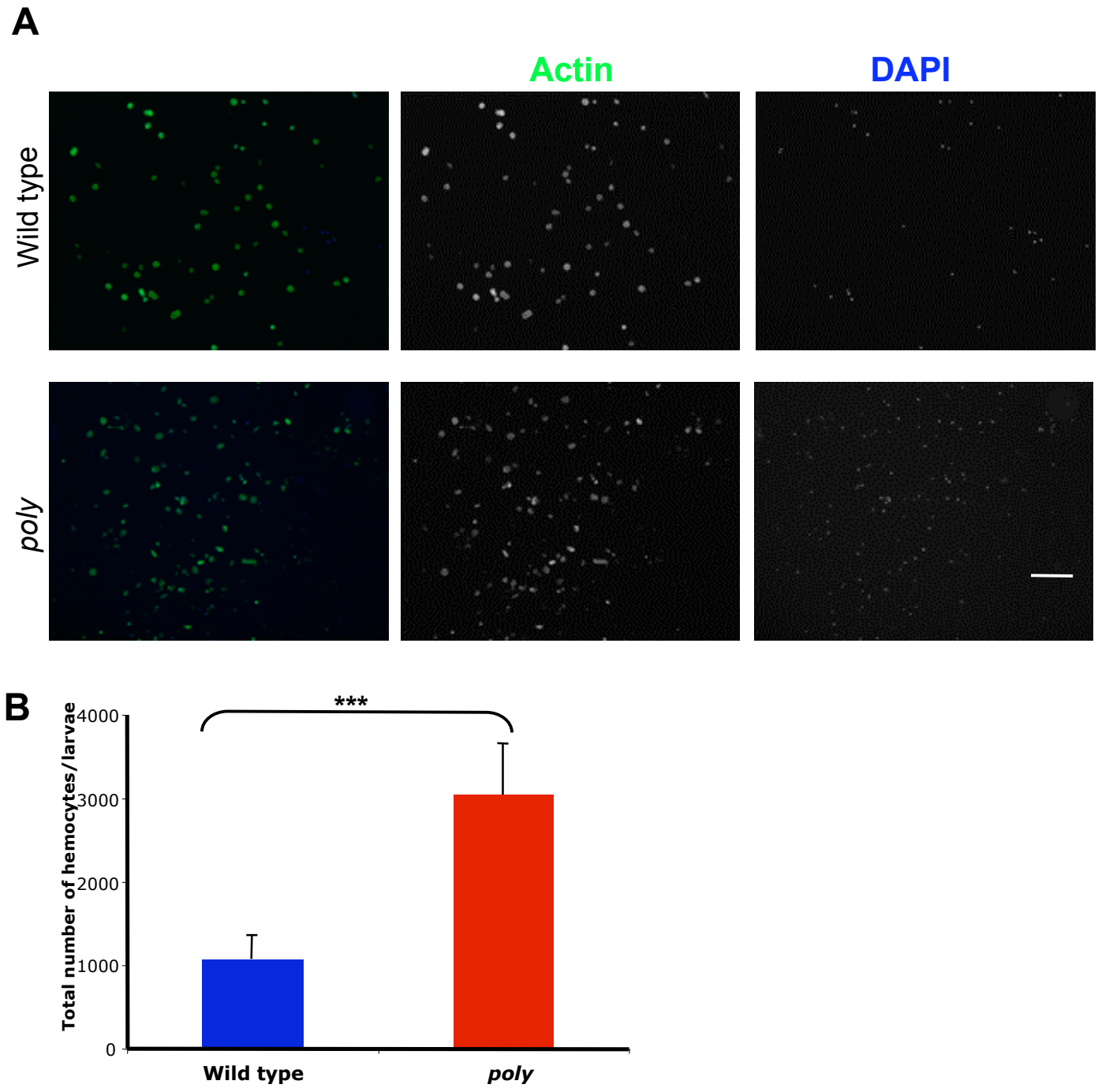

Figure 6.2. *poly* mutation leads to an increased number of hemocytes.

Hemocytes were isolated by bleeding third instar wild type and *poly* larvae. A) Hemocytes were then immunostained for actin (Phalloidin-Alexafluor 488, green) and DNA (DAPI, blue). A higher number of hemocytes was consistently observed in *poly* (lower panel) mutants compared to wild type (higher panel). Scale bar presents 100 μm. B) Quantification of hemocyte numbers was carried out on wild type and *poly* larvae. Larvae corresponding to each genotype were bled and the total number of hemocytes per larvae was determined by performing cell counts. Error bars represent standard deviation of cell counts performed on 10 larvae for each genotype. Triple asterisks represent significant difference ($p<0.001$) between cell counts of wild type and *poly* larvae. Cell counts were performed by the MSc by research student Swati Naidu.

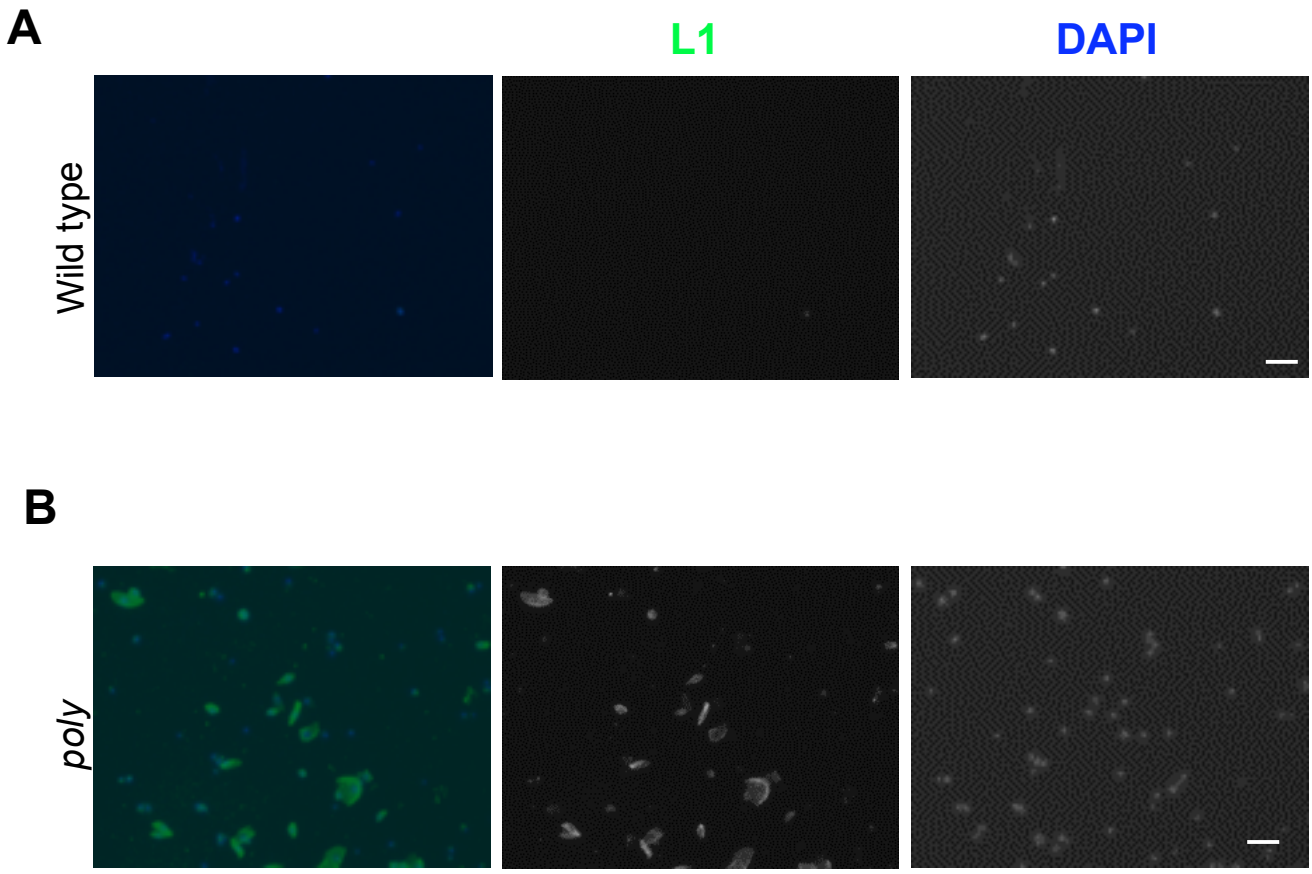

Figure 6.3. Staining of hemocytes isolated from wild type and *poly* mutants with lamellocyte-specific L1 antibody reveals presence of lamellocytes in *poly* mutant animals.

Hemocytes were isolated by bleeding third instar wild type A) and *poly* B) larvae. Hemocytes were then immunostained with the lamellocyte-specific L1 antibody (green) and DNA (DAPI, blue). L1 staining was absent in wild type A) hemocytes, whereas L1 positive cells were present at high frequency in hemocytes isolated from B) *poly* larvae. Scale bar presents 40 μm.

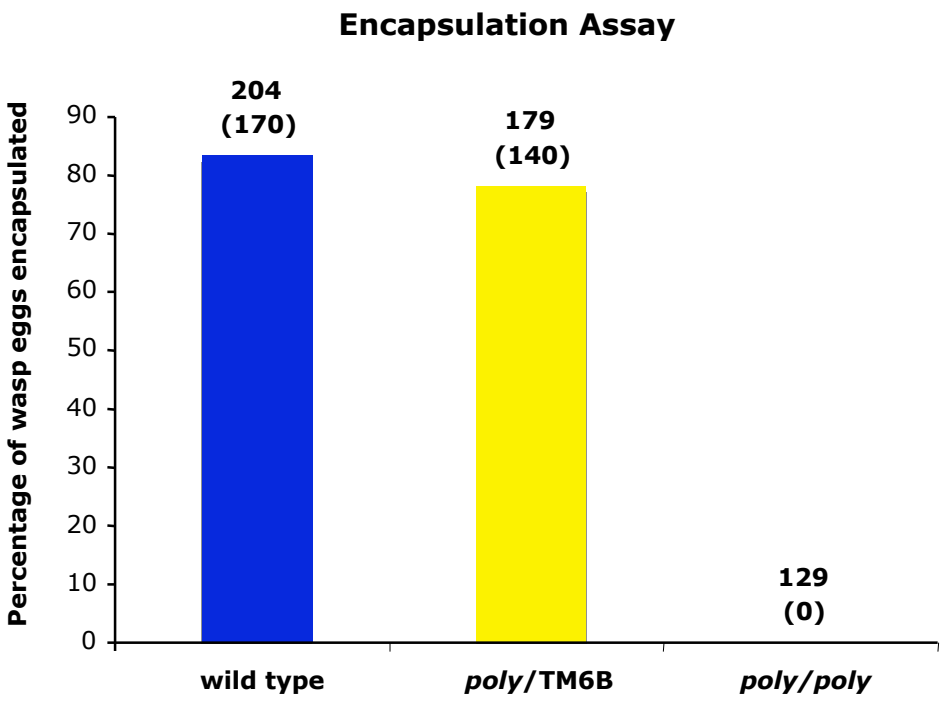

Figure 6.4. Encapsulation assay carried out following parasitisation by the was *Leptopilina boulardi* reveals that *poly* mutants fails to encapsulate.

Encapsulation rate of control (wild type and heterozygous flies of genotype *poly/TM6B*) and *poly* mutant larvae was calculated following parasitisation by the wasp *Leptopilina boulardi*. The total number of parasitised larvae examined is indicated on the top of each bar, while the number in parenthesis indicates the number of larvae presenting a dark capsule around the wasp egg, indicating a successful encapsulation process.

Gene name	Fold change	Related Signaling Pathway
Drosomycin	1.25	Toll pathway
Relish	1.91	Imd pathway
Diptericin	2.34	Imd pathway
AttacinA	2.9	Imd pathway

Figure 6.5. Microarray analysis on wild type and *poly* larvae revealed up-regulation of genes involved in the immune response in *poly* mutant animals.

Microarray analysis was carried out on wild type and *poly* third instar larvae. Analysis of differential gene expression revealed up-regulation of genes involved in the immune response in *poly* mutant larvae. The fold-change in expression levels revealed by microarray analysis are represented in the second column in this Table. The corresponding signalling pathway in which these genes take part is represented in the last column of the Table.

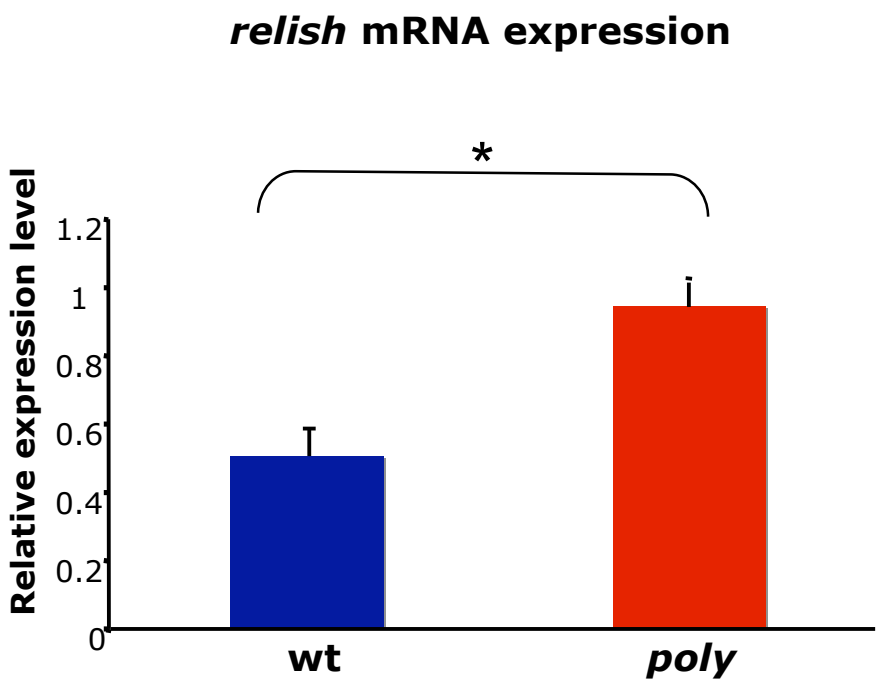

Figure 6.6. Real-time PCR on wild type and *poly* larvae reveals up-regulation of *rel* mRNA levels in *poly* mutant animals.

rel transcript levels were assessed by real-time qPCR on RNA isolated from wild type and *poly* mutant larvae. *rel* levels were normalized to *actin5C* levels. The error bars derive from reactions carried on biological triplicate samples. Each biological sample was obtained by extracting RNA from 5-7 larvae. Asterisk represents significant difference ($p<0.05$) in *rel* expression levels between wild type and *poly* larvae.

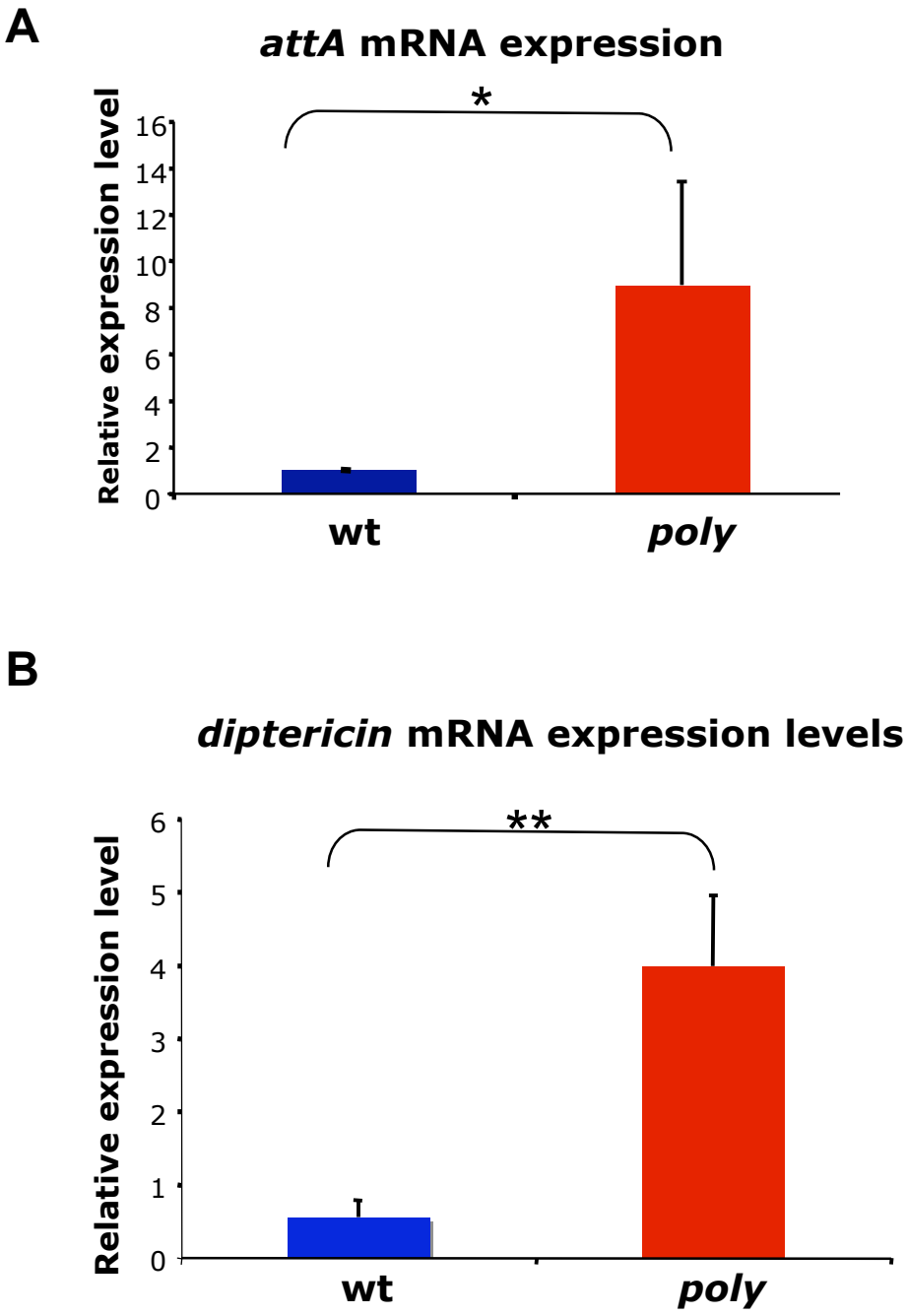

Figure 6.7. Real-time PCR on wild type and *poly* larvae reveals up-regulation of *attA and dpt* mRNA levels in mutant animals.

A) *attA* and B) *dpt* transcript levels were assessed by real-time qPCR on RNA isolated from wild type and *poly* mutant larvae. Expression levels of both *attA* and *dpt* were normalized to *actin5C* levels. The error bars derive from reactions carried on biological triplicate samples. Each biological sample was obtained by extracting RNA from 5-7 larvae. Asterisk and double asterisks represent significant differences at A) ($p<0.05$) in *attA* and B) ($p<0.01$) in *dpt* expression levels between wild type and *poly* larvae.

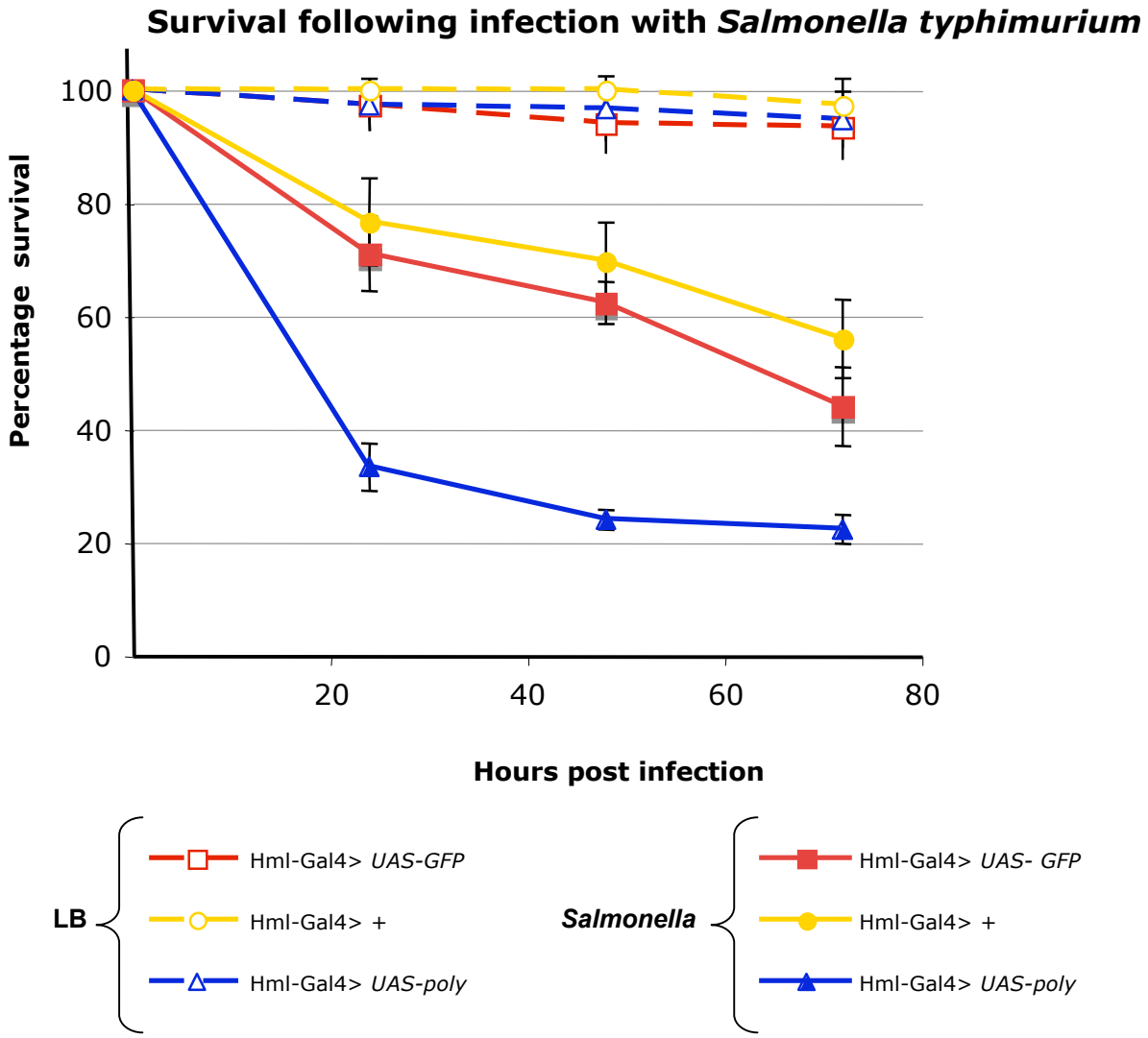

Figure 6.8. Poly over-expression in hemocytes leads to sensitivity to *Salmonella typhimurium* infection.

Survival rate of *Drosophila* infected with bacteria as indicated. 5- to 7-day old flies previously raised at 25ºC were infected with *Salmonella thyphimurium* by septic injury of the thorax with a thin needle previously dipped into the bacterial solution that had been gown in LB broth overnight. Injections by using LB solution alone were used as controls. The survival rate was followed at 25ºC. The genotype of flies are as follows: *Hml-Gal4* > *UAS-GFP* (*Hml-Gal4*/+ ; *UAS-GFP*/ +); *Hml-Gal4* > + (*Hml-Gal4*/+); *Hml-Gal4*> *UAS-poly* (*Hml-Gal4*/ + *; UAS-poly*/ +). Each data point was obtained by monitoring the survival of 25-30 male and 25-30 female flies (giving therefore a total of 50-60 flies). The average of results obtained from three experiments are represented in this graph. Errors bars represent standard deviation of three experiments.

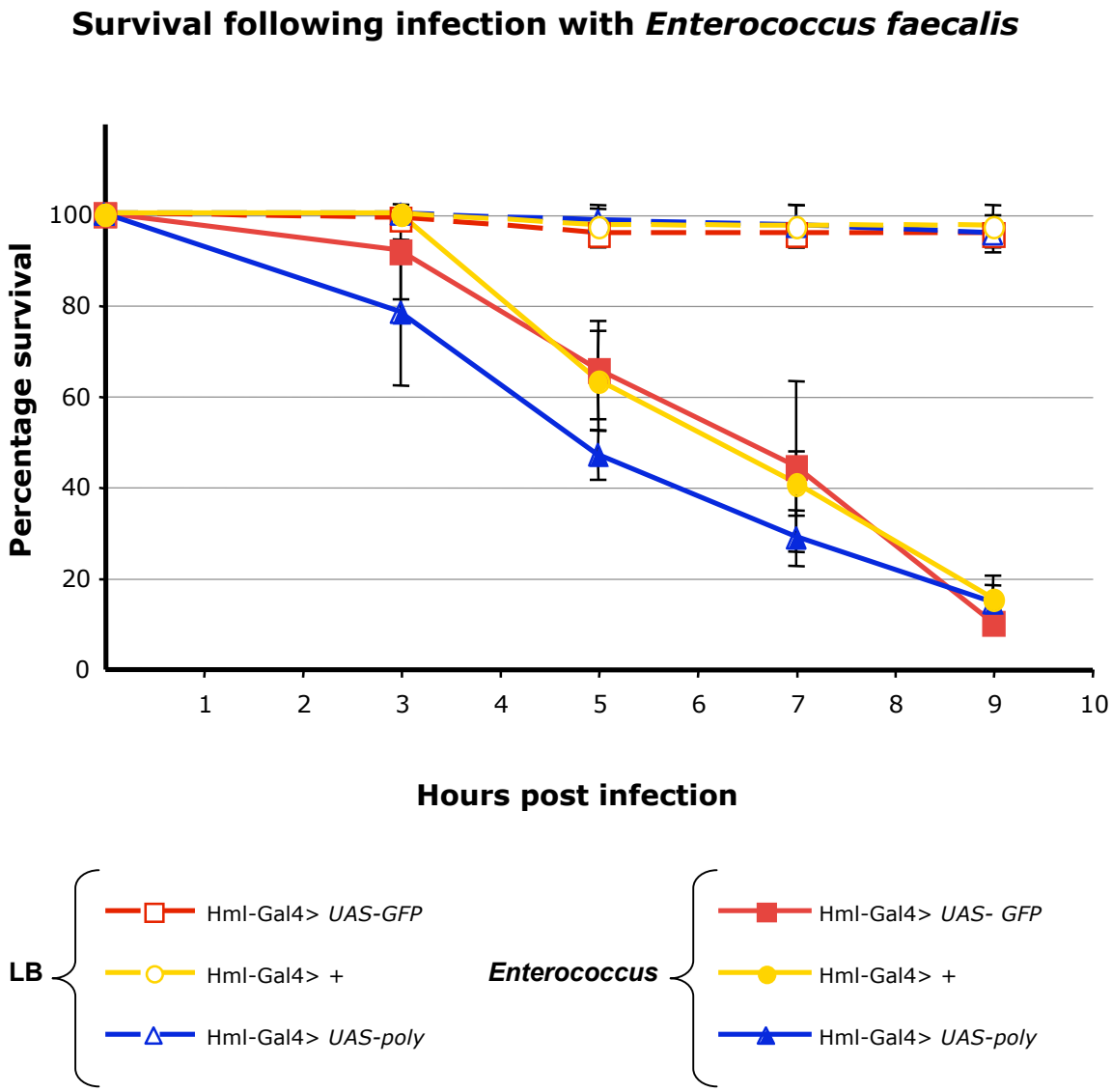

Figure 6.9. Poly over-expression in hemocytes does not affect survival following *Enterococcus faecalis* infection.

Survival rate of *Drosophila* infected as indicated. 5- to 7-day old flies previously raised at 25ºC were infected with *Enterococcus faecalis* by septic injury of the thorax with a thin needle previously dipped into the bacterial solution (OD= 0.7). Injections using LB solution alone were used as controls. The survival rate was followed at 25ºC. The genotypes of flies are as follows: *Hml-Gal4 > UAS-GFP* (*Hml-Gal4*/+ ; *UAS-GFP*/ +); *Hml-Gal4* > + (*Hml-Gal4*/+); *Hml-Gal4> UAS-poly* (*Hml-Gal4/ + ; UAS-poly/ +).* Each data point was obtained by monitoring the survival of 25-30 male and 25-30 female flies (giving therefore a total of 50-60 flies). The average of results obtained from three experiments are represented in this graph. Errors bars represent standard deviation of three experiments.

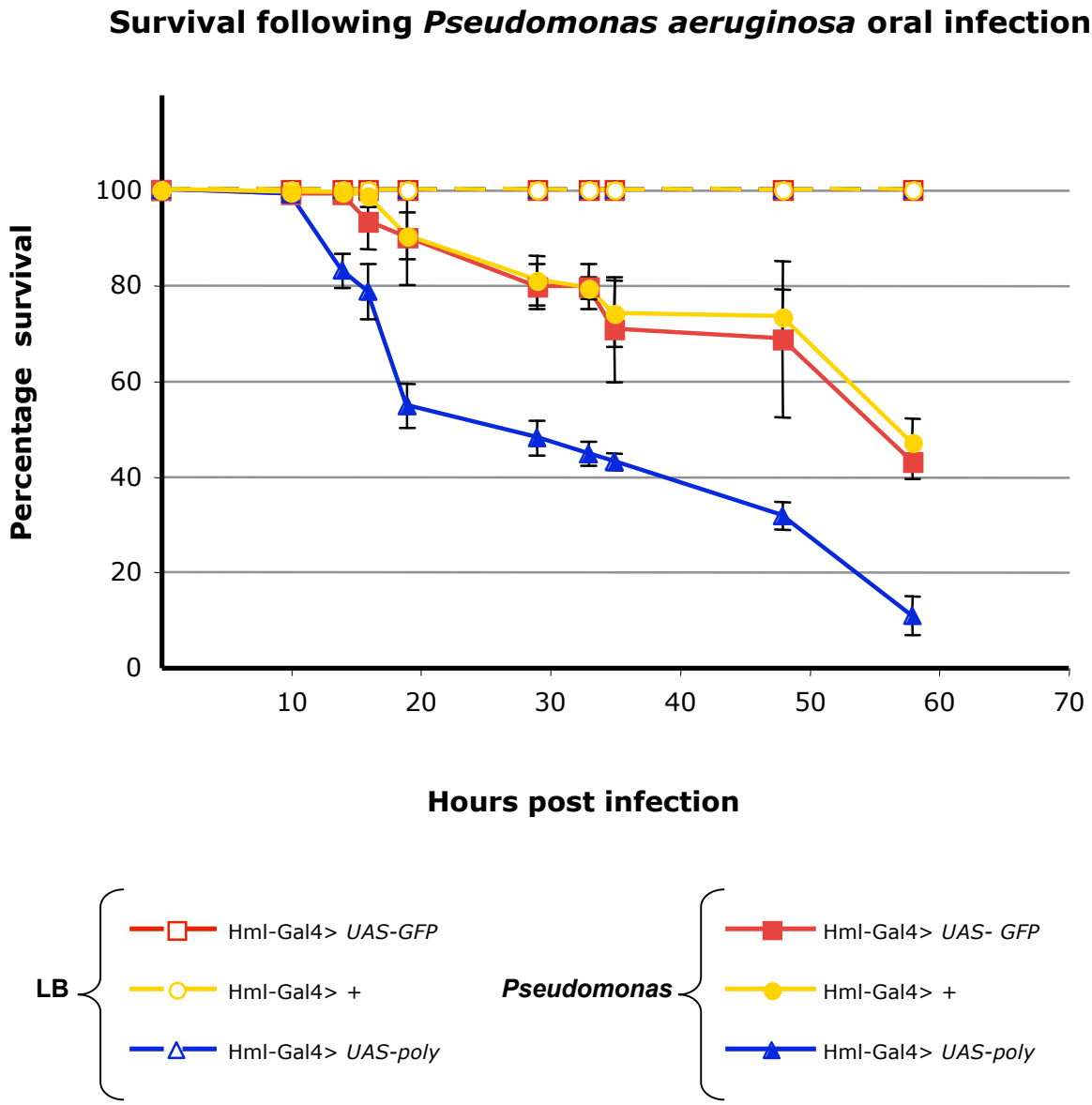

Figure 6.10. Poly over-expression in hemocytes leads to sensitivity to *Pseudomonas aeruginosa* infection.

Survival rate of *Drosophila* infected with bacteria as indicated 5- to 7-day old flies previously raised at 25ºC were infected with *Pseudomonas aeruginosa* by oral ingestion. LB solution alone diltuted in sterile sucrose solution was used as control. The survival rate was followed at 25ºC. The genotypes of flies are as follows: *Hml-Gal4 > UAS-GFP* (*Hml-Gal4*/+ ; *UAS-GFP*/ +); *Hml-Gal4 >* + (*Hml-Gal4/*+); *Hml-Gal4> UAS-poly* (*Hml-Gal4/ + ; UAS-poly/ +).* Each data point was obtained by monitoring the survival of 25-30 male and 25-30 female flies (giving therefore a total of 50-60 flies). The average of results obtained from three experiments are represented in this graph. Errors bars represent standard deviation of three experiments.

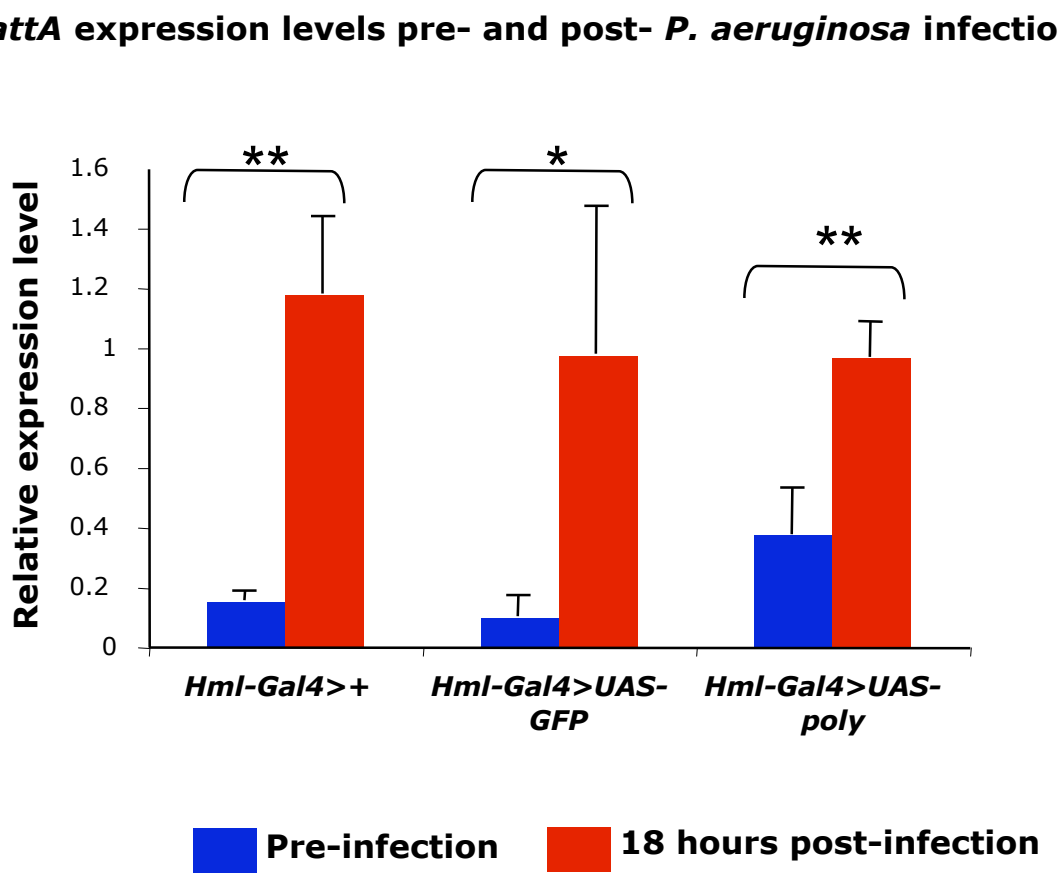

Figure 6.11. Expression of *attA* following *P. aeruginosa* infection.

attA transcript levels were assessed by real-time qPCR on RNA isolated from control (*Hml-Gal4>+, Hml-Gal4>UAS-GFP*) and *Hml-Gal4>UAS-poly* larvae before and 18 hours after *Pseudomonas aeruginosa* oral infection. Expression levels of *attA* were normalized to *actin5C* levels. The error bars derive from reactions carried on biological triplicate samples. Each biological sample was obtained by extracting RNA from 10 flies. Asterisk and double asterisks represent significant differences with p-values of $p<0.05$ and $p<0.01$ respectively. *attA* expression levels were found to be significantly increased post-infection in both control flies and flies over-expressing *poly* in hemocytes.

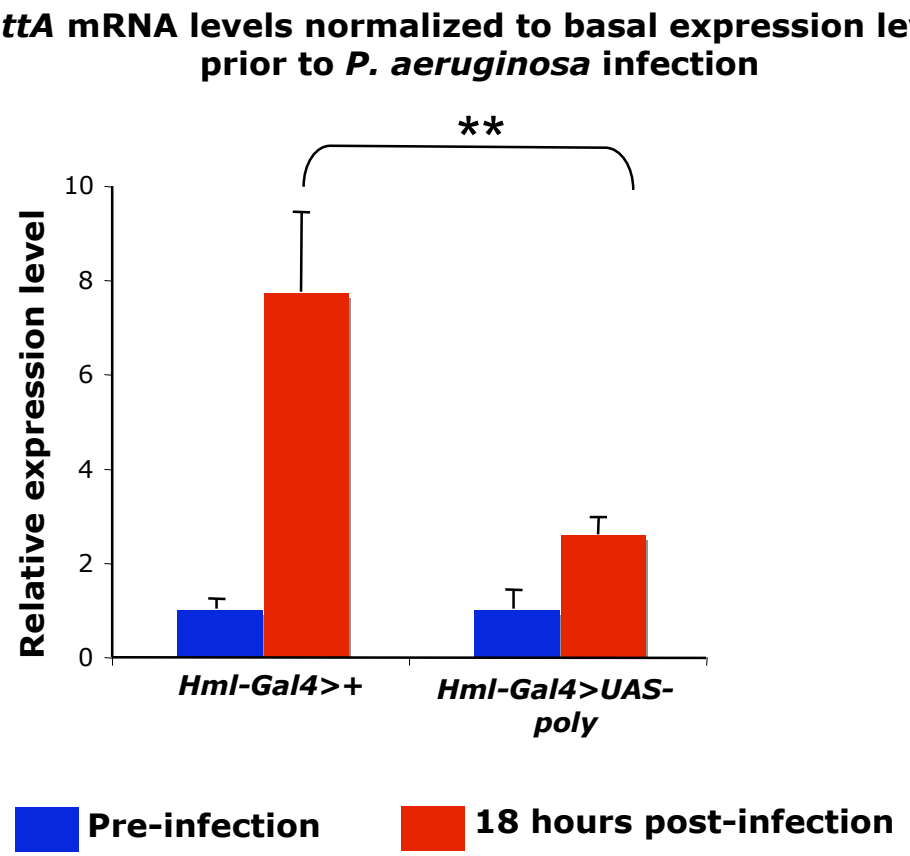

Figure 6.12. Expression of *attA* following infection normalized to basal expression levels prior to infection of *P. aeruginosa*.

attA transcript levels were assessed by real-time qPCR on RNA isolated from control (*Hml-Gal4>+*) and *Hml-Gal4>UAS-poly* larvae before and 18 hours after *Pseudomonas aeruginosa* oral infection. Expression levels of *attA* were normalized to *actin5C* levels. AttA expression levels following infection were further normalized to basal expression levels (prior to infection) for each genotype to determine the fold induction of *attA* expression for each genotype. The error bars derive from reactions carried on biological triplicate samples. Each biological sample was obtained by extracting RNA from 10 flies. Double asterisks represent significant differences with a value $p<0.01$. The fold induction of *attA* expression following infection was found to be significantly different between control flies and flies over-expressing *poly* in hemocytes.

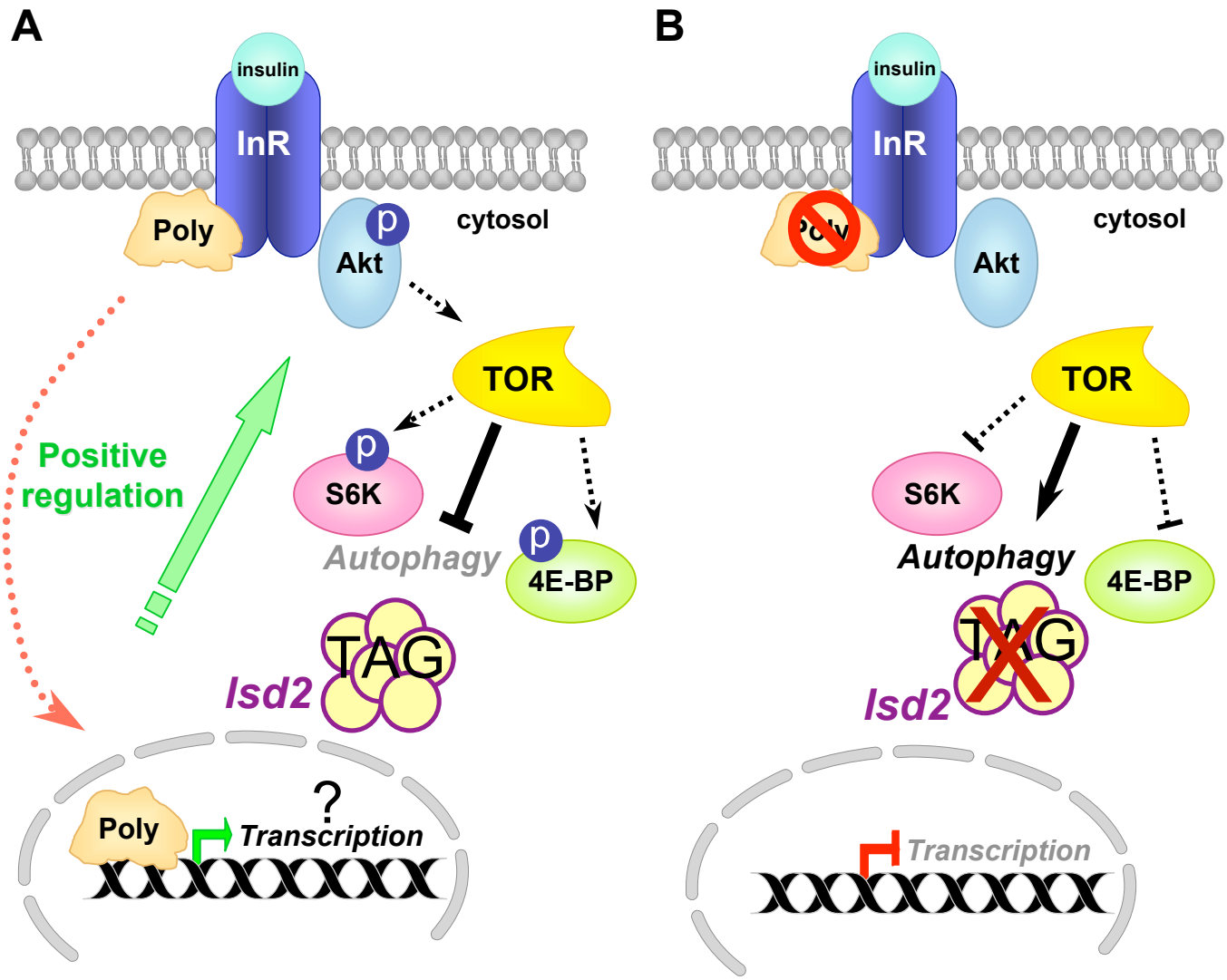

Figure 8.1. Model for the function of Poly in the InR/TOR signalling pathway.

A) The formation of a protein complex between Poly and Insulin Receptor allows it to accomplish its role as positive regulator of InR/TOR signalling. The activation of InR signalling leads to a change in the subcellular localisation of Poly and to its movement into the nucleus, allowing it to accomplish its potential role during transcription. This has an overal effect of increasing the phosphorylation levels of various positive regulators of the InR/TOR pathway, such as Akt and S6K, as well as inhibiting negative regulators of cell growth such as autophagy. Furthermore, anabolic metabolism is promoted resulting in increase of TAG and Lsd2 levels. B) The absence of Poly leads to a decrease in the activation of positive regulators of cell growth such as Akt and S6K kinases. 4E-BP transcript levels increase while the protein itself becomes hypophosphorylated consistent with an overall downregulation of the InR/TOR signalling. Furthermore, autophagy – a negative effector of InR/TOR signalling – becomes constitutively active. Anabolic metabolism is down-regulated as indicated by a decrease in TAG and lsd2 levels.

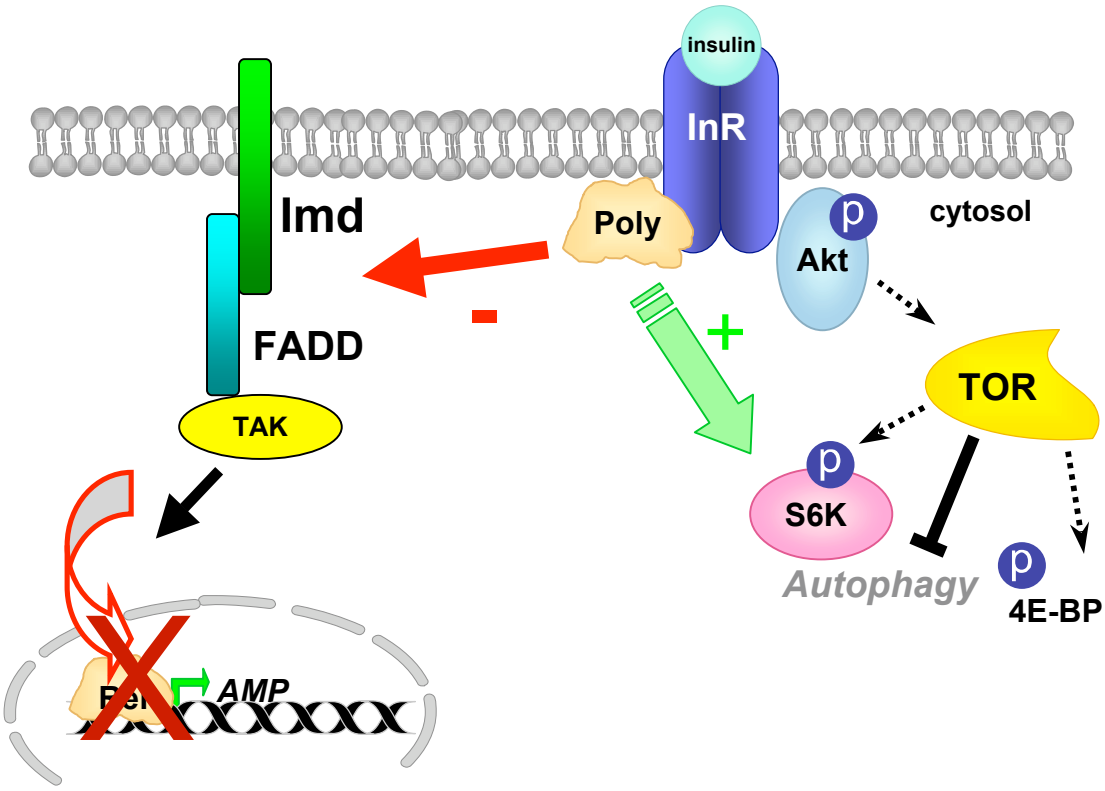

Figure 8.2. Model for a direct involvement of Poly in the humoral immune response in *Drosophila*.

The interaction of Poly with Insulin Receptor allows it to accomplish its role as positive regulator of InR/TOR signalling. At the same time, Poly could be playing a role as a co-regulator of InR/TOR within the immune response by exerting an inhibitory effect on the humoral immune response (most likely via the Imd pathway) at the absence of infection.